ACTIVATION OF C-H AND C-F BONDS BY CYCLOPENTADIENYL IRIDIUM COMPLEXES

CHAN PEK KE
(B. Sc. (Hons.), NUS)

A THESIS SUBMITTED

FOR THE DEGREE OF DOCTOR OF PHILOSOPHY

DEPARTMENT OF CHEMISTRY

NATIONAL UNIVERSITY OF SINGAPORE

2007

Acknowledgements

I would like to express my heartfelt gratitude to my supervisor, A/P Leong Weng Kee for his mentorship, inspiration, invaluable advice and help; my co-supervisors, A/P Marc Garland and Dr Zhu Yinghuai (Institute of Chemical and Engineering Sciences, A*STAR) for their support and my boss, Andy Naughton for his kind understanding.

I am grateful to my past and current group members: the postgraduates Padma, Jiehua, Janet, Sridevi, Chunxiang, Garvin, Kong, Xueling and Changhong for helpful discussion, friendship and encouragement; the lively undergraduates Yanqin, Guihua, Tommy, Aifen, Jieying, Benny, Hwee Hwee, Xueping, Huifang, Audrey and Jeremiah for injecting life into the lab and the research and student assistants Gao Lu, Mui Ling, Meien and Jialin for maintaining a comfortable working environment in the lab.

I also wish to thank Karl I. Krummel (Department of Chemical and Biomolecular Engineering, NUS) for his help in setting up the experiments for in situ IR studies and BTEM deconvolution.

Technical support from the following people is also sincerely appreciated: Yanhui and Peggy from the NMR laboratory, Mdm Wong and Mdm Chen from the Mass Spectrometry laboratory and Mdm Choo and Zing from the Elemental Analysis laboratory.

I definitely have to thank my family, especially my husband, James for motivating me, believing in me and giving me the moral support.

Finally, I thank God for His grace.

TABLE OF CONTENTS

Summary

The activation of C-H bonds by cyclopentadienyl iridium complexes and its derivatives and the reactivity of the iridium complex $Cp^*Ir(CO)_2$, **2a** with fluoroaromatics have been investigated.

The first part of the thesis deals with the photochemical reactivity of iridium complexes containing side-chain-functionalized cyclopentadienyl ligands in saturated hydrocarbon solvents as compared to the parent complex **2a**. In situ infrared measurements were carried out to detect any reaction intermediates with the help of the band-targeted entropy minimization (BTEM) algorithm for deconvolution of the data matrix to obtain pure component spectra of individual species present in the reaction mixture. Photolysis of the aminoethyl-functionalized analogue $Cp^*{\wedge}Ir(CO)_2$, **2b** in a degassed cyclohexane solution led to the formation of the dihydride species $Cp^*{\wedge}Ir(CO)(H)_2$, **5b** in addition to the hydridoalkyl species $Cp^*{\wedge}Ir(CO)(C_6H_{11})(H)$, **3b**. Complex **5b** was obtained from the *β*-hydride elimination of cyclohexene from **3b**. Photolysis of other side-chain-functionalized complexes $Cp{\wedge}Ir(CO)_2$, **2c** and Cp^{BZ} $Ir(CO)_2$, **2d** in cyclohexane also resulted in the formation of their corresponding hydridoalkyl and dihydride species. When the photolysis was carried out under a carbon monoxide atmosphere, the cluster $Ir_4(CO)_{12}$ was obtained together with the hydridoalkyl species instead of the dihydride species. Formation of cyclohexanecarboxaldehyde from the carbonylation of cyclohexane was also observed.

In the search for solvents that are inert to C-H activation by the iridium complexes, attempts were made to carry out the photoirradiation in non-hydrocarbon solvents. In the process, it was discovered that **2a** reacted with hexafluorobenzene (C_6F_6) photochemically to give $Cp^*Ir(CO)(\eta^2\text{-}C_6F_6)$, **15** and $[Cp^*Ir(C_6F_5)(\mu\text{-}CO)]_2$, **16**. Subsequently, the reactions of **2a** with several other substituted fluoroaromatics were carried out in order to study the regioselectivity of the reaction and these constitute the second part of the thesis.

The reaction of **2a** with pentafluorobenzonitrile (C_6F_5CN) proceeded at room temperature in the presence of water to give $Cp^*Ir(CO)(COOH)(p\text{-}C_6F_4CN)$, **18a** in

essentially quantitative yield. A similar reaction with pentafluoropyridine (C_5F_5N) produced Cp*Ir(CO)(COOH)(*p*-C_5F_4N), **22a**. The reactions were highly regioselective, giving only *para*-substituted products. In an alcoholic media, the corresponding alkoxylcarbonyls Cp*Ir(CO)(COOR)(*p*-C_6F_4CN) and Cp*Ir(CO)(COOR)(*p*-C_5F_4N) were formed.

Several pieces of experimental evidence suggest that the formation of the metallocarboxylic acids occurred via a nucleophilic substitution pathway. Two nucleophilic substitution steps are believed to be involved: (i) attack by **2a** on the fluoroarene and (ii) attack by water or hydroxide ion, probably via a general base-catalyzed mechanism, on one of the carbonyls to form the carboxylic acid group.

Compound **18a** exhibited several properties typical of metallocarboxylic acids such as dehydration in the presence of a strong acid (HBF_4) to form the corresponding metal carbonyl cation $[Cp^*Ir(CO)_2(p\text{-}C_6F_4CN)]^+[BF_4]^-$, **20**; decarboxylation in the presence of bases to form the metal hydride Cp*Ir(CO)(H)(*p*-C_6F_4CN), **19a**; and esterification in alcohols in the absence of an acid or a base as catalyst. Compound **18a** also reacted with the triosmium cluster $Os_3(CO)_{10}(NCCH_3)_2$ to form $Os_3(CO)_{10}(\mu\text{-}H)(\mu\text{-}OOCR)$ (R = Cp*Ir(CO)(*p*-C_6F_4CN)], **21** in which the iridium and osmium centers are joined by the bridging carboxylate group.

Compound Numbering Scheme

Formula	Structure
1 $[Cp^*Ir(Cl)(\mu\text{-}Cl)]_2$	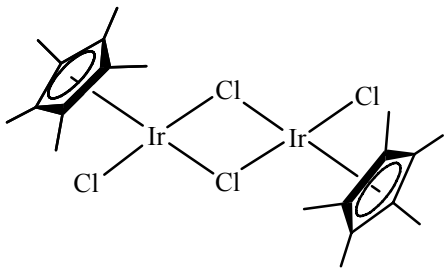
2a $Cp^*Ir(CO)_2$ **2b** $Cp^{*\wedge}Ir(CO)_2$ **2c** $Cp^{\wedge}Ir(CO)_2$ **2d** $Cp^{BZ}Ir(CO)_2$	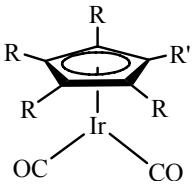 R = Me, R' = Me **2a** R = Me, R' = $(CH_2)_2N(Me)_2$ **2b** R = H, R' = $(CH_2)_2N(Me)_2$ **2c** R = H, R' = CH_2Ph **2d**
3a $Cp^*Ir(CO)(C_6H_{11})(H)$ **3b** $Cp^{*\wedge}Ir(CO)(C_6H_{11})(H)$ **3c** $Cp^{\wedge}Ir(CO)(C_6H_{11})(H)$ **3d** $Cp^{BZ}Ir(CO)(C_6H_{11})(H)$	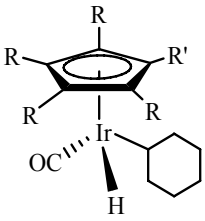 R = Me, R' = Me **3a** R = Me, R' = $(CH_2)_2N(Me)_2$ **3b** R = H, R' = $(CH_2)_2N(Me)_2$ **3c** R = H, R' = CH_2Ph **3d**
4a $Cp^*Ir(CO)(C_5H_9)(H)$ **4b** $Cp^{*\wedge}Ir(CO)(C_5H_9)(H)$	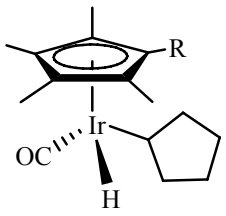 R = Me **4a** R = $(CH_2)_2N(Me)_2$ **4b**
5a $Cp^*Ir(CO)(H)_2$ **5b** $Cp^{*\wedge}Ir(CO)(H)_2$ **5c** $Cp^{\wedge}Ir(CO)(H)_2$ **5d** $Cp^{Bz}Ir(CO)(H)_2$	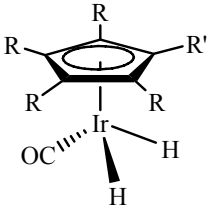 R = Me, R' = Me **5a** R = Me, R' = $(CH_2)_2N(Me)_2$ **5b** R = H, R' = $(CH_2)_2N(Me)_2$ **5c** R = H, R' = CH_2Ph **5d**
6 $Ir_4(CO)_{12}$	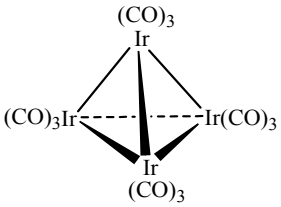

7a $Cp^*Ir(CO)(PPh_3)$

7b $Cp^{BZ}\ Ir(CO)(PPh_3)$

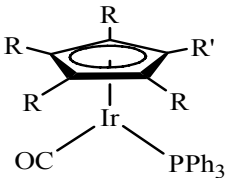

R = Me, R' = Me **7a**

R = H, R' = CH_2Ph **7b**

8a $Cp^*Ir(CO)(C_6H_{11})(Cl)$

8b $Cp^*{}^{\wedge}Ir(CO)(C_6H_{11})(Cl)$

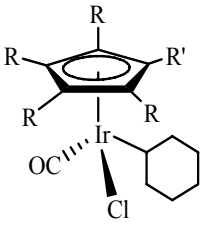

R = Me, R' = Me **8a**

R = Me, R' = $(CH_2)_2N(Me)_2$ **8b**

9a $Cp^*Ir(CO)(Cl)_2$

9b $Cp^*{}^{\wedge}Ir(CO)(Cl)_2$

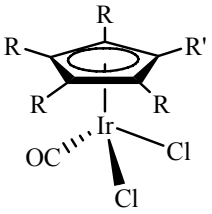

R = Me, R' = Me **9a**

R = Me, R' = $(CH_2)_2N(Me)_2$ **9b**

10 $Cp^*Ir(CO)$ [PhC=CHC(Ph)=CCH=CCl(Ph)]

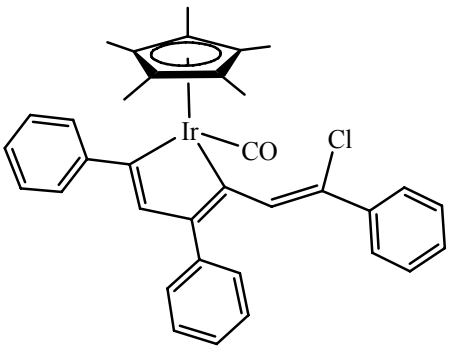

11 $Cp^*Ir(CO)(\eta^2\text{-PhC}\equiv\text{C-C}\equiv\text{CPh})$

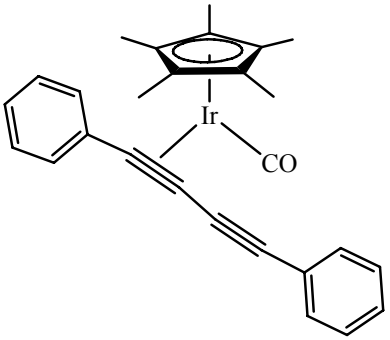

12a $Tp^*Rh(CO)_2$

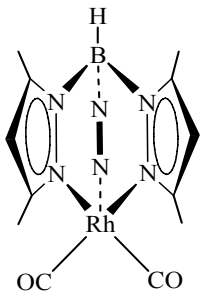

12b $C_{40}H_{40}RhBN_6O$

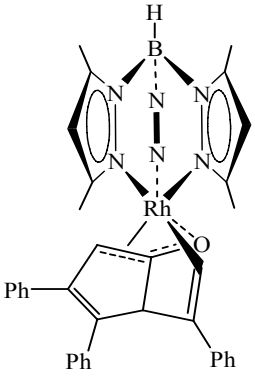

12b-d $C_{40}H_{37}D_3RhBN_6O$

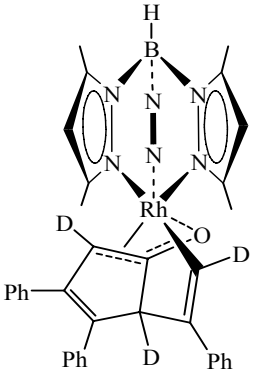

13 $C_{46}H_{30}Ir_2O_4$

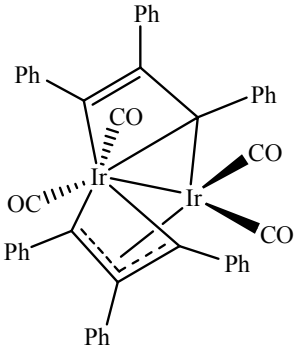

14a $C_{46}H_{30}Ir_2O_4$

14b $C_{46}H_{30}Rh_2O_4$

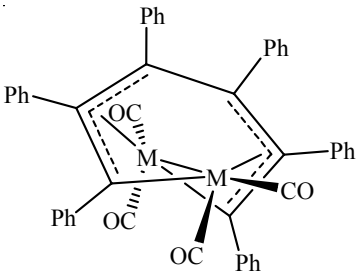

M = Ir **14a**
= Rh **14b**

15 $Cp^*Ir(CO)(\eta^2\text{-}C_6F_6)$

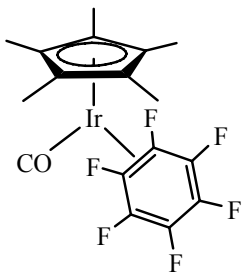

16 $[Cp^*Ir(C_6F_5)(\mu\text{-}CO)]_2$

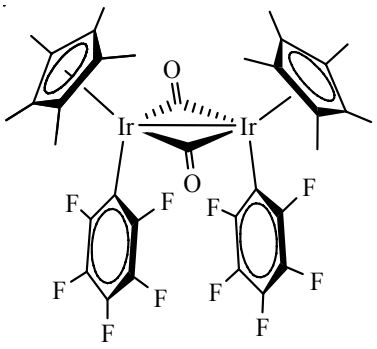

17 $Cp^*Ir(CO)(C_6F_5)Cl$

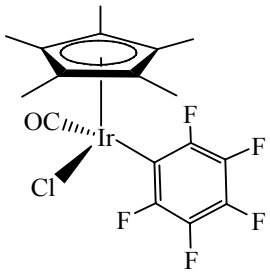

18a $Cp^*Ir(CO)(COOH)(p\text{-}C_6F_4CN)$
18b $Cp^*Ir(CO)(COOMe)(p\text{-}C_6F_4CN)$
18c $Cp^*Ir(CO)(COO^iPr)(p\text{-}C_6F_4CN)$
18d $Cp^*Ir(CO)(COOC_5H_9)(p\text{-}C_6F_4CN)$

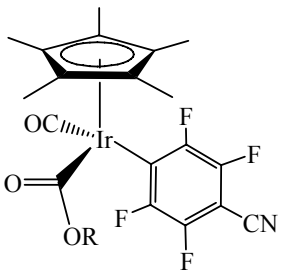

R = H **18a**
= Me **18b**
= ^{i}Pr **18c**
= Cyclopentyl **18d**

19a $Cp^*Ir(CO)(H)(p\text{-}C_6F_4CN)$
19b $Cp^*Ir(CO)(Cl)(p\text{-}C_6F_4CN)$

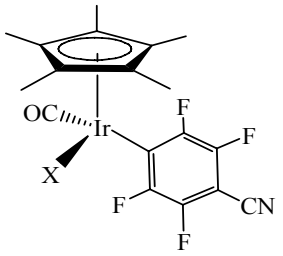

X = H **19a**
= Cl **19b**

20 $[Cp^*Ir(CO)_2(p\text{-}C_6F_4CN)][BF_4]$

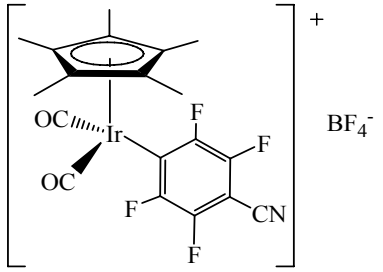

21 $Os_3(CO)_{10}(\mu\text{-}H)(\mu\text{-}OOC)[IrCp^*(CO)(p\text{-}C_6F_4CN)]$

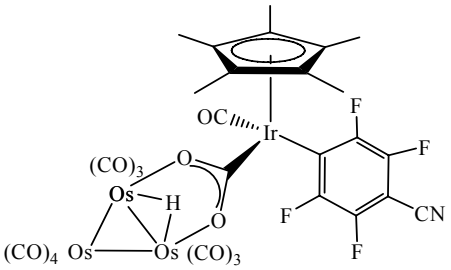

22a $Cp^*Ir(CO)(COOH)(p\text{-}C_5F_4N)$

22b $Cp^*Ir(CO)(COOMe)(p\text{-}C_5F_4N)$

22c $Cp^*Ir(CO)[COO(CH_2)_2CH_2Cl](p\text{-}C_5F_4N)$

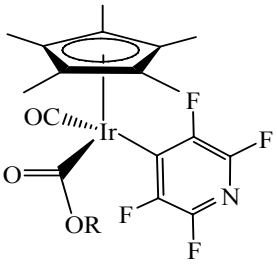

R = H **22a**
= Me **22b**
= $(CH_2)_2CH_2Cl$ **22c**

23 $Os_3(CO)_{10}(\mu\text{-}H)(\mu\text{-}OOC)[IrCp^*(CO)(p\text{-}C_5F_4N)]$

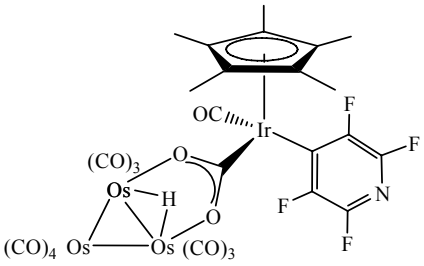

24a $Cp^*Ir(CO)(COOMe)(p\text{-}C_6F_4CF_3)$

24b $Cp^*Ir(CO)(COO^nPr)(p\text{-}C_6F_4CF_3)$

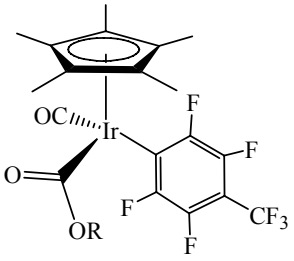

R = Me **24a**
= ^{n}Pr **24b**

25 $Cp^*Ir(CO)(H)(p\text{-}C_6F_4CF_3)$

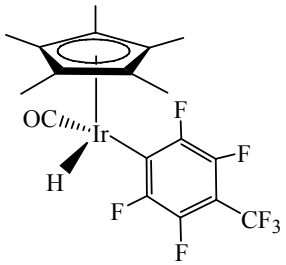

26 $Cp^*Ir(CO)(COOH)(p\text{-}C_6F_4CHO)$

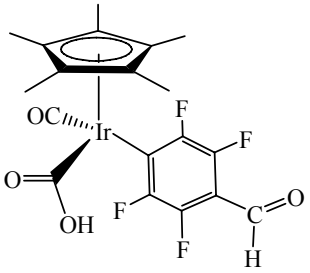

27 Cp*Ir(CO)(COOH)(*p*-$C_6F_4NO_2$)

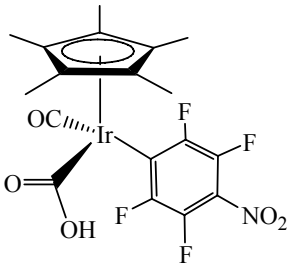

28 Cp*Ir(CO)(H)[2,4-$C_6F_3(CN)_2$]

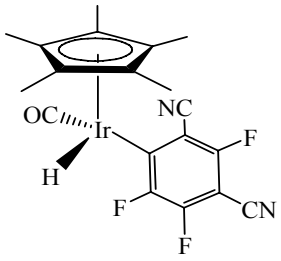

29 Cp*Ir(CO)(COOMe)[2,4-$C_6F_3(CN)_2$]

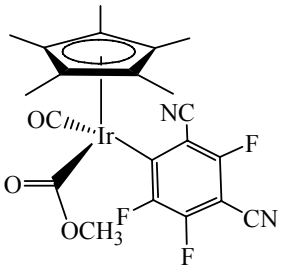

30 [Cp*Ir(CO)(PPh_3)(*p*-C_6F_4CN)][F]

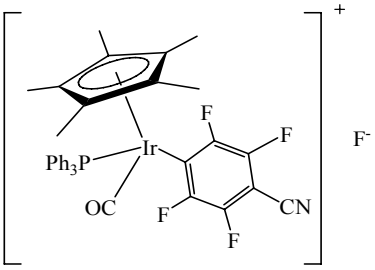

31 Cp*$(CO)_2$Ir→BF_3

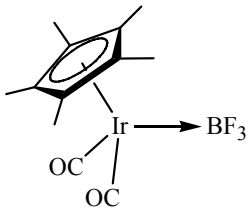

32a Cp*Ir(PPh_3)$(Cl)_2$

32b Cp*Ir(PMe_3)$(Cl)_2$

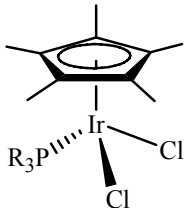

R = Ph **32a**
= Me **32b**

List of Tables

List of Figures

Abbreviations and Nomenclature

Standard abbreviations and IUPAC nomenclature are used throughout this thesis. Less common usages are as follows:

Cp^	2-[(dimethylamino)ethyl]cyclopentadienyl
Cp*^	1-[2-(N,N-dimethylamino)ethyl]-2,3,4,5-tetramethylcyclopentadienyl
Cp^{Bz}	benzylcyclopentadienyl
Tp*	hydridotris(3,5-dimethylpyrazolyl)borate
dcm	dichloromethane
hex	hexane
tol	toluene
thf	tetrahydrofuran

Infrared (IR) Spectroscopy

ν_{co}	stretching frequency in the carbonyl region (1600 – 2200 cm^{-1})
vw	very weak
w	weak
m	medium
s	strong
vs	very strong
sh	shoulder
br	broad

Nuclear Magnetic Resonance (NMR) Spectroscopy

δ	chemical shift
J	coupling constant
s	singlet
d	doublet
dd	doublet of doublet
t	triplet
q	quartet
m	multiplet
NOESY	Nuclear Overhauser Effect Spectroscopy
COSY	Correlation Spectroscopy

Mass Spectrometry (MS)

EI	Electron Impact
ESI	Electrospray Ionization
FAB	Fast Atom Bombardment
m/z	mass to charge ratio

Chapter 1: Activation of Unreactive Bonds by Homogeneous Transition Metal Catalyst

1.1 Overview

Many petrochemical processes rely on the use of heterogeneous catalysts due to their greater stability at high temperatures and their ease of separation.[1] However, there is a growing interest in the use of homogeneous catalysts, which offer the advantages of higher selectivity, greater catalytic activity, greater control of temperature on catalyst site, better control of catalyst and ligand concentrations and more facile mixing. In addition, regio-, stereo- and even enantio- selectivity can be achieved using chiral catalysts.[2]

The study of the activation of chemical bonds is important in the search for new synthetic routes to valuable products from cheap and abundant, but traditionally unreactive precursors. Many soluble transition metal complexes have been found to be able to activate chemical bonds. The activation of a bond by a metal complex is referred to as the weakening of the chemical bond upon coordination to the metal center or upon oxidative addition to the metal center. Unreactive chemicals refer to compounds which, under normal conditions, do not react with other substances or with themselves. Two major classes of such compounds are saturated hydrocarbons and molecular nitrogen. Hydrocarbons, which are readily available from oil and petroleum is the largest fraction of the world's primary energy source while dinitrogen is a major component of the earth's atmosphere. They represent inexpensive potential sources of carbon and nitrogen, respectively.

Activation of other inert bonds such as C-Cl, C-F and C-O bonds is important in the destruction of certain man-made environmental toxins such as chlorofluorocarbons (CFC) and polychlorinated biphenyls (PCB) while the activation of specific C-C bonds has great potential on specialty chemical synthesis.[3]

In this chapter, an overview on the activation of general classes of inert bonds by soluble transition metal complexes will be covered, with emphasis on the activation of C-H bonds in saturated hydrocarbons.

1.2 Activation of general classes of unreactive bonds

1.2.1 Activation of molecular dinitrogen

Catalytic dinitrogen activation is one of the most challenging fields in organometallic chemistry. The high strength of a N-N bond (226 kcal mol^{-1}) and its low basicity makes efficient catalytic transformation available only under drastic conditions. An example is the Haber process for the production of ammonia, which requires high temperature and pressure. The first metal-N_2 complex was isolated by Allen and Senoff in 1965. Since then, fully characterized Metal-N_2 complexes have been reported for almost all the d-block transition metals. However, simple coordination of N_2 to a metal center does not immediately lead to activation of the molecule as the coordinated N_2 tends to dissociate under certain reaction condition and there is a lack of well-defined reactions for the conversion of coordinated N_2 into nitrogen-containing compounds. The first example of a mild, catalytic conversion of N_2 to ammonia catalyzed by a high valent Mo complex was only reported in 1995. Mo and W-N_2 complexes were found to undergo N-H, N-C and N-Si bond formation at the coordinated N_2 to give a variety of nitrogeneous ligands and compounds [3]

1.2.2 Activation of C-Cl and C-F bonds

Simple polyhalogenated alkanes such as tetrachloromethane are reactive due to the ease of formation of the trichloromethane radical. However, other chlorocarbons may not be so easily activated. For example, the C-Cl bond strength in PCB is 96 kcal mol^{-1} for C_6H_5-Cl. Therefore, unlike bromo and iodoarenes, chloroarenes usually remain inert under S_N1 and Ullmann-type reaction conditions. Many late transition metal complexes (Ni, Pd, Co, Rh) are capable of activating C-Cl bond via nucleophilic, electrophilic and radical pathways under mild conditions.

The challenges in the activation of C-F bonds rival those of C-H activation. Activation of the C-F bond is of importance due to the environmental hazards associated with the use of fluorocarbons. Fluorocarbons are highly resistant to oxidative degradation which makes them useful for many applications. However, an important disadvantage associated

with the use of fluoroalkanes is their global-warming and ozone-depletion potential. The atmospheric lifetime of perfluorocarbons is estimated to be greater than 2000 years. The inertness of C-F bonds is a consequence of the strength of the C-F bond and the high electronegativity of fluorine. The C-F bond energy is typically 120-125 kcal mol^{-1} for sp^3 C-F bonds and the low σ-basicity of the fluorine lone pairs makes fluorocarbons very poor ligands.

Compared to their saturated counterparts, fluorinated alkenes and arenes are much more reactive due to the presence of the π-electron system, which is susceptible to nucleophilic attack and fluoride is a good leaving group.[4] For instance, perfluoroarenes can be defluorinated by $[CpFe(CO)_2]^-$ (Fp) to give a mixture of fluoroaromatics bound to Fp (Scheme 1.1).[5]

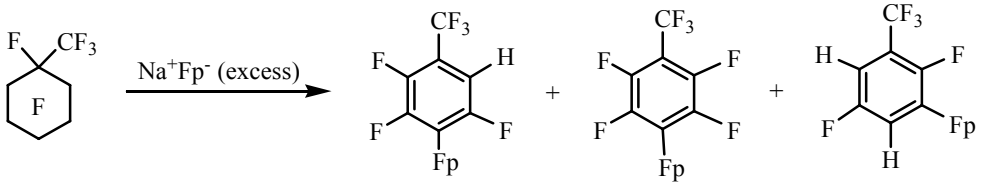

Scheme 1.1

Oxidative addition of a C-F bond across a metal center can also occur with suitably designed ligands containing fluoroarenes (Scheme 1.2).[6]

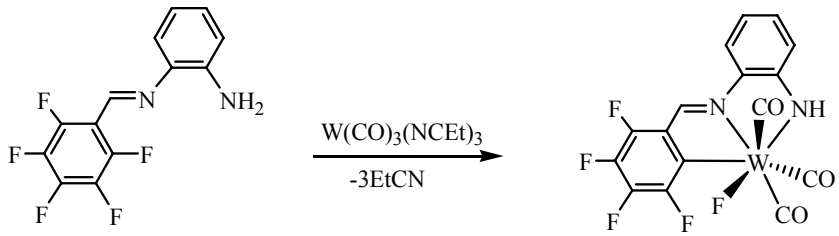

Scheme 1.2

Photoirradiation is another way to provide energy to activate a C-F bond. Jones and Perutz *et. al.* have reported the photochemical oxidative addition of the C-F bond in the hexafluorobenzene ligand in $Cp^*Rh(PMe_3)(\eta^2\text{-}C_6F_6)$ to give $Cp^*Rh(PMe_3)(C_6F_5)F$.[7]

Activation of an sp^3 C-F bond is more difficult but several examples of stoichiometric and catalytic reactions promoted by transition metal complexes are known. The hydrolysis of

CF_2 groups bound to transition metal centers is more facile because it is driven by the formation of strong H-F and C=O bonds (Scheme 1.3).[8]

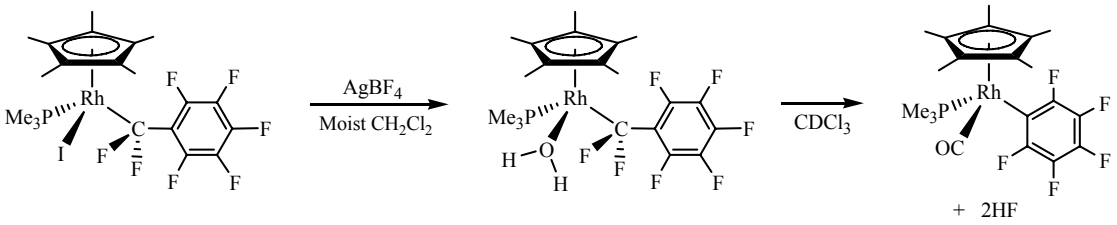

Scheme 1.3

Catalytic synthesis of perfluoronaphthalene from perfluorodecalin using Group 4 metallocenes has been reported by Crabtree, Richmond and Kiplinger *et. al.* utilizing Mg or Al as the terminal reductant (Scheme 1.4). Turnover numbers up to 12 have been achieved.

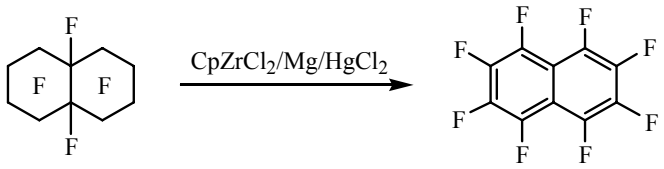

Scheme 1.4

1.2.3 Activation of C-C bonds

The lack of reactivity of the C-C single bond can be attributed to its thermodynamic stability and kinetic inertness. Oxidative addition of a C-C bond to a transition metal center provides a direct method for C-C bond cleavage. However, through this process, less stable M-C bonds (*ca* 70 kcal mol^{-1}) are formed at the expense of a more stable C-C bond (*ca* 85 kcal mol^{-1}). The σ-orbital of a C-C single bond is highly directional, constrained along the C-C bond axis. Moreover, there may be several substituents on both ends, making interaction with metal orbitals difficult, thus rendering the C-C bond quite inert. Many of the reported examples involve the activation of strained cyclic compounds (Scheme 1.5). Oxidative addition of strained three or four-membered rings across a metal center is thermodynamically driven by relief of the structural strain of the rings upon formation of the metal adducts. The biggest challenge is the insertion of a transition metal into an unstrained bond between two sp^3 carbon atoms in a selective fashion.[9]

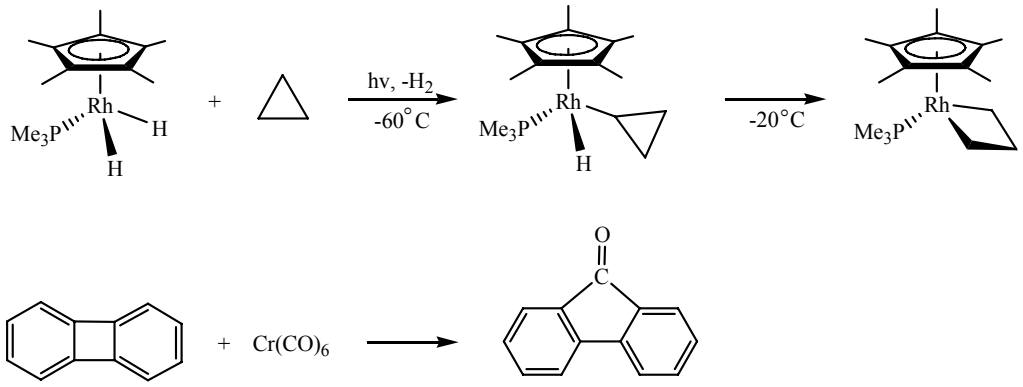

Scheme 1.5

1.2.4 Activation of C-H bonds

The plentiful supply of alkanes in oil and natural gas makes it attractive to explore their use as chemical feedstocks for the catalytic synthesis of organic molecules. However, alkanes are among the most chemically inert organic molecules known. Methane, the main constituent of natural gas is one of the most common but least reactive molecules in nature. Its C-H bond energy is 104 kcal mol^{-1}. Selective and efficient transformation of hydrocarbons into functionalized molecules such as alcohols, ketones and acids is hence of great industrial importance. The potential use of alkanes has stimulated interest in the search for metal complexes that are capable of activating C-H bonds in saturated hydrocarbons because alkanes would be a much cheaper feedstock for the organic chemical industry compared to alkenes.[10,11]

The next few sections will be devoted to the discussion on the activation of C-H bonds. In addition to the activation of inert sp^3 C-H bonds in saturated alkanes, the activation of sp^2 and sp C-H bonds in alkenes and alkynes will also be discussed briefly.

1.3 C-H bond activation by transition metal complexes

1.3.1 Intramolecular and intermolecular C-H bond activation

Intramolecular C-H activation by electron-rich metal complexes is a very common reaction in organometallic chemistry and has been known since the 1960s. It involves the cleavage of a C-H bond in the ligand linked to the metal center via an atom such as nitrogen or phosphorus. The process is named orthometallation or cyclometallation although it is not restricted to "ortho" protons.[12, 13] An example of orthometallation with H/D exchange of the hydrogen on the ligand with deuterium and another involving cyclometallation with elimination of HX are given in Scheme 1.6.[14]

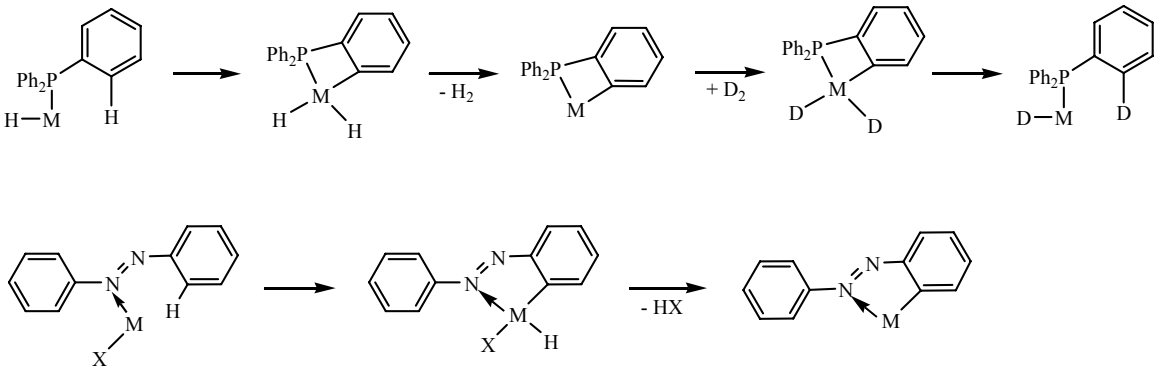

Scheme 1.6

Intermolecular C-H activation would be a more important goal owing to the possibility of selectively activating and functionalizing hydrocarbons into valuable organic products. Several late transition metal complexes capable of intermolecular C-H activation have been reported and they will be discussed in Section 1.3.4

1.3.2 Five classes of C-H activation

C-H bond activation by transition metal complexes can be grouped into five classes based on their overall stoichiometry as suggested by Labinger and Bercaw.[15]

i) Oxidative addition

Oxidative addition of C-H bonds across a metal center is typical for electron-rich, low valent complexes of a late transition metal. The reactive species is a coordinatively unsaturated intermediate generated *in situ* thermally or photochemically from a suitable

precursor. The M-H and M-hydrocarbyl bonds formed will be much more prone to functionalization than the unreactive C-H bond (equation 1).

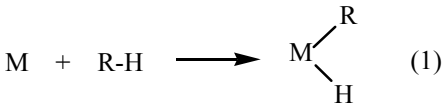

ii) Sigma-bond metathesis

This reversible reaction occurs for alkyl or hydride complexes of "early" transition metal complexes according to equation 2, where an interchange of alkyl fragments or an exchange of hydrogen and alkyl fragment occurs.

iii) Homolytic or radical activation

This involves the reversible breaking of C-H bond with the attachment of the two fragments into two separate metal centers (equation 3).

iv) 1,2 addition

This involves the addition of a C-H bond into an M=X bond where X can be a heteroatom containing ligand or an alkylidene (equation 4).[2]

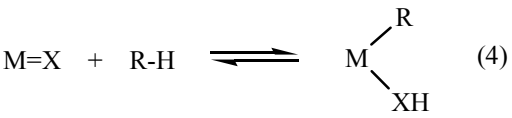

v) Electrophilic addition

This occurs usually in a strongly polar medium such as water or an anhydrous strong acid and involves the use of an electrophilic metal center to break the C-H bond. It is still not certain whether the reaction is concerted or proceeds via an oxidative addition pathway (Scheme 1.7).[2]

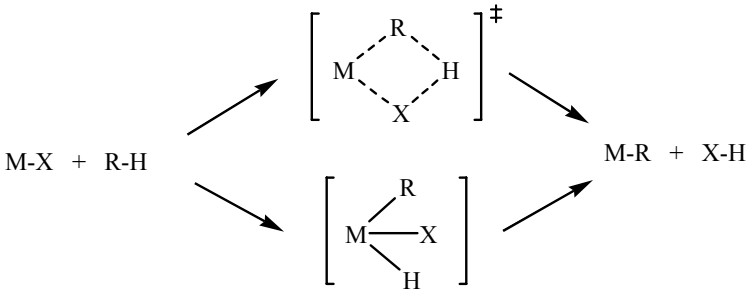

Scheme 1.7

1.3.3 Activation of different types of C-H bonds

Although sp^3 C-H bonds have the lowest bond energy compared to sp^2 and sp C-H bonds, they are the most difficult bonds to activate among the three (Table 1.1).[16] The chemical inertness of alkanes is a consequence of several factors. Alkanes have low proton affinities and acidity and they are held together by strong localized C-H and C-C bonds so that the molecules have no empty orbitals of low energy or filled orbitals of high energy that could readily participate in a chemical reaction.

Table 1.1. Properties of some hydrocarbons.

	D(R-H)[a]/ kcal mol^{-1}	I. P.[b]/ eV	E. A.[c]/ eV	P. A.[d]/ eV	pK_a
CH_4	104	12.7		5.3	40
C_2H_6	98	11.5		5.6	42
C_6H_{12} (cyclohexane)	94	9.9			45
C_6H_6	109	9.2		7.5	37
$H_2C{=}CH_2$	106	10.5	-1.1	6.9	36
$HC{\equiv}CH$	120	11.4	-1.8		25

[a] C-H bond energy; [b] ionization potential; [c] electron affinity; [d] proton affinity.

Activation of sp^2 C-H bonds is more well established due to the kinetic advantage associated with the prior π-coordination of the arene ring to the metal center; a route unavailable to alkanes.[17] Jones and Perutz reported the formation of an equilibrium mixture of $[CpRh(PMe_3)\{\eta^2\text{-}C_6H_4(CF_3)_2\}]$ and $[CpRh(PMe_3)\{C_6H_3(CF_3)_2\}(H)]$ upon irradiation of a solution of $[CpRh(PMe_3)(C_2H_4)]$ in 1,4-$C_6H_4(CF_3)_2$ (Scheme 1.8).[18]

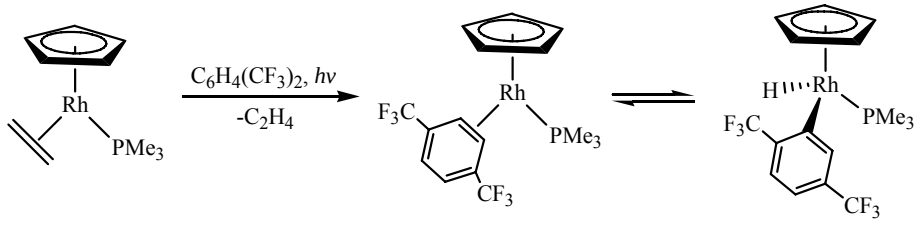

Scheme 1.8

Acetylenic C-H bonds (sp) are the strongest (120 kcal mol^{-1} for HC≡CH) compared to sp^2 and sp^3 C-H bonds. However, terminal alkynes are acidic and the end hydrogen can be removed as a proton by a strong base. Several metal complexes in low oxidation state can also activate C-H bonds in acetylenes via oxidative addition (Scheme 1.9).

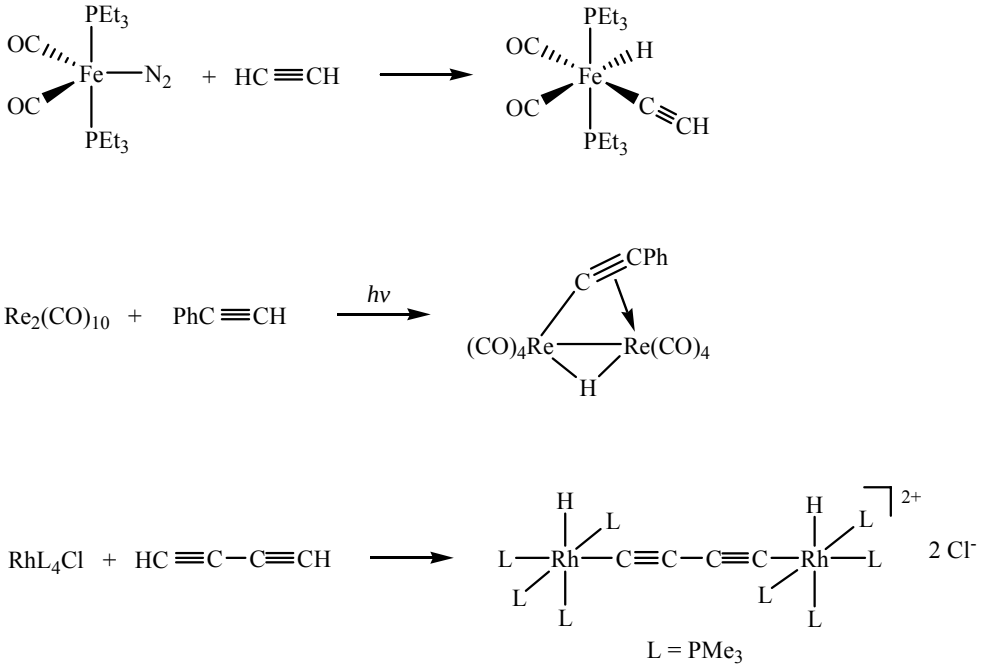

Scheme 1.9

It is possible to induce alkanes to react by exposure to highly reactive species such as superacids or free radicals or by heating at high temperatures. However, it is difficult to control the selectivity of such processes. Examples of this are seen in butane oxidation and naptha cracking. A wide spectrum of products is produced, and a tremendous amount of energy is expended to separate the products to produce fundamental chemical feedstocks.[19] A

variety of enzymes can efficiently and selectivity catalyze alkane oxidation at physiological temperatures and pressures, but they are mainly applicable to small-scale production of specialized chemicals. The lack of selectivity under classical conditions prompted the search for homogeneous transition metal complexes that are able to catalyze C-H activation under mild and neutral conditions.[20]

1.3.4 Photochemical sp^3 C-H activation by cyclopentadienyl iridium and rhodium complexes

UV initiated photo-dissociation of CO or H_2 from group 9 organometallic compounds of the type Cp*MLL' (where M = Ir, Rh; L = CO, PMe_3; L' = CO, H_2) have been known to generate 16-electron Cp*ML fragments that are capable of activating the otherwise inert C-H bonds in hydrocarbon solvents and methane to form hydridoalkyl species Cp*ML(R)(H) (Scheme 1.10).[21]

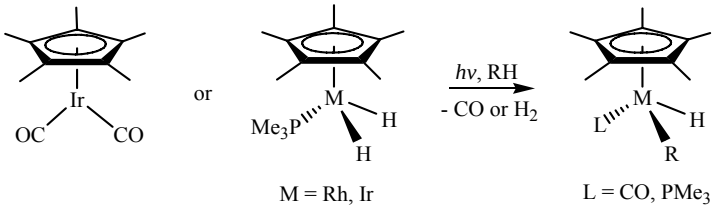

Scheme 1.10

While the hydridoalkyl iridium complexes Cp*Ir(PMe_3)(R)(H) is stable up to *ca* 110 ºC, the rhodium analogues are quite unstable, undergoing reductive elimination of alkanes at -20 ºC. The corresponding phenyl derivatives of these complexes are more stable. Cp*Rh(PMe_3)(Ph)(H) loses benzene only at 60 ºC while Cp*Ir(PMe_3)(Ph)(H) is stable even at 200 ºC.

The rhodium and iridium complexes Cp*M(PMe_3)$(H)_2$ show selectivity in the activation of C-H bonds in different molecules (intermolecular selectivity) and for different types of C-H bonds in the same molecule (intramolecular selectivity), as demonstrated in competition studies with various hydrocarbon substrates (Table 1.2).

Table 1.2. Relative kinetic selectivities for activation of different types of C-H bonds by various metal fragments on per hydrogen basis.

Product distributions reflect the relative reactivity of one C-H bond in each hydrocarbon.

									
k_{rel}[Cp*Ir]	1.0	2.63	1.6	-	0.09	4.0		2.7(1º)[a]; 1.0(2º)[a]	1.5(1º)[a]; 1.0(2º)[a]
k_{rel}[Cp*Rh]	1.0	10.4	1.8	0.14	0.06	19.5	15(1º); 0(2º)	5.9(1º); 0(2º)	2.6(1º); 0(2º)
k_{rel}[Tp*Rh]	1.0	18.4	1.7	-	-	70	14.9(1º); 0(2º)	-	15(1º); 0(2º)

[Cp*Ir] = Cp*Ir(PMe_3); [Cp*Rh] = Cp*Rh(PMe_3); [Tp*Rh] = Tp*Rh(CNR), where R is neopentyl).
[a]Relative intramolecular selectivity only; values not relative to cyclohexane.

The rate of attack of the metal center on a particular C-H bond seems to depend on steric effects and C-H acidities rather than bond energies. For all three complexes, activation of benzene is preferred over alkanes, smaller cycloalkanes are preferred over larger cycloalkanes and normal alkanes are preferred over cycloalkanes. In the normal alkanes, activation of a primary C-H bond is preferred over secondary C-H bonds. The selectivity demonstrated by the complexes is as follows: Tp*Rh > Cp*Rh > Cp*Ir. This is particularly apparent for the activation of C-H bonds in the same molecule. With acyclic alkanes, the rhodium complex inserts only into primary C-H bonds while both terminal and internal C-H activation was observed with the iridum complex.[2,10,21c]

The activation of sp^3 C-H bonds of alkanes using Cp*Ir(PMe_3)$(H)_2$ has been extended to functionalized organic molecules (Scheme 1.11). Under photochemical activation, alcohols or amine showed C-H activation instead of X-H activation. With methanol and ethanol, products from subsequent transformation of the initially formed species were obtained.

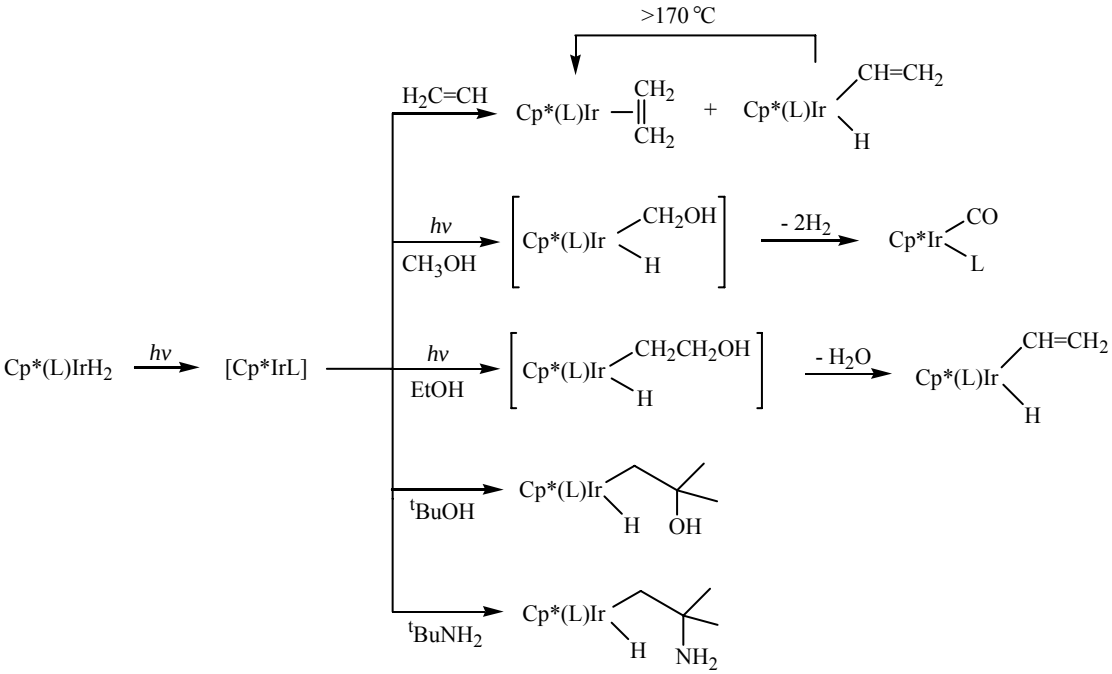

Scheme 1.11

Due to the high reactivity of the intermediates generated by photoirradiation, the substrate often serves as the solvent medium for reaction. However, liquefied noble gases and supercritical fluids were found to be inert solvent for carrying out photochemical C-H activation. Liquefied noble gases such as krypton and xenon are useful for carrying out C-H activation of gaseous substrates and solids. Activation of methanol and ethanol in liquid xenon gave O-H activation instead of C-H activation observed in alcoholic media (Scheme 1.12).[10]

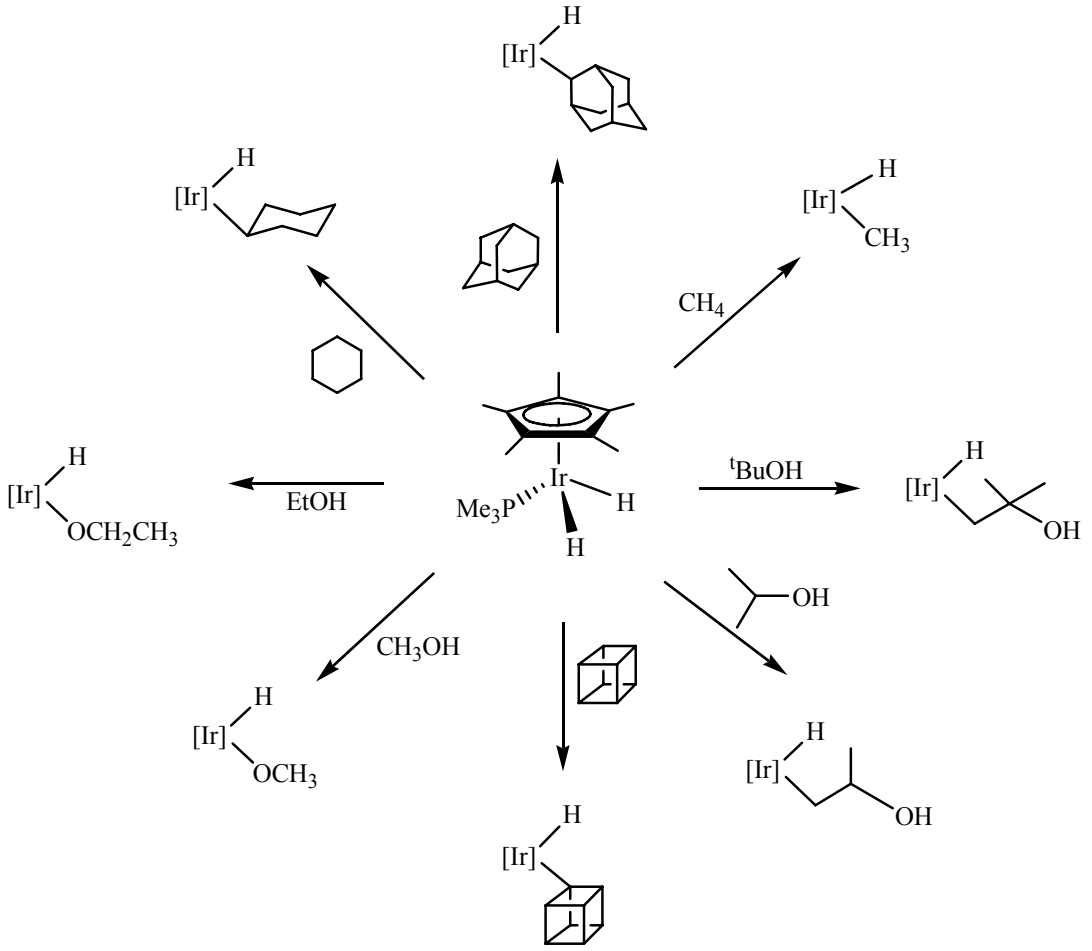

Scheme 1.12

Supercritical carbon dioxide has been used for C-H activation studies at ambient temperatures due to its chemical inertness towards unsaturated metal centers and good miscibility with metal complexes such as $Cp^*Ir(CO)_2$ and gases such as H_2.[22] C-H activation has also been carried out in supercritical ethane, where the fluid is both the reactant and the solvent for the photochemical activation of C_2H_6 by $Cp^*Ir(CO)_2$.[23]

1.3.5 Mechanism of C-H activation

Studies on the mechanism, kinetics, and thermodynamics of the activation process in solution, gas phase, low temperature matrices and liquid noble gases have been carried out by various research groups.[24] For $Cp^XM(CO)_2$ (Cp^X = Cp or Cp*; M = Ir or Rh), spectroscopic measurements have shown that the primary photoproduct is a coordinatively-unsaturated 16-electron species $[Cp^XM(CO)]$ obtained via dissociation of a CO ligand. This species is

extremely reactive and forms a solvent adduct complex [$Cp^XM(CO)\cdots S$] before undergoing C-H activation to give $Cp^XM(CO)(R)(H)$. [24b,25]

The activation of C-H bond was initially believed to occur via a three-centered transition state (Figure 1.1). However, the discovery of stable η^2-dihydrogen adducts suggest that an analogous species formed by interaction of a C-H sigma bond with a metal center might be an intermediate for the reaction before oxidative cleavage of the C-H bond to form the metal alkyl hydride occurs (equation 5).[2,26] Stable agostic complexes with a C-H bond coordinated to a metal center are known. The proton on the coordinated C-H bond is much more acidic than in the uncoordinated state.[15,27] George *et. al*. have directly observed $CpRe(CO)_2$(n-heptane) sigma-alkane complex by time-resolved infrared spectroscopy at room temperature. Bergman and Harris have also reported ultrafast studies on C-H activation of hydrocarbons by $Tp^*Rh(CO)_2$ (Tp^* = hydrotris(3,5-dimethylpyrazolyl)borate) using femtosecond transient absorption spectroscopy in which two carbonyl stretching vibrations were assigned to the alkane sigma species η^3-$Tp^*Rh(CO)(\sigma$-$C_6H_{12})$ and η^2-$Tp^*Rh(CO)(\sigma$-$C_6H_{12})$.[28] The primary photoprocess also involves the dissociation of one CO ligand. Formation of the solvated species followed by de-chelation and C-H activation of the alkane then occurs to give the final product (Scheme 1.13).

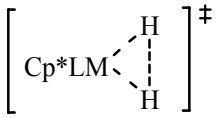

Figure 1.1. 3-centered transition state in the activation of C-H bond.

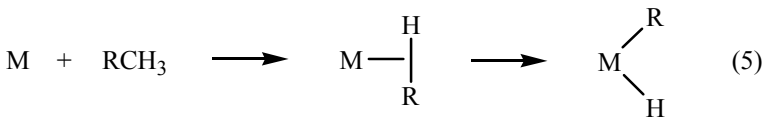

(5)

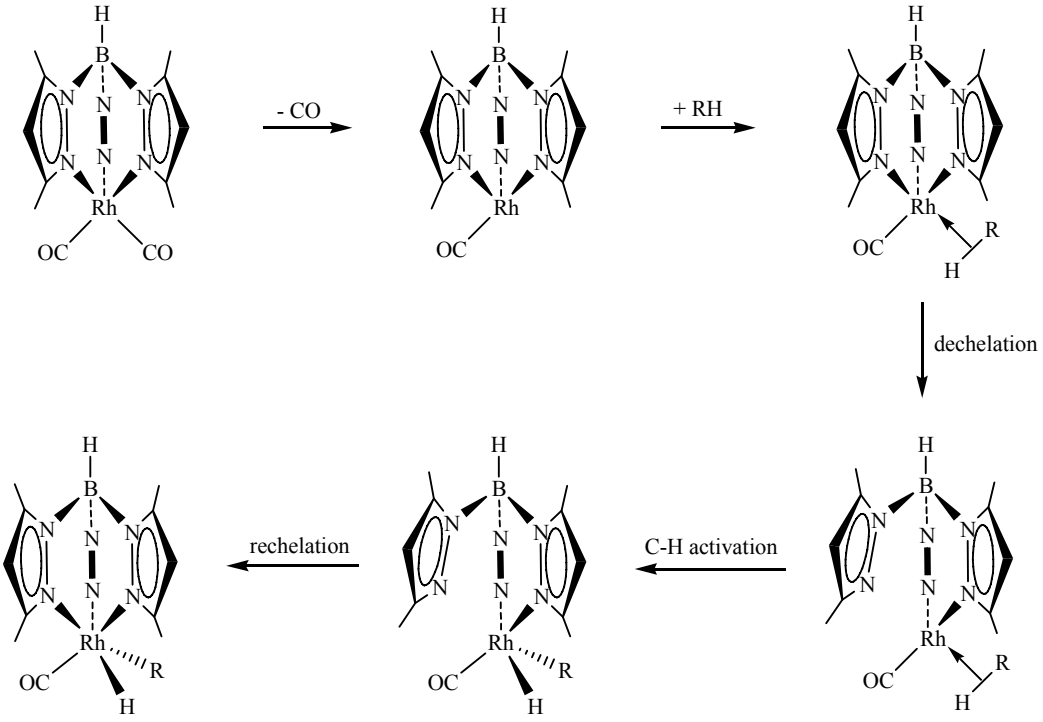

Scheme 1.13

1.4 Functionalization of C-H bonds

Insertion of small molecules into the M-C bond of activated hydrocarbons allow functionalization of hydrocarbons into new organic products. Many metal complexes that activate C-H bonds are, however, coordinatively saturated and the lack of ligand lability prevents potentially reactive molecules in solution from coordinating to the metal center. As a result, generally, only strong electrophiles are reactive with the oxidative addition adducts of hydrocarbons with low valent metals.[29]

Although $Cp^*(PMe_3)Ir(R)(H)$ are some of the most thermally stable hydridoalkyl species known, they are coordinatively saturated and their reluctance to open up a new coordination site at the metal centre makes it difficult for coordination of an additional unsaturated ligand such as CO, alkyne or alkene without dissociation of the alkane. Replacement of the hydrogen with a better anionic leaving group such as the weakly coordinating OTf group would allow a coordination site to be generated more readily. Thus $Cp^*(PMe_3)IrMe(OTf)$ and $[Cp^*(PMe_3)IrMe(CH_2Cl_2)][BAr_f]$ were found to cleave the C-H bonds of a variety of organic molecules selectively (Schemes 1.14 and 1.15).[30]

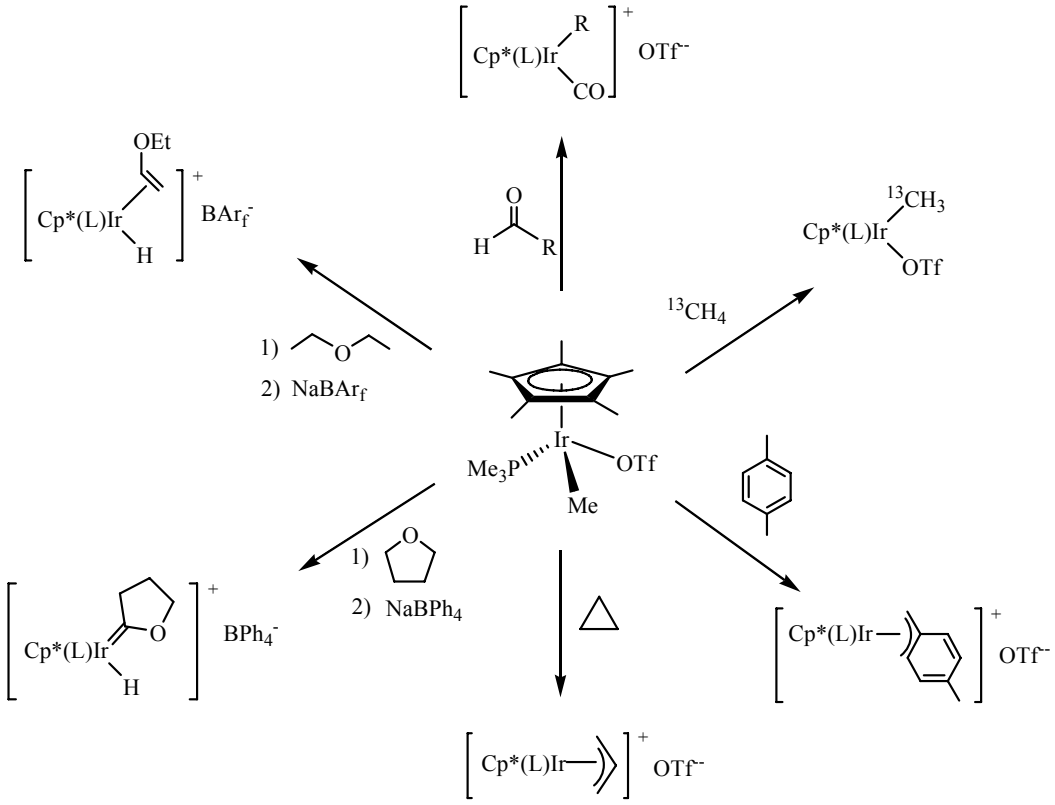

L = PMe_3; OTf = OSO_2CF_3; BAr_f = B[3,5-$(CF_3)_2C_6H_3]_4$

Scheme 1.14

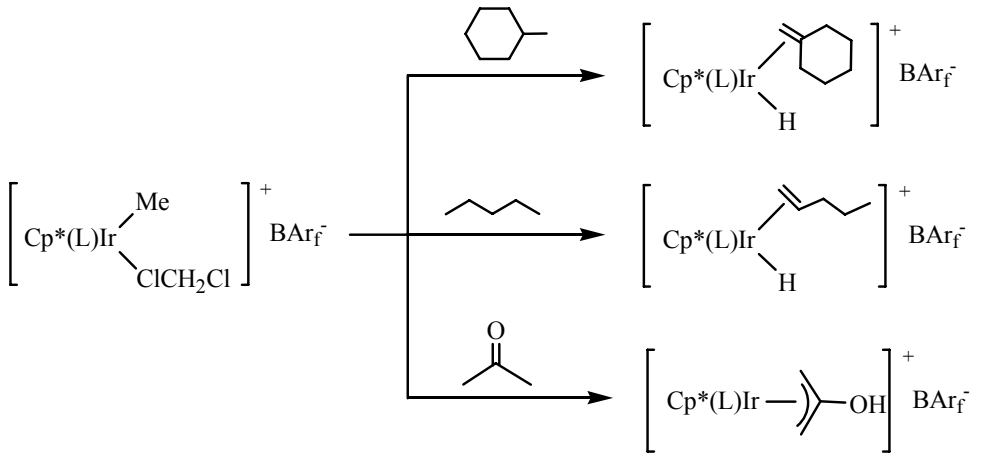

Scheme 1.15

For commercially valuable products to be produced, the functionalized organic molecule must be eliminated from the metal complex easily. There are several factors that favor such reactions:

i) A thermodynamically favorable overall reaction. The reaction can be driven by removal of product(s), or by an external source of energy, such as light.

ii) A low valent metal center.

iii) Presence of good electron-donating ligands such as hydride, phosphine or cyclopentadienyl.

iv) Vacant coordination site on the molecule.

v) The functionalizing group does not bind so strongly as to represent a thermodynamic sink for the catalytic cycle.[31]

Some examples of the insertion of molecules such as CNR, CO and olefins into activated C-H bonds are given in Scheme 1.16, two of which are photochemically driven.[29,32,33,34]

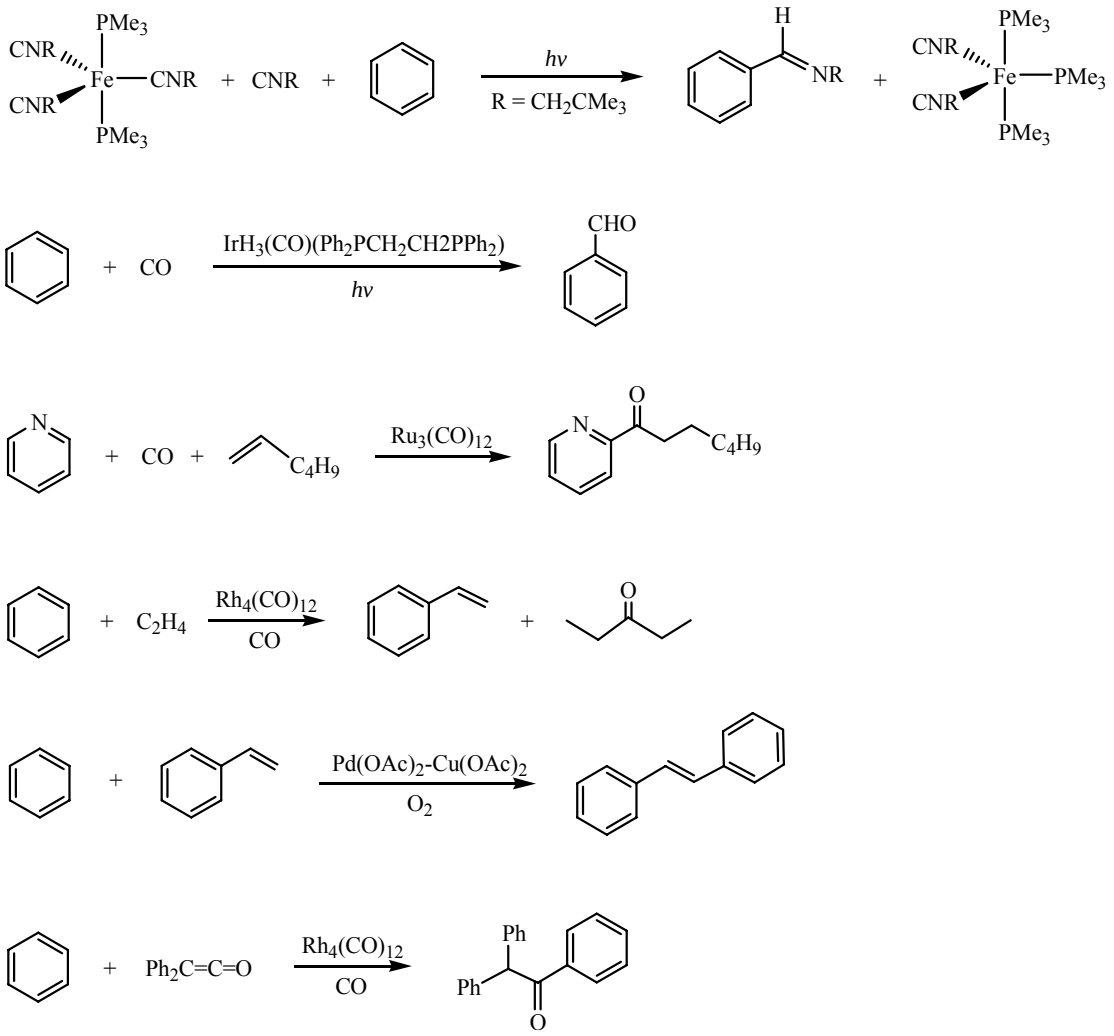

Scheme 1.16

Although there have been several reports on the transition metal catalyzed functionalization of C-H bonds, many of them deal with sp^2 C-H bonds on aromatic rings. Bergman has reported the stoichiometric functionalization of sp^3 C-H bond activated by $Cp^*M(PMe_3)(H)_2$ (M = Rh, Ir). Treatment of the hydrioalkyl complex with bromoform produces an alkyl bromide complex from which the corresponding alkyl bromide can be obtained in high yield by treatment with Br_2 (for rhodium) or mercuric chloride followed by Br_2 (for iridium) (Scheme 1.17).[35]

Such photochemically assisted conversion of alkane to alkyl halide offers an advantage over free-radical halogenation of alkane due to their improved selectivity for terminal C-H bond functionalization.

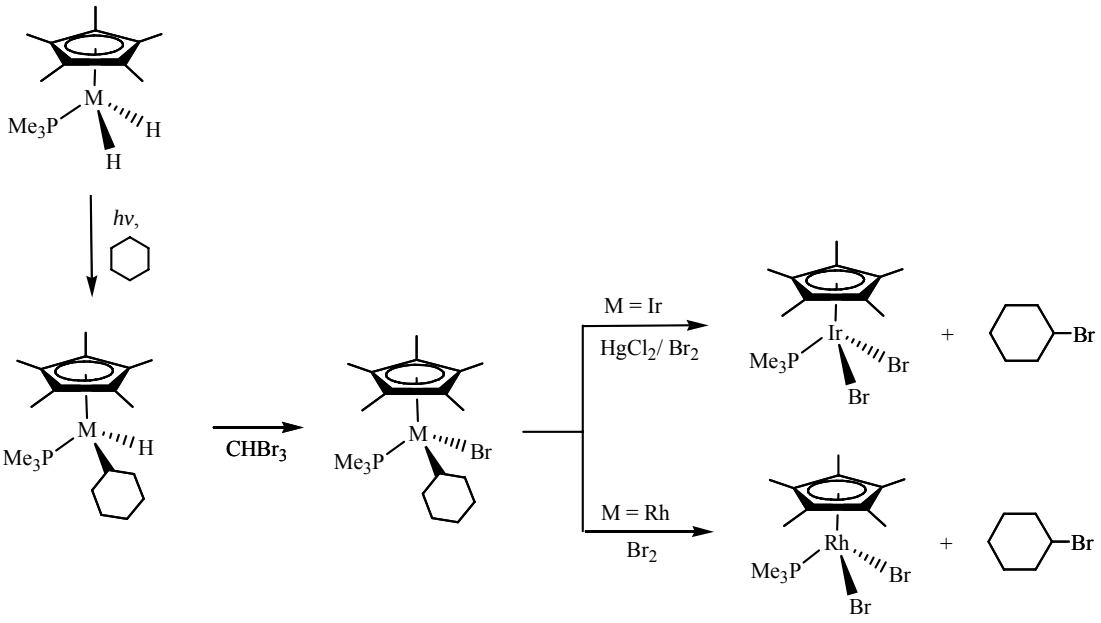

Scheme 1.17

Some of the best examples of catalytic alkane functionalization were reported by Tanaka *et. al.* who discovered that $RhCl(CO)(PMe_3)_2$ can catalyze the functionalization of hydrocarbons (insertion of small molecules and dehydrogenation), including alkanes under mild conditions using photoirradiation (Scheme 1.18).[32,36] A turnover number of 930 (in 68 h) in cyclooctane dehydrogenation has been achieved under nitrogen purge.

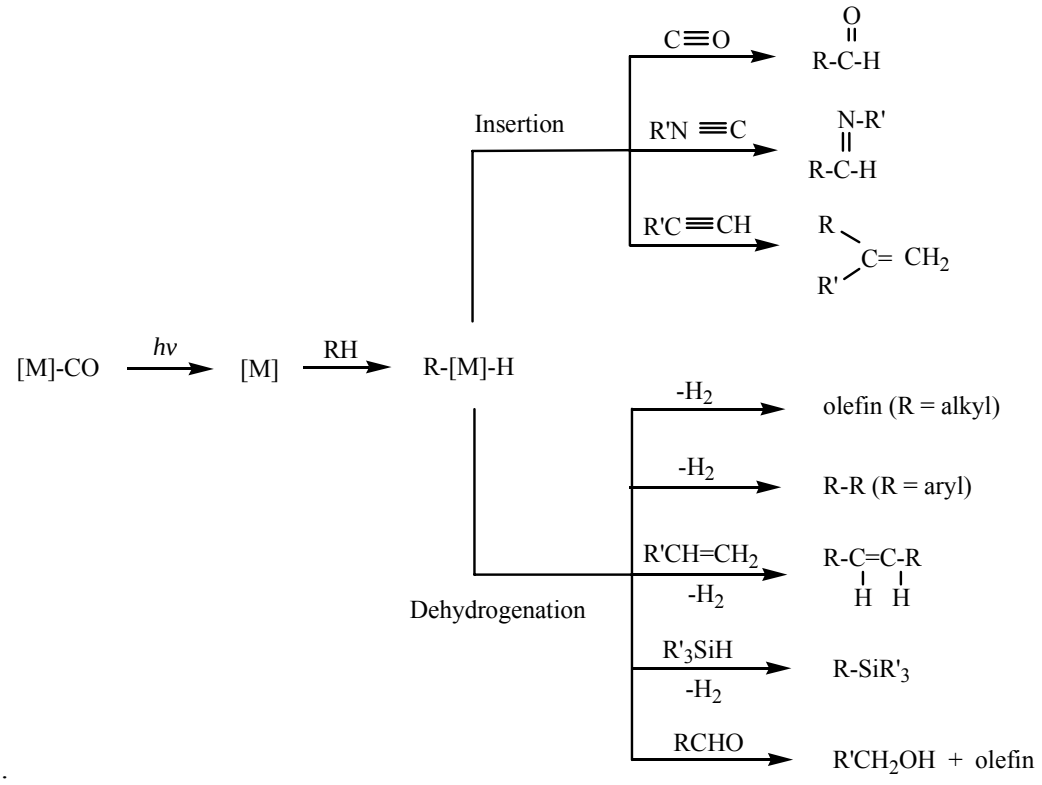

Scheme 1.18

1.5 Chiral C-H bond activation

C-H activation of alkanes by a metal complex to form diastereomers has been reported by Bergman *et. al.* Photolysis of $Cp^*Ir(PMe_3)(H)_2$ in dimethylcyclopropane resulted in the formation of a pair of diastereomeric cyclopropyl-activated complexes **A1**, **A2** and a methyl-activated complex **B** (Scheme 1.19). Complex **B** can be converted to a 1:1 mixture of the thermodynamically favored complexes **A1** and **A2** by thermolysis at 140 ºC.[37]

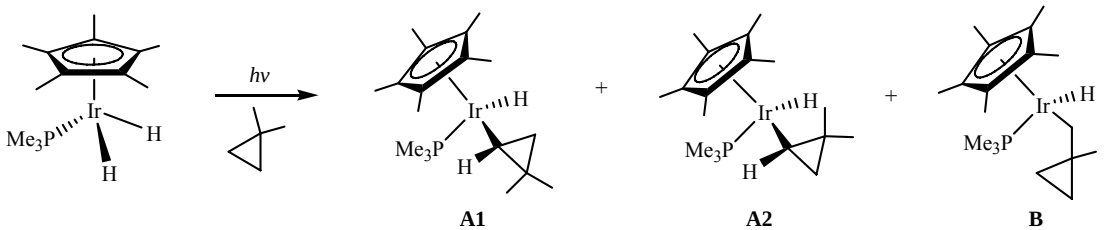

Scheme 1.19

Enantioselective C-H activation has also been achieved through the use of a tethered iridium-phosphine complex. The planar chiral iridium complex **C** was able to activate the C-H bond of cyclohexane with high diastereoselectivity to afford a single diastereomer **D** and of benzene to give a 1:1 mixture of the two diastereomers **E1** and **E2** (Scheme 1.20).

Thermolysis of **D** in benzene at 150 ºC results in the formation of both diastereomers **E1** and **E2**.[2,38]

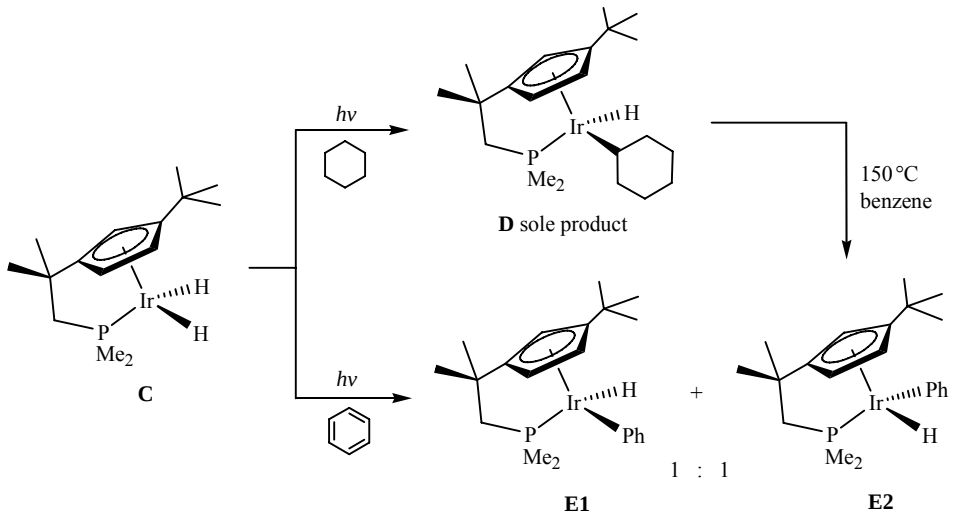

Scheme 1.20

Rhodium and iridium complexes with quinolyl-functionalized Cp ligands are known. Such ligands have a predefined geometry so that the nitrogen donor atom is in a suitable position for coordination to the metal center. Since nitrogen donors typically do not bind strongly to electron-rich metals in low oxidation states; only hemilabile bonding is expected. However, due to the close proximity of the donor to the metal center, stabilization of the low-coordinate species will always be possible. This prevents decomposition of the active species, which is necessary in catalytic transformations. The quinolyl-Cp rhodium complex **G1** has been synthesized by the reaction of **F** with $[(C_2H_4)_2RhCl]_2$. Chelation of the nitrogen donor on the quinolyl side arm to the rhodium metal center in **G1** can be achieved photochemically via loss of an ethene molecule. This coordination is reversible; **G2** converts back to **G1** slowly in the dark with the liberated ethene (Scheme 1.21).

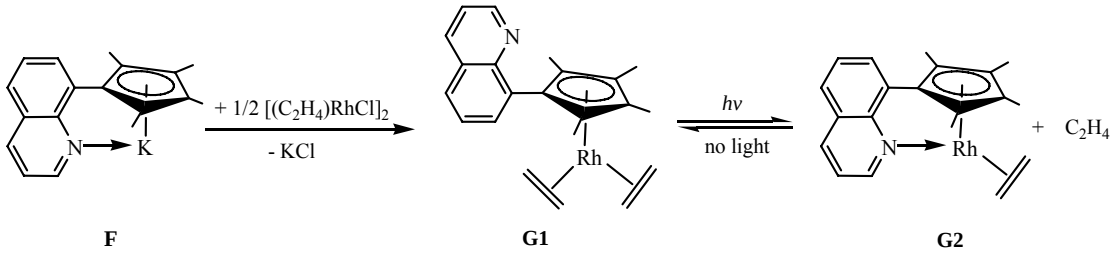

Scheme 1.21

Photolysis of **G1** in C_6D_6 under vacuum or argon leads to H/D exchange between C_6D_6 and a coordinated ethene ligand. The proposed mechanism of the H/D exchange is shown in Scheme 1.22. Photodissociation of an ethene ligand leads to the formation of **G2** stabilized by an intramolecular coordination of the quinolyl nitrogen atom. The weak Rh-N bond allows the oxidative addition of the C-D bond of the solvent to the Rh center to form **H1** followed by the insertion of the olefin ligand into the Rh-D bond. Reductive elimination of a hydrogen atom from the ethyl group on **I** followed by the reductive elimination of a molecule of benzene from **H1'** regenerates **G1**. The cycle is repeated to effect complete deuterium incorporation into the ethene molecules.[39]

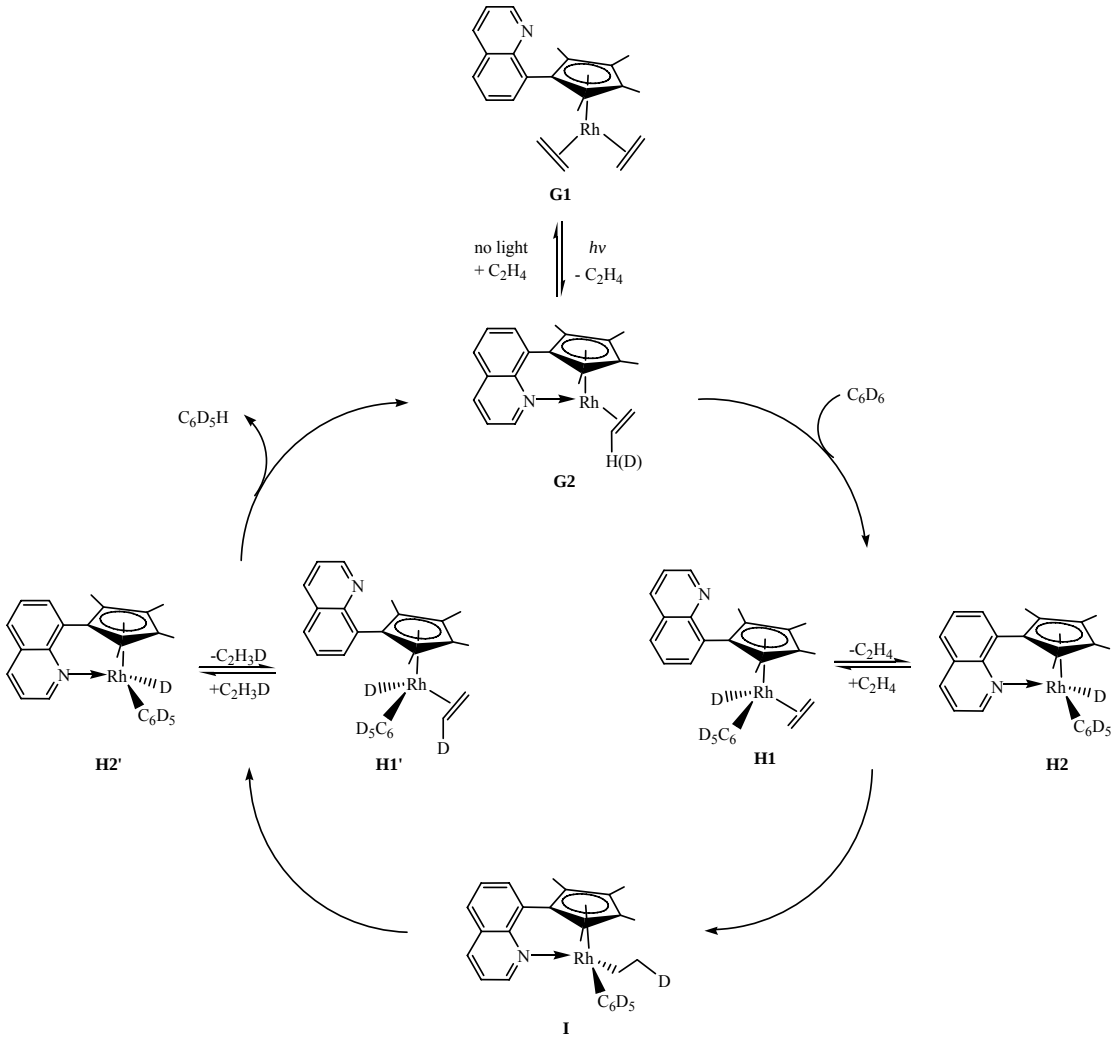

Scheme 1.22

A variety of other functionalised cyclopentadienyl ligands containing donor groups on the side-chain are known.[40] These bidentate ligands can give rise to chelate complexes

where both the cyclopentadienyl ring and the donor group on the side-chain are interacting with the metal center (Figure 1.2).[41]

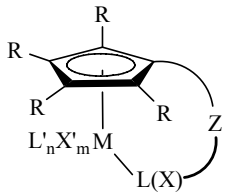

Carbon: X = CH_2, CO(acyl); L = $CH{=}CH_2$, C_6H_5
Nitrogen: X = NR', N; L = NR'_2, NC_5H_3(pyridyl)
Phosphorus: X = PR'; L = PR'_2
Oxygen: X = O; L = OR'
Sulphur: L = SR'

Figure 1.2. Chelate metal complexes with side-arm functionalized cyclopentadienyl ligands.

Reversible coordination of the donor group on the side chain to the metal center can be achieved where there is a combination of a "hard" donor group (nitrogen) and a "soft" metal center (group 9 transition metal) (Scheme 1.23). This otherwise unfavored "hard-soft" combination is stabilized to a certain extent by the chelate effect leading to a hemilable behaviour where the donor group can coordinate to the metal center or act as a spectator ligand.[40a]

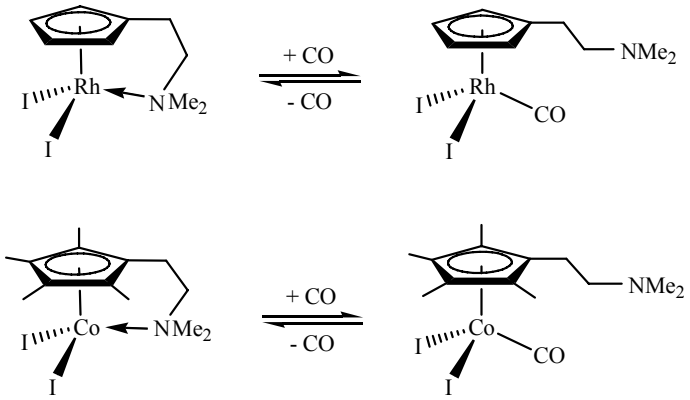

Scheme 1.23

1.6 Aim and objectives of this project

The activation of sp^3 C-H bonds remains an important goal in synthetic chemistry. While the activation of alkanes by cyclopentadienyl complexes of group 9 transition metal complexes have been reported by several groups, these complexes are coordinatively saturated and photoirradiation is required for ligand dissociation to generate a reactive species. The lack of ligand lability also hinders functionalization of the activated hydrocarbon by preventing coordination of an additional reactant to the metal center.

Transition metal complexes containing a cyclopentadienyl ligand with a donor group tethered via a side-chain which can coordinate reversibly may therefore be useful. Complexes such as Cp^Rh(I)$_2$(CO) and Cp*^Co(I)$_2$(CO), where the metals are in the +III oxidation state, are able to form tethered complexes but intramolecular coordination of the amino group to the metal center is not known for compounds of the type Cp*^ML$_2$ (M = Co, Rh, Ir; L = CO or C_2H_4) where the metal is in the +I oxidation state. The photochemical reaction of Cp*^Ir(CO)$_2$ in cyclohexane therefore became of interest. Photodissociation of one of the CO ligand was known to occur with the Cp* analogue. It was hoped that with the amine analogue, intramolecular coordination of the nitrogen donor to the iridium center would occur following dissociation of CO to produce a tethered iridium complex which would be capable of C-H activation, and of H/D exchange like that observed in the tethered quinolyl-functionalized Cp-Rh system described in Scheme 1.22.

Infrared spectroscopy offers the advantages of speed and high sensitivity, which is useful for the monitoring of reactions using low concentration of metal complexes as catalyst. However, the spectra would usually consist of overlapping peaks from different species present in the reaction, in contrast to NMR spectra in which the resonances are more dispersed.[42] In situ IR monitoring offers advantages over the traditional method of withdrawing aliquots from the reaction mixture, which would usually require cooling and depressurization. These can result in an inaccurate representation of the species present in the reaction mixture, as the species may exist as different forms under different operating conditions. An algorithm that has been proven useful in the deconvolution of complex spectra

in such cases is the band-target entropy minimization (BTEM) algorithm, which allows for the recovery of pure component spectra from the experimental spectra.[43]

Hence in this project, we aim to explore the feasibility of employing an iridium complex containing an aminoethyl-functionalized cyclopentadienyl ligand for C-H activation. The specific objectives are:

1) To study the photochemical reaction of such a complex in hydrocarbon solvents.
2) Detect any intermediates in the photochemical reaction with the help of BTEM deconvolution.
3) Functionalize cycloalkanes by carrying out the photolysis under a CO atmosphere to see if carbonylation of cycloalkanes can occur.

References

[1] Dickson, R. S. In *Homogeneous Catalysis with Compounds of Rhodium and Iridium*; Catalysis by Metal Complexes; Kluwer Academic Publishers: U. S. A., 1985; Chapter 1; pp1-7.

[2] Jones, W. D. In *Activation of Unreactive Bonds and Organic Synthesis*; Murai, S. Eds.; Topics in Organometallic Chemistry 3; Springer: New York; 1999, pp9-46.

[3] Gossage, R. A.; Koten, G. In *Activation of Unreactive Bonds and Organic Synthesis*; Murai, S. Eds.; Topics in Organometallic Chemistry 3; Springer: New York, 1999; pp1-8.

[4] (a) Kiplinger, J. L.; Richmond, T. G.; Osterberg, C. E. *Chem. Rev.* **1994**, *94*, 373-431. (b) Burdeniuc, J.; Jedlicka, B.; Crabtree, R. H. *Chem. Ber.* **1997**, *130*, 145-154.

[5] Richmond, T. G. In *Activation of Unreactive Bonds and Organic Synthesis*; Murai, S. Eds.; Topics in Organometallic Chemistry 3; Springer: New York, 1999; pp243-269.

[6] Richmond, T. G.; Osterberg, C. E.; Arif, A. M. *J. Am. Chem. Soc.* **1987**, *109*, 8091-8092.

[7] Belt, S. T.; Helliwell, M.; Jones, W. D.; Partridge, M. G.; Perutz, R. N. *J. Am. Chem. Soc.* **1993**, *115*, 1429-1440.

[8] Hughes, R. P.; Lindner, D. C. *J. Am. Chem. Soc.* **1997**, *119*, 11544-11545.

[9] Murakami, M.; Ito, Y. In *Activation of Unreactive Bonds and Organic Synthesis*; Murai, S. Eds.; Topics in Organometallic Chemistry 3; Springer: New York, 1999; pp97-129.

[10] Bergman, R. G. In *Homogeneous Transition Metal Catalyzed Reactions*; W. R. Moser, D. W. Slocum, Eds.; Advances in Chemistry Series 230; American Chemical Society: Washington, DC, 1992; Chapter 14; pp211-220.

[11] Dickson, R. S. In *Homogeneous Catalysis with Compounds of Rhodium and Iridium*; Catalysis by Metal Complexes; Kluwer Academic Publishers: U. S. A. 1985; Chapter 2; pp8-39.

[12] Shilov, A. E.; Shul'pin, G. B. In *Activation and Catalytic Reactions of Saturated Hydrocarbons in the Presence of Metal Complexes*; Catalysis by Metal Complexes Volume 21; Kluwer Academic Publishers: The Netherlands, 2000; Chapter 4; pp 127-189.

[13] Piet, W. N. M. van Leeuwen In *Homogeneous Catalysis Understanding the Art;* Kluwer Academic Publishers: The Netherlands, 2004; Chapter 2; pp29-62.

[14] Piet, W. N. M. van Leeuwen In *Homogeneous Catalysis Understanding the Art*; Kluwer Academic Publishers: The Netherlands, 2004; Chapter 19; pp387-401.

[15] Labinger, J. A.; Bercaw, J. E. *Nature* **2002**, *417*, 507-514.

[16] Shilov, A. E.; Shul'pin, G. B. In *Activation and Catalytic Reactions of Saturated Hydrocarbons in the Presence of Metal Complexes*; Catalysis by Metal Complexes Volume 21; Kluwer Academic Publishers: The Netherlands, 2000; Chapter 1; pp 8-20.

[17] (a) Jones, W. D.; Feher, F. J. *Acc. Chem. Res.* **1989**, *22*, 91-100. (b) Jones, W.D.; Feher, F. J. *J. Am. Chem. Soc.* **1984**, *106*, 1650-1663.

[18] Belt, S. T.; Dong, L.; Duckett, S. B.; Jones, W. D.; Partridge, M. G.; Perutz, R. N. *J. Chem. Soc. Chem. Commun*. **1991**, 266-269.

[19] Tanaka, M. *Chemtech* **1989**, 59-64.

[20] Dyker, G. *Angew. Chem. Int. Ed.* **1999**, *38*, 1698-1712.

[21] (a) Janowicz, A. H.; Bergman, R. G. *J. Am. Chem. Soc.* **1982**, *104*, 352-354. (b) Hoyano, J. K.; Graham, W. A. G. *J. Am. Chem. Soc.* **1982**, *104*, 3723-3725. (c) Janowicz, A. H.; Periana,

R. A.; Buchanan, J. M.; Kovac, C. A.; Stryker, J. M.; Wax, M. J.; Bergman, R. G. *Pure & Applied Chem*. **1984**, *56*, 13-23. (d) Belt, S. T.; Grevels, F. W.; Klotzbucher, W. E.; McCamley, A.; Perutz, R. N. *J. Am. Chem. Soc.* **1989**, *111*, 8373-8382.

[22] Jobling, M.; Howdle, S. M.; Healy, M. A. Poliakoff, M. *J. Chem. Soc., Chem. Commun* **1990**, 1287-1290.

[23] Banister, J. A.; Cooper, A. I.; Howdle, S. M.; Jobling, M.; Poliakoff, M. *Organometallics* **1996**, *15*, 1804-1812.

[24] (a) Buchanan, J. M.; Stryker, J. M.; Bergman, R. G. *J. Am. Chem. Soc.* **1986**, *108*, 1537-1550. (b) Bromberg, S. E.; Lian, T.; Bergman, R. G.; Harris, C. B. *J. Am. Chem. Soc.* **1996**, *118*, 2069-2072. (c) Dunwoody, N.; Sun, S.; Lees, A. J. *Inorg. Chem*. **2000**, *39*, 4442-4451. (d) Bengali, A. A.; Schultz, R. H.; Moore, C. B.; Bergman, R. G. *J. Am. Chem. Soc.* **1994**, *116*, 9585-9589.

[25] Lees, A. J. *J. Organ*omet. Chem. **1998**, *554*, 1-11.

[26] Vetter, A. J.; Flaschenriem, C.; Jones, W. D. *J. Am. Chem. Soc.* **2005**, *127*, 12315-12322.

[27] Crabtree, R. H. In *Selective Hydrocarbon Activation: Principles and Progress;* Davies, J. A.; Watson, P. L.; Liebman, J. F.; Greenberg, A. Eds.; VCH Publishers: New York, 1990, Chapter 1; pp1-17.

[28] Harris, C. B. *Science* **1997**, *278*, 260-263.

[29] Jones, W. D.; Chandler, V. L.; Feher, F. J. *Organometallics* **1990**, *9*, 164-174.

[30] Klei, S. R.; Golden, J. T.; Burger, P.; Bergman, R. G. *J. Mol. Catal. A:Chem.* **2002**, *189*, 79-94.

[31] Jones, W. D. In *Selective Hydrocarbon Activation: Principles and Progress;* Davies, J. A.; Watson, P. L.; Liebman, J. F.; Greenberg, A. Eds.; VCH Publishers: New York, 1990, Chapter 5; pp113-148.

[32] Tanaka, M.; Sakukara, T. In *Homogeneous Transition Metal Catalyzed Reactions*; W. R. Moser, D. W. Slocum, Eds.; Advances in Chemistry Series 230; American Chemical Society: Washington, DC, 1992; Chapter 12; pp181-196.

[33] Lail, M.; Arrowood, B. N.; Gunnoe, T. B. *J. Am. Chem. Soc.* **2003**, *125*, 7506-7507.

[34] Kakiuchi, F.; Murai, S. *Acc. Chem. Res*, **2002**, *35*, 826-834.

[35] Periana, R. A.; Bergman, R. G. Organometallics **1984**, *3*, 508-510.

[36] (a) Tokunaga, Y.; Sakakura, T.; Tanaka, M. J. Mol. Catal. **1989**, *56*, 305-314. (b) Sakakura, T.; Sodeyama, T.; Sasaki, K.; Wada, K.; Tanaka, M. *J. Am. Chem. Soc.* **1990**, *112,* 7221-7229. (c) Tanaka, M.; Sakakura, T. *Pure Appl. Chem.* **1990**, *62*, 1147-1150. (d) Sakakura, T.; Abe, F.; Tanaka, M. *Chem. Lett.* **1991**, 359-362.

[37] Mobley, T. A.; Schade, C.; Bergman, R. G. *Organometallics* **1998**, *17*, 3574-3587.

[38] Mobley, T. A.; Bergman, R. G. *J. Am. Chem. Soc.* **1998**, *120*, 3253-3254.

[39] Kohl. G.; Rudolph, R. Pritzkow, H.; Enders, M. *Organometallics* **2005**, *24*, 4774-4781.

[40] (a) Muller, C.; Vos, D.; Jutzi, P. *J. Organomet. Chem.* **2000**, *600*, 127-143. (b) Blais, M. S.; Chien, J. C. W.; Rausch, M. D. *Organometallics* **1998**, *17*, 3775-3783. (c) Dooley, T.; Fairhurst, G.; Chalk, C. D.; Tabatabaian, K.; White, C. *Transition Met. Chem.* **1978**, *3*, 299-302. (d) Blais, M. S.; Rausch, M. D. *J. Organomet. Chem.* **1995**, *502*, 1-8. (e) Butenschon, H. *Chem. Rev.* **2000,** *100*, 1527-1564. (f) Jutzi, P.; Siemeling, U. *J. Organomet. Chem.* **1995**, *502*, 175-185. (g) Hughes, A. K.; Meetsma, A.; Teuben, J. H. *Organometallics* **1993**, *12*, 1936. (h) Jutzi, P.; Kristen, M.O.; Dahlhaus, J.; Neumann, B.; Stammler, H.G. *Organometallics* **1993**, *12*, 2980-2985. (i) Jutzi, P.; Redeker, T. *J. Inorg. Chem*. **1998**, 663-674. (i) Fujita, K.; Nakamura, M.; Yamaguchi, R. *Organometallics* **2001**, *20*, 100-105. (j) Jutzi, P.; Dahlhaus, J. *Phosphorus, Sulfur, and Silicon* **1994**, *87*, 73-82.

[41] Okuda, J. *Comments. Inorg. Chem*. **1994**, *16*, 185-205.

[42] Whyman, R. In *Homogeneous Transition Metal Catalyzed Reactions*; W. R. Moser, D. W. Slocum, Eds.; Advances in Chemistry Series 230; American Chemical Society: Washington, DC, 1992; Chapter 2; pp19-31.

[43] (a) Chew, W.; Widjaja, E.; Garland, M. *Organometallics* **2002**, *21*, 1982-1990. (b) Widjaja, E.; Li, C.; Garland, M. *Organometallics* **2002**, *21*, 1991-1997.

Chapter 2: C-H Activation by Cyclopentadienyl Iridium Complexes

2.1 Cyclopentadienyl complexes of group 9 transition metal and their derivatives in the C-H activation of hydrocarbons

There has been much interest in the activation of C-H bonds in saturated hydrocarbons due to the potential use of alkanes as chemical feedstocks for the synthesis of organic molecules.[1] For example, activation of the C-H bond in cyclohexane by $Cp^*Ir(CO)_2$, **2a** was reported by Graham et. al. in 1982. The reaction proceeded photochemically to give a stable hydridoalkyl species, $Cp^*Ir(CO)(C_6H_{11})(H)$, **3a** (Scheme 2.1).

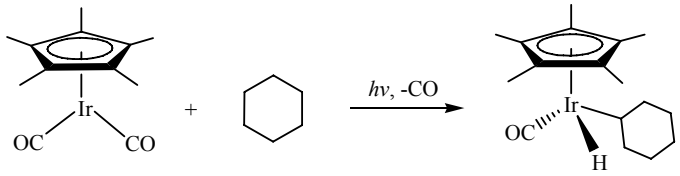

2a **3a**

Scheme 2.1

Many functionalised cyclopentadienyl ligands containing side-chain donor groups (-OR, -NRR', -PRR', $-CH=CH_2$) have appeared in the literature. In particular, we were interested in aminoethyl-functionalized cyclopentadienyl ligands because of their "hard-soft" combination of electron donors; the cyclopentadienyl ligand is known to stabilize transition metals in high as well as low oxidation states whereas the amino group favors coordination to metals in high oxidation states. To metals in low oxidation states, only weak interactions are anticipated, which may be strengthened by the chelate effect.[2] As a result, an aminoethyl-functionalized cyclopentadienyl ligands may be expected to behave as a hemilabile ligand, allowing reversible coordination of the nitrogen donor to the metal center (Scheme 2.2).

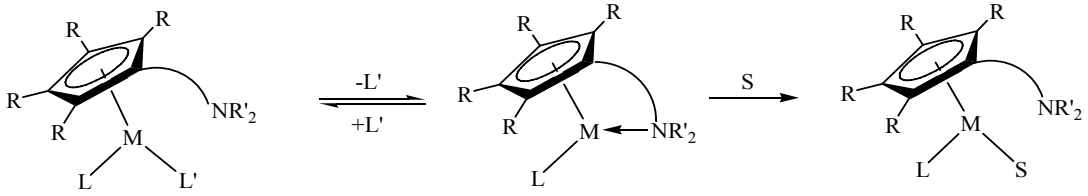

R = H, Alkyl
S = Substrate

Scheme 2.2

The reversible coordination of the amino side-chain to a reactive metal centre is of general interest in catalysis as it may stabilize a highly reactive, electronically and sterically unsaturated intermediate by weakly occupying the vacant coordination site until the actual substrate coordinates and replaces the amino group.[3] The intramolecular coordination of the amino group on the side-arm of the cyclopentadienyl ligand to the metal center in group 9 transition metal complexes have been achieved via the synthetic route outlined in Scheme 2.3. The amino group in these complexes can be reversibly displaced by CO. In the case of the cobalt and rhodium complexes, the CO ligand is only weakly bound to the metal center. Hence **Ic** and **IIc** converts back to **Ib** and **IIb** readily upon removal of the carbon monoxide atmosphere. The iridium analogue **IIIc** is, however, stable and converts back to **IIIb** only upon heating or photolysis.[4]

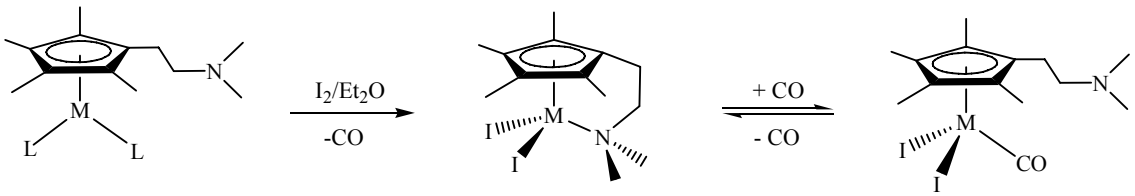

L = CO; M = Co **Ia**
L = C_2H_4; M = Rh **IIa**
M = Ir **IIIa**

M = Co **Ib**
= Rh **IIb**
= Ir **IIIb**

M = Co **Ic**
= Rh **IIc**
= Ir **IIIc**

Scheme 2.3

We were interested to study the ability of aminoethyl-functionalised cyclopentadienyl iridium dicarbonyl complexes in the activation of saturated hydrocarbons and if it was possible to achieve intramolecular coordination of the nitrogen atom to the iridium center from these dicarbonyl complexes photochemically via the dissociation of a CO ligand since the 16-electron species $[Cp^XIr(CO)]$ (Cp^X = Cp or Cp*) was obtained as a primary photoproduct via photo-dissociation of a CO ligand for the Cp^X analogue (Scheme 2.4).[5]

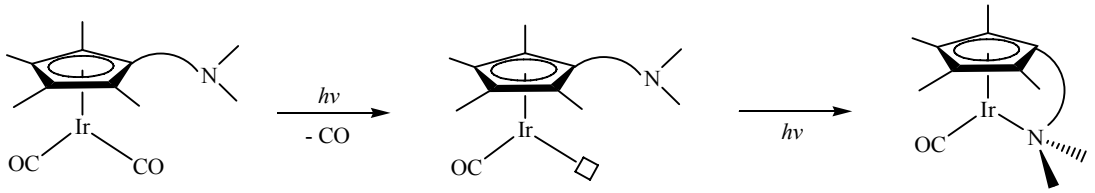

Scheme 2.4

2.2 C-H Activation of saturated hydrocarbon by cyclopentadienyl iridium complexes

$Cp^*Ir(CO)_2$, **2a** was synthesized from $[Cp^*Ir(Cl)_2]_2$, **1** following a literature procedure.[6] The functionalised cyclopentadienyl iridium complexes $Cp^*\text{^}Ir(CO)_2$, **2b**, $(Cp\text{^}Ir(CO)_2$, **2c**, and Cp^{BZ} $Ir(CO)_2$, **2d**; where $Cp^*\text{^}$ = $C_5Me_4CH_2CH_2NMe_2$, $Cp\text{^}$ = $C_5H_4(CH_2)_2NMe_2$ and Cp^{BZ} = $C_5H_4CH_2Ph$ were synthesized by reacting $Ir(CO)_3Cl$ with the appropriate salt of the cyclopentadienyl ligand using an analogous route to that reported for $CpIr(CO)_2$ (Scheme 2.5).[7] $Cp^*Ir(CO)(PPh_3)$, **7a** and $Cp^{Bz}Ir(CO)(PPh_3)$, **7b** can be synthesized from the reaction of **2a** or **2d** with excess triphenylphosphine. Alternatively, **7b** can also be synthesized from the reaction of $Cp^{BZ}Tl$ with trans-chlorocarbonylbis(triphenylphosphine)iridium.

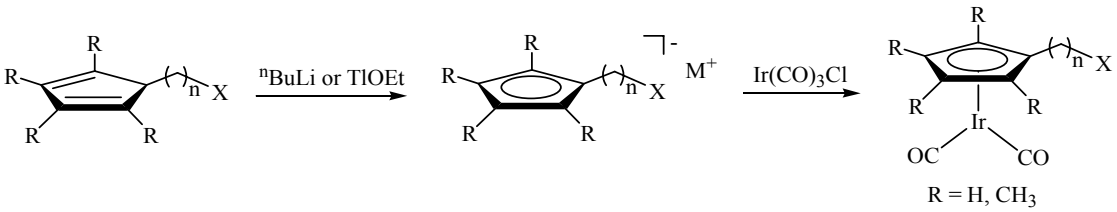

Scheme 2.5

2.2.1 Activation of cyclohexane

Photo-irradiation was carried out using a UV source as the absorption maxima of **2b** taken in cyclohexane were found to be in the UV range (210 and 280 nm).

Upon UV irradiation of a degassed solution of **2b** in cyclohexane, the solution darkened slowly from yellow to orange-brown. Monitoring the photolysis via infrared spectroscopy showed initial formation of the corresponding hydridoalkyl species $Cp^*\text{^}Ir(CO)(C_6H_{11})(H)$, **3b** ($\nu_{co}$: 1981 cm^{-1}), the CO stretching vibration of which is essentially identical to that of the $Cp^*IrCO(Cy)(H)$ analogue.[8] As the photolysis progressed, a new species showing a carbonyl stretch at 1996 cm^{-1} in the infrared, and a hydride resonance at δ -15.90 in the ^1H NMR, was formed (Scheme 2.6). This was assigned to the dihydride complex

Cp*^Ir(CO)$(H)_2$, **5b**, by comparison of the spectroscopic data with that of the analogue, Cp*Ir(CO)H_2, **5a** [ν_{co}: 1996 cm^{-1}, ^{1}H NMR (hydride resonance): δ -15.76];[8,9] the latter was reported to form when **2a** was irradiated under a hydrogen atmosphere. The ^{1}H NMR spectrum also shows a minor species, **A** with hydride resonance at δ -17.51, the identity of which has not been established. It could be a species resulting from intramolecular C-H activation of the dimethylamino group on the Cp*^ ligand, or an acyl species, Cp^*Ir(CO)(H)(COC_6H_{11}) from a CO insertion into the Ir-C bond of **3b**. Since irradiation of **2b** was carried out in the absence of hydrogen gas, the formation of **5b** may have resulted from *β*-hydrogen elimination of cyclohexene from **3b**; indeed, cyclohexene was detected by GC-MS analysis of the reaction solution.

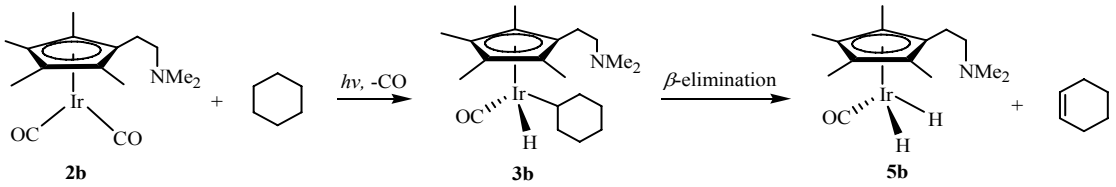

2b **3b** **5b**

Scheme 2.6

Similar irradiation of **2c** in cyclohexane also resulted in the formation of the corresponding hydridoalkyl species Cp^Ir(CO)(C_6H_{11})(H), **3c**, although there appeared to be some decomposition during irradiation. Similar results could also be achieved in a shorter time via irradiation with a 266 nm laser; for **2c**, the ratio of **2c** to the corresponding hydridoalkyl species **3c** as determined by the relative intensities of the CO absorbance was 3.29 after 6 h UV irradiation, while the ratio was 1.96 after 45 min irradiation with the laser. With $Cp^{Bz}Ir(CO)_2$, **2d**, which has a benzyl group as the side arm, Cp^{Bz}Ir(CO)(C_6H_{11})(H), **3d**, was obtained together with a small amount of another product that has a CO stretch at 2012 cm^{-1} and a hydride resonance at δ -14.61. Resonances in the region of δ -17.5 were, however, not observed in the reactions involving **2c** or **2d**. In contrast, the phosphine derivatives Cp*Ir(CO)(PPh_3), **7a** and Cp^{Bz}Ir(CO)(PPh_3), **7b** were found to be inactive in the C-H activation of cyclohexane. This may be attributed to the difficulty of CO dissociation in these

complexes; in the synthesis of **7a** and **7b** from **2a**, we have found that the second CO was not substituted even in the presence of excess phosphine (1.5 equivalents).

The hydridoalkyl species Cp*Ir(CO)(H)(C_6H_{11}), **3a** can be converted to the more stable chloroalkyl species Cp*Ir(CO)(Cl)(C_6H_{11}), **8a** by stirring in tetrachloromethane (CCl_4).[1b] Following the reported procedure, stirring the product mixture containing **2a** and **3a** in the presence of CCl_4 gave a yellow precipitate which was identified to be Cp*Ir(CO)Cl_2, **9a** (ν_{CO} 2058 cm^{-1}) in addition to **8a**. Compound **9a** was formed from the reaction of **2a** with CCl_4. Compound **2a** also decomposed slowly in chloroform to form **9a**. In a dichloromethane solution, **2a** did not convert to **9a** in the absence of light, but converted completely to **9a** upon 2.5 h of UV irradiation. For the analogous reaction using **2b**, stirring the product mixture in CCl_4 yielded Cp*^Ir(CO)(Cl)(C_6H_{11}), **8b** (ν_{CO} 2009 cm^{-1}) and Cp*^Ir(CO)$(Cl)_2$, **9b** (ν_{CO} 2058 cm^{-1}).

2.2.2 Photolysis in cyclohexane under a CO atmosphere

Photolyses under a CO atmosphere were carried out to find out if CO insertion into the Ir-C_6H_{11} bond in the hydridoalkyl species can occur to give carbonylation products.

Photolysis of a solution of **2a** or **2b** in cyclohexane under a CO atmosphere (1 bar) showed the initial formation of **3a** or **3b,** respectively. Upon prolonged photolysis, a new species, **6** showing carbonyl stretches at 2029 and 2069 cm^{-1} was detected together with **3a** or **3b** instead of **5a** or **5b**. A species containing a CO stretch at 1733 cm^{-1} was also detected. This was confirmed to be cyclohexanecarboxaldehyde ($C_6H_{11}CHO$) by ^1H NMR and GC-MS characterization. Formation of the corresponding aldehyde in reactions carried out with cyclopentane has also been observed by ^1H NMR spectroscopy. The aldehydes could have been formed by carbonylation of the hydridoalkyl species followed by reductive elimination. Carbonylation of hydrocarbons catalyzed by group 9 transition metal complexes such as RhCl(CO)$(PMe_3)_3$ under UV irradiation has been reported,[10] but 18-electron Cp*Ir complexes have not been known to carbonylate hydrocarbons as it was believed that coordination of an incoming CO ligand would result in dissociation of the hydrocarbon.[11] The yield of

cyclohexanecarboxaldehyde was determined by GC-FID and it was found that a 1 h UV irradiation of **2a** in cyclohexane under CO (1 bar) afforded 72 % of cyclohexanecarboxaldehyde (wrt [Ir]). Carrying out the photolysis in vacuo (absence of external CO source) for the same length of time also gave the aldehyde, but in a much lower yield (1 %).

The effect of CO pressures on the yield of the aldehyde was studied as high CO pressure may inhibit the initial CO dissociation from the iridium dicarbonyl complex while favoring the insertion of CO into the Ir-C bond to form the putative $Cp^*Ir(CO)(COC_6H_{11})(H)$ acyl intermediate. In situ IR measurement at high CO pressures was carried out as described in Section 2.2.4. Photolyses at various CO pressures (1.3 to 17.4 bar), however, did not show any significant trend in the yield of aldehyde with CO pressure.

Compound **6** was not formed if a cyclohexane solution of **2b** was stirred under a CO atmosphere without irradiation. However, if the cyclohexane solution of **2b** was first irradiated, and then a CO atmosphere introduced, a mixture of **2b**, **3b** and **6** was obtained; the changes in the relative intensities in the infrared spectra suggested that **5b** was completely converted to **6**, while **3b** was partially converted to **6**. If this mixture was degassed and then subjected to irradiation, a mixture of **2b**, **3b** and **5b** was obtained. All these are summarized by Scheme 2.7 and the spectra given in Figure 2.1, and suggest that **6** was formed by the reversible decomposition of **3b** and **5b**. The Cp* analogue, **2a** undergoes similar reaction under a CO atmosphere to give **3a** and **6**.

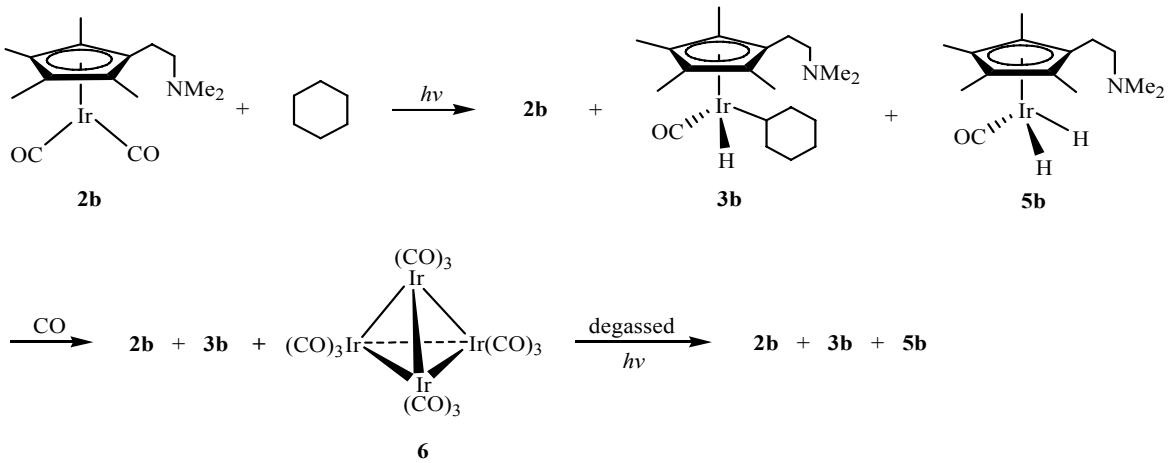

Scheme 2.7

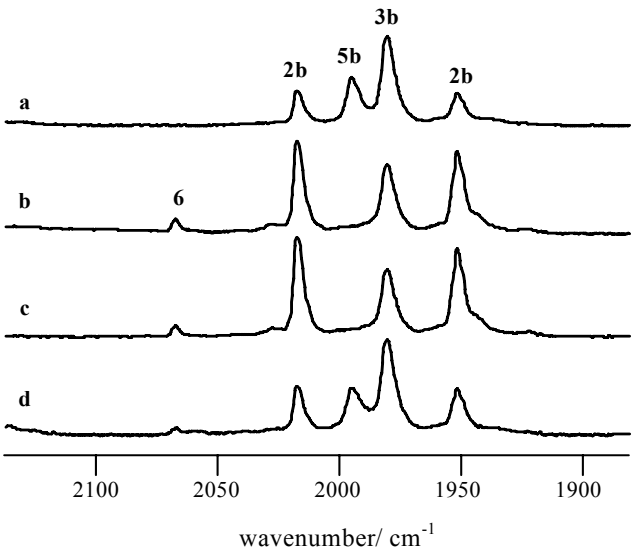

Figure 2.1. IR spectra for the solution of **2b** in cyclohexane: (a) after 6 h UV irradiation in degassed solution, followed by (b) stirring overnight under 1 atm of CO, (c) degassing and stirring overnight in degassed solution, and (d) UV irradiation in degassed solution for 3 h.

Compound **6** was identified to be $Ir_4(CO)_{12}$ by an independent synthesis[12] and it was found that upon irradiation of a degassed suspension of **6** in cyclohexane in the presence of Cp*H, partial conversion to **2a** was observed. Further irradiation resulted in the formation of **3a** in low yield. At the end of the 6.5 h irradiation, suspended **6** was still visible. Thus, the low conversion rates may be attributed to the low solubility of **6** in cyclohexane.

The ratio of **2a**:**3a** formed by the photolysis of **2a** in degassed cyclohexane solution versus that under a carbon monoxide atmosphere (1 bar) was determined by monitoring the reactions using IR spectroscopy (Table 2.1). It was found that the conversion of **2a** to **3a** proceeded faster in the degassed solution and the amount of **3a** increased with the length of photolysis. For the reaction under a CO atmosphere, cluster **6** was detected after 30 min of photolysis and increased in amount with time; the ratio of **3a** to **2a** was quite constant after 30 min. This indicates that while **3a** is being formed from **2a**, it is continuously being converted to **6**.

Table 2.1. Changes in **3a:2a** absorbance ratio with length of photolysis.

Photolysis time/ min	**3a:2a** absorbance ratio	
	In degassed solution	**Under CO**
15	0.67	0.56
30	1.03	0.65
45	1.27	0.63
60	1.61	0.66

2.2.3 Activation of cyclopentane

In line with earlier reports that smaller rings showed higher reactivity toward C-H activation,[1c, 13] it was found that the C-H activation of cyclopentane by **2b** was indeed more facile; the ratio of **4b**:**2b** (by absorbance) was 2.22 after 10 min, compared to the **3b**:**2b** ratio of 1.94 after the same length of irradiation. These figures also indicate that activation with **2b** was faster than that of **2a**. The ratio of the absorbance intensities of **3a**:**2a** was 0.67 after 15 min of irradiation in cyclohexane compared to 0.86 for **3b**:**2b** after 5 min of irradiation (Tables 2.1 and 2.2).

Table 2.2. Changes in **3b:2b and 4b:2b** absorbance ratio with length of photolysis in cyclohexane and cyclopentane respectively.

Photolysis time/ min	**In cyclohexane 3b:2b**	**In cyclopentane 4b:2b**
5	0.86	1.02
10	1.94	2.22

As in the case of **2b** in cyclohexane, irradiation in cyclopentane in degassed solution led to the formation of both **4b** and **5b**. On stirring the resulting solution overnight under a CO atmosphere, both **4b** and **5b** were converted completely to **6** (Scheme 2.8 and Figure 2.2). Irradiation of a solution of **2b** in cyclopentane under 1 atmosphere of hydrogen or argon also gave **4b** and **5b** without the formation of cluster **6** (same products as activation in vacuo). A

minor species **B**, with hydride resonance at δ -17.71 was also present in the product mixture obtained from photolyses in a degassed solution, under hydrogen or argon but not in the reaction under a CO atmosphere.

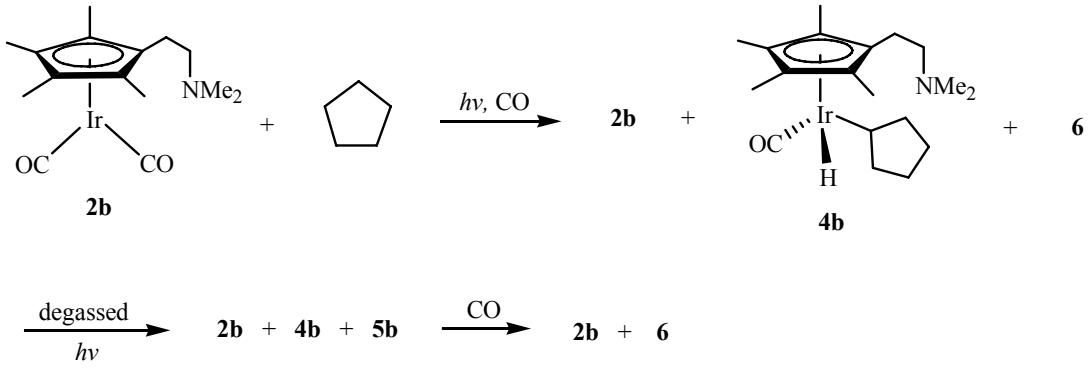

Scheme 2.8

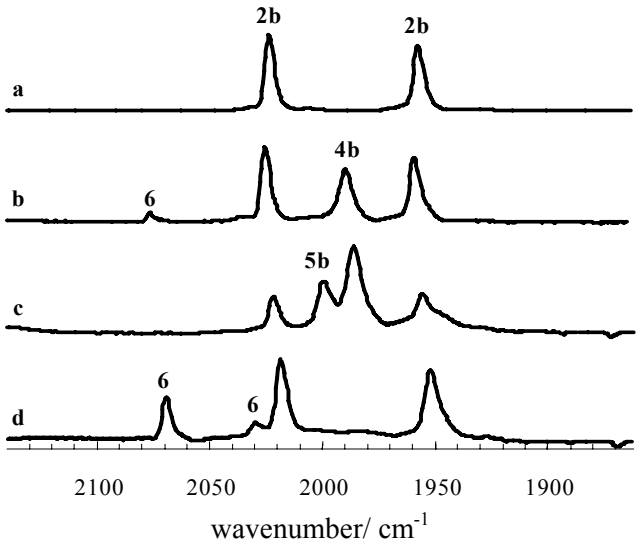

Figure 2.2. IR spectrum for the solution of **2b** in cyclopentane: (a) after 2 h stirring under CO, followed by (b) 3 h UV irradiation under CO, (c) degassing and irradiation for 3 h and finally (d) stirring overnight under 1 atm of CO.

Although the hydridocyclohexyl and cyclopentyl species **3b** and **4b** cannot be interconverted thermally (i.e. heating a solution of **3b** in cyclopentane at 70 ºC for 20 h did not give **4b**), they can do so photochemically. Hence, irradiation of a solution of **3b** in cyclopentane resulted in complete conversion of **3b** to **4b** (Scheme 2.9).

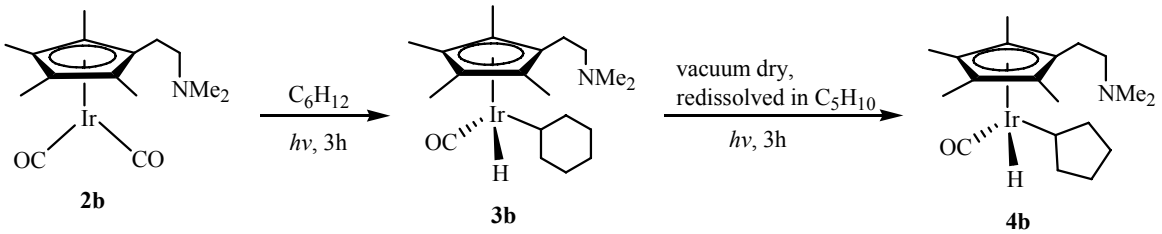

Scheme 2.9

2.2.4 In situ infrared monitoring of reaction

To gain further insights into the process, particularly with respect to the detection of compounds that we have hitherto not isolated or identified, in situ infrared measurements on the C-H activation of cyclohexane was carried out and iterative band targeted entropy minimisation (iBTEM) was used for deconvolution of the data matrix. The iBTEM algorithm has been proven to be useful for picking up signals due to species present in low concentration, having low absorbance, is unstable, or has peaks that overlap with those due to other species.[14]

The schematic diagram for the set-up used for the in situ infrared measurements is shown in Figure 2.3. Three different reactors were used and they are shown in Figures 2.4 – 2.6. The quartz reactor shown in Figure 2.4 was purchased commercially. The reaction vessel is cooled by flowing water through two cooling jackets. For photolysis using a smaller volume of solution, a modified quartz tube shown in Figure 2.5 was used. The reaction mixture can be cooled by immersing the quartz tube into a cooling jacket. The reaction mixture was channeled continuously between the reactor and the IR cell via viton and tygon tubings using a peristaltic pump. For measurements at high CO pressures, the reactor is made of sapphire and the sample is circulated via steel tubings into the high pressure cell (Figure 2.6).

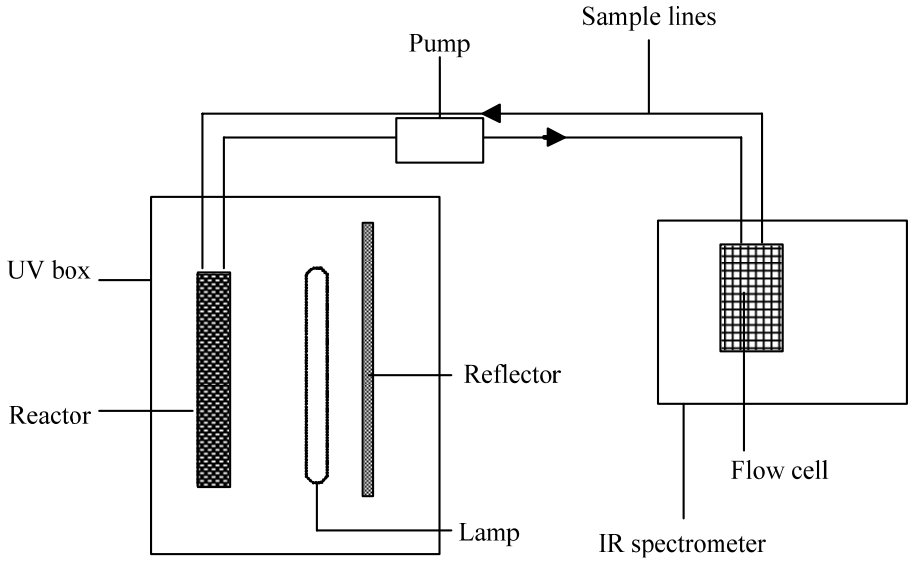

Figure 2.3. Schematic diagram of the set-up used for in situ infrared measurements.

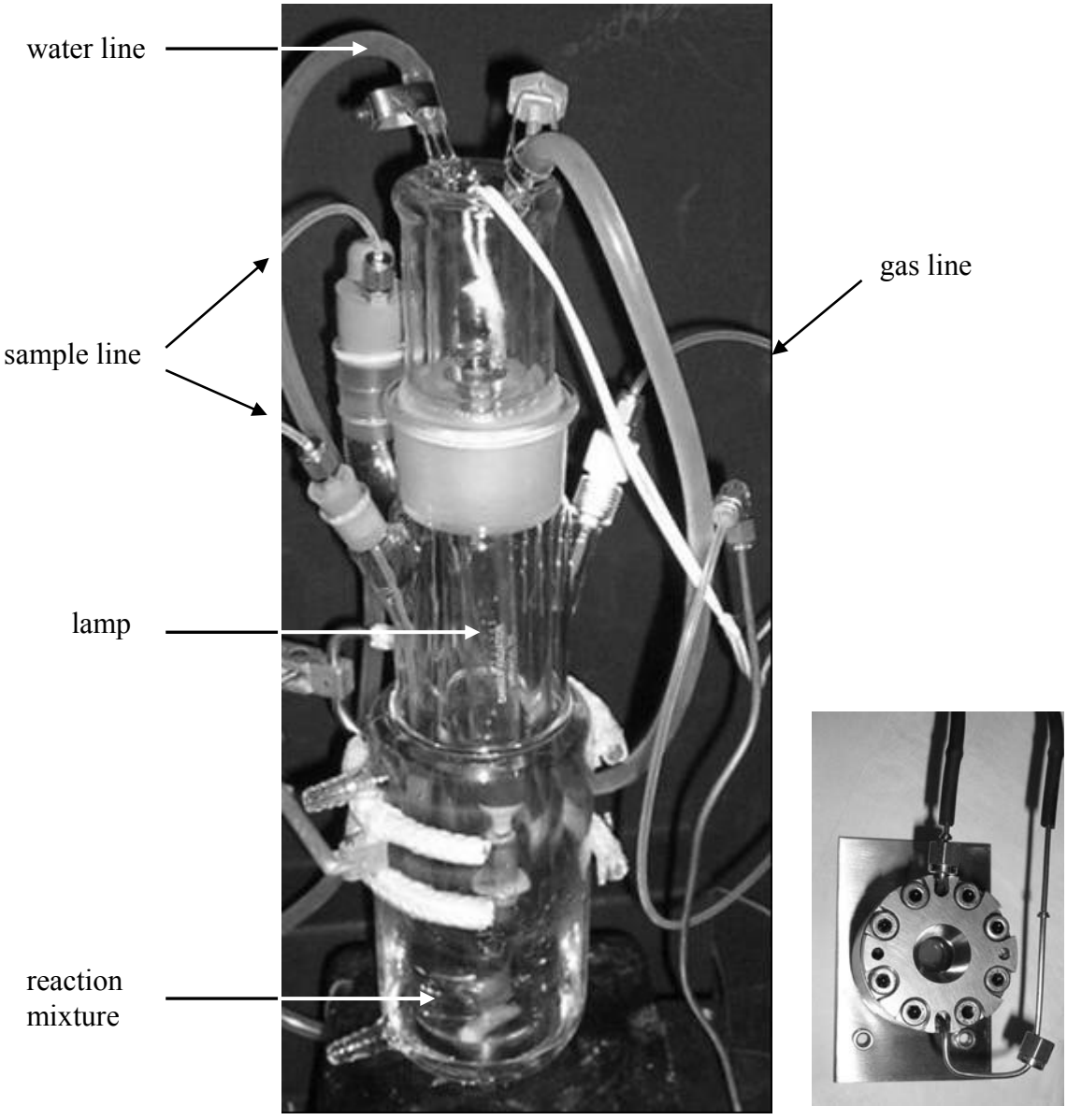

Figure 2.4. (a) UV reactor set-up for large volume reaction (ca. 250 ml). (b) Flow cell used for IR measurement.

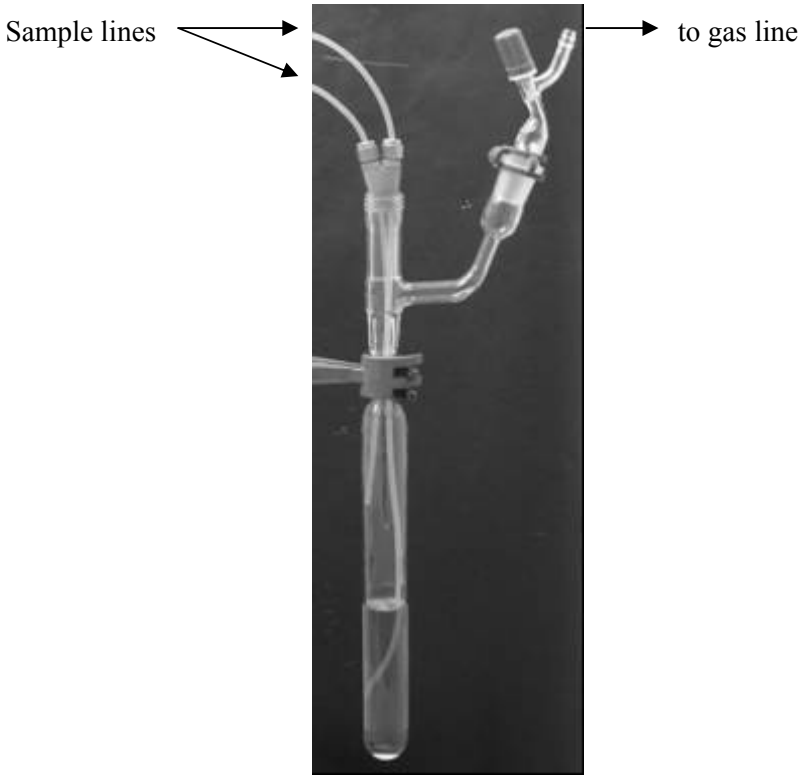

Figure 2.5. UV reactor set-up for small volume reaction (*ca*. 70 ml).

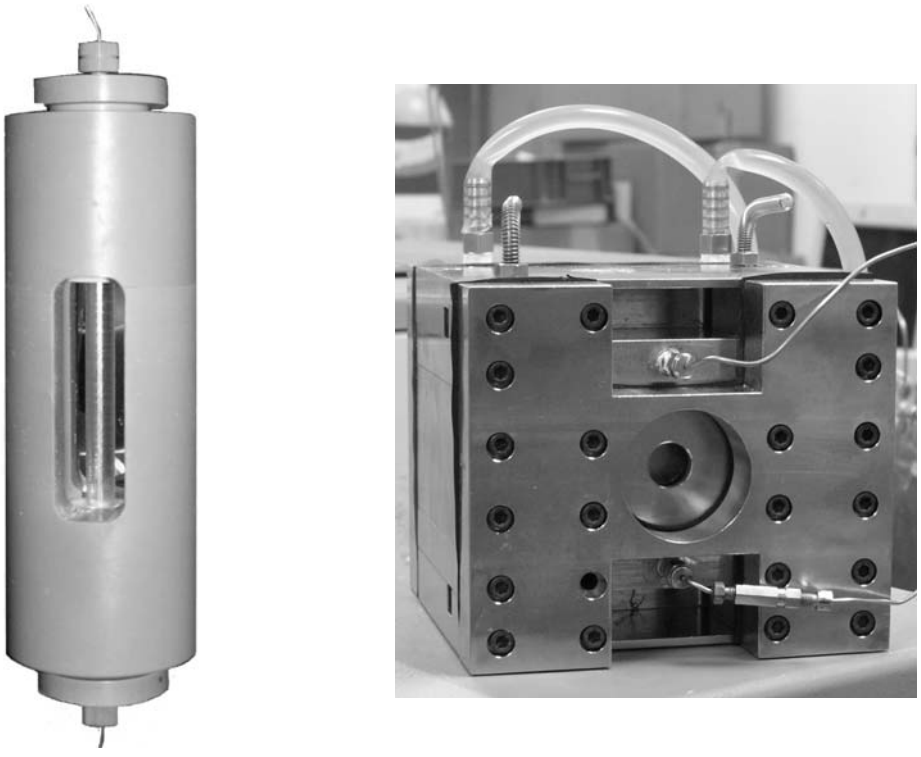

(a) **(b)**

Figure 2.6. Apparatus for IR measurement at high CO pressures. (a) Industrial sapphire tube. (b) High pressure cell (AMTIR windows).

Measurements were made for both **2a** and **2b**; for each complex, spectra were collected at 5 minute intervals over several hours. For **2a**, the reaction was done under an argon atmosphere or under a CO atmosphere and a total of 232 spectra was collected. iBTEM numerical analysis was carried out on the resulting spectra over the range 2200 – 1650 cm^{-1}. (Chart 2.1). The individual IR spectra of **2a**, **3a** and **6** were recovered, together with the C=O stretch for cyclohexanecarboxaldehyde. In addition, there were carbonyl stretches assignable to two other species, **C** and **D** (Figure 2.7).

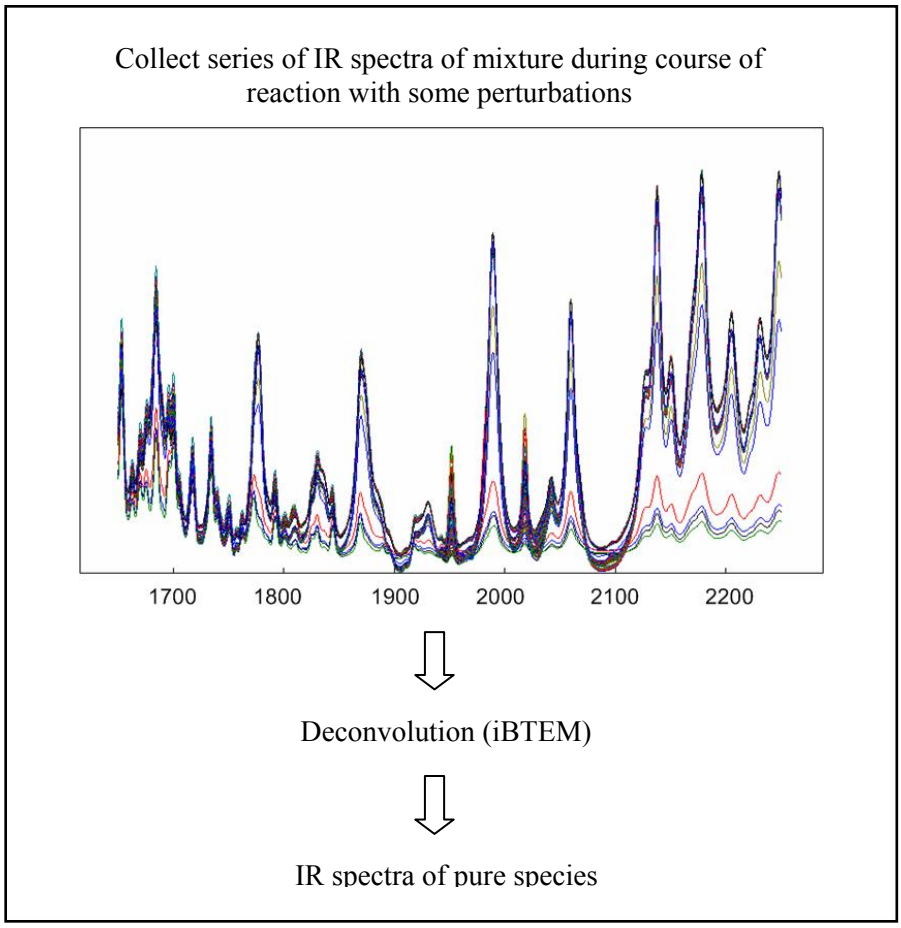

Chart 2.1

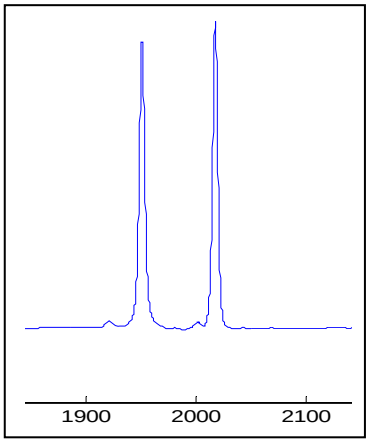

2a: 1952, 2018 cm^{-1}

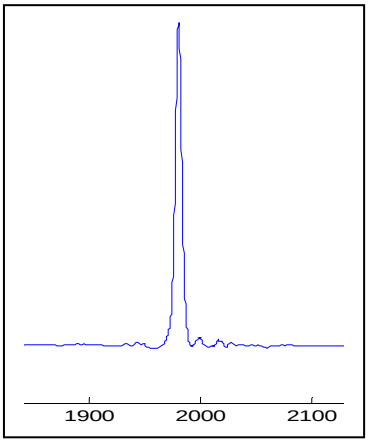

3a: 1981 cm^{-1}

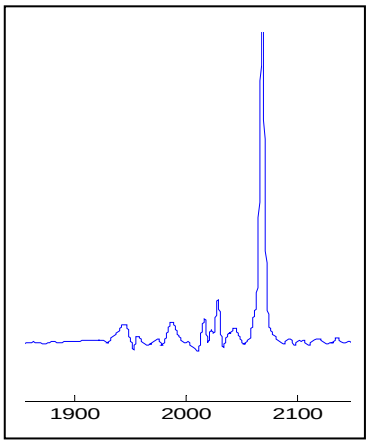

6: 2029, 2068 cm^{-1}

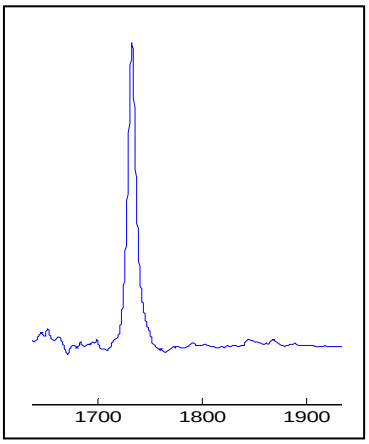

$C_6H_{11}CHO$: 1733 cm^{-1}

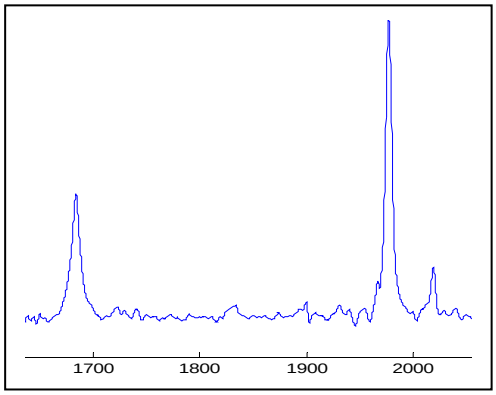

C: 1685, 1976 cm^{-1}

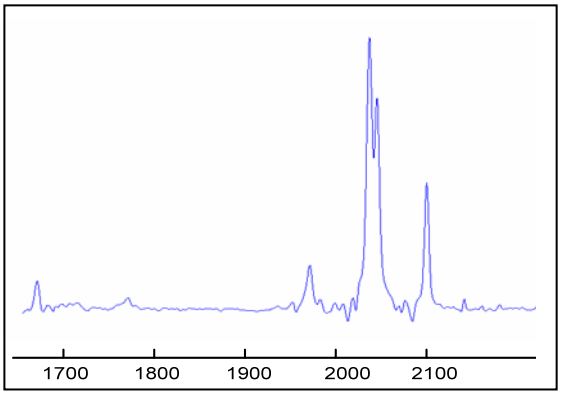

D: 1666, 1967, 2034, 2043, 2097 cm^{-1}

Figure 2.7. Pure component IR spectra of individual species recovered from deconvolution of the IR spectra of the reaction mixture.

The IR spectra of unknowns **C** and **D** show a peak at 1685 and 1666 cm^{-1} respectively which are typical of the carbonyl stretching frequencies of metal-acyl complexes.[15] In the IR

spectrum of **C**, a terminal CO stretch was observed in addition to the CO stretch due to the acyl group. Unknown **C** could be the acyl intermediate $Cp^*Ir(CO)(COC_6H_{11})(H)$ formed by CO insertion into the Ir-C_6H_{11} bond prior to the dissociation of $C_6H_{11}CHO$. A FAB-MS analysis of the reaction mixture yielded a molecular ion peak at m/z 467 in the positive ion mode corresponding to a species of the formulation $[Cp^*Ir(CO)(COC_6H_{11})]^+$. The IR spectrum of **D** showed four terminal CO stretches in addition to the acyl CO stretch, suggesting a $Ir(CO)_4(COR)$ type of species. The trigonal bipyramidal intermediate $Rh(CO)_4(COR)$ has been observed in the $Rh_4(CO)_{12}$-catalyzed hydroformylation of alkene. However, the pattern of the CO stretching vibrations of **D** does not match that of $Rh(CO)_4(COR)$ fully (Figures 2.7 and 2.8); **C** may be a structural isomer, and could have been formed from the reaction of cluster **6** with cyclohexene (from reductive elimination of **3a**), CO and H_2 (from decomposition of **5a**) present in the reaction mixture. We have not been able to isolate **C** and **D** from the reaction mixture for further characterization.

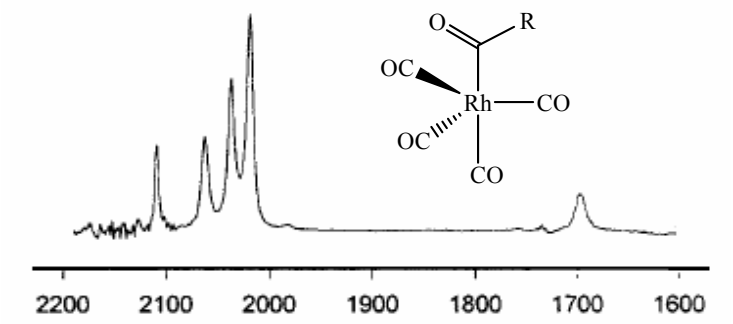

Figure 2.8. IR spectrum of $Rh(CO)_4(COR)$ (υ_{CO} 2110, 2063, 2037, 2020, 1698 cm^{-1} for R = cyclopentyl).[15b]

2.2.5 Attempts at intramolecular coordination of the amine group on 2b

In all the above studies, there has not been any observed intramolecular coordination of the amine group to the iridium center. This may be because the activation of cyclohexane or cyclopentane by the unsaturated intermediate is much more facile than the intramolecular coordination of the nitrogen atom to the iridium center or the tethered complex could have been formed but immediately activate the solvent to form the observed hydridoalkyl species. We have observed that the activation of cylopentane was faster with **2b** compared to **2a** (see Section 2.2.3). It was suggested in the C-H activation of alkanes by **2a** that after initial excitation by UV photons, ~ 99 % of the excited state molecules relax quickly through non-dissociative excited states, decaying to the ground state without the loss of CO. Only ~ 1 % of the excited molecules lose a CO, leaving a coordinatively unsaturated intermediate capable of C-H activating the surrounding solvent, thus accounting for the low quantum yield observed for the formation of the C-H activated hydridoalkyl species.[5a] The faster reaction observed with **2b** could be due to the ability of the amine group to stabilize the unsaturated intermediate, thus favoring the dissociation of CO.

Attempts were made at using solvents that do not contain any C-H bonds such as perfluorinated solvents and carbon disulfide. Photolysis of Cp* analogue without the side arm, **2a** in hexafluorobenzene and carbon disulfide were done in order to establish the stability of **2a** in these solvents. Photolysis of **2a** in carbon disulfide resulted in a gradual darkening of the solution from yellow to brown. Although the IR spectrum did not show any change in the carbonyl region, the ^{1}H NMR spectrum shows new resonances between δ 1.5 to 1.7 (1:2 integration ratio wrt Cp* resonance of **2a** in ^{1}H NMR spectrum) suggesting that **2a** has reacted with CS_2. Complex **2a** was also found to react with hexafluorobenzene. The reaction of **2a** with hexafluorobenzene and other fluoroarenes will be discussed in Chapter 3. Thus far, we have not been able to identify a solvent truly "inert" to C-H activation

2.3 Attempted activation of sp C-H bond

2.3.1 Reaction of 2a with phenylacetylene

In an extension to the activation of sp^3 C-H bonds using **2a**, the activation of sp C-H bonds by **2a** was attempted.

Photolysis of a solution of **2a** in neat phenylacetylene gave a red solution but the IR spectrum of the crude showed only CO stretches due to **2a**. Removal of unreacted **2a** by extraction with hexane gave a red oil that gave only peaks in the phenyl region but no methyl resonances for the Cp* ligand in the ^{1}H NMR spectrum. Room temperature stirring of a solution of **2a** in neat phenylacetylene and heating up to 133 ºC without UV irradiation gave no reaction from IR and NMR analysis.

An attempt to facilitate loss of a CO ligand from **2a** to generate a coordinatively unsaturated intermediate capable of C-H activation was made by performing the reaction in the presence of trimethylamine N-oxide (TMANO) in phenylacetylene at 100 ºC. The product mixture did not give any carbonyl stretches in the IR spectrum. The ^{1}H NMR spectrum is complicated, showing many peaks between δ 8.0 – 7.0 and δ 2.0 – 1.0. The FAB spectrum (+ve ion mode) shows the molecular ion peak at 1246 corresponding to the mass of Cp*Ir + 9 PhC≡CH and fragments corresponding to subsequent loss of six PhC≡CH.

2.3.2 Reaction of $Cp^*Ir(CO)Cl_2$ with phenylacetylene and lithium phenylacetylide

Phenylacetylene was reacted with another iridium complex, $Cp^*Ir(CO)Cl_2$, **9a** at room temperature. The ^1H NMR spectrum of the crude mixture shows no resonance in the hydride region, indicating that species such as Cp*Ir(CO)(C≡CPh)(H) from the activation of the sp C-H bond was not formed. TLC separation gave two yellow bands. The major product Cp*Ir(CO)[PhC=CHC(Ph)=CCH=CCl(Ph)], **10** was isolated from band 1 and characterized spectroscopically, including by a x-ray crystallographic study; an ORTEP plot showing the molecular structure, together with selected bond parameters, is given in Figure 2.9.

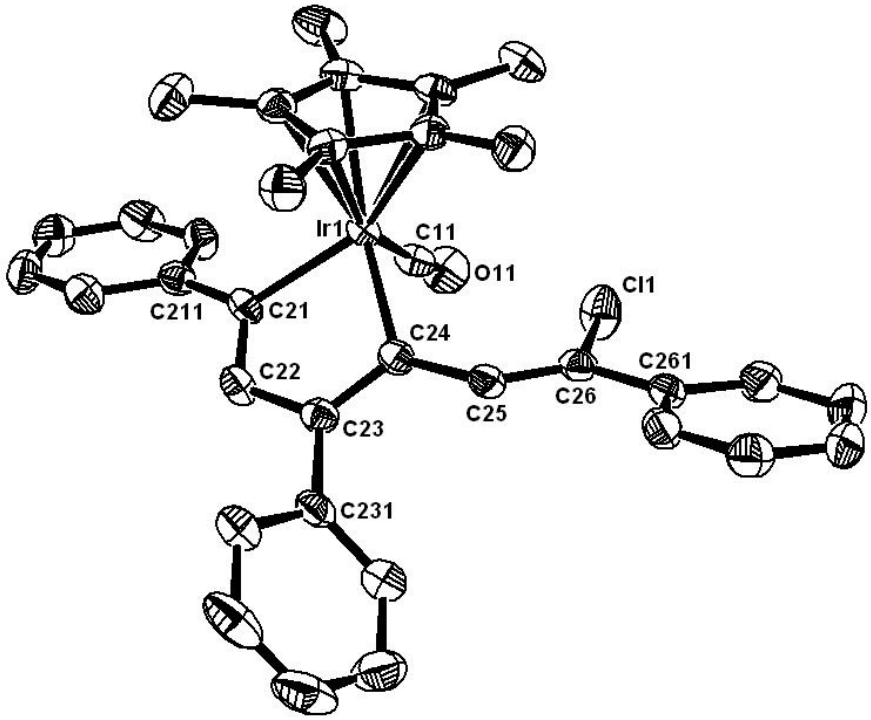

Figure 2.9. ORTEP diagram of **10.** Thermal ellipsoids are drawn at 50% probability level. The hydrogen atoms have been omitted for clarity. Selected bond distances (Å) and angles (°): Ir1-C21 = 2.068(4); Ir1-C24 = 2.091(5); Ir1-C11 = 1.846(5); C21-C211 = 1.479(7); C21-C22 = 1.340(7); C22-C23 = 1.443(7); C23-C231 = 1.490(7); C23-C24 = 1.360(6); C24-C25 = 1.461(7); C25-C26 = 1.337(6); C26-C261 = 1.476(7); Cl1-C26 = 1.752(5); C11-Ir1-C24 = 96.3(2); C11-Ir1-C21 = 94.2(2); C22-C21-Ir1 = 113.7(4); C23-C24-Ir1 = 113.3(4); C21-C22-C23 = 117.5(4); C24-C23-C22 = 114.9(4).

The molecular structure of **10** shows coupling of three phenylacetylene molecules. The stoichiometry indicates that a molecule of HCl has been eliminated, and a chloride ligand has migrated to C26 (Scheme 2.10). The ligand backbone shows alternating long (C211-C21), short (C21-C22), long (C22-C23), short (C23-C24) pattern with the length of the shorter bonds typical of a C=C double bond and the longer bonds between a C-C single and C=C double bond.

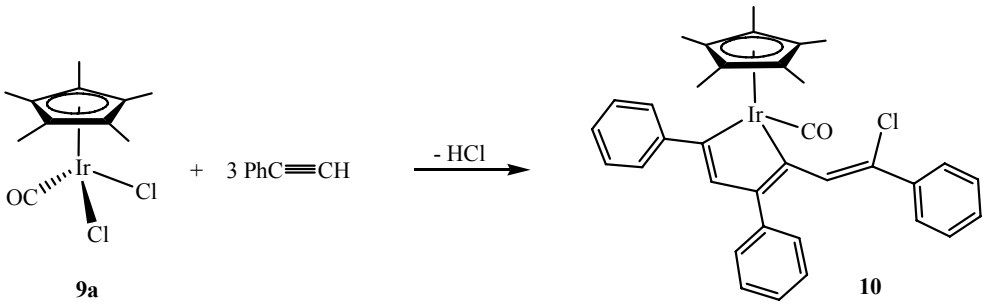

9a **10**

Scheme 2.10

Band 2 was impure and gave a CO stretching vibration at 2025 cm^{-1} in the IR spectrum. It decomposed when re-eluted on TLC.

The reaction of **9a** with lithium phenylacetylide proceeded rapidly at -78 ºC, giving a product with peaks at 2159 and 1937 cm^{-1} in the IR spectrum assignable to C≡C and CO stretching vibrations, respectively. The product was purified by TLC to give Cp*Ir(CO)(η^2-PhC≡C-C≡CPh), **11**, which was fully characterized, including by a single crystal x-ray crystallographic study; an ORTEP plot showing the molecular structure, together with selected bond parameters, is given in Figure 2.10.

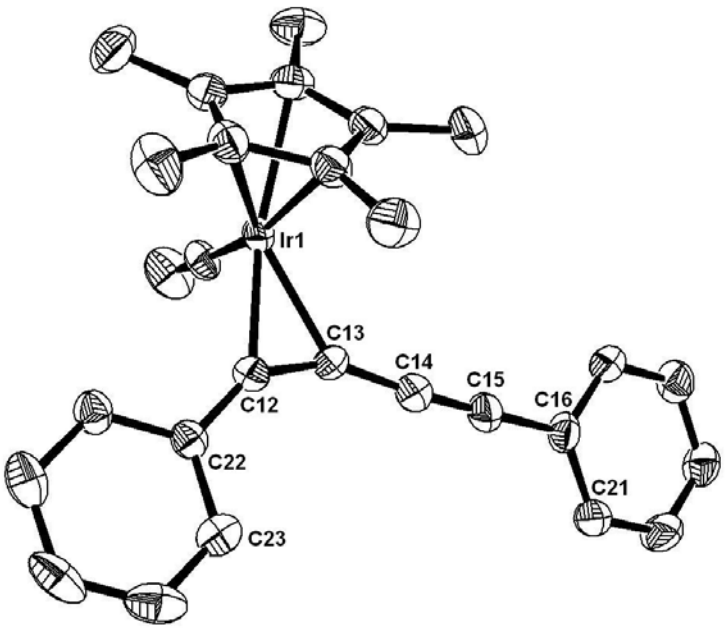

Figure 2.10. ORTEP diagram of **11.** Thermal ellipsoids are drawn at 50% probability level. The hydrogen atoms have been omitted for clarity. Selected bond distances (Å) and angles (°): Ir1-C12 = 2.084(5); Ir1-C13 = 2.112(5); C12-C13 = 1.295(7); C12-C22 = 1.435(6); C13-C14 = 1.376(7); C14-C15 = 1.205(7); C15-C16 = 1.438(7); C13-C12-Ir1 = 73.2(3); C12-C13-Ir1 = 70.8(3); C13-C12-C22 = 146.2(5); C12-C13-C14 = 153.3(5); C15-C14-C13 = 175.4(6); C14-C15-C16 = 175.0(6).

The molecular structure of **11** shows that the diyne is η^2-bonded to the iridium center via one of the C-C triple bond. The difference between the bond lengths Ir(1)-C(12) and Ir(1)-C(13) are not as large as the reported Rh(I) diyne compound, trans-[RhI(η^2-PhC≡CC≡CPh)(P^iPr_3)$_2$][16] (2,034(3) and 2.124(3) Å respectively). The C(12)-C(13) bond is elongated by ca. 0.09 Å compared to C(14)-C(15) bond. The C13-C14 bond length [1.376(7) Å] approaches that of a C-C double bond (1.34 Å).

The reaction of **9a** with lithium phenylacetylide represents an unexpected oxidative coupling of two phenyacetylide ligands; the metal center is reduced from Ir(III) to Ir(I). A literature report on the reaction of lithium acetylides with the closely related phosphine derivatives [Cp*$MCl_2(PEt_3)$] (M = Rh, Ir) gave stepwise displacement of the chloride ligands

to give monoalkynyl and bis(alkynyl) complexes [Cp*M(C≡CR)Cl(PEt_2)] and [Cp*M($C≡CR)_2$(PEt_2)] (R = Ph, $SiMe_3$; M = Rh, Ir) respectively; the alkyne is bonded to the metal center via the terminal carbon atom and there was no coupling of the alkynyl ligands.

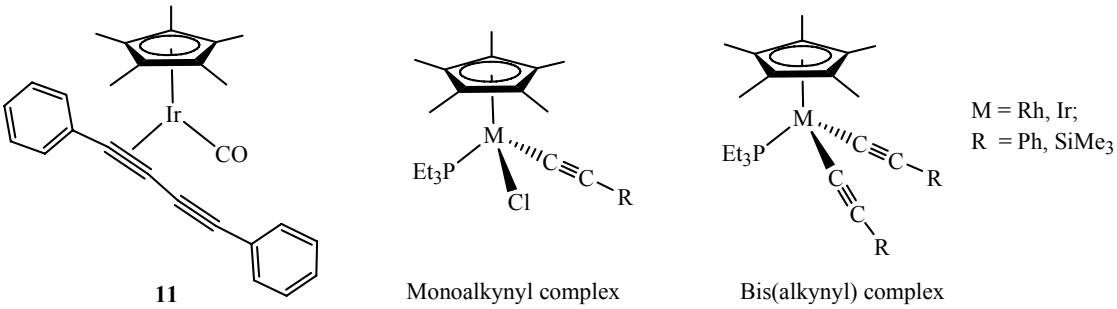

11 Monoalkynyl complex Bis(alkynyl) complex

Chart 2.2

An attempt to react **9a** with phenylacetylene using 2 equivalents of triethylamine as a base in a one pot reaction gave poor conversion to **11**. Increasing the amount of triethylamine resulted in the formation of an unidentified product, **F** with peaks at 2134 and 2047 cm^{-1} in the IR spectrum and Cp* resonance at δ 2.02 in the ^1H NMR spectrum instead of **11**. The FAB spectrum of the product mixture shows peaks at 940 corresponding to the mass of Cp*Ir + 6 PhCCH and fragments due to subsequent loss of five PhCCH units while the EI spectrum shows peaks at 306 corresponding to the mass of three PhCCH molecules. The phenylacetylene molecules may have undergone trimerization and two molecules of the trimerized product may have been attached to the iridium center.

2.3.3 Reaction of Tp*Rh($CO)_2$ with alkynes

A closely related compound, Tp*Rh($CO)_2$, **12a** is known to activate C-H bonds in saturated hydrocarbons efficiently.[17] Product formation can be driven to completion by removal of CO by nitrogen purge.[18] When a solution of **12a** was stirred in neat phenylacetylene for 20 h at room temperature, the solution turned from yellow to red. Addition of hexane to a toluene extract of the product mixture, gave a yellow precipitate, **12b**. The reaction was found to occur only with large excess of phenyacetylene. With 1 to 10

equivalents of phenylacetylene in a toluene solution, **12b** was not formed although the reaction mixture turned red. Compound **12b** has been completely characterized, including by a single crystal X-ray crystallographic study; an ORTEP plot showing the molecular structure, together with selected bond parameters, is given in Figure 2.11.

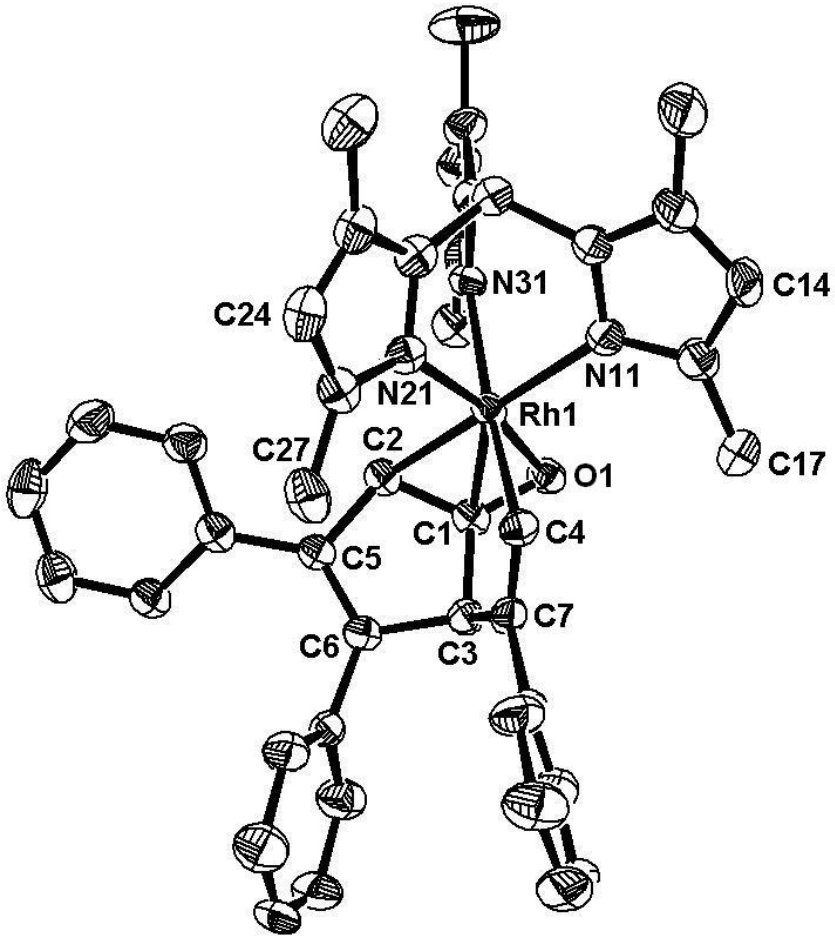

Figure 2.11. ORTEP diagram of **12b.** Thermal ellipsoids are drawn at 50% probability level. The hydrogen atoms have been omitted for clarity. Selected bond distances (Å) and angles (°): Rh1-C4 = 1.994(5); Rh1-C1 = 2.110(6); Rh1-C2 = 2.230(6); Rh1-O1 = 2.105(4); C1-O1 = 1.287(6); C1-C2 = 1.411(8); C1-C3 = 1.522(8); C2-C5 = 1.484(7); C3-C6 = 1.509(8); C3-C7 =1.531(8); C4-C7 = 1.334(8); C5-C6 = 1.350(8); C4-Rh1-O1 = 67.57(18); C1-O1-Rh1 = 67.57(18); C1-O1-Rh1 = 72.4(3); O1-C1-C2 = 126.7(5); C1-C3-C7 = 105.6(4); C7-C4-Rh1 = 123.3(5).

An interesting feature of **12b** is the insertion of one of the CO ligand from the starting Tp*Rh(CO)$_2$ complex into the ligand formed by the coupling of three phenylacetylene molecules. The inserted CO ligand is still bonded to the rhodium center although the bonding is via the oxygen atom instead of the carbon atom. The C1-O1 bond [1.287(6) Å] is longer than a typical C-O double bond (1.22 Å).

The ^{1}H NMR spectrum of **12b** is shown in Figure 2.12(a). The alkenic protons derived from the phenylacetylene ligands and the resonances due to the C-H protons on the Tp* ligand were distinguished by repeating the reaction using PhC≡CD. The ^{1}H NMR spectrum of the product obtained (**12b-d)** is shown in Figure 2.12(b). The disappearance of the resonances at δ 5.2 and 6.1 confirmed that they are due to alkenic protons. The resonance due to one of the alkenic protons is highly deshielded (H^f) and overlaps with the resonances due to phenyl groups. This is consistent with the Chemdraw prediction that H^f would be the most deshielded alkenic proton and the integration ratio of the resonances in the two spectra.[19] The other three resonances at δ 5.87, 5.82 and 5.79 are due to C-*H* groups on the Tp* ligand. A 2D NOESY spectrum of **12b** exhibited crosspeaks between the resonances for H^a, H^b, H^d and H^e with the phenylic resonances, indicating the spatial proximity between the protons giving rise to these resonances and the phenyl ring. H^c also gave a crosspeak with H^e distinguishing them from the other protons [Figures 2.13(a) and (b)].

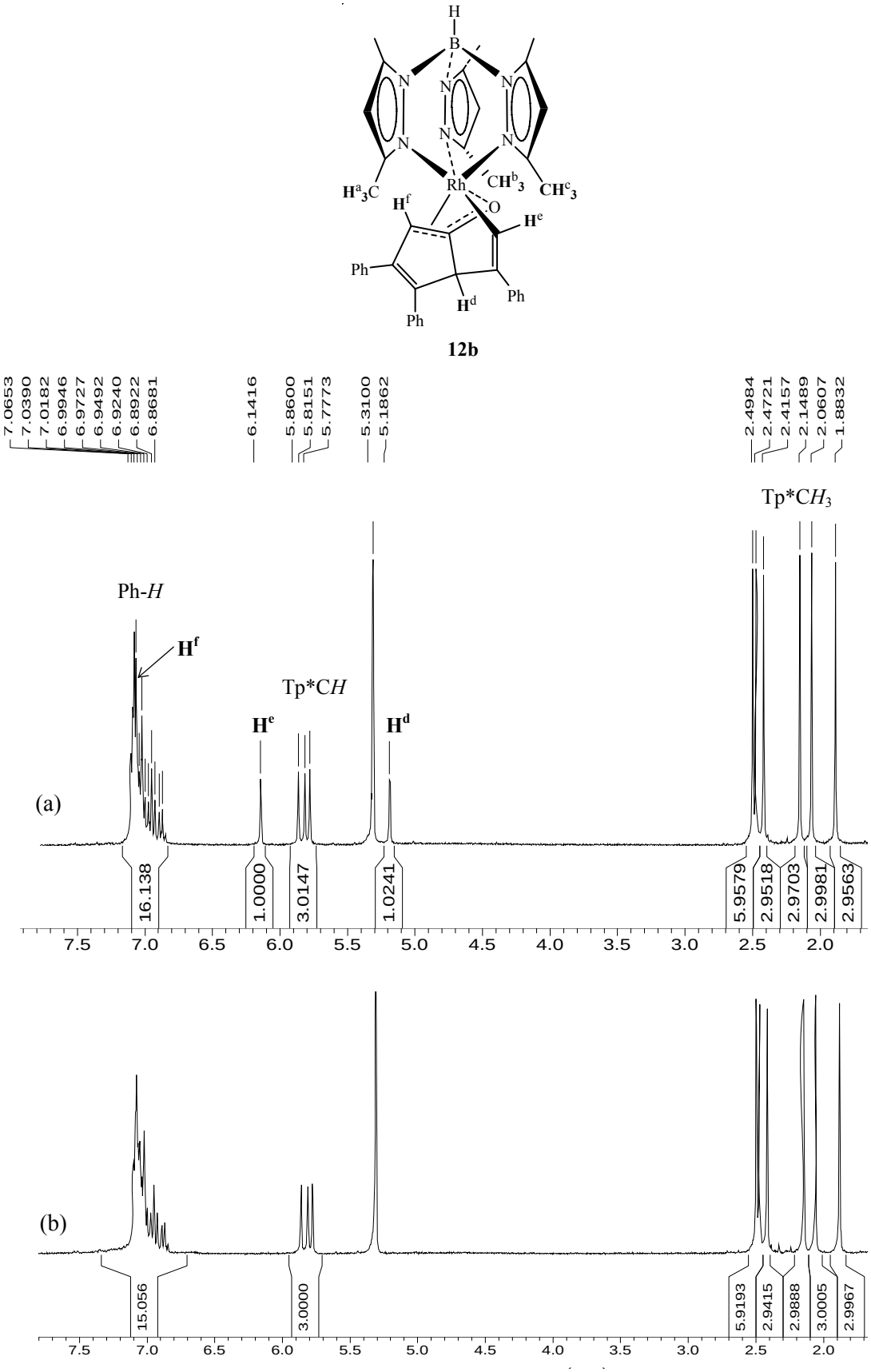

Figure 2.12. ^{1}H NMR spectrum, in the alkenic and aromatic regions, of (a) **12b** (b) **12b-d** (in CD_2Cl_2).

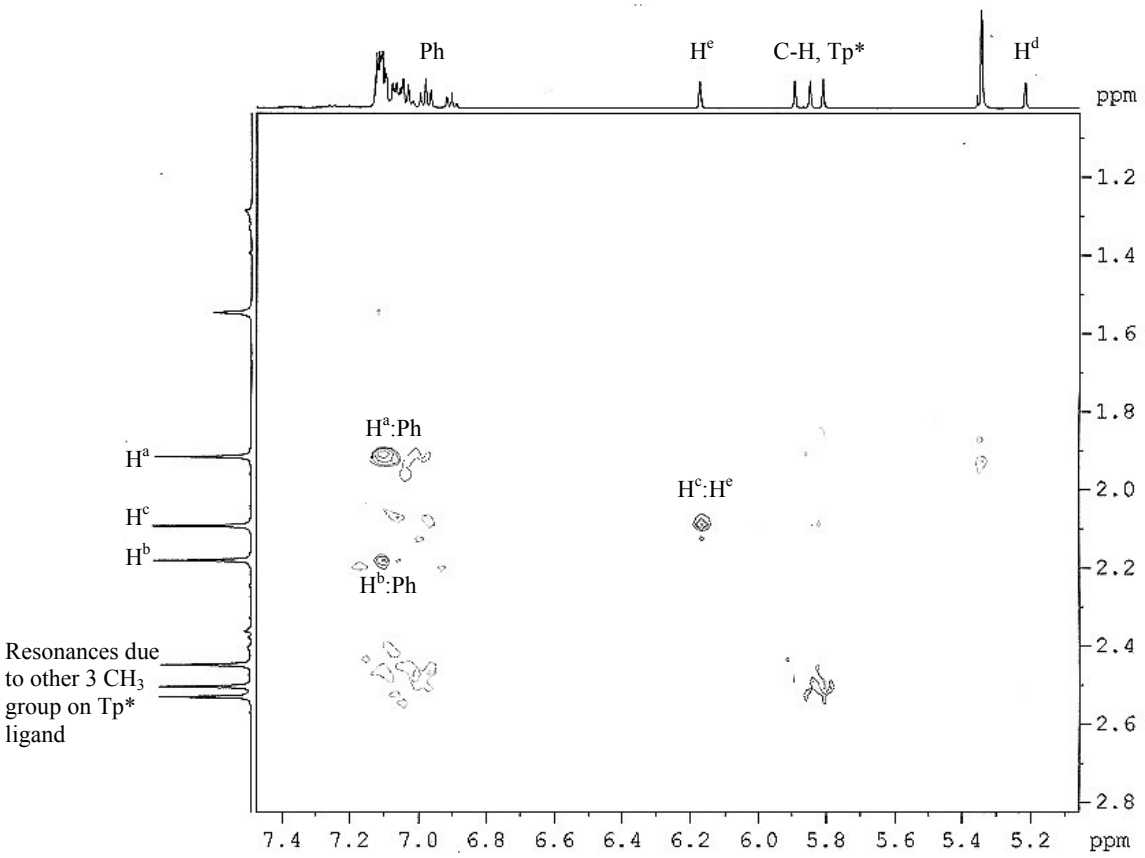

(a)

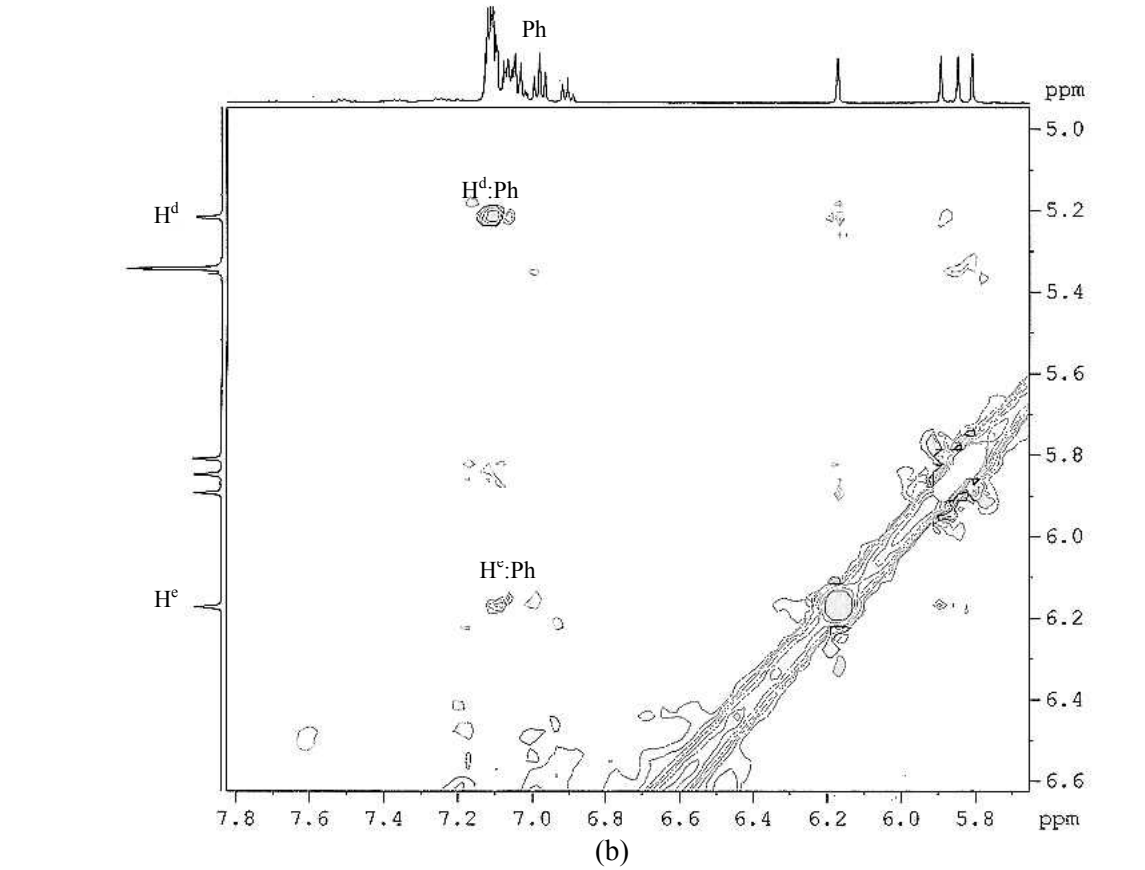

(b)

Figures 2.13(a) and **(b).** Expanded portions of the ^{1}H NOESY spectrum of **12b** in CD_2Cl_2.

Several organic products due to coupling of the phenylacetylene molecules were also detected in minor quantities from the GC-MS of the supernatant (Chart 2.3).

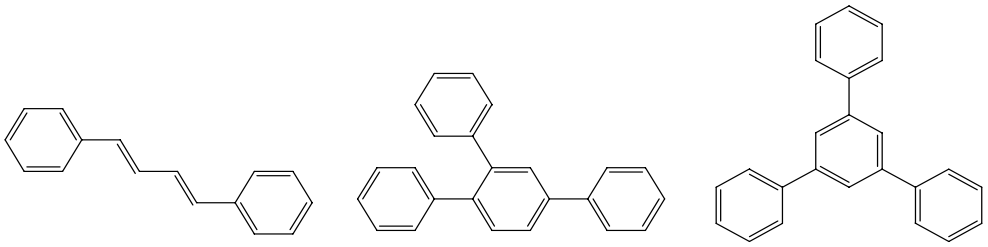

(1E,3E)-1,4-diphenylbuta-1,3-diene 1,2,4-triphenylbenzene 1,3,5triphenylbenzene

Chart 2.3

The analogous reaction of **12a** with ^{t}butylacetylene did not give any organometallic product. The GC-MS spectrum of the product mixture after removal of the volatiles shows the presence of 1,3,5-tri-tert-butylbenzene resulting from the cyclotrimerization of the terminal alkyne. Likewise, **12a** did not give any organometallic products with the internal alkyne diphenylacetylene (excess) at room temperature or upon heating to 110 ºC. The GC-MS spectrum of the product mixture shows mainly unreacted diphenylacetylene and small amounts of other organic products such as cis and trans–stilbene.

2.4 Reaction of triphenylcyclopropenyl cation with $[M(CO)_4]^-$ (M = Ir, Rh)

2.4.1 Transition metal cyclopropenyl complexes

Although C-H activation of saturated hydrocarbon solvents by group 9 transition metal carbonyl complexes containing Cp ligand (and it's derivatives such as Cp*, Ind, Tp and Tp*) are well studied, those involving complexes containing other ring systems are not well-established. In an extension to the cyclopentadienyl system, we attempted to synthesize cyclopropenyltricarbonyliridium complexes to study their C-H activation ability.

η^3-Cyclopropenyl is the simplest cyclic enyl ligand. It is able to undergo $\eta^1 \rightarrow \eta^3$ ring-slippage in a similar fashion to its acylic η^3-propenyl (allyl) analogue. It is known to bind to transition metal centres via η^1-, η^2- and η^3- coordination.[20] η^3-cyclopropenyl complexes are valence isomeric relatives of metallacyclobutadienes (Scheme 2.11).

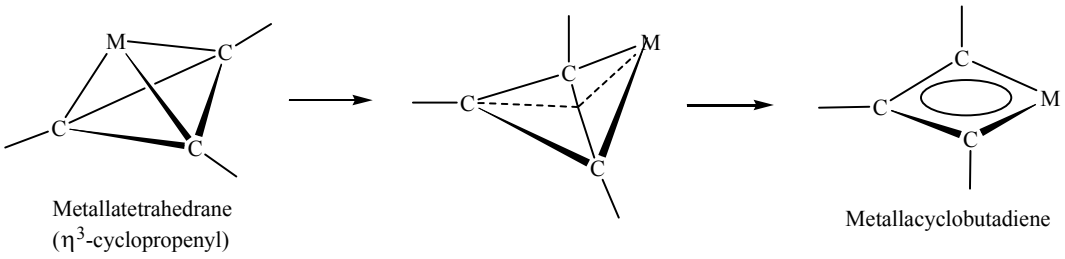

Metallatetrahedrane (η^3-cyclopropenyl)

Metallacyclobutadiene

Scheme 2.11

η^2- cyclopropenyl complexes are rare. One example is the platinum complex shown below, which has an approximate plane of symmetry passing through the metal atom and the distal C of the C_3 unit.[21]

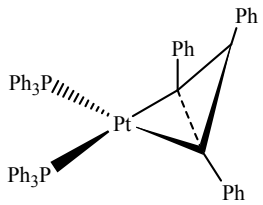

Chart 2.4

Compared to cyclopentadienyl transition metal complexes, there are far fewer reports of cyclopropenyl complexes in the literature. The complexes shown below were synthesized via the reaction of cyclopropenyl cation or halide with anionic or neutral metal complexes.[22,23,24]

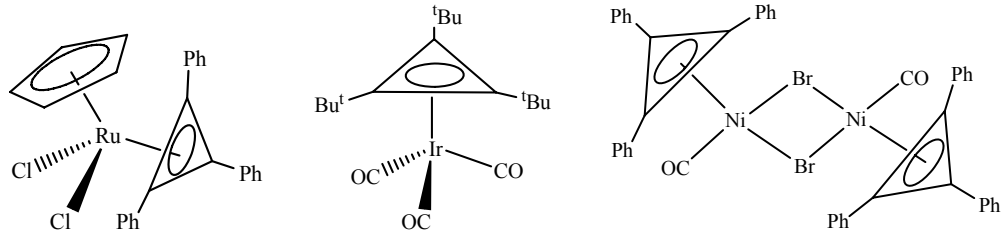

Chart 2.5

However, cyclopropenyl rings are also known to undergo ring opening reactions with some transition metal complexes. A common product from the reaction of cyclopropenyl cations with transition metal anions is the η^3-oxycyclobutenyl complex which may be formed via CO insertion pathways (Scheme 2.12).[25, 26]

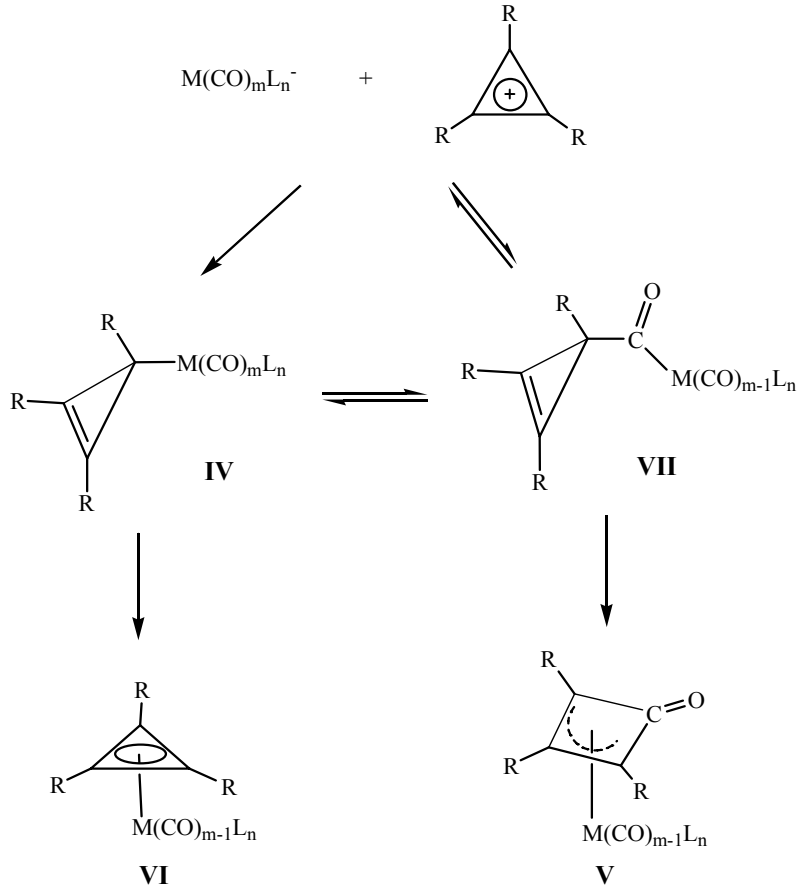

Scheme 2.12

For example, the reaction between $[CpFe(CO)_2]^-$ and $[C_3Ph_3]^+$ afforded **IV** whereas reaction with the more bulky $[C_3{}^tBu_3]^+$ gave only **V** via ring expansion from **VII**. It was proposed that the latter reaction proceeded via direct electrophilic attack on CO ligand rather than at the metal center to give **IV** due to steric reasons. Compounds **IV** and **V** do not interconvert when heated, but they can interconvert under photochemical activation.

An example of an oxidative addition of a metal ion across a C-C bond was reported for the reaction between $[C_3Ph_3][BF_4]$ and $[IrCl(CO)(PMe_3)_2]$. The cyclopropenium ring is opened by, and adds oxidatively to, the Ir centre to form **VIII.**[27]

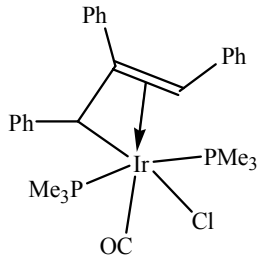

VIII

A similar cyclopropenyl ring opening was reported in the case of a rhenium compound; **IX** can be converted to **X** by uv irradiation or by refluxing in hexane (Scheme 2.13).[28]

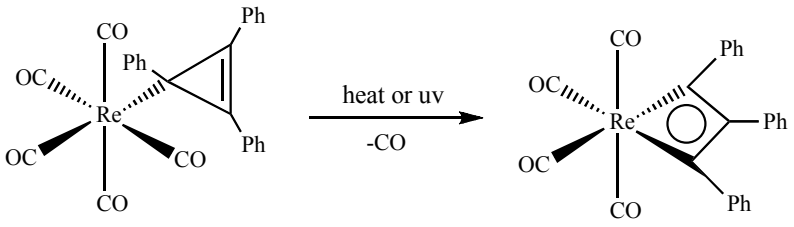

IX **X**

Scheme 2.13

2.4.2 Reaction of $C_3Ph_3BF_4$ with $[M(CO)_4]^-$ (M = Ir, Rh)

Following the literature method for the preparation of $[(\eta^3\text{-}C_3{}^tBu_3)Ir(CO)_3]$, $C_3Ph_3BF_4$ was reacted with $[PPN][Ir(CO)_4]$ at room temperature in dichloromethane. The solution darkened to deep red within a few minutes. Preparative TLC was carried out in a glove box as the products were air-sensitive in solution. TLC separation gave a purple (band 1) and a yellow band (band 2) that overlapped. The two bands could not be completely separated even after another round of elution. Two isomers **13** and **14a** were isolated from bands 1 and 2, respectively (Scheme 2.14). Their molecular structures have been determined by single crystal X-ray crystallographic studies and revealed ring opening of the two cyclopropenyl ligands.

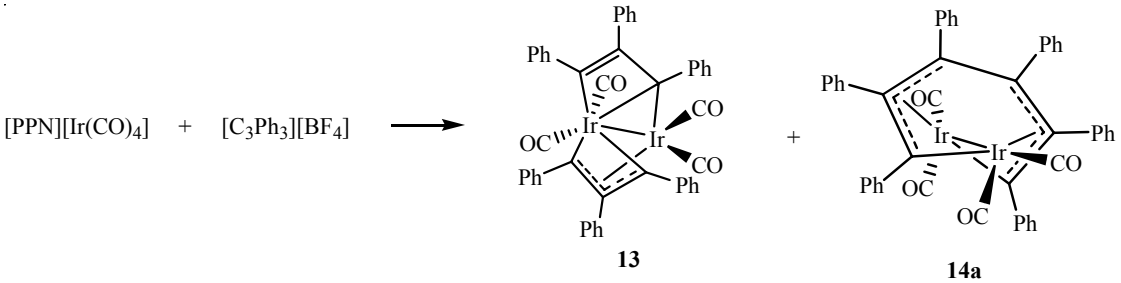

Scheme 2.14

A similar reaction of $[C_3Ph_3][BF_4]$ with $[PPN][Rh(CO)_4]$ in dichloromethane gave **14b**, which is the rhodium analogue of **14a**. In this case, the reaction was cleaner. TLC separation gave a single red band, leaving an immovable pale red band on the baseline.

The ORTEP plots of **13**, **14a** and **14b** together with selected bond parameters, are given in Figures 2.14, 2.15 and Tables 2.3-2.5.

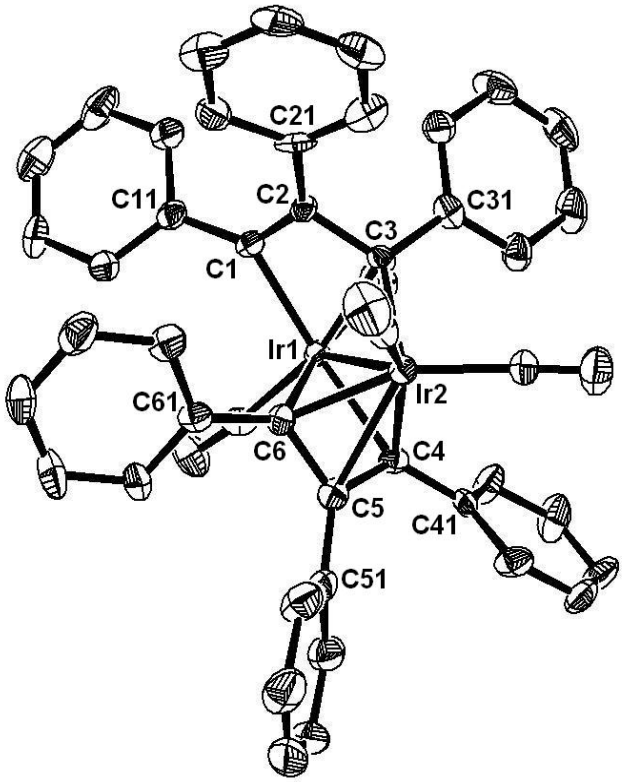

Figure 2.14. ORTEP diagram of **13.** Thermal ellipsoids are drawn at 50% probability level. The hydrogen atoms have been omitted for clarity.

Table 2.3. Selected bond distances (Å) and angles (°) for **13**.

bond distances (Å)		angles (°)	
Ir(1)-C(1)	2.132(6)	C(1)-Ir(1)-C(6)	90.2(2)
Ir(1)-C(3)	2.136(7)	C(1)-Ir(1)-Ir(2)	94.85(18)
Ir(1)-C(4)	2.204(6)	C(6)-Ir(1)-Ir(2)	50.29(16)
Ir(1)-C(6)	2.179(7)	C(3)-Ir(2)-C(4)	96.8(2)
Ir(1)-Ir(2)	2.6926(4)	C(2)-C(1)-Ir(1)	99.5(4)
Ir(2)-C(3)	2.113(6)	C(1)-C(2)-C(3)	101.8(6)
Ir(2)-C(4)	2.156(7)	C(2)-C(3)-Ir(2)	114.6(4)
Ir(2)-C(5)	2.327(7)	C(5)-C(4)-Ir(2)	78.1(4)
Ir(2)-C(6)	2.120(7)	C(4)-C(5)-C(6)	102.9(6)
C(1)-C(2)	1.334(10)		
C(2)-C(3)	1.504(9)		
C(4)-C(5)	1.423(9)		
C(5)-C(6)	1.443(9)		

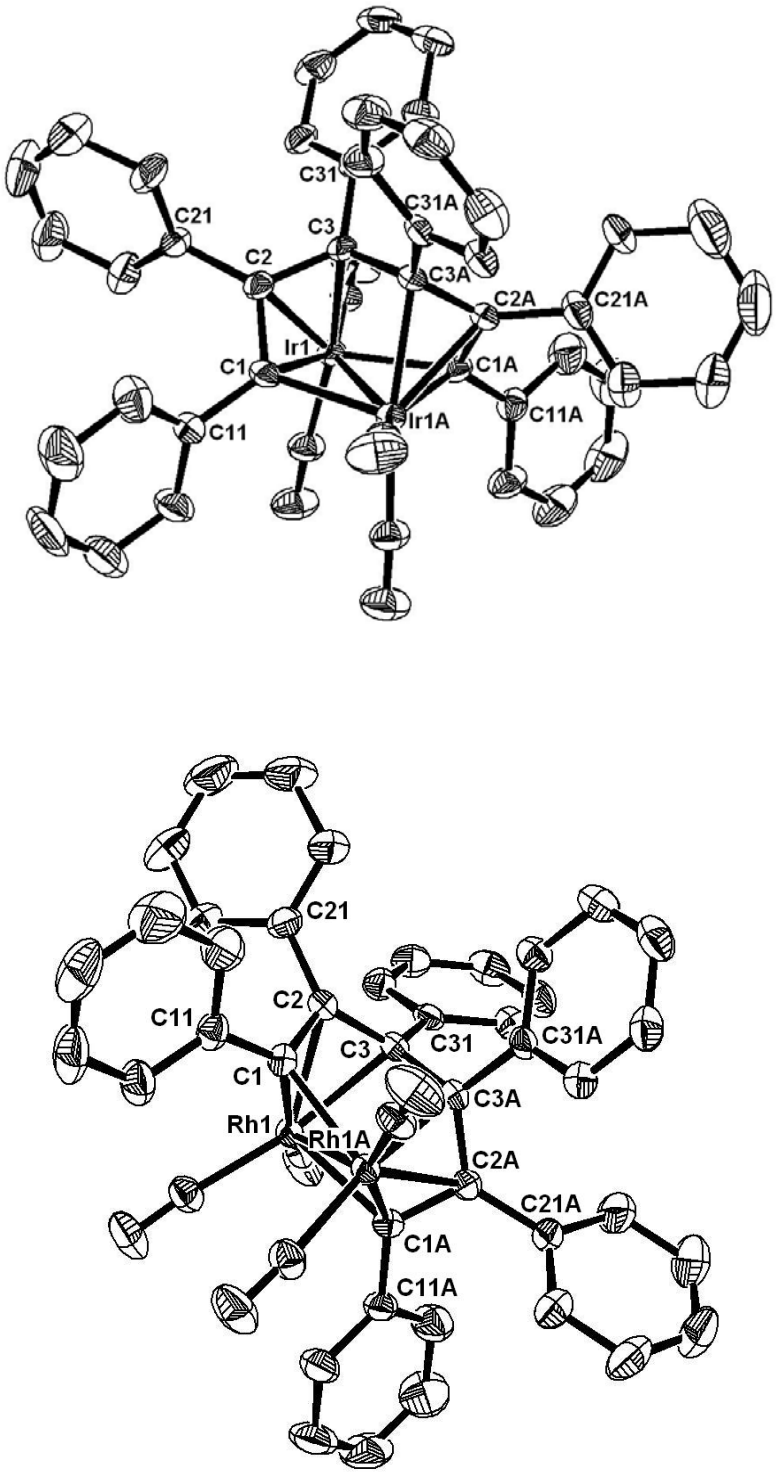

Figure 2.15. ORTEP diagrams of **14a** (top) and **14b** (bottom). Thermal ellipsoids are drawn at 50% probability level. The hydrogen atoms have been omitted for clarity.

Table 2.4. Selected bond distances (Å) for **14a** and **14b**.

	14a	**14b**
M1-C1	2.144(7)	2.098(3)
M1-C2	2.246(6)	2.237(3)
M1-C3	2.176(6)	2.172(2)
M1-C1A	2.136(7)	2.180(3)
M1-M1A	2.6974(5)	2.6963(4)
C1-C2	1.424(9)	1.415(3)
C2-C3	1.458(9)	1.455(4)
C3-C3A	1.539(12)	1.529(5)

Table 2.5. Selected bond angles (°) for **14a** and **14b**.

	14a	**14b**
C1-M1-M1A	50.81(18)	52.30(7)
C2-C1-M1	75.0(4)	76.36(16)
C1-C2-C3	110.6(5)	111.0(2)
C2-C3-C3A	114.9(6)	115.3(2)
C1A-M1-M1A	51.05(18)	49.59(7)

The molecular structure of **13** shows no coupling between the two ring-opened propenyl ligands; the distance between C1 and C3 [2.205 Å] shows that there is essentially no bond between them, indicating that the C1-C3 bond in the cyclopropenyl ligand has been broken. This is also the case for the other cyclopropenyl ligand (distance between C4 and C6 is 2.241 Å). The bond angles C1-C2-C3 and C4-C5-C6 has also opened to 101.8(6)° and 102.9(6)°, respectively.

An interesting feature of the molecular structure of **13** is the difference in the way the two ring-opened cyclopropenyl ligands bridge the Ir-Ir centers. The bond lengths in one of the ring-opened propenyl ligand are distinctly different. The C1-C2 bond length [1.334(10) Å) is typical of a double bond and the C2-C3 bond length [1.504(9) Å) is slightly shorter than a single bond. C3 has bonding interaction with both the iridium atoms while C1 has bonding interaction with only Ir1. In contrast, there is no distinct difference in bond lengths of the other ring-opened cyclopropenyl ligand. The bond lengths C4-C5 [1.423(9) Å] and C5-C6

[1.443(9) Å] are intermediate between that of a single and double bond as in the case of **14a** and **14b**.

The molecular structures of **14a** and **14b** show that ring opening and coupling of two cyclopropenyl rings have occurred; the resulting six carbon chain is bound to the metal centres in a similar fashion. The C-C bond lengths within a ring-opened cyclopropenyl ligand are typical of other known η^3-cyclopropenyl ligands which lie in between that of a single and double bond (1.54 Å and 1.34 Å respectively). They are joined by a single bond (C3-C3A) to form a six-membered acyclic chain, which wraps around the M-M bond.

Attempts to prevent cleavage of the cyclopropenyl ring by performing the reactions at a lower temperature (-78 °C) were unsuccessful; evaporation of the solvent under reduced pressure at low temperature gave essentially the same products. Attempts to dislodge the coupled ligand from **14a** by heating and reaction under high CO pressure also did not give any detectable organic species in the GC-MS analysis of the product mixture.

Although cyclopropenyl ring opening is known, formation of dinuclear complexes such as **13** and **14** has not been reported. The formation of compound **13** may involve initial binding of the cyclopropenyl ring to the Ir centre via a η^1-coordination mode followed by the loss of two CO ligands for each metal center. The two iridium centers are then bridged by two ring-opened cyclopropenyl ligands. It is, however, not clear why dinuclear species containing a metal-metal bond are observed here, while compounds obtained from the reaction of cyclopropenyl cations with transition metal complexes that were reported in the literature are monomeric (see Section 2.4.1).

2.5 Conclusion

Cyclopentadienyl iridium dicarbonyl complexes in which there is a side-chain carrying an amino group photochemically activate C-H bonds of cycloalkanes to give the corresponding hydridoalkyl species in a similar way to the reported complex $Cp^*Ir(CO)_2$. In a degassed solution or under an argon or hydrogen atmosphere, the dihydride species is formed in additional to the hydridoalkyl species while under an atmosphere of carbon monoxide, the cluster $Ir_4(CO)_{12}$ is produced. Intramolecular coordination of the amine group to the iridium center has not been observed. Employing in situ infrared measurements and using iterative band targeted entropy minimisation to analyse the spectra, allowed the detection the presence of many hitherto undetected products and intermediates in the C-H activation reaction of such iridium species, including a carboxaldehyde. The formation of the carboxaldehyde shows that the iridium complex can be photochemically activated to promote the carbonylation of alkanes.

Attempts at the activation of sp C-H bonds were made. Unexpected products such as **12b** where there is a CO insertion and coupling of three phenylacetylene molecules were isolated.

Attempted synthesis of cyclopropenyl iridium complexes from the reaction of a cyclopropenyl salt with an anionic metal carbonyl $[M(CO)_4]^-$ resulted in ring opening of the cyclopropenyl ligand to form complexes **13** and **14**.

2.6 Experimental

General

All operations were carried out using standard Schlenk techniques under an inert argon atmosphere unless otherwise stated. All solvents used were of AR grade except for cyclohexane (99.9%) and were distilled from appropriated drying agents and stored under argon prior to use. Cp^H,[29] Cp*^H,[30] $C_5H_5CH_2Ph$ ($Cp^{Bz}H$),[31] $[C_3Ph_3][BF_4]$,[32] $Cp^*Ir(CO)_2$, **2a**,[33] $Cp^*Ir(CO)Cl_2$, **9a**,[34] $Tp^*Rh(CO)_2$, **12a**,[35] $[PPN][Ir(CO)_4]^-$ and $[PPN][Rh(CO)_4]^-$[36] were prepared following published procedures. Compound **2a** was purified by column chromatography (alumina, activated, neutral, 50-200 microns, Acros / 100% hexane). Thallium salts of the corresponding cyclopentadienyl derivatives were prepared following a literature method.[37] The complexes $Cp^*{}^\wedge Ir(CO)_2$, **2b**, $Cp^\wedge Ir(CO)_2$, **2c** and $Cp^{Bz}Ir(CO)_2$, **2d**, were synthesized by a procedure analogous to that used for the synthesis of $CpIr(CO)_2$.[7] $Cp^*Ir(CO)(PPh_3)$, **7a** and $Cp^{Bz}Ir(CO)(PPh_3)$, **7b** were synthesized from the reaction of **2a** or **2d** with PPh_3 in nonane.[38] Alternatively, **7b** can also be synthesized form the reaction of $Cp^{Bz}Tl$ and $IrCl(CO)(PPh_3)_2$ as described in the literature.[39] All other reagents were purchased commercially and used as supplied.

Column chromatography was done using a silica gel packed column. TLC was done using plates coated with silica gel 60 F_{254} of 0.25 mm thickness.

NMR spectra were recorded either on a Bruker ACF 300 MHz or Bruker DPX 300 MHz spectrometer. Chemical shifts reported are with respect to residual solvent peaks. UV absorption spectra of starting complexes were recorded in cyclohexane on a Shimadzu 160 spectrometer. Gas Chromatography (GC) analyses were performed on a HP 6890 gas chromatograph equipped with a HP 5973 mass selective detector and a ZB-1 (30 m x 0.25 mm x 0.25 μm) capillary column, or with an HP5890 Series II plus equipped with an FID detector and a DB-5 (30 m x 0.32 mm x 0.25 μm) capillary column. Photolyses were carried out with either a Hanovia 450W UV lamp with a nominal λ_{max} of 254 nm, or a continuum Surelite III 10 ns pulse Nd-YAG laser operating at 3 mJ/pulse of 266 nm radiation.

Infrared spectra for routine analysis were recorded on a Bio-Rad FTS 165, a Digilab Excalibur Series FTS 3000MX, or a Shimadzu IR Prestige-21 FTIR-8400S FT-IR spectrometer at a resolution of 1 cm^{-1} using a solution IR cell with NaCl windows and a pathlength of 0.1 mm. Infrared spectra for in situ studies under ambient pressure were recorded on a Perkin Elmer 2000 FTIR spectrometer at a resolution of 4 cm^{-1} using a high pressure heatable liquid cell with ZnSe windows and a pathlength of 0.1 mm from Specac. Infrared spectra for high pressure studies were taken in a thermostatted high pressure cell constructed of 316 stainless steel and AMTIR windows with a pathlength of 0.5 mm.[40] Only carbonyl stretches in the 1600 – 2200 cm^{-1} region are reported except for the reactions involving acetylenes and acetylides.

BTEM deconvolution was carried out by Karl I. Krummel from the Department of Chemical and Biomolecular Engineering, National University of Singapore. All algorithms were implemented in MATLAB. Calculations were performed on an Intel Pentium III compatible personal computer of 551 MHz processing speed with 1 GB of RAM.

X-ray structure determination was carried out by A/P W. K. Leong. Crystals were mounted on quartz fibres. X-ray data were collected on a Bruker AXS APEX system, using Mo Kα radiation, with the SMART suite of programs.[41] Data were processed and corrected for Lorentz and polarization effects with SAINT,[42] and for absorption effects with the programme, SADABS.[43] Structural solution and refinement were carried out with the SHELXTL suite of programs.[44] The structures were solved by either direct methods or Patterson maps to locate the heavy atoms, followed by difference maps for the light, non-hydrogen atoms. Organic hydrogen atoms were placed in calculated positions.

2.6.1 Synthesis of cyclopentadienyl iridium complexes and their derivatives

Preparation of Cp*^Ir(CO)$_2$, 2b

Cp*^Li was prepared in situ from Cp*^H (98.2 mg, 0.509 mmol) and ^{n}BuLi (0.3 ml of 2.2M solution, 0.66 mmol) in hexane. The suspension was cannula transferred into a

suspension of $Ir(CO)_3Cl$ (102.0 mg, 0.327 mmol) in hexane (10 ml) in a Carius tube. The mixture was degassed and heated at 70 ºC for 2 d. The resultant mixture was cooled and filtered through celite to remove unreacted starting materials. The yellow filtrate was dried under reduced pressure to give **2b** as yellow oil.

IR (cyclohexane) 1954, 2020 cm^{-1}; ^1H NMR ($CDCl_3$) δ 2.60-2.54 (m, 2H, C*H*$_2$-N) 2.27 (s, 6H, N-C*H*$_3$), 2.26-2.19 (m, 2H, C*H*$_2$), 2.15 (s, 6H, ring C*H*$_3$), 2.16 (s, 6H, ring C*H*$_3$). The ^1H NMR data matched the literature values.[45, 4a]

Preparation of $Cp^{\wedge}Ir(CO)_2$, 2c

A degassed suspension of $Cp^{\wedge}Tl$ (432.0 mg, 1.27 mmol) and $Ir(CO)_3Cl$ (217.0 mg, 0.696 mmol) in hexane (20 ml) was heated in a Carius tube at 80 ºC for 2 d. The resultant mixture was cooled and filtered through celite to remove unreacted starting materials. The yellow filtrate was dried under reduced pressure to give **2c** as yellow oil.

IR (cyclohexane) 1967, 2034 cm^{-1}; ^1H NMR ($CDCl_3$) δ 5.52 (m, 2H, C_5H_4), 5.37 (m, 2H, C_5H_4), 2.58-2.36 (m, 4H, C*H*$_2$C*H*$_2$), 2.26 (s, 6H, N-C*H*$_3$). The ^1H NMR data matched the literature values.

Preparation of $Cp^{Bz}Ir(CO)_2$, 2d

The complex $Cp^{Bz}Ir(CO)_2$, **2d** was prepared from $Cp^{Bz}Tl$ (55.0 mg, 0.154 mmol) and $Ir(CO)_3Cl$ (21.2 mg, 0.068 mmol) in an analogous manner to give **2d** as a yellow oil.

IR (cyclohexane) 1969, 2036 cm^{-1}; ^1H NMR ($CDCl_3$) δ 7.23 (m, 5H, C_6H_5), 5.45 (m, 2H, C_5H_4), 5.37 (m, 2H, C_5H_4), 3.77 (s, 2H, C*H*$_2$). The IR data matched the literature values.

Preparation of $Cp^{Bz}Ir(CO)(PPh_3)_2$, 7b

A degassed suspension of $Cp^{Bz}Tl$ (60.0 mg, 0.166 mmol) and $IrCl(CO)(PPh_3)_2$ (90.0 mg, 0.115 mmol) in toluene (20 ml) was heated in a Carius tube at 80 ºC for 3 d in an analogous method to the literaure which uses toluene as a solvent. Alternatively, **7b** can be prepared from the reaction of **2d** (80.0 mg, 0.198 mmol) with PPh_3 (78.0 mg, 0.29 mmol) in refluxing nonane (5 ml) for 15 h using a similar procedure to that for the preparation of **7a** described in the literature.[38]

IR (nonane) 1931 cm^{-1}. ^{31}P NMR (C_6D_6) δ 17.55 (s). The ^{1}H NMR and ^{31}P NMR chemical shifts in $CDCl_3$ matched the literature values.

2.6.2 Preparative photolysis

A solution of the metal complex in the hydrocarbon solvent (l mg/ml) was placed in a closed quartz tube, degassed by three cycles of freeze-pump-thaw, and then irradiated with a 450W water-cooled, medium pressure, mercury lamp placed approximately 15 cm away while continuously stirred. For reaction under CO atmosphere, the quartz tube was refilled with 1 atm of CO from the Schlenk line after degassing. For the laser irradiation, dichroic mirrors were used to direct the pulses; cooling by water circulation was not necessary.

Table 2.6. Summary of photochemical reactions of **2a** – **2d**, **7a** and **7b**.

Starting Ir compound	Solvent	Atmosphere	Length of photolysis*	Products
2a	Cyclohexane	In vacuo	5 h	**3a**
		1 atm CO	5 h	**3a** + **6**
	Cyclopentane	In vacuo	5 h	**4a**
2b	Cyclohexane	In vacuo	up to 16 h	**3b** + **5b** + **A**
		1 atm argon	4 h	**3b** + **5b** + **A**
		1 atm CO	6 h	**3b** + **6**
	Cyclopentane	In vacuo	10 h	**4b** + **5a** + **B**
		1 atm hydrogen	3 h	**4b** + **5a** + **B**
		1 atm argon	4 h	**4b** + **5a** + **B**
		1 atm CO	3 h	**4b** + **6**
2c	Cyclohexane	In vacuo	up to 6 h	**3c** + **5c**
			up to 2 h 15 min (laser)	**3c** + **5c**
2d	Cyclohexane	In vacuo	5 h	**3d** + **5d**
7a	Cyclohexane	In vacuo	5	No C-H activation
7b	Cyclohexane	In vacuo	3	No C-H activation
	Cyclopentane	In vacuo	3	No C-H activation

* UV irradiation unless otherwise stated.

Table 2.7. IR and NMR data of products.

Compound	ν_{CO}/ **cm^{-1}** (in cyclohexane)	**^{1}H NMR** (hydride region)[a] (in d_8-toluene)
3a	1981	-16.48
3b	1981	-16.47
3c	1995	-16.45
3d	1997	-16.48
4a	1980 (cyclopentane)	-15.71 (C_6D_6)
4b	1982 (cyclopentane)	-15.80; -15.70 (C_6D_6)
5a	1996	-15.76 (C_6D_6)
5b	1996	-15.90
5c	2010	-16.06
5d	2012	-14.61
6	2069, 2029	-
9a	2058 (dcm)	-
9b	2058 (dcm)	-
A	-	-17.51
D	-	-17.71

[a]all resonances reported are singlets.

Photolysis of 6 and Cp*H in cyclohexane

To a suspension of **6** (10.0 mg, 9.1 μmol) in cyclohexane (10 ml) was added Cp*H (4.9 mg, 36.0 μmol). The mixture was subjected to 4 h irradiation in vacuo. IR analysis shows the presence of CO stretches due to **2a** and unreacted **6**. The CO stretches due to **3a** appeared after an additional 2.5 h of irradiation.

Reversible activation in hydrocarbon solvents

A solution of **2b** in cyclohexane (5 ml) was photolysed for 3 h at 0 ºC during which **2b** was partially converted to **3b** and **5b**. The volatiles were removed under reduced pressure and the residue was redissolved in cyclopentane (5 ml). The reaction mixture was degassed by three cycles of freeze-pump-thaw and heated in a Carius at 70 ºC for 20 h. IR analysis showed only the presence of **3b**, **5b** and unreacted **2b**. The solution was photolysed for 3 h in cyclopentane. IR analysis showed that **3b** has been consumed with the formation of **4b**.

2.6.3 In situ infrared measurements

For ambient pressure measurements, a well-stirred solution of **2a** or **2b** in cyclohexane was circulated between the quartz reactor and a ZnSe cell through viton (internal diameter 2.06mm) and tygon tubings using a peristaltic pump (MASTERflex C/L 5910 pump systems model 77120-62). UV irradiation was carried out through the quartz reactor. The reactor was fan cooled and the temperature was not controlled. The atmosphere was either argon or carbon monoxide.

For the high pressure measurements, a solution of **2a** in cyclohexane was circulated between a 100 ml stainless steel autoclave type reactor, a high pressure cell of original design (AMTIR windows) and an industrial sapphire tube (Almaz Optics, Inc, Marlton, New Jersey) of 5 mm internal diameter (I.D.) via stainless steel tubings of 1/16 inch I.D. under various CO pressures. UV irradiation was carried out through the sapphire tube. The temperature was kept at 20 °C via cryostat control.

2.6.4 Reaction with alkynes

Reaction of 2a with phenylacetylene

i) With UV irradiation

Compound **2a** (8.0 mg, 20.9 μmol) was dissolved in phenylacetylene (1 ml) in a Carius tube. The reaction mixture was degassed by three cycles of freeze-pump-thaw and subjected to UV photolysis for 4.5 h. The reaction mixture turned red but IR analysis shows only CO stretching vibrations due to **2a**. Unreacted **2a** was removed by extraction with hexane. The remaining red oil did not show resonance due to the Cp* ligand in the ^{1}H NMR.

i) Without UV irradiation

Compound **2a** (10.0 mg, 26.0 μmol) was dissolved in phenylacetylene (0.5ml) and stirred at room temperature for 15 h. IR and NMR analysis show only the presence of starting materials.

The reaction mixture was heated at 100 ºC for 15 h and subsequently at 133 ºC for 15 h in a Carius tube. IR analysis shows only carbonyl stretches due to **2a**.

TMANO (2 eq) was added and the mixture was heated at 100 ºC for 15h. IR analysis of the crude mixture shows no carbonyl stretching vibrations.

^{1}H NMR ($CDCl_3$): δ 8.0 – 7.0 (m, aromatic), 1.0 – 2.0 (many small peaks).

MS FAB$^+$ (*m*/*z*): 1246 $[M]^+$, 1142 $[M - (PhCCH)]^+$. (and fragments corresponding to subsequent loss of 6 PhC≡CH units).

Reaction of Cp*Ir(CO)Cl_2, 9a with phenylacetylene

Compound **9a** (25.0 mg, 58.7 μmol) was dissolved in phenylacetylene (3 ml) and stirred at room temperature for 4 d. The volatiles were removed under reduced pressure. The residue was redissolved in a minimum amount of dcm and 2/3 of the crude was subjected to two rounds of TLC separation using dcm:hexane (3:7, v/v) as eluent followed by dcm:hexane (4:7, v/v) to give two major yellow bands and several other faint bands. Band 1 (R_f = 0.65)

yielded a product identified to be Cp*Ir(CO)[PhC=CHC(Ph)=CCH=CCl(Ph)], **10** (7.4 mg, 27%). X-ray diffraction quality crystals of **10** were grown from a toluene/hexane solution at 5 ºC.

IR (dcm): ν_{CO} 1995 (s) cm^{-1}. ^1H NMR ($CDCl_3$): δ 7.7-7.0 (m, 17H, aromatic), 1.71 (s, 15H, Cp*C*H*$_3$). MS FAB^+ (*m*/*z*): 696 $[M]^+$. HR-MS FAB^+ (*m*/*z*): calcd for $C_{35}H_{32}OClIr$: 696.1771, found: 696.1744.

Band 2 was close to the baseline and overlapped with a faint purple band (total amount: 2.9 mg). It was unstable on TLC. When the impure band was isolated and re-eluted with dcm:hexane (1:1, v/v), it decomposed to a product with no CO stretch in the IR spectrum.

IR before re-TLC (dcm): ν_{CO} 2025 (s) cm^{-1}. ^1H NMR ($CDCl_3$): δ 7.7-6.5 (m), 1.90 (s) MS FAB^+ (*m*/*z*): 908.

Crude:

IR (dcm): ν_{CO} 2032 cm^{-1}. ^1H NMR ($CDCl_3$): δ 7.7 - 7.0 (m, aromatic), 1.1 - 2.0 (many peaks).

* When the reaction of Cp*Ir(CO)Cl_2 with phenylacetylene was done using stoichiometric amount of phenylacetylene (and again using 20 equivalents of phenylacetylene) at room temperature, there was no product formation.

Reaction of 9a with lithium phenylacetylide

Lithium phenylacetylide was freshly prepared from the reaction of 2.2 M ^{n}BuLi (0.75 ml) with phenylacetylene (0.21 ml) in THF (made up to 10 ml) at -78 °C using a dry-ice/acetone bath. The desired amount of the phenylacetylide solution was syringed out while cold. To a solution of **9a** (72.0 mg, 169 μmol) in THF (2 ml) was added the lithium phenylacetylide (2 eq.) at -78 °C. The solution was stirred for 15 min before warming up to room temperature. Any unreacted lithium phenylacetylide was destroyed by quenching with "wet" THF. The solution was concentrated under reduced pressure and subjected to TLC separation using ether: hexane (1:4, v/v) as eluent to yield a yellow band identified to be **11**

(42.9 mg, 46%; R_f = 0.55). X-ray diffraction quality crystals of **11** were grown from a dcm/hexane solution at 5 ºC.

IR (KBr): $\nu_{C\equiv C}$ 2159 (w), ν_{CO} 1937 (s) cm^{-1}. IR (Hex): $\nu_{C\equiv C}$ 2165 (w), ν_{CO} 1971 (s) cm^{-1}. IR (THF): $\nu_{C\equiv C}$ 2161 (w), ν_{CO} 1956 (s) cm^{-1}. ^{1}H NMR (CD_2Cl_2): δ 7.7 - 7.2 (m, 10H, aromatic), 2.05 (s, 15H, Cp*C*H*$_3$). MS FAB$^+$ (*m*/*z*): 558 $[M]^+$, 530 $[M - CO]^+$. Anal. Calcd for $C_{27}H_{25}OIr$: C, 58.15; H, 4.52. Found: C, 58.21; H, 4.27. HR-MS FAB$^+$ (*m*/*z*): calcd for $C_{27}H_{25}OIr$: 558.1535, found: 558.1549.

Reaction of 9a with phenylacetylene in the presence of triethylamine

i) To a solution of **9a** (10.0 mg, 23.5 μmol) in THF (3 ml) was added phenylacetylene (5.2 μl, 2 eq) and triethylamine (6.6 μl, 2 eq). The solution was stirred at room temperature for 3 h. The volatiles were removed under reduced pressure and the residue was extracted with hexane to give two weak intensity peaks due to CO stretching vibrations of **10** and an unidentified product, **E** (2041 cm^{-1}). The remaining residue contained unreacted **9a** and another unidentified product **F**. The ratio of **F** to **9a** is 2:3 from ^{1}H NMR integration.

ii) To a solution of **9a** (10.0 mg, 23.5 μmol) in THF (3 ml) was added phenylacetylene (5.2 μl, 20 eq) and triethylamine (0.66 ml, 200 eq). The solution was stirred at room temperature for 3 h during which **9a** is completely consumed. The volatiles were removed under reduced pressure. The residue was insoluble in hexane. Extraction with dcm afforded **F** as the major product.

F:

IR (dcm): ν_{CO} 2047 (s) cm^{-1}. ^{1}H NMR ($CDCl_3$): δ 7.5-7.0 (m, aromatic), 2.03 (s, Cp*C*H*$_3$) and many small peaks between 2.0-1.5. MS FAB$^+$ (*m*/*z*): 940 $[M]^+$, 838 $[M – (PhCCH)]^+$, 736 $[M – 2(PhCCH)]^+$, 634 $[M – 3(PhCCH)]^+$. MS EI$^+$ (*m*/*z*): 306 $[3(PhCCH)]^+$.

Reaction of Tp*Rh(CO)$_2$, 12a with phenylacetylene

Compound **12a** (60.0 mg, 132 μmol) was dissolved in phenylacetylene (3 ml) and stirred at room temperature for 20 h during which the solution turned from yellow to red. The excess phenylacetylene was removed under reduced pressure and the residue was redissolved in a minimum amount of toluene. Hexane (4 ml) was added to precipitate out **12b** as a yellow solid. The solid was separated from the superrnatant by cannula filtration and washed with hexane (3 x 2 ml). It can be further purified by TLC with dcm: hexane (1:4, v/v) as eluent to give a yellow band (45.8 mg, 47%; R_f 0.13). X-ray diffraction quality crystals of **12b** were grown from a toluene/ hexane solution at 5 ºC.

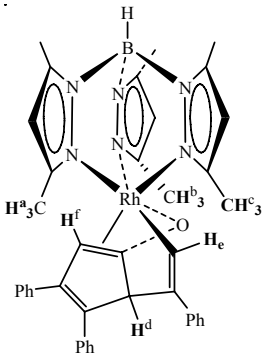

^{1}H NMR ($CDCl_3$): δ 7.1 – 6.8 (m, 16H, aromatic), 6.21 (s, 1H, H^e), 5.81 (s, 1H, Tp*C*H*), 5.75 (s, 2H, Tp*C*H*), 5.18 (s, 1H, H^d), 2.50 (s, 3H, Tp*CH_3), 2.48 (s, 3H, Tp*CH_3), 2.41 (s, 3H, Tp*CH_3), 2.20 (s, 3H, Tp*CH^b_3), 2.09 (s, 3H, Tp*CH^c_3), 1.89 (s, 3H, Tp*CH^a_3). ^{1}H NMR (CD_2Cl_2): δ 7.1 – 6.8 (m, 16H, aromatic), 6.14 (s, 1H, H^e), 5.86 (s, 1H, Tp*C*H*), 5.82 (s, 1H, Tp*C*H*), 5.78 (s, 1H, Tp*C*H*), 5.19 (s, 1H, H^d), 2.50 (s, 3H, Tp*CH_3), 2.47 (s, 3H, Tp*CH_3), 2.42 (s, 3H, Tp*CH_3), 2.15 (s, 3H, Tp*CH^b_3), 2.06 (s, 3H, Tp*CH^c_3), 1.88 (s, 3H, Tp*CH^a_3). MS FAB$^+$ (*m*/*z*): 734 $[M]^+$. Anal. Calcd for $C_{40}H_{40}BN_6ORh$: C, 65.41; H, 5.49; N, 11.44. Found: C, 65.24; H, 5.75; N, 10.81. HR-MS FAB$^+$ (*m*/*z*): Calcd for $C_{40}H_{40}{}^{[11]}BN_6O^{[103]}Rh$: 734.2406, found: 734.2402.

Organic products in the supernatant detected by GC-MS:

Compound	Quality	Retention time/ min
Styrene	94	7.49
(1*E*,3*E*)-1,4-diphenylbuta-1,3-diene	99	18.63
1,2,4-triphenylbenzene	99	23.23
1,3,5triphenylbenzene	99	25.15

*Reaction of **12a** with phenylacetylene only occurred in the presence of large excess of phenylacetylene (more than 100 eq.) When the reaction was done using stoichiometric amount of phenylacetylene (and up to 10 eq. of phenylacetylene) in toluene at room temperature, **12b** was not formed although the solution turned red.

The reaction was repeated with **12a** (30.0 mg, 65.8 μmol) in PhC≡CD (0.5 ml). The mixture was stirred at room temperature for 17 h.

12b-d:

^{1}H NMR (CD_2Cl_2): δ 7.1 – 6.8 (m, 15H, aromatic), 5.86 (s, 1H, Tp*C*H*), 5.81 (s, 1H, Tp*C*H*), 5.78 (s, 1H, Tp*C*H*), 2.50 (s, 3H, Tp*CH_3), 2.47 (s, 3H, Tp*CH_3), 2.41 (s, 3H, Tp*CH_3), 2.15 (s, 3H, Tp*C$H^b{}_3$), 2.06 (s, 3H, Tp*C$H^c{}_3$), 1.88 (s, 3H, Tp*C$H^a{}_3$). MS FAB$^+$ (*m*/*z*): 737 $[M]^+$

Reaction of 12a with ^{t}butylacetylene

Compound **12a** (10.0 mg, 21.9 μmol) was suspended in ^{t}butylacetylene (0.2 ml) and stirred at room temperature for 1 d. No observable changes occurred. THF (0.5 ml) was added and the solution was stirred overnight at room temperature. The excess ^{t}butylacetylene was removed under reduced pressure. IR analysis shows that **12a** remained unreacted. 1,3,5-tri-^{t}butylbenzene (t_r = 15.31 min, Q = 95) was detected in the GC-MS spectrum.

Reaction of 12a with Diphenylacetylene

A solution of **12a** (10.0 mg, 21.9 μmol) and diphenylacetylene (39.2 mg, 219 μmol) in toluene (5 ml) was stirred at room temperature for 15 h. IR analysis showed no change in the carbonyl stretching region. Diphenylacetylene (350.0 mg, 1.96 mmol) was added and the solution was heated at 110 °C for 1 d. IR analysis showed no change in the CO stretching region.

GC-MS analysis of the crude mixture showed mainly unreacted diphenylacetylene and small amounts of other organic products.

Compound	Quality	Retention time, t_r/ min
E – stilbene	98	17.14
Cis – stilbene	96	15.81

2.6.5 Reaction of $[M(CO)_4]^-$ with $[C_3Ph_3][BF_4]$

Reaction of $[PPN][Ir(CO)_4]^-$ with $[C_3Ph_3][BF_4]$

$[PPN][Ir(CO)_4]$ (106.0 mg, 126 μmol) was dissolved in dcm (5 ml) in a Schlenk tube. A suspension of $[C_3Ph_3][BF_4]$ (45.0 mg, 127 μmol) in dcm (5 ml) was added dropwise at room temperature. The solution turned wine-red and darkened to deep purple within a few minutes. The solution was stirred at room temperature for 0.5 hour after which the solvent was removed under reduced pressure. The resultant purple oil was extract with toluene (3 x 2 ml). The residue is soluble in dcm and found to contain $[PPN][BF_4]$ (51.8 mg, 66%). The toluene extract was concentrated under reduced pressure and subjected to TLC separation using ether:hexane (1:2, v/v) as eluent to give two major bands which overlapped. The two bands could not be completely separated even after another round of elution. Other minor bands were not characterized as their IR spectra did not show any CO vibrations. X-ray diffraction quality crystals of **13** and **14a** were grown from a dcm/ hexane solution at 5 ºC.

Band 1 (purple) (R_f = 0.57) afforded black crystals identified to be **13** (17.3 mg, 13%). IR (toluene): ν_{CO} 2059 (m), 2037 (vs), 2011 (m), 1990 (m) cm^{-1}. IR (hex): ν_{CO} 2061 (m), 2041 (vs), 2016 (m), 1996 (m) cm^{-1}. ^1H NMR ($CDCl_3$): δ 7.5 – 6.7 (m, aromatic). MS FAB^+ (*m*/*z*): 1030 $[M]^+$. HR-MS FAB^+ (*m*/*z*): calcd for $C_{46}H_{30}O_4{}^{[191]}Ir^{[193]}Ir$: 1030.1374, found: 1030.1381. HR-MS FAB^+ (*m*/*z*): calcd for $C_{46}H_{30}O_4{}^{[193]}Ir_2$: 1032.1397, found: 1032.1422.

Band 2 (yellow) (R_f = 0.54) afforded dark red crystals identified to be **14a** (43.4 mg, 34%). IR (tol): ν_{CO} 2055 (s), 2030 (vs), 1990 (m), 1976 (s) cm^{-1}. IR (hex): ν_{CO} 2059 (m), 2054 (w), 2033 (vs), 1996 (w) 1990 (w), 1981 (s) cm^{-1}. ^1H NMR ($CDCl_3$): δ 7.5 – 6.7 (m,

aromatic). Anal. Calcd for $C_{46}H_{30}O_4Ir_2$.1/2ether: C, 54.15; H, 3.58. Found: C, 54.02; H, 3.54. MS FAB^+ (*m*/*z*): 1030 $[M]^+$. HR-MS FAB^+ (*m*/*z*): calcd for $C_{46}H_{30}O_4{}^{[191]}Ir^{[193]}Ir$: 1030.1374, found: 1030.1339. HR-MS FAB^+ (*m*/*z*): calcd for $C_{46}H_{30}O_4{}^{[193]}Ir_2$: 1032.1397, found: 1032.1362.

The same reaction was repeated at -78 °C in a dry ice-acetone bath. The stirred solution was slowly warmed up until the reaction was completed (as indicated by the disappearance of peaks in the carbonyl stretching region due to $[Ir(CO)_4]^-$ from IR monitoring). Evaporation of the solvent under reduced pressure at low temperature gave essentially the same products.

Reaction of $[PPN][Rh(CO)_4]^-$ with $[C_3Ph_3][BF_4]$

$[PPN][Rh(CO)_4]$ (90.0 mg, 119 μmol) was dissolved in dcm (5 ml) in a Schlenk tube and cooled to -78 °C in a dry ice-acetone bath. A suspension of $[C_3Ph_3][BF_4]$ (45.0 mg, 127 μmol) in dcm (5 ml) was added dropwise. The solution was stirred and allowed to warm to room temperature during which the solution darkened to wine-red. The solvent was removed under reduced pressure and the residue was redissolved in a minimum amount of dcm and subjected to TLC separation. Elution with dcm:hexane (1:3, v/v) as eluent afforded a red band leaving an immovable pale red band on the baseline. The red band was identified to be $C_{46}H_{30}O_4Ir_2$, **14b** (49.4 mg, 49%, R_f 0.37). X-ray diffraction quality crystals of **14b** were grown from a hexane solution at 5 ºC.

IR (KBr): ν_{CO} 2054 (m), 2031 (vs), 2009 (s), 1995 (w) cm^{-1}. IR (hex): ν_{CO} 2060 (m), 2045 (vs), 2014 (s), 2004 (w) cm^{-1}. ^1H NMR ($CDCl_3$): δ 7.8 - 6.8 (m, aromatic). MS FAB^+ (*m*/*z*): 824 $[M - CO]^+$, 796 $[M - 2(CO)]^+$, 768 $[M - 3(CO)]^+$, 740 $[M - 4(CO)]^+$. Anal. Calcd for $C_{46}H_{30}O_4Rh_2$: C, 64.81; H, 3.55. Found: C, 64.83; H, 4.03. HR-MS FAB^+ (*m*/*z*): calcd for $C_{46}H_{30}O_4{}^{[103]}Rh_2$: 852.0249, found: 852.0259.

Table 2.8. Crystal data for **10**, **11** and **12b**.

Compound	**10**	**11**	**12b**
Empirical formula	$C_{35}H_{32}ClIrO$	$C_{27}H_{25}IrO$	$C_{41.75}H_{43.50}BCl_{3.50}N_6ORh$
Formula weight	696.26	557.67	883.12
Temperature	223(2)	223(2)	223(2)
Crystal system	Monoclinic	Monoclinic	Monoclinic
Space group	$P2_1/n$	$P2_1/c$	$P2_1/c$
Unit cell dimensions			
a (Å)	7.6184(3)	18.4357(8)	11.2103(6) Å
b (Å)	19.6501(8)	16.7744(7)	11.0618(6) Å
c (Å)	19.0083(9)	7.2934(3)	33.8705(18) Å
α (°)	90	90	90
β (°)	90.8320(10	94.3090(10)	99.363(2)
γ (°)	90	90	90
Volume ($Å^3$)	2845.3(2)	2249.09(16)	4144.2(4)
Z	4	4	4
Density calc. (Mg m^{-3})	1.625	1.647	1.415
Absorption coefficient (mm^{-1})	4.813	5.951	0.678
F(000)	1376	1088	1814
Crystal size (mm^3)	0.12 x 0.10 x 0.08	0.26 x 0.20 x 0.06	0.14 x 0.06 x 0.06
Theta range for data collection (°)	2.07 to 26.37.	2.22 to 26.37	2.04 to 26.37
Index ranges	$-9 \le h \le 9$	$-23 \le h \le 22$	$-14 \le h \le 13$
	$0 \le k \le 24$	$0 \le k \le 20$	$0 \le k \le 13$
	$0 \le l \le 23$	$0 \le l \le 9$	$0 \le l \le 42$
Reflections collected	24986	34349	52807
Independent reflections	5832 [R(int) = 0.0497]	4591 [R(int) = 0.0393]	8471 [R(int) = 0.1215]
Completeness to theta (%)	= 26.37°; 100.0	= 26.37°; 100.0	= 26.37°; 100.0
Max. and min. transmission	0.6994 and 0.5959	0.7166 and 0.3068	0.9604 and 0.9110
Data / restraints / parameters	5832 / 0 / 348	4591 / 0 / 362	8471 / 15 / 515
Goodness-of-fit on F^2	1.079	1.164	1.116
Final R indices [$I>2\sigma(I)$]	R1 = 0.0369, wR2 = 0.0786	R1 = 0.0335, wR2 = 0.0819	R1 = 0.0800, wR2 = 0.1498
R indices (all data)	R1 = 0.0476, wR2 = 0.0829	R1 = 0.0369, wR2 = 0.0836	R1 = 0.1211, wR2 = 0.1667
Largest diff. peak and hole ($e.Å^{-3}$)	1.430 and -0.843	2.672 and -0.641	1.063 and -0.692

Table 2.9. Crystal data for **13**, **14a**, **14b**.

Compound	**13**	**14a**	**14b**
Empirical formula	$C_{46}H_{30}Ir_2O_4$	$C_{46}H_{30}Ir_2O_4$	$C_{46}H_{30}Rh_2O_4$
Formula weight	1031.10	1031.10	852.52
Temperature	223(2)	223(2)	223(2)
Crystal system	Triclinic	Monoclinic	Monoclinic
Space group	$P\bar{1}$	C2/c	C2/c
Unit cell dimensions			
a (Å)	11.2098(8)	12.8167(11)	12.7410(3)
b (Å)	11.6987(8)	19.5537(18)	19.6927(4)
c (Å)	16.2944(12)	15.4177(14)	15.4404(3)
α (°)	71.4880(10)	90	90
β (°)	74.6470(10	106.897(2)	106.5150(10)
γ (°)	65.5560(10)	90	90
Volume ($Å^3$)	1822.5(2)	3697.1(6)	3714.24(14)
Z	2	4	4
Density calc. (Mg m^{-3})	1.879	1.852	1.525
Absorption coefficient (mm^{-1})	7.339	7.236	0.932
F(000)	984	1968	1712
Crystal size (mm^3)	0.34 x 0.08 x 0.04	0.16 x 0.10 x 0.08	0.27 x 0.14 x 0.09
Theta range for data collection (°)	2.02 to 26.37	2.08 to 29.48	2.07 to 30.40
Index ranges	$-13 \le h \le 14$	$-16 \le h \le 16$	$-18 \le h \le 17$
	$-13 \le k \le 14$	$0 \le k \le 25$	$0 \le k \le 27$
	$0 \le l \le 20$	$0 \le l \le 21$	$0 \le l \le 21$
Reflections collected	16752	15398	19917
Independent reflections	7438 [R(int) = 0.0347	4689 [R(int) = 0.0555]	5453 [R(int) = 0.0449]
Completeness to theta (%)	= 26.37°; 99.8	= 29.48°; 91.1	= 30.40°; 96.9
Max. and min. transmission	0.7578 and 0.1893	0.5952 and 0.3906	0.9208 and 0.7869
Data / restraints / parameters	7438 / 0 / 469	4689 / 0 / 235	5453 / 0 / 235
Goodness-of-fit on F^2	1.020	1.059	1.085
Final R indices [$I>2\sigma(I)$]	R1 = 0.0386, wR2 = 0.0782	R1 = 0.0480, wR2 = 0.0967	R1 = 0.0430, wR2 = 0.0883
R indices (all data)	R1 = 0.0591, wR2 = 0.0850	R1 = 0.0689, wR2 = 0.1042	R1 = 0.0554, wR2 = 0.0944
Largest diff. peak and hole (e.$Å^{-3}$)	1.776 and -1.140	3.458 and -1.125	0.862 and -0.360

References

[1] (a) Janowicz, A. H.; Bergman, R. G. *J. Am. Chem. Soc.* **1982**, *104*, 352-354. (b) Hoyano, J. K.; Graham, W. A. G. *J. Am. Chem. Soc.* **1982**, *104*, 3723-3725. (c) Janowicz, A. H.; Periana, R. A.; Buchanan, J. M.; Kovac, C. A.; Stryker, J. M.; Wax, M. J.; Bergman, R. G. *Pure & Applied Chem*. **1984**, *56*, 13-23. (d) Bengali, A. A.; Schultz, R. H.; Moore, C. B.; Bergman, R. G. *J. Am. Chem. Soc.* **1994**, *116*, 9585-9589. (d) Belt, S. T.; Grevels, F. W.; Klotzbucher, W. E.; McCamley, A.; Perutz, R. N. *J. Am. Chem. Soc.* **1989**, *111*, 8373-8382.

[2] Muller, C.; Vos, D.; Jutzi, P. *J. Organomet. Chem*. **2000**, *600*, 127-143.

[3] Jutzi, P.; Redeker, T. *Eur. J. Inorg. Chem.* **1998**, 663-674.

[4] (a) Jutzi, P.; Kristen; M. O.; Dahlhaus, J.; Neumann, B.; Stammler, H. G. *Organometallics* **1993**, *12*, 2980-2985. (b) Jutzi, P.; Kristen; M. O.; Neumann, B.; Stammler, H. G. *Organometallics* **1994**, *13*, 3854-3861.

[5] (a) Bromberg, S. E.; Lian, T.; Bergman, R. G.; Harris, C. B. *J. Am. Chem. Soc.* **1996**, *118*, 2069-2072. (b) Lees, A. J. *J. Organomet. Chem*. **1998**, *554*, 1-11.

[6] Ball, R.G.; Graham, W. A. G.; Heinekey, D. M.; Hoyano, J. K.; McMaster, A. D.; Mattson, B. M.; Michel, S. T. *Inorg. Chem*. **1990**, *29*, 2023-2025.

[7] Gardner, S. A.; Andrews, P. S.; Rausch, M. D. *Inorg. Chem*. **1973**, *12*, 2396-2402.

[8] (a) Graham, W. A. G. *J. Organomet. Chem*, **1986**, *300*, 81-91. (b) Heinekey, D. M.; Fine, D. A..; Harper, T. G. P.; Michel, S. T. *Can. J. Chem*, **1995**, *73*, 1116-1125.

[9] Heinekey, D. M.; Fine, D. A.; Harper, T. G. P.; Michel, S. T. *Can. J. Chem*, **1995**, *73*, 1116-1125.

[10] (a) Sakakura, T.; Sodeyama, T.; Sasaki, K.; Wada, K.; Tanaka, M. *J. Am. Chem. Soc.* **1990**, *112,* 7221-7229. (b) Rosini, G. P.; Zhu, K. M.; Goldman, A. S. *J. Organomet. Chem*. **1995**, *504*, 115-121. (c) Rosini, G. P.; Boese, W. T.; Goldman, A. S. *J. Am. Chem. Soc.* **1994**, *116*, 9498-9505.

[11] Tanaka, M.; Sakukara, T. In *Homogeneous Transition Metal Catalyzed Reactions*; Moser, W. R.; Slocum, D. W. Eds.; Advances in Chemistry Series 230; American Chemical Society: Washington, DC, 1992; Chapter 12; pp181-196.

[12] Pruchnik, F. P.; Waijda-Hermanowicz, K.; Koralewicz, M. *J. Organomet. Chem*. **1990**, *384*, 381-383.

[13] Bergman, R. G. *Science* **1984**, *223*, 902-908.

[14] (a) Chew, W.; Widjaja, E.; Garland, M. *Organometallics* **2002**, *21*, 1982-1990. (b) Widjaja, E.; Li, C.; Garland, M. *Organometallics* **2002**, *21*, 1991-1997.

[15] (a) Feng, J.; Garland, M. *Organometallics* **1999**, *18*, 417-427. (b) Liu, G.; Volken, R.; Garland, M. *Organometallics* **1999**, *18*, 3429-3436. (c) Cordaro, J. G.; Bergman, R. G. *J. Am. Chem. Soc.* **2004,** *126*, 16912-16929.

[16] Werner, H.; Gevert, O.; Haquette, P. Organometallics **1997**, *16*, 803-806.

[17] (a) Bloyce, P. E.; Mascetti, J.; Rest, A. J.; *J. Organomet. Chem.* **1993**, *444*, 223-233. (b) Slugovc, C.; Padilla-Martinez, I.; Sirol, S.; Carmona. E. *Coord. Chem. Rev.* **2001**, *213*, 129-157.

[18] Jones, W. D. In *Activation of Unreactive Bonds and Organic Synthesis*; Murai, S. Eds.; Topics in Organometallic Chemistry 3; Springer: New York, 1999, pp9-45.

[19] Chemdraw Ultra 7.0, Cambridgesoft Corporation, Cambridge, USA, **2001**.

[20] Shen, J-K.; Tucker, D. S.; Basolo, F.; Hughes, R. P. *J. Am. Chem. Soc.* **1993**, *115*, 11312-11318.

[21] Hughes, R. P.; Tucker, D. S.; Rheingold, A. L. *Organometallics*, **1993**, *12*, 3069-3074.

[22] Ditchfield, R.; Hughes, R. P.; Tucker, D. S.; Bierwagen, E. P.; Robbins, J.; Robinson, D. J.; Zakutansky, J. A. *Organometallics*, **1993**, *12*, 2258-2267.

[23] Lichtenberger, D. L.; Hoppe, M. L.; Subramanian, L.; Kober, E. M.; Hughes, R. P.; Hubbard, J. L.; Tucker, D. S. *Organometallics*, **1993**, *12*, 2025-2031.

[24] Gowling, E. W.; Kettle, S. F. A. *Inorg. Chem.* **1963**, *3*, 604-605.

[25] Hughes, R. P.; Kläui, W.; Reisch, J. W.; Müller, A. *Organometallics*, **1985**, *4*, 1761-1766.

[26] Donaldson, W. A.; Hughes, R. P. *J. Am. Chem. Soc.* **1982**, *104*, 4846-4859.

[27] Tuggle, R. M.; Weaver, D. L. *J. Am. Chem. Soc.* **1970**, *92*, 5523-5524.

[28] Lowe, C.; Shklover, V.; Berke, H. *Organometallics*, **1991**, *10*, 3396-3399.

[29] Wang, T. F.; Lee, T. Y. *J. Organomet. Chem*. **1992**, *423*, 31-38.

[30]Jutzi, P.; Dahlhaus, J. *Synthesis* **1993**, *7*, 684-686.

[31] Singh, P.; Rausch, M. D. *J. Organomet. Chem*. **1988**, *352*, 273-282.

[32] Hughes, R. P.; Lambert, J. M. J.; Whitman, D. W.; Hubbard, J. L.; Henry, W. P.; Rheingold, A. L. *Organometallics* **1986**, *5*, 789-797.

[33] Ball, R.G.; Graham, W. A. G.; Heinekey, D. M.; Hoyano, J. K.; McMaster, A. D.; Mattson, B. M.; Michel, S. T. *Inorg. Chem*. **1990**, *29*, 2023-2025.

[34] Kang, J. W.; Maitlis, P. M.; *J. Organomet. Chem*. **1971**, *26*, 393-399.

[35] Purwoko, A. A.; Lees, A. *J. Inorg. Chem*. **1996**, *35*, 675-682.

[36] Garlaschelli, L.; Della Pergola, R.; Martinengo, S. *Inorg. Synth.*, **1989**, *28*, 211-215.

[37] Blais, M. S.; Chien, J. C. W.; Raush, M. D. *Organometallics* **1998**, *17*, 3775-3783.

[38] Wang, D.; Angelici, R. J. *Inorg. Chem*. **1995**, *35*, 1321-1331.

[39] Gusev, O. V.; Sergeev, S.; Saez, I. M.; Maitlis, P. M. *Organometallics* **1994**, *13*, 2059-2065.

[40] Gao, F.; Ng, K. P.; Li, C.; Krummel, K. I.; Allian, A. D.; Garland, M. *J. Catal*. **2006**, *237*, 49-57.

[41] SMART, version 5.628, Bruker AXS Inc.: Madison, Wisconsin, USA, **2001**.

[42] SAINT+, version 6.22a, Bruker AXS Inc.: Madison, Wisconsin, USA, **2001**.

[43] Sheldrick, G. M. SADABS: **1996**.

[44] SHELXTL version 5.1, Bruker AXS Inc.: Madison, Wisconsin, USA, **1997**.

[45] Blais, M. S.; Rausch, M. D. *J. Organomet. Chem*. **1995**, *502*, 1-8.

Chapter 3: Reaction of $Cp^*Ir(CO)_2$ with Fluoroarenes and Fluoropyridines

3.1 Introduction

The results in the previous chapter suggest that solvents inert to C-H activation are required to enable coordination of the Cp^ side arm to the iridium center upon photodissociation of the CO ligand. $Cp^*Ir(CO)_2$, **2a** and $Cp^*Ir(PMe_3)(H)_2$ have been known to activate all organic solvents containing C-H bonds upon UV irradiation.[1]

Graham *et. al.* have reported using perfluorohexane as an inert solvent in the activation of methane gas by **2a**[2] and Lees *et. al.* have reported the use of C_6F_6 as an inert solvent in the study of the photochemistry of **2a** in benzene,[3] although Bergman *et. al.* found that the intermediate formed from heating a sample of $Cp^*Ir(PMe_3)(Cy)(H)$ in benzene at 130 ˚C reacted with C_6F_6 and other fluorocarbons.[4]

In the search for solvents that are inert to C-H activation by **2a** and $Cp^*{}^\wedge Ir(CO)_2$, **2b**, attempts were made at using non-hydrocarbon solvents such as fluorocarbons (C_6F_6) and carbon disulfide (CS_2). However, **2b** was completely insoluble in perfluorohexane, while solvents like hexafluorobenzene (C_6F_6) and carbon disulfide (CS_2) were found to react with the iridium species under UV irradiation.

This chapter will describe the reaction of **2a** with C_6F_6 as well as with other substituted fluoroarenes and fluoropyridines. Substituent effects and regioselectivity will also be discussed.

3.2 UV irradiation of $Cp^*Ir(CO)_2$, 2a in C_6F_6

Fluorinated solvents might be a possible inert media for C-H activation reactions involving **2a** and its derivatives due to the high C-F bond dissociation energy (154 kcal/mol for C_6F_6).

UV irradiation of a solution of **2a** in C_6F_6 (10 mg/ ml) resulted in a gradual colour change from yellow to orange-red. Prolonged irradiation resulted in slow precipitation of tan solids. Complex **2a** was completely consumed after 20 h of irradiation to give two carbonyl containing species **15** and **16** which were identified to be $[Cp^*Ir(CO)(\eta^2\text{-}C_6F_6)]$ and $[Cp^*Ir(CO)(C_6F_5)]_2$, respectively, by spectroscopic characterization as well as by single crystal X-ray crystallographic analysis.

The formation of $\eta^2\text{-}C_6F_6$ complexes similar to **15** have been previously reported for complexes containing d^6 and d^8 metal centers. They can be synthesized by photolysis or by thermal means (Scheme 3.1).[5,6,7,8]

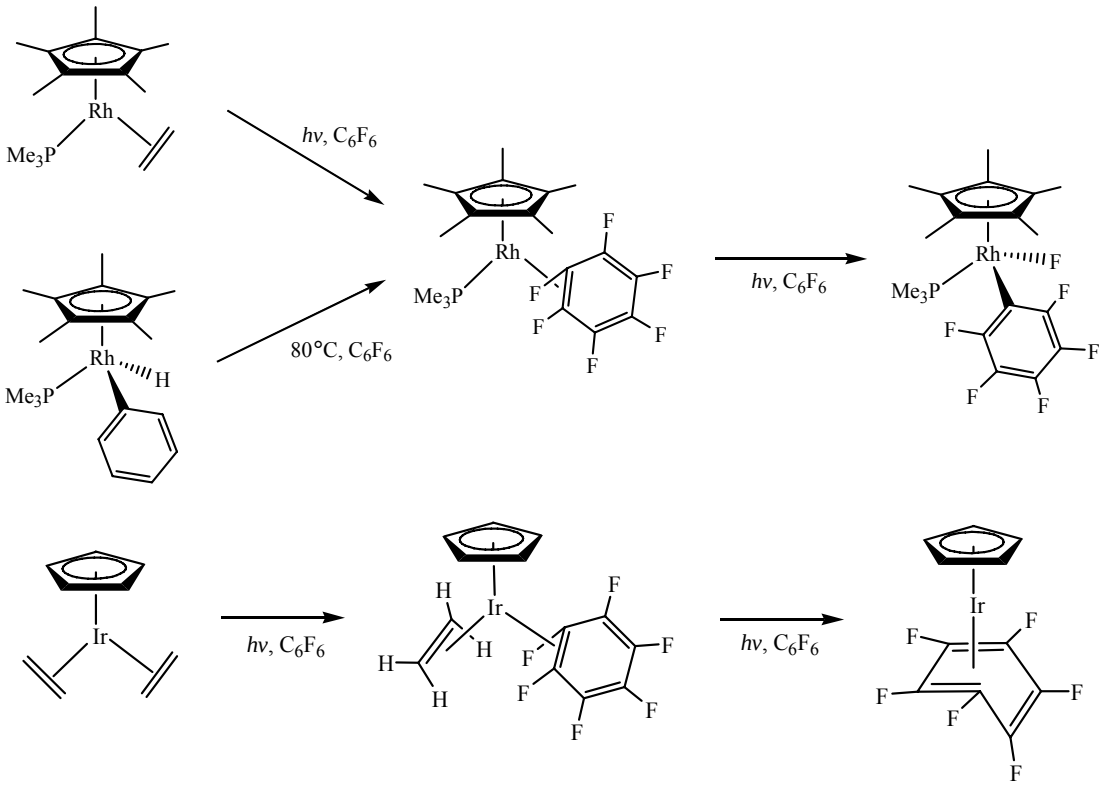

Scheme 3.1

The formation of **16** was, however, rather unexpected. No dimeric structures similar to **16** containing C_6F_5 ligands have been reported. The known complexes $LRh(PMe_3)(\eta^2\text{-}C_6F_6)$

(where L = Cp or Cp*) gave C-F activated complexes $LRh(PMe_3)(C_6F_5)(F)$ upon prolonged irradiation. The C-F insertion product was suggested to be formed from the η^2-C_6F_6 complex due to the sequential formation of $Cp^*Rh(PMe_3)(\eta^2\text{-}C_6F_6)$ and $Cp^*Rh(PMe_3)(C_6F_5)(F)$.[7b] A group 10 metal complex, $(^tBu_2PC_2H_4P^tBu_2)Ni(\eta^2\text{-}C_6F_6)$ has also been found to undergo C-F oxidative addition to afford a mononuclear product, $(^tBu_2PC_2H_4P^tBu_2)Ni(C_6F_5)(F)$ (Scheme 3.2). A similar C-F insertion intermediate, $Cp^*Ir(CO)(C_6F_5)(F)$ may have been formed from the photolysis of **15** which underwent fluorine elimination to give the dimeric complex **16**.

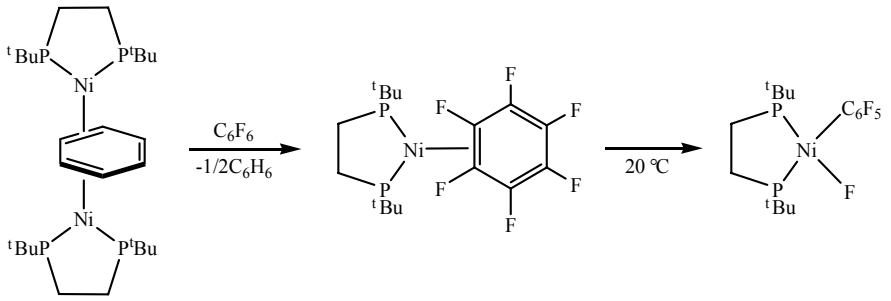

Scheme 3.2

The ^{19}F-NMR spectrum of **15** shows three sets of multiplets at δ -71.36, -77.92 and -97.91 corresponding to the three pairs of inequivalent fluorines. The resonances have been assigned by comparison with that of the known η^2-C_6F_6 iridium and rhodium complexes, $CpIr(C_2H_4)(\eta^2\text{-}C_6F_6)$ and $CpRh(PMe_3)(\eta^2\text{-}C_6F_6)$. The ^{19}F resonances for **16** were similarly assigned by comparison with the known compound $CpIr(PMe_3)(C_6F_5)H$.[7b]

The reaction was monitored by infrared spectroscopy. Initially, the IR spectrum of the carbonyl stretching region shows only peaks due to **2a** and a new peak at 2026 cm^{-1} due to the terminal CO stretch of **15**. Further irradiation resulted in an additional peak at 1778 cm^{-1} due to the bridging CO stretch of **16** (Scheme 3.3).

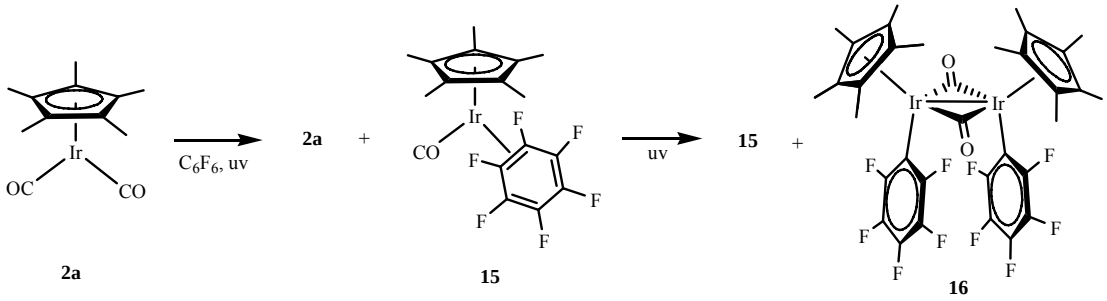

Scheme 3.3

After complex **2a** has been completely consumed, the ^{1}H NMR spectrum of the product mixture shows the presence of **15** and **16** in a 5 :1 ratio from the integration of their Cp* methyl resonances.

The products were unstable on silica gel plates and re-crystallization from toluene and cyclopentane did not give complete separation of the products.

Attempts to increase the yield of **16** by increasing the length of photolysis led to slow precipitation of tan solids containing a mixture of unidentified products. Conversion of compound **15** to **16** could not be achieved thermally as heating the reaction mixture containing **2a** and **15** in C_6F_6 at 80 °C did not result in the formation of **16**. The relative proportion of **2a** and **15** stayed essentially the same.

When a more diluted sample of **2a** in C_6F_6 (4.4 mg/ml) was irradiated for 6 h, complex **16** was not obtained. Instead, **2a** was completely converted into **15** and another product **17**. The later showed a terminal carbonyl stretch at 2052 cm^{-1} in its IR spectrum, a singlet at δ 1.92 due to the methyl protons of a Cp* ring in its ^{1}H NMR spectrum and three sets of ^{19}F resonances in a 2: 1: 2 integration ratio with the same coupling pattern as **16**, suggesting the presence of a η^1-C_6F_5 ligand. Complex **17** may have resulted from the reaction of **2a** with an impurity in C_6F_6. A GC-MS analysis of a commercial sample of C_6F_6 showed that the main impurities detected were C_6F_5H and C_6F_5Cl. The ^{1}H NMR and ^{19}F NMR spectra of a solution of **2a** in C_6F_5H after UV irradiation shows complicated mixtures of unidentified products, but compounds **16** or **17** were not formed. Similarly, irradiation of a solution of **2a** in C_6F_5Cl afforded an intractable mixture, but **16** was not present. However, irradiating a solution of **2a** with C_6F_5Cl (10 μl) in C_6F_6 (1 ml) resulted partial conversion to **15** and **17**. The ratio of **2a**: **15**: **17** from ^{1}H NMR integration is 1: 8: 5. Mass spectrometry (FAB) of the mixture showed a set of peaks assignable to $[Cp^*Ir(CO)(C_6F_5)]^+$. Thus **17** is proposed to have the formulation $Cp^*Ir(CO)(C_6F_5)Cl$ (Figure 3.1). Attempts to purify **17** by re-crystallization were unsuccessful.

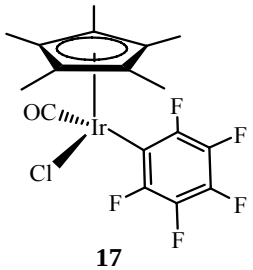

17

Figure 3.1. Proposed structure of **17**.

A similar observation has previously been reported in which the photolysis of $Cp^*Rh(PMe_3)(C_2H_4)$ in C_6F_6 afforded $Cp^*Rh(PMe_3)(C_6F_5)Cl$. It was suggested that the chloro species came from the reaction of the $Cp^*Rh(PMe_3)(C_6F_5)F$ product with the C_6F_5Cl impurity in C_6F_6 because photolysis of $Cp^*Rh(PMe_3)(C_2H_4)$ in C_6F_6 doped with 1% C_6F_5Cl gave $Cp^*Rh(PMe_3)Cl_2$ instead of $Cp^*Rh(PMe_3)(C_6F_5)Cl$.[7b] In our case, only **17** and not the analogous $Cp^*Ir(CO)Cl_2$, was observed. The faster consumption of **2a** in the presence of added C_6F_5Cl suggests that **17** could be formed directly from the reaction of **2a** with C_6F_5Cl. Formation of **17** from the reaction of **16** with C_6F_5Cl was unlikely as the photolysis of **2a** to give **15** and **16** took 20 h for complete consumption of **2a** while the photolysis of **2a** in C_6F_6 doped with 1 % C_6F_5Cl gave 90 % consumption of **2a** to give **15** and **17** in only 1 h 45 min..

Compound **16** might be formed from the elimination of HCl from the intermediates obtained from the reaction of **2a** with the impurities C_6F_5H and C_6F_5Cl found in the commercial sample of C_6F_6 [i.e. $Cp^*Ir(CO)(C_6F_5)(H)$ and $[Cp^*Ir(CO)(C_6F_5)(Cl)]$] (Scheme 3.4). Irradiation of a solution of **2a** in C_6F_6 doped with C_6F_5Cl and C_6F_5H should increase the production of **16**. However, **16** was not detected when a solution of **2a** in C_6F_6 doped with 1 % C_6F_5Cl and 1 % C_6F_5H was irradiated, suggesting that this proposed route was not likely.

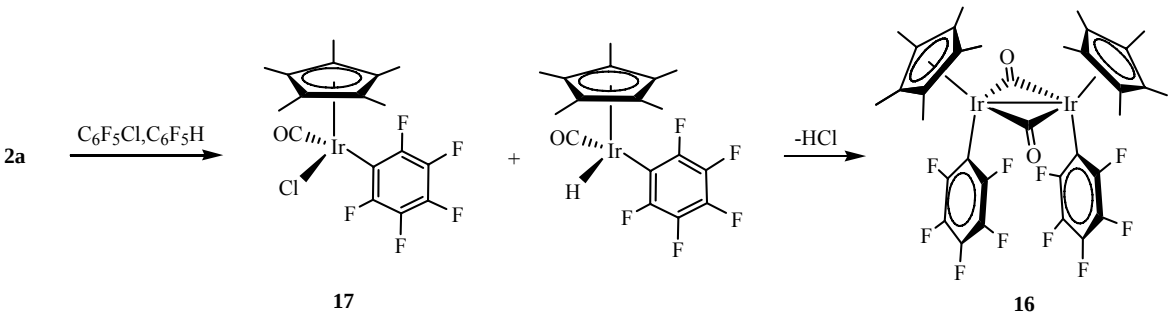

Scheme 3.4

Crystallographic studies

Diffraction quality crystals from the cyclohexane extract were grown by keeping a toluene/hexane solution of the mixture at 5 °C for a few weeks, during which the solvent evaporated to give orange-red and yellow crystals and together with some dark yellow oil. The crystals were mechanically separated and the orange-red and yellow crystals were identified to be [Cp*Ir(CO)(η^2-C_6F_6)], **15** and [Cp*Ir(CO)(C_6F_5)]$_2$, **16**, respectively. The ORTEP plot of **15**, together with selected bond parameters is shown in Figure 3.2. Selected bond parameters for **15** and other known η^2-C_6F_6 complexes are tabulated in Table 3.1.

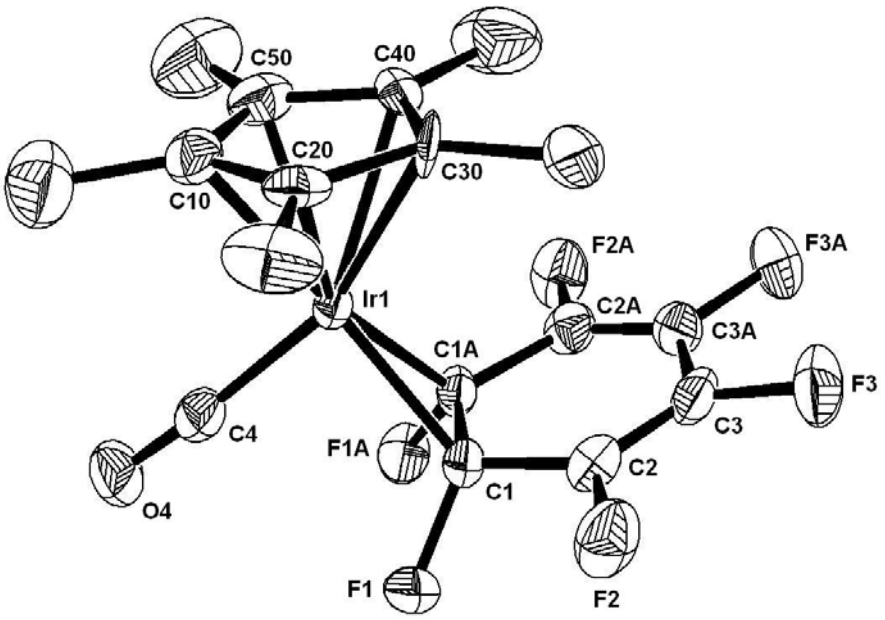

Figure 3.2. ORTEP diagram of **15.** Thermal ellipsoids drawn at 50% probability level. The hydrogen atoms have been omitted for clarity. Selected bond distances (Å) and angles (°): Ir1-C4 = 1.863(9); Ir1-C1 = 2.071(6); C4-O4 = 1.124 (11); F1-C1 = 1.390(6); F2-C2 = 1.340(8); F3-C3 = 1.351(7); C1-C2-C3-C3A = 1.4(6).

Table 3.1. Comparison of bond distances (Å) and dihedral angles (°) of **15** with reported η^2-C_6F_6 complexes.

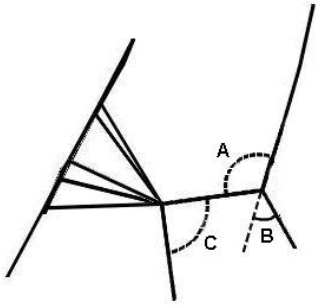

(a)

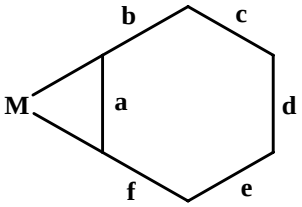

M = Ir, Rh

(b)

A = Dihedral angle between C1-C2-C3-C3A-C2A-C1A and C1-C1A-Ir1.
B = Dihedral angle between C1-C2-C3-C3A-C2A-C1A and F1-C1-C1A-F1A.
C = Bond angle between C4 and C1-C1A-Ir1.

	15	$CpIr(C_2H_4)$ (η^2-C_6F_6)	$CpRh(PMe_3)$ (η^2-C_6F_6)	(η^5:η^1-$C_5H_5SiMe_2CH_2PPh_2$)Rh (η^2-C_6F_6)
a (Å)	1.465(11)	1.47(2)	1.397(12)	1.446(9)
b (Å)	1.469(9)	1.42(2)	1.473(8)	1.451(8)
c (Å)	1.317(10)	1.33(2)	1.331(8)	1.326(9)
d (Å)	1.428(13)	1.43(2)	1.354(12)	1.420(10)
e (Å)	1.317(10)	1.34(3)	1.331(8)	1.333(8)
f (Å)	1.469(9)	1.43(2)	1.473(8)	1.460(9)
A (°)	115.0 (4)	114.6 (1)	108.6 (0.3)	109.6 (4)
B (°)	47.0 (5)	47.9 (1)	43.8 (0.5)	38.0 (5)
C (°)	90.2 (3)	95.8 (8)	-	-

The molecular structure of **15** shows the iridium center coordinated to the hexafluorobenzene ligand (C_6F_6) via a η^2 coordination mode. The structure retains an almost planar C_6F_4 unit; the dihedral angle formed by C1-C2-C3-C3A is only 1.4°, and F2 and F3 are bent out of the arene plane by 2.9° and 5.5°, respectively. The bond angle subtended by C4 and the C_6F_6 ligand at the iridium centre (C) is 90.2°. The fluorines on the bonding carbons (F1 and F1A) bend strongly away from the aromatic plane (B = 47.0°). This angle is similar to that reported for $CpIr(C_2H_4)(\eta^2$-$C_6F_6)$ and they are larger compared to that for the Rh compounds. The angle between the Ir1-C1-C1A plane and the C_6 plane (A) is likewise very close to that reported for $CpIr(C_2H_4)(\eta^2$-$C_6F_6)$ but larger than that for the Rh compounds.

The coordinated C-C bond in **15** is significantly lengthened compared to that of free C_6F_6 (1.394 Å) but comparable to that in $CpIr(C_2H_4)(\eta^2\text{-}C_6F_6)$ and $(\eta^5{:}\eta^1\text{-}C_5H_5SiMe_2CH_2PPh_2)Rh(\eta^2\text{-}C_6F_6)$. This is, however, in contrast to that reported for $CpRh(PMe_3)(\eta^2\text{-}C_6F_6)$ (1.397 Å) which is not significantly different from that of the free C_6F_6. The C-C bond lengths for the rest of the ring (C2C3C3AC2A) resembles a free diene structure with a short (C2-C3), medium (C3-C3A), short (C3A-C2A) pattern, as observed for the other compounds. Hence, the C_6F_6 ligand resembles a coordinated alkene in geometry.

The ORTEP diagram showing the molecular structure of **16** and a wireframe diagram showing the view along the C_6F_5 plane, are given in Figure 3.3. The C_6F_5 rings are oriented perpendicular to the plane defined by the bridging carbonyl.

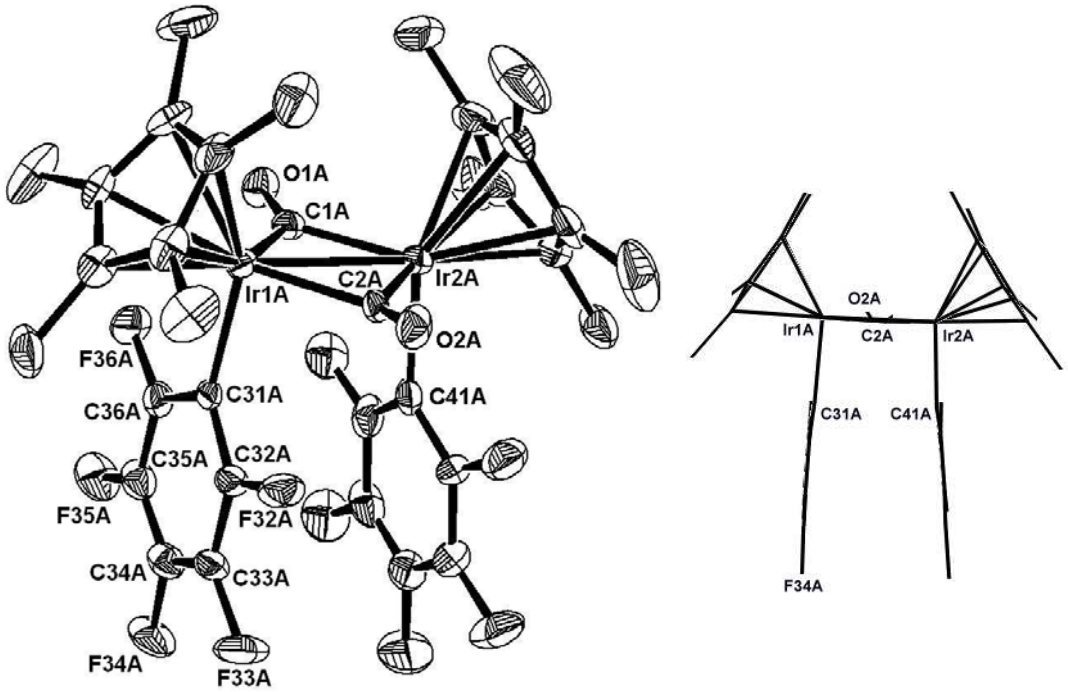

(a) (b)

Figure 3.3(a). ORTEP diagram of **16.** Thermal ellipsoids drawn at 30% probability level. The hydrogen atoms have been omitted for clarity. Selected bond distances (Å) and angles (°): Ir1A-C1A = 2.011(14); Ir1A-C2A = 2.036(13); Ir2A-C2A = 2.010(15); Ir1A-C31A = 2.093(13); Ir2A-C41A = 2.088(15); Ir1A-Ir2A = 2.7576(8); C31A-C32A = 1.40(2); C32A-C33A = 1.40(2); C33A-C34A = 1.36(3); C34A-C35A = 1.36(2); C35A-C36A = 1.40(2); C31A-C36A = 1.38(2); C31A-Ir1A-Ir2A = 93.5(3); C41A-Ir2A-Ir1A = 93.9(4); C41A-Ir2A-Ir1A-C31A = -10.5(4).

(b). Wireframe diagram of **16** viewed along the plane of the C_6F_5 rings and showing the planarity of the aromatic rings.

The two Cp* rings are in a cis arrangement, in contrast to the trans arrangement observed in many homo- or heterodinuclear complexes containing Cp* ligands (Figure 3.4).[9]

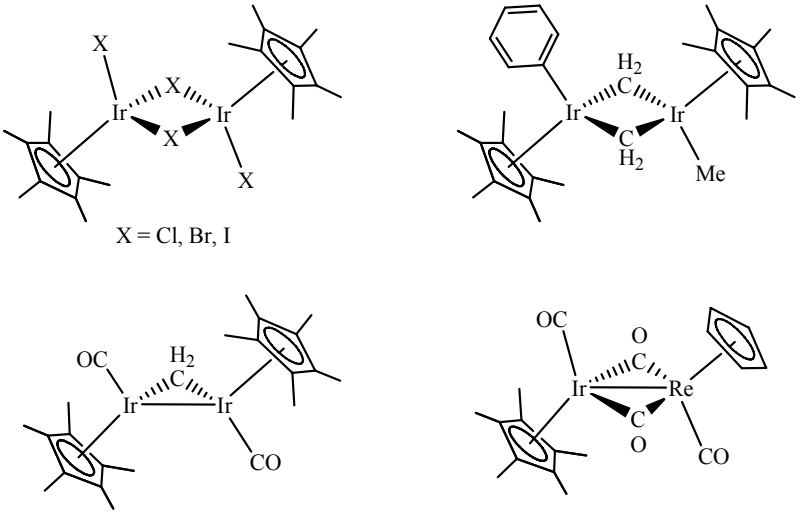

Figure 3.4. Examples of Cp*Ir homodinuclear or heterodinuclear complexes that have Cp* or Cp ligands in a trans arrangement.

3.3 Reaction of 2a with substituted fluoroarenes and fluoropyridines

As an extension to the study of C-F activation of hexafluorobenzene by **2a**, the reaction of various substituted fluoroarenes and fluoropyridines with **2a** was investigated to study the regioselectivity of the reaction.

In contrast to the reaction of hexafluorobenzene with **2a**, which requires UV photoactivation to give **15** and **16**, the reaction of **2a** with pentafluorobenzonitrile (C_6F_5CN) proceeded at room temperature to give a slow precipitation of a white powder, Cp*Ir(CO)(COOH)(*p*-C_6F_4CN), **18a** in a yellow solution; the reaction proceeded more rapidly in the presence of a small amount of water, to afford **18a** in essentially quantitative yield (Scheme 3.5).

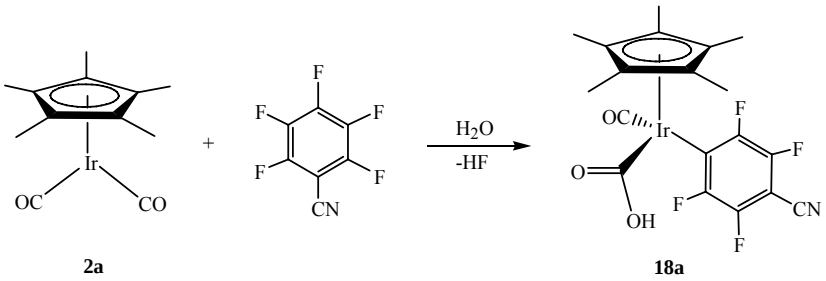

2a **18a**

Scheme 3.5

Compound **18a** has been completely characterized, including by a single crystal X-ray crystallographic study; an ORTEP plot showing the molecular structure, together with selected bond parameters, is given in Figure 3.5.

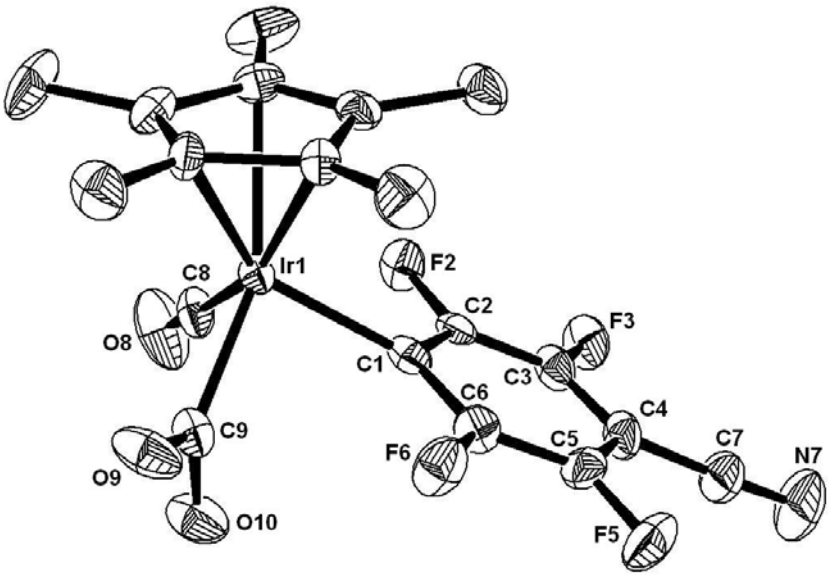

Figure 3.5. ORTEP diagram of **18a**. Thermal ellipsoids drawn at 50% probability level. The hydrogen atoms have been omitted for clarity. Selected bond distances (Å) and angles (°): Ir1-C1 = 2.090(8); Ir1-C8 = 1.906(10); Ir1-C9 = 2.040(6); C8-O8 = 1.143(12); O9-C9 = 1.227(9); O10-C9 = 1.330(10); C8-Ir1-C1 = 89.8(4); Ir1-C1-C^*_{Ar}[a] = 173.0(10); C^*_{CN}[b]-C4-C^*_{Ar} = 176.2(10); C8-Ir1-C9 = 86.9(3); C9-Ir1-C1 = 88.9(3); O9-C9-O10 = 118.8(6); O9-C9-Ir1 = 122.9(5); O10-C9-Ir1 = 118.3(5).

[a] C^*_{Ar} = centroid of the fluoroarene C_6 plane.
[b] C^*_{CN} = centroid of the CN bond.

The most important structural feature of **18a** is the M-COOH moiety. The earliest reported example of a metallocarboxylic acid appears to be also an iridium species,[10] although there have since been a number of other examples; these were generally obtained via attack of OH^- on a carbonyl ligand.[11] The reactivity of metallocarboxylic acids will be further discussed in Chapter 5. Several of the reported metallocarboxylic acids exist as hydrogen-bonded dimers in solid state.[11e] X-ray structural analysis however did not reveal any evidence of hydrogen-bonded dimers in **18a**.

The ^{1}H NMR spectrum of **18a** shows a singlet at δ 1.96 due to the methyl protons of the Cp* ring and a broad singlet at δ 8.45 for the proton of the carboxylic acid group; the identity of the latter was confirmed by its disappearance when D_2O was added to the NMR

sample. This signal is typical of a metallocarboxylic acid (7-11 ppm) and upfield of that for organic carboxylic acids (10-13 ppm).[11e] The ^{19}F NMR spectrum of **18a** shows two sets of multiplets at δ -34.27 and δ -59.17 in a 1:1 integration ratio, consistent with a *para*-substituted fluoroarene. There are no other signals due to *ortho*- or *meta*- substituted fluoroarenes, demonstrating the high regioselectivity of the reaction.

A similar reaction with pentafluoropyridine (C_5F_5N) afforded Cp*Ir(CO)(COOH)(*p*-C_5F_4N), **22a**, in which the substitution also occurred exclusively at the *para* position.

Attempts at the reaction of **2a** with a number of other fluoroaromatics C_6F_5X (where X = NH_2, OMe, H, Cl, F, COOMe, CH_2CN, CF_3 in order of electron-withdrawing ability) under similar conditions failed while the reaction with C_6F_5CHO and $C_6F_5NO_2$ gave mixtures.

Reaction of **2a** with a number of partially fluorinated fluoroarenes and fluoropyridines as well as a disubstituted fluoroarene was also carried out in order to study the substituent effect and regioselectivity of the reaction (Chart 3.1).

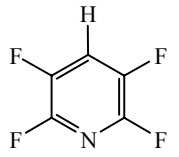

2,3,5,6-Tetrafluoropyridine
(**A**)

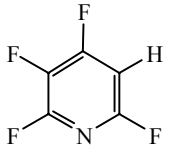

2,4,5,6-Tetrafluoropyridine
(**B**)

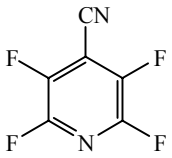

2,3,5,6-Tetrafluoro-4-pyridinecarbonitrile
(**C**)

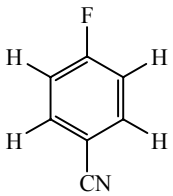

4-Fluorobenzonitrile
(**D**)

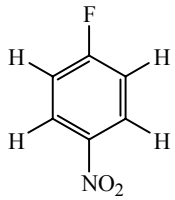

1-Fluoro-4-nitrobenzene
(**E**)

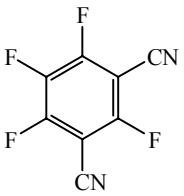

Tetrafluoroisophthalonitrile
(**F**)

Chart 3.1

It was found that the reaction with ligand **E** gave only trace conversion to the expected product, Cp*Ir(CO)(COOH)(*p*-$C_6H_4NO_2$), **27** (7%) while there was no reaction with ligands **A**-**D**. The site of substitution of the arene on **27** was proposed to be at the *para* position based on the absence of resonances in the ^{19}F NMR spectrum. The reaction with ligand **F** occurs with only 1.3 equivalents of the fluoroarene.

From the above results, it can be seen that:

1) Reaction only occurs when there is one or more highly electron-withdrawing substituent(s). For fluoroarenes containing a substituent less electron-withdrawing than CN, no reaction occurred at room temperature while those carrying a substituent more electron-withdrawing than CN gave rapid reaction.
2) Reaction is highly regioselective. When the *para* position is not available, substitution at other positions did not occur even when there are highly electron-withdrawing substituents (**C**).
3) Reaction occurs with highly fluorinated compounds. With fluoroarene **B**, when a fluorine atom at the *meta* position was substituted with a hydrogen atom, no reaction was observed although the *para* position was available. With fluoroarene **D**, reaction did not occur even though there is an electron-withdrawing CN group and the *para*-fluorine is available.
4) Reaction is enhanced if there is a second electron-withdrawing substituent that is not *para* to the first substituent (**F**).

The room temperature reaction of **2a** with $C_6F_5NO_2$ and C_6F_5CHO afforded a mixture of products. Attempts were made to slow down the reaction with smaller equivalents of the fluoroarene as a hexane solution. It was hoped that the product formed would precipitate out. However, it was found that for C_6F_5CHO, at least 20 equivalents of the fluoroarene was required to observe precipitation of an impure orange oil. Mass spectrometry (FAB^+) showed that the expected product, Cp*Ir(CO)(COOH)(C_6F_4CHO) was present in the mixture. For the reaction with $C_6F_5NO_2$, reaction took place with 1 equivalent of the fluoroarene. However, the ^1H NMR spectrum of the crude still shows a complicated mixture. Lowering the reaction

temperature did not give a cleaner reaction and mass spectroscopy did not show the presence of peaks due to the expected product, Cp*Ir(CO)(COOH)($C_6F_4NO_2$).

The higher reactivity with the nitro group was also demonstrated in the reaction of **2a** with neat 4-fluorobenzonitrile and 1-fluoro-4-nitrobenzene. While there was no reaction with 4-fluorobenzonitrile, trace conversion (7%) to the metallocarboxylic product was obtained from the reaction with 1-fluoro-4-nitrobenzene (by integration of the Cp* methyl resonances in the ^{1}H NMR spectrum).

The susceptibility of the fluoroarenes toward nucleophilic aromatic substitution increases with an increase in the number of electron-withdrawing substituents. This is evident from the reaction with 1,3-$C_6F_4(CN)_2$; while the reaction with C_6F_5CN and C_5F_5N occurred only in large excess or in neat solutions of the fluorinated compounds, only 1.3 equivalents of 1,3-$C_6F_4(CN)_2$ was needed. Furthermore, while the metallocarboxylic acids **18a** and **22a** could be isolated from the reaction with C_6F_5CN and C_5F_5N, only the hydride species Cp*Ir(CO)(H){2,4-$C_6F_4(CN)_2$}, **28** was isolated in the reaction with 1,3-$C_6F_4(CN)_2$. The structure of **28** was proposed based on spectroscopic evidence. There are two CN stretches (2252 and 2242 cm^{-1}) and a terminal carbonyl stretch (2052 cm^{-1}) in its IR spectrum; two singlets (δ 1.53 and -14.39) due to the methyl protons of the Cp* ring and the hydride, respectively, in its ^{1}H NMR spectrum and three sets of ^{19}F resonances in a 1:1:1 integration ratio (Figure 3.6), consistent with the expected substitution *para* to one of the CN substituents (i.e. substitution at position 1). If the substitution occurred at position 2 or 3, two sets of resonances in a 1:2 integration ratio are expected in the ^{19}F NMR spectrum. The assignments are based on their coupling patterns, coupling constants and chemical shifts; F^c being next to two electron-withdrawing CN group is expected to be the most deshielded. F^a is coupled to F^b and F^c while F^b is only coupled to F^a because *ortho* > *para* >> *meta* coupling. The mass spectrum (-ve mode) shows the highest m/z ion peak at 537 corresponding to [Cp*Ir(CO){2,4-$C_6F_3(CN)_2$}]$^-$.

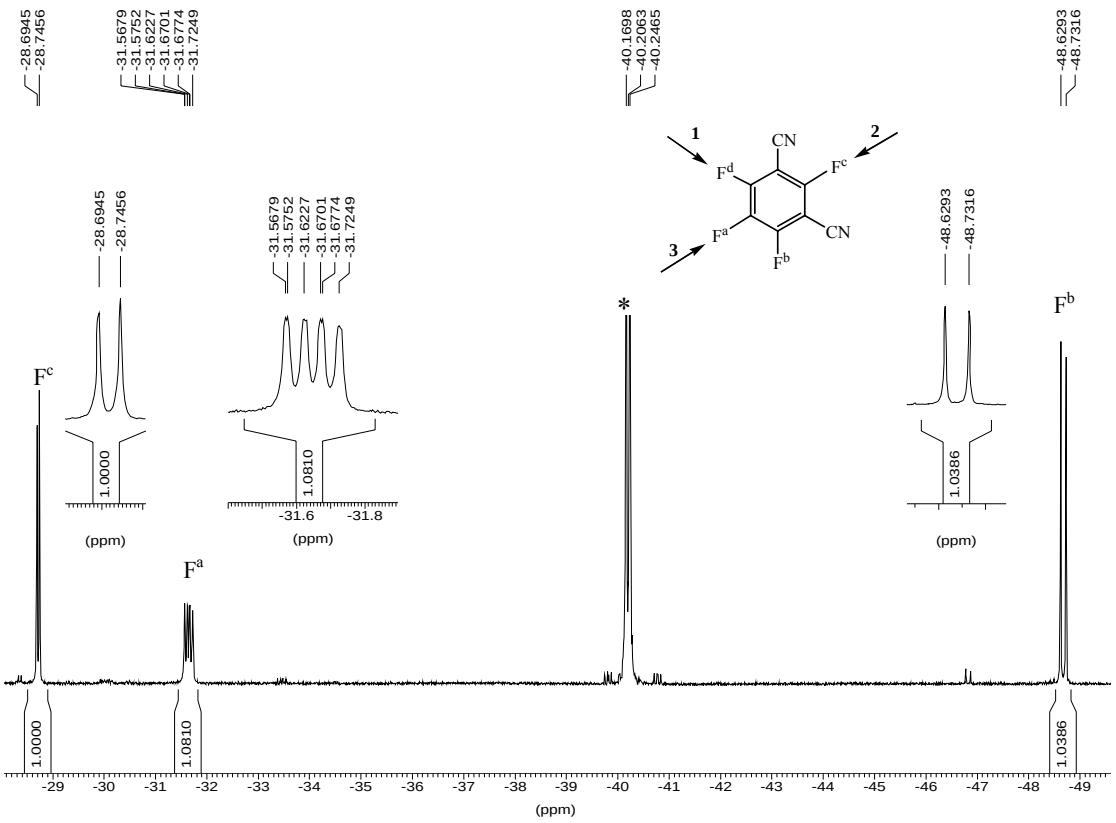

Figure 3.6. ^{19}F NMR spectrum of **28**. *Resonances due to unreacted 1,3-$C_6F_4(CN)_2$ (δ -26.52, -40.21, -82.28).

It is likely that analogous metallocarboxylic acid Cp*Ir(CO)(COOH)[2,4-$C_6F_4(CN)_2$] may have been formed initially but it undergoes spontaneous decarboxylation to give **28** (Scheme 3.6).

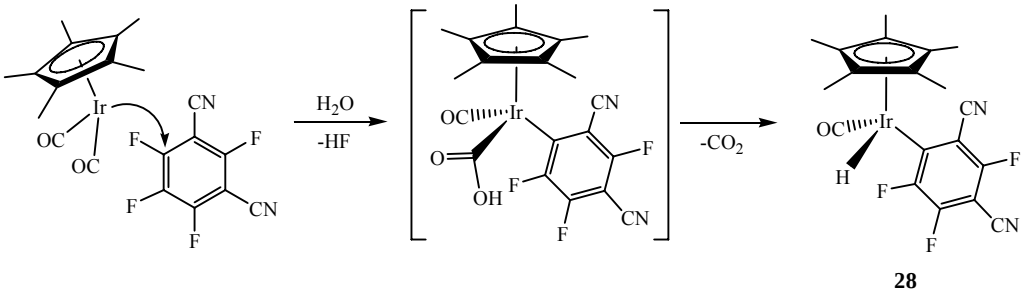

Scheme 3.6

Although C_6F_5CN and C_5F_5N are different ring systems and hence the electron-withdrawing ability of the substituents cannot be compared directly, the reaction of **2a** with a 1:1 molar ratio of C_6F_5CN and C_5F_5N at room temperature gave, after 16 h, a ^{19}F NMR spectrum which shows that **22a** and **18a** were formed in a 1:1.4 molar ratio, indicating that C_6F_5CN was more susceptible to nucleophilic attack compared to C_5F_5N.

3.4 Conclusion

Photoirradiation of **2a** in hexafluorobenzene resulted in the formation of a η^2-arene complex, **15** and a dimer, **16** with the C_6F_5 ligand bonded to the iridium center in a η^1-coordination mode. Complex **2a** reacts with highly fluorinated arenes carrying electron-withdrawing substituent(s) (e.g. C_6F_5X where X = CN, CHO) and pentafluoropyridine without irradiation. Cleavage of a C-F bond occurs to give *para*-substituted products exclusively, demonstrating the high regioselectivity of the reaction.

3.5 Experimental

General experimental as described in Section 2.6. $Cp^*Ir(CO)_2$, **2a** was synthesized and purified as described in Section 2.6. All other reagents were purchased commercially and used without further purification.

3.5.1 UV photolysis of 2a in fluoroarenes

Unless otherwise stated, all photolyses were carried out using a 450W medium pressure mercury lamp (peak emission at 254 nm) placed approximately 15 cm away from the reaction vessel, with magnetic stirring. The reaction vessel was cooled by circulating ice-water through a quartz cooling jacket.

UV photolysis of 2a in hexafluorobenzene, C_6F_6

i) To a quartz tube containing **2a** (20.0 mg, 52.2 μmol) was added C_6F_6 (2 ml). The reaction mixture was degassed by three cycles of freeze-pump-thaw and irradiated for 20 h during which the solution darkened from yellow to orange-brown, with some brown precipitate. Irradiation was continued until **2a** was completely consumed (by IR spectroscopy). The volatiles were removed under reduced pressure and the residue was extracted with *ca.* 20 ml of cyclohexane. Removal of solvent from the extract gave a brownish-yellow oil (26.9 mg). The ^{1}H NMR spectrum of the extract shows a mixture of $Cp^*Ir(CO)(\eta^2\text{-}C_6F_6)$, **15** and $[Cp^*Ir(C_6F_5)(\mu\text{-}CO)]_2$, **16** (5:1 ratio by ^{1}H NMR integation) and some small peaks due to unidentified compounds. Re-crystallization from toluene and cyclopentane gave a larger proportion of **15** in the supernatant, but complete separation was not obtained.

Prolonged irradiation gave slow precipitation of tan solids containing a mixture of unidentified products.

ii) A quartz tube containing **2a** (22.0 mg, 57.4 μmol) in C_6F_6 (5 ml) was irradiated for 9 h. The ^{1}H NMR spectrum of the extract showed a mixture of $Cp^*Ir(CO)(\eta^2\text{-}C_6F_6)$, **15** and

Cp*Ir(CO)(C_6F_5)Cl, **17** (1.5: 1 ratio by ^{1}H NMR integation). Extraction with cyclohexane (20 ml) gave a yellow powder (29.7 mg). Repeated recrystallization from cyclopentane at 0 ºC gave pure **15** (8.0 mg, 28 %).

iii) A quartz tube containing **2a** (30.0 mg, 78.2 μmol) in C_6F_6 (6 ml) was irradiated for 6 h. The ^{1}H NMR spectrum of the crude mixture shows a mixture of **15**, **16** and small amounts of **17**.

15:

IR (cyclohexane): ν_{CO} 2027 (s) cm^{-1}. ^{1}H NMR ($CDCl_3$): 1.89 (s, 15H, Cp*C*H*$_3$). ^{19}F NMR ($CDCl_3$): δ -71.36 (m, 2F, F^2, F^{2A}), -77.92 (m, 2F, F^1, F^{1A}), -97.91 (m, 2F, F^3, F^{3A}) where F^1 and F^{1A} are bound to the coordinated carbon atoms; F^2 and F^{2A} are ortho to F^1 and F^{1A}. Anal. Calcd for $C_{17}H_{15}F_6IrO \cdot 0.25C_6H_{12}$: C, 39.50; H, 3.23. Found: C, 39.90; H, 3.13. MS FAB$^+$ (*m*/*z*): 523[M – F] $^+$, 495[M – F - (CO)]$^+$, 356[M – (C_6F_6)]$^+$. HR-MS FAB$^+$ (*m*/*z*): calcd for $C_{17}H_{15}O_1F_5{}^{193}Ir$ [M – F]$^+$: 523.0670, found: 523.0667.

16:

IR (cyclohexane): ν_{CO} 1778 (s) cm^{-1}. ^{1}H NMR ($CDCl_3$): 1.82 (s, 15H, Cp*C*H*$_3$). ^{19}F NMR ($CDCl_3$): δ -38.98 (m, 2F, F_{ortho}), -85.23 (t, J = 19.6, 2F, F_{para}), -88.48 (m, 2F, F_{meta}). MS FAB$^+$ (*m*/*z*): 523[M /2] $^+$.

17:

IR (cyclohexane): ν_{CO} 2052 (s) cm^{-1}. IR (dcm): ν_{CO} 2048 (s) cm^{-1}. ^{1}H NMR ($CDCl_3$): 1.93 (s, 15H, Cp*C*H*$_3$). ^{19}F NMR ($CDCl_3$): δ -37.45 (m, 2F, F_{ortho}), -83.99 (t, J = 20, 2F, F_{para}), -87.11 (m, 2F, F_{meta}). MS FAB$^+$ (*m*/*z*): 523[M – Cl] $^+$

X-ray diffraction quality crystals of **15** and **16** were grown from a toluene/ hexane solution at 5 ºC.

UV Photolysis of 2a in pentafluorobenzene (C_6F_5H)

A quartz tube containing **2a** (10.0 mg, 26.1 μmol) in C_6F_5H (1 ml) was irradiated for 1h 40 min. The IR spectrum shows that **2a** has been completely consumed. The ^{1}H and ^{19}F

NMR spectra are complicated but **16** is absent. IR (cyclohexane): ν_{CO} 2040 (s), 2024 (vs), 2000 (w) cm^{-1}

UV photolysis of 2a in chloropentafluorobenzene (C_6F_5Cl)

A quartz tube containing **2a** (10.0 mg, 26.1 μmol) in C_6F_5Cl (1 ml) was irradiated for 2 h during which the solution turned brown. The product mixture could not be dried completely and gave a complicated ^1H NMR spectrum that did not show the presence of **16**.

UV photolysis of 2a in C_6F_6/ C_6F_5Cl mixture

To a quartz tube containing **2a** (10.0 mg, 26.1 μmol) in C_6F_6 (1 ml) was added C_6F_5Cl (10 μl, 77.4 μmol). The reaction mixture was degassed by three cycles of freeze-pump-thaw and irradiated for 1 h 45 min. The solution turned from yellow to red. The ^1H NMR spectrum shows the presence of **2a**, **15** and **17** in a 1: 8: 5 ratio.

UV photolysis of 2a in C_6F_6/ C_6F_5Cl/ C_6F_5H mixture

To a quartz tube containing **2a** (10.0 mg, 26.1 μmol) in C_6F_6 (1 ml) was added C_6F_5Cl (10 μl, 77.4 μmol) and C_6F_5H (8 μl, 72.0 μmol). The reaction mixture was degassed by three cycles of freeze-pump-thaw and irradiated for 1 h 45 min. The solution turned from yellow to red. The ^1H and ^{19}F NMR spectra shows the presence of **15** and **17**. Complex **16** was not formed.

3.5.2 Reaction of 2a with fluoroarenes and fluoropyridines in the presence of water

To a Carius tube containing **2a** was added the fluoroarene or fluoropyridine and deionized H_2O. The reaction mixture was degassed by three cycles of freeze-pump-thaw and stirred at room temperature. The amount of substrate used is summarized in the Table 3.2.

Table 3.2. Reaction of **2a** with fluoroarenes and fluoropyridines in the presence of water.

Amount of 2a /mg	Amount of 2a /μmol	Fluoroarene or fluoropyridine	Amount of Fluoroarene or fluoropyridine	Distilled water /ml	Time	Product
10.0	26.1	$C_6F_5NH_2$	150 mg (excess)	0.1	60°C, 1d; 80°C in toluene, 1d	No reaction
10.0	26.1	C_6F_5OMe	0.5 ml	0.1	16 h	No reaction
5.0	13.0	C_6F_5H	0.5 ml	0.1	16 h	No reaction
10.0	26.1	C_6F_5Cl	0.5 ml	0.1	16 h	No reaction
5.0	13.0	C_6F_6	0.5 ml	0.1	16 h	No reaction
10.5	27.4	C_6F_5COOMe	0.25 ml	0.1	16 h	No reaction
10.0	26.1	$C_6F_5CH_2CN$	0.5 ml	0.1	16 h	No reaction
5.0	13.0	$C_6F_5CF_3$	0.5 ml	0.1	16 h	No reaction
51.5	134	C_6F_5CN	1.5 ml	0.2	16 h	Cp*Ir(CO)(COOH)(*p*-C_6F_4CN), **18a**
10.0	26.1	C_6F_5CHO	0.3 ml	0.2	6 h	Cp*Ir(CO)(COOH)(*p*-C_6F_4CHO), **26** + mixture of unknown compounds
5.0	13.0	$C_6F_5NO_2$	0.5 ml	0.1	5 min	Mixture
22.8	59.5	C_5F_5N	0.5 ml	0.1	2 d	Cp*Ir(CO)(COOH)(*p*-C_5F_4N), **22a**
10.0	26.1	C_5F_4NH , **A**	0.5 ml	0.1	16 h	No reaction
10.0	26.1	C_5F_4NH, **B**	0.25 ml	0.1	3 d	No reaction
10.5	27.4	*p*-$C_5F_4N(CN)$, **C**	96.0 mg (20 x excess)	0.1	16 h	No reaction
10.0	26.1	*p*-$C_6H_4F(CN)$, **D**	200.0 mg in toluene (3 ml)	0.25	16 h	No reaction
9.6	25.0	*p*-$C_6H_4F(NO_2)$, **E**	0.25 ml	0.25	16 h	Poor conversion
10.0	26.1	1,3-$C_6F_4(CN)_2$, **F**	a) 5.2 mg, 26.0 μmol in toluene (2 ml) b) 26 mg ,130.0 μmol in C_6D_6 (0.6 ml) (NMR scale)	0.1 0.1	16 h 18 h	Cp*Ir(CO)(H)[2,4-$C_6F_3(CN)_2$], **28**

With pentafluorobenzonitrile, C_6F_5CN

Cp*Ir(CO)(COOH)(*p*-C_6F_4CN), **18a** precipitated out of solution as a white solid. The mixture was filtered via a cannula and the solvent was removed from the supernatant under reduced pressure. Additional product was recovered from the supernatant by precipitation from a hexane-dichloromethane solution by slow evaporation. Combined yield: 76.6 mg (99%). X-ray diffraction quality crystals of **18a** were obtained by slow evaporation from a C_6F_5CN solution under reduced pressure in a Carius tube.

IR (KBr): ν_{OH} 3447 (br), 2700 (br, w), ν_{CN} 2237 (w), ν_{CO} 2036 (s), 1624 (m) cm^{-1}. ^1H NMR ($CDCl_3$): δ 8.45 (brs, 1 H, IrCOO*H*), 1.96 (s, 15H, Cp*C*H*$_3$). ^{19}F NMR ($CDCl_3$): δ -34.27 (m, 2F, F_{meta}), -59.17 (m, 2F, F_{ortho}). MS FAB^+ (*m*/z): 576$[M + H]^+$, 558$[M – OH]^+$, 530$[M – OH - CO]^+$, 502$[M – OH – 2CO]^+$. Anal. Calcd for $C_{19}H_{16}F_4NO_3Ir$: C, 39.72; H, 2.81; F, 13.23; N, 2.44. Found: C, 39.84; H, 2.60; F, 13.20; N, 2.68. HR-MS FAB^+ (*m*/z): calcd for $C_{19}H_{17}F_4NO_3Ir$ $[M + H^+]$: 576.0774, found: 576.0757.

D_2O exchange: To a sample of **18a** in $CDCl_3$ (0.5 ml) in an NMR tube was added D_2O (1 drop). The peak at δ 8.45 disappeared.

With pentafluoropyridine, C_5F_4N

Cp*Ir(CO)(COOH)(*p*-C_5F_4N), **22a** precipitated out of solution as a white solid. The mixture was filtered through cannula and the solvent was removed form the supernatant under reduced pressure. The residue obtained from the supernatant was washed with hexane (3 x 1 ml) to remove unreacted **2a** (7.9 mg, 35%). Combined yield of **22a**: 19.4 mg (59%).

IR (KBr): ν_{OH} 3448 (br), 2705 (br, w), ν_{CO} 2040 (s), 1628 (m) cm^{-1}. ^1H NMR: ($CDCl_3$): δ 1.98 (s, 15H, Cp*C*H*$_3$). ^{19}F NMR ($CDCl_3$): δ - 20.60 (m, 2F, F_{meta}), -42.88 (m, 2F, F_{ortho}). MS FAB^+ (*m*/*z*): 552$[M + H]^+$, 534$[M – OH]^+$, 506$[M – OH - CO]^+$, 478$[M – OH – 2CO]^+$. Anal. Calcd for $C_{17}H_{16}F_4NO_3Ir$: C, 37.09; H, 2.93; F, 13.80; N, 2.54. Found: C, 37.20; H, 2.83; F, 13.62; N, 2.82. HR-MS FAB^+ (*m*/*z*): calcd for $C_{17}H_{17}F_4NO_3Ir$ $[M + H]^+$: 552.0774, found: 552.0777.

With 2,3,4,5,6-pentafluorobenzaldehyde, C_6F_5CHO.

i) Neat C_6F_5CHO

Reaction mixture turned from yellow to pale brown. Removal of volatiles under reduced pressure yielded a brown oil which contained Cp*Ir(CO)(COOH)(*p*-C_6F_4CHO), **26** as the major product and a mixture of unknown compounds in minor quantities.

26 (crude)**:**

IR (dcm): ν_{CO} 2046 (s), 1719 (m), 1700 (m), 1652 (s), 1627 (m) cm^{-1}. ^1H NMR ($CDCl_3$): 10.27 (s, 1H, C*H*O), 1.98 (s, 15H, Cp*C*H*$_3$). ^{19}F NMR ($CDCl_3$): δ -37.16 (m, 2F, F_{meta}), -71.13 (m, 2F, F_{ortho}). MS FAB^+ (*m*/*z*): 561[M – (OH)] $^+$, 533[M – (COOH)]$^+$, 505[M – (COOH) - (CO)]$^+$. HR-MS FAB^+ (*m*/*z*): calcd for $C_{19}H_{16}O_3F_4$[193]Ir [M – (OH)]$^+$: 561.0683, found: 561.066.

ii) In hexane

To a Carius tube containing **2a** (10.0 mg, 26.1 μmol) was added C_6H_5CHO (30 μl, 10 eq.) in hexane (1 ml) and deionized water (0.1 ml). The solution was stirred at room temperature for 30 min. No change was observed. The reaction was repeated with 20 and 30 eq. of C_6H_5CHO in hexane. When 20 eq. of C_6H_5CHO was added, orange oil started to precipitate. When 30 eq. of C_6H_5CHO was added, more orange oil precipitated.

Crude:

^1H NMR (C_6D_6): 10.36 (s, 1H, C*H*O), 1.37 (s, 15H, Cp*C*H*$_3$). Other resonances: 1.79 (s), 1.74 (s). ^{19}F NMR (C_6D_6): δ -38.15 (m, 2F, F_{meta}), – 70.71 (m, 2F, F_{ortho}). Other resonances: -69.19 (m), – 69.61 (m), -85.69 (m).

With pentafluoronitrobenzene, $C_6F_5NO_2$.

i) In neat $C_6F_5NO_2$.

Immediate darkening of solution from yellow to light brown was observed. The solution was concentrated under reduced pressure and hexane (1 ml) was added to precipitate some brown oil.

ii) In hexane

To a Carius tube containing **2a** (10.0 mg, 26.1 μmol) was added $C_6F_5NO_2$ (0.34 μl, 1 eq.) in hexane (1 ml) and deionized water (0.1 ml). The mixture was stirred at room temperature for 30 min after which the volatiles were removed under reduced pressure. The ^1H and ^{19}F NMR spectra taken in $CDCl_3$ gave complicated spectra.

With 1-fluoro-4-nitrobenzene, *p*-$FC_6H_4(NO_2)$

Reaction mixture turned slightly brown. Removal of volatiles under reduced pressure gave yellow solids. The integration ratio of the methyl resonance of the Cp* ligand in **27** to **2a** in the ^1H NMR spectrum is 1: 14 (7% conversion).

^1H NMR ($CDCl_3$): 1.94 (s, 15H, Cp*CH_3) and other small peaks.

With tetrafluoroisophthalonitrile 1,3-$C_6F_4(CN)_2$

i) IR spectrum shows a mixture of **28**, unreacted **2a** and 1,3-$C_6F_4(CN)_2$.

ii) An NMR scale reaction was done with 5 eq. of 1,3-$C_6F_4(CN)_2$ in C_6D_6.

28:

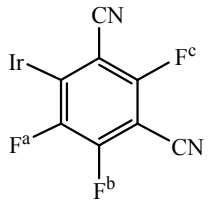

IR (dcm): ν_{CN} 2252, 2242(w), ν_{CO} 2052 (s) cm^{-1}

^1H NMR (C_6D_6): 1.53 (s, 15H, Cp*CH_3), -14.39 (s, 1H, Ir-*H*). ^{19}F NMR (C_6D_6): δ - 28.72 (d, $^5J_{FF}$ = 14, 1F, F^c), -31.65 (dd, $^3J_{FF}$ = 28, $^5J_{FF}$ = 14, 1F, F^a), -48.68 (d, $^3J_{FF}$ = 28, 1F, F^b). MS FAB^- (*m*/*z*): 537[M – H].

iii) To a Carius tube containing **2a** (10.0 mg, 26.1 μmol) and 1,3-$C_6F_4(CN)_2$ (7.0 mg, 35.0 μmol) was added C_6D_6 (1 ml) and deionized H_2O (0.1 ml). The reaction mixture was degassed by three cycles of freeze-pump-thaw, sonicated and stirred for 40 h at room temperature. Half the solution was syringed into an NMR tube containing 1,3,5-triphenylbenzene (6.0 mg, 19.5 μmol) and a ^{1}H NMR spectrum was taken immediately. Yield of **28**: 92% (^{1}H NMR).

Competitive reaction in C_6F_5CN/ C_5F_5N

To a Carius tube containing **2a** (5.4 mg, 14.1 μmol) was added C_5F_5N (0.25 ml), C_6F_5CN (0.274 ml) (1:1 molar ratio) and deionized H_2O (0.2 ml). The reaction mixture was degassed by three cycles of freeze-pump-thaw and stirred at room temperature for 16 h. The volatiles were removed under reduced pressure and the ^{1}H NMR spectrum of the residue was taken in $CDCl_3$. The integration ratio of the fluorine resonances of **22a**: **18a** in the ^{19}F NMR spectrum is 1: 1.4.

Table 3.3. Crystal data for **15**, **16** and **18a**.

Compound	**15**	**16**	**18a**
Empirical formula	$C_{17}H_{15}F_6IrO$	$C_{34.10}H_{30.20}Cl_{0.20}F_{10}Ir_2O_2$	$C_{19}H_{16}F_4IrNO_3$
Formula weight	541.49	1053.47	574.53
Temperature	223(2)	223(2)	213(2)
Crystal system	Orthorhombic	Monoclinic	Monoclinic
Space group	$Cmc2_1$	$P2_1/n$	C2/m
Unit cell dimensions			
a (Å)	12.5662(3)	11.7894(11)	13.3143(8)
b (Å)	8.2197(2)	35.409(3)	8.8432(6)
c (Å)	15.8285(4)	17.3432(16)	16.7447(10)
α (°)	90	90	90
β (°)	90	104.342(2)	108.601(3)
γ (°)	90	90	90
Volume ($Å^3$)	1634.93(7)	7014.3(11)	1868.5(2)
Z	4	8	4
Density calc. (Mg m^{-3})	2.200	1.995	2.042
Absorption coefficient (mm^{-1})	8.232	7.679	7.204
F(000)	1024	3986	1096
Crystal size (mm^3)	0.36 x 0.32 x 0.24	0.36 x 0.30 x 0.10	0.17 x 0.10 x 0.06
Theta range for data collection (°)	2.57 to 26.37	2.11 to 26.37	2.57 to 30.50
Index ranges	$0 \le h \le 15$	$-14 \le h \le 14$	$-18 \le h \le 17$
	$0 \le k \le 10$	$0 \le k \le 44$	$0 \le k \le 12$
	$-19 \le l \le 15$	$0 \le l \le 21$	$0 \le l \le 23$
Reflections collected	6923	98672	8728
Independent reflections	1432 [R(int) = 0.0250]	14331 [R(int) = 0.0533]	2879 [R(int) = 0.0358]
Completeness to theta (%)	= 26.37°; 100.0	theta = 26.37°; 100.0	= 30.50°; 95.3
Max. and min. transmission	0.2427 and 0.1556	0.5139 and 0.1686	0.6718 and 0.3739
Data / restraints / parameters	1432 / 61 / 145	14331 / 0 / 886	2879 / 0 / 256
Goodness-of-fit on F^2	1.067	1.362	1.076
Final R indices [$I>2\sigma(I)$]	R1 = 0.0207, wR2 = 0.0529	R1 = 0.0641, wR2 = 0.1595	R1 = 0.0346, wR2 = 0.0719
R indices (all data)	R1 = 0.0208, wR2 = 0.0529	R1 = 0.0739, wR2 = 0.1630	R1 = 0.0386, wR2 = 0.0737
Largest diff. peak and hole (e.$Å^{-3}$)	1.316 and -0.526	2.118 and -1.388	1.800 and -1.355

References

[1] Bergman, R. G. In *Homogeneous Transition Metal Catalyzed Reactions*; W. R. Moser, D. W. Slocum, Eds.; Advances in Chemistry Series 230; American Chemical Society: Washington, DC, 1992; Chapter 14; pp 211-220.

[2] Hoyano, J. K.; McMaster, A. D.; Graham, W. A. G. *J. Am. Chem. Soc*. **1983**, *105*, 7190-7191.

[3] Lees, A. J.; Marx, D. E. *Inorg. Chem.* **1988,** *27*, 1121-1122.

[4] Buchanan, J. C.; Stryker, J. M.; Bergman, R. G. *J. Am. Chem. Soc*. **1986**, *108*, 1537-1550.

[5] Bach, I.; Pörschke, K-R; Goddard, R.; Kopiske, C.; Krüger, C.; Rufińska, A.; Seevogel, K. *Organometallics* **1996**, *15*, 4959-4966.

[6] Bell, T. W.; Helliwell, M.; Partridge, M. G.; Perutz, R. N. *Organometallics* **1992**, *11*, 1911-1918.

[7] (a) Belt, S. T.; Duckett, S. B.; Helliwell, M.; Perutz, R. N. *J. Chem. Soc., Chem. Commun.* **1989**, 928-930. (b) Belt, S. T.; Helliwell, M.; Jones, W. D.; Partridge, M. G.; Perutz, R. N. *J. Am. Chem. Soc*. **1993**, *115*, 1429-1440.

[8] Lefort, L.; Crane, T. W.; Farwell, M. D.; Baruch, D. M.; Kaeuper, J. A.; Lachicotte, R. J.; Jones, W. D. *Organometallics* **1998**, *17*, 3889-3899.

[9] (a) Churchill, M. R.; Julis, S. A. *Inorg. Chem.* **1979**, *18*, 1215-1221. (b) Isobe, K.; Miguel, V.; Maitlis, P. M. *J. Organomet. Chem.* **1983**, *250*, C25-C27. (c) Heinekey, D. M.; Michel, S. T.; Schulte, G. K. *Organometallics* **1989**, *8*, 1241-1246. (d) Zhuang, J. M.; Batchelor R. J.; Einstein, F. W**.** B.; Jones, R. H.; Hader, R.; Sutton, D. *Organometallics* **1990**, *9*, 2723-2727.

[10] Kolomnikov, I.S.; Kukolev, V.P.; Koreshkov, Yu.D.; Mosin, V.A.; Vol'pin, M.E. *Izv. Akad. Nauk SSSR, Ser. Khim*. **1972**, 2371.

[11](a) Pinkes, J. R.; Masi, C. J.; Chiulli, R.; Steffey, B.D.; Cutler, A.R. *Inorg. Chem.* **1997**, *36*, 70-79. (b) Gibson, D. H.; Mehta, J. M.; Ye, M.; Richardson, J. F.; Mashuta, M. S. *Organometallics* **1994**, *13*, 1070-1072. (c) Mandal, S. K.; Ho, D. M.; Orchin, M. *J. Organomet. Chem*. **1992**, *439*, 53-64. (d) Gibson, D. H.; Ong, T. S. *J. Am. Chem. Soc.* **1987**, *109*, 7191-7193. (e) Bennett, M. A. *J. Mol. Catal*. **1987**, *41*, 1-20. (f) Gibson, D. H.; Owens,

K.; Ong, T. S. *J. Am. Chem. Soc*. **1984**, *106*, 1125-1127. (g) Carlos, F.; Barrientos, P.; Gilchrist, A. B.; Sutton, D. *Organometallics* **1983**, *2*, 1265-1266. (h) Sweet, J.; Graham, W. A. G.; *Organometallics* **1982**, *1*, 982-986. (i) Grice, N.; Kao, S. C.; Pettit, R. *J. Am. Chem. Soc*. **1979**, *101*, 1627-1628.

Chapter 4: Possible Pathways for the Formation of the Metallocarboxylic Acid, Cp*Ir(CO)(COOH)(C_6F_4CN)

4.1 Synthetic routes to metallocarboxylic acids

Metallocarboxylic acids (hydroxycarbonyls) have been proposed to be key intermediates in several reactions of catalytic importance,[1] including the oxidation of carbon monoxide by transition metal ions such as Hg^{2+},[2] iron carbonyl-catalyzed water-gas shift reaction,[3] carbon dioxide fixation and reduction, in the exchange of metal carbonyls with oxygen-labelled water,[4] and reactions of metal carbonyls with water to form the corresponding hydrides.[5]

There are fewer known hydroxycarbonyl complexes that have been structurally and/or spectroscopically characterized compared to alkoxycarbonyl complexes probably due to their lower stabilities. For example, metallocarboxylic acids have only been characterized for Mo, Re, Fe, Ru, Ir and the platinum triad but alkoxycarbonyls have been characterised for all group 7 to 10 metals as well as for Hg.[6]

Metallocarboxylic acids are most commonly prepared via nucleophilic attack of water or hydroxide ions on an electrophilic CO ligand bound to a metal centre. The attack is favoured by high charge on the metal, electron-withdrawing groups on the other ligands and little M→CO back-bonding.[7]

Another method of preparing metallocarboxylic acids involves insertion of CO into a M-OH bond. This route has only been reported for platinum group metals.[8,9] Some of the synthetic methods for the formation of metallocarboxylic acids are shown in Scheme 4.1.

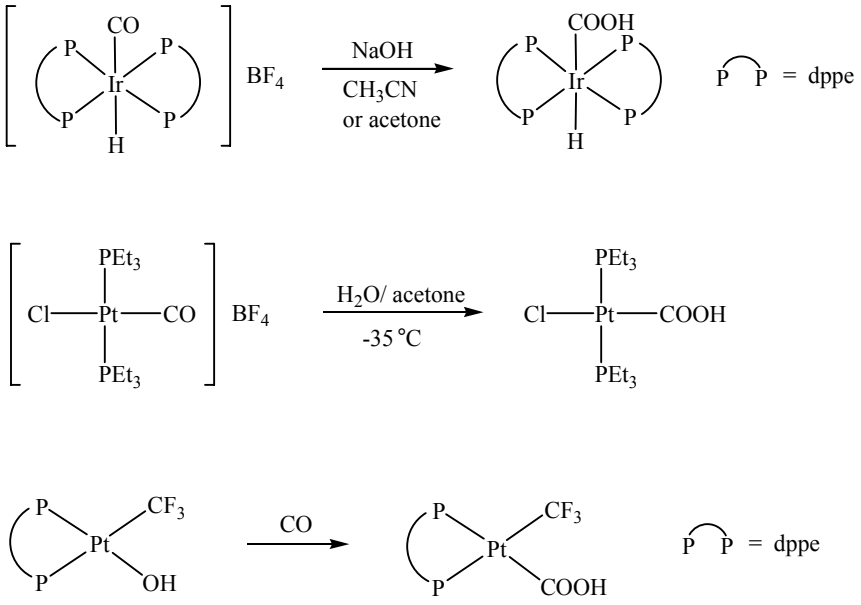

Scheme 4.1

From the examples above, it can be seen that the metal complexes susceptible to nucleophilic attack by water to form the corresponding metallocarboxylic acids are usually cationic metal carbonyls. It is therefore of interest to find out how the metallocarboxylic acid is formed in our case, where the starting complex is a neutral iridium dicarbonyl.

In the course of our studies, a report on the formation of an Ir(III) hydroxycarbonyl complex starting from a neutral Ir(I) complex, Tp'Ir(CO)$_2$ [Tp' = hydrotris(pyrazolyl)borate or hydrotris(3,5-dimethylpyrazolyl)borate] which bears some relation to our work appeared; the proposed mechanism for the reaction is shown in Scheme 4.2.[10]

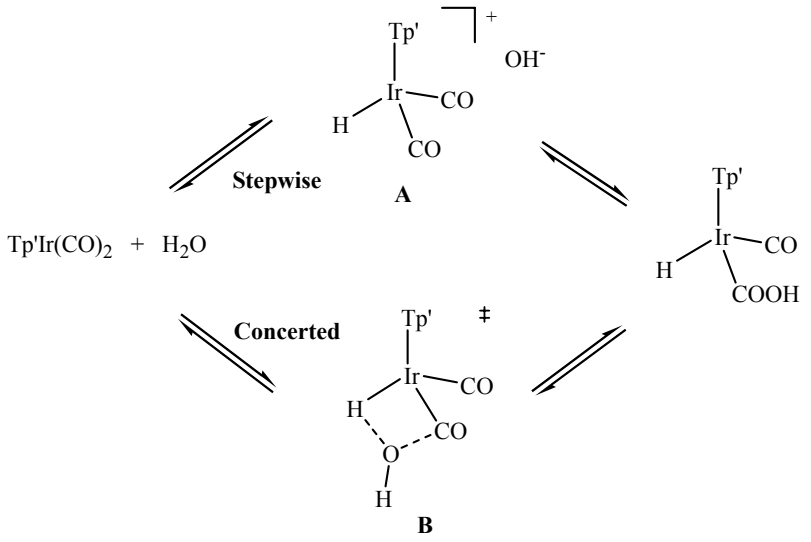

Scheme 4.2

It was proposed that the iridium (I) complex was oxidized to an iridium(III) intermediate (**A**) by protonation. Nucleophilic attack on one of the CO ligand then generated the metallocarboxylic acid. Protonation of the iridium centre and nucleophilic attack on CO can also occur in a concerted manner via transition state **B**. The reaction showed a kinetic isotope effect of k_{H2O}/k_{D2O} = 1.4 at 20 ºC, indicating that an O-H or O-D bond cleavage was involved in the rate-determining step. D_2O has a smaller self-ionization constant compared to H_2O, hence protonation of the iridium centre by H_2O is faster.

4.2 Possible reaction pathways

The several possibilities for the reaction pathway leading from **2a** to **18a** which we have considered are summarized in Scheme 4.3. Pathway **a** involves a CO dissociation and a C-F activation to form an Ir-F species (**F**) via an Ir-(η^2-C_6F_5CN) intermediate (**D**). This is similar to the mechanism proposed for C-H activation of hydrocarbons by Cp*Ir$(CO)_2$, **2a**; dissociation of a CO ligand to form the coordinatively-unsaturated 16-electron species [Cp*Ir(CO)] led to C-H activation of hydrocarbons to form Cp*Ir(CO)(R)(H).[11] The Ir-F bond may undergo hydrolysis to form an Ir-OH bond which can undergo CO insertion to form the metallocarboxylic acid. CO insertion into M-OH bonds to form metallocarboxylic acids has been reported for Ni, Pt and Pd complexes.[8,9] Alternatively, the coordination of the fluoroarene to the iridium center may take place without CO dissociation to give the 20-electron species Cp*Ir$(CO)_2$(η^2-C_6F_5CN) (**C**), or a ring slippage complex (η^3-Cp*)Ir$(CO)_2$(η^2-C_6F_5CN) (**E**).

Pathway **b** involves an initial nucleophilic aromatic substitution of **2a** at the perfluorinated ring leading to a cationic intermediate (**G**). Intermediate **G** can undergo attack by water or OH^- on one of the carbonyl carbon to form the COOH moiety,[9,12] or a nucleophilic attack by fluoride ion may occur to form a fluoroacyl species such as Cp*Ir(CO)(COF)(C_6F_4CN) (**H**); the latter is expected to be sensitive to moisture,[13] and hence

may then undergo hydrolysis of the COF moiety to COOH. Our task is thus to examine these possibilities.

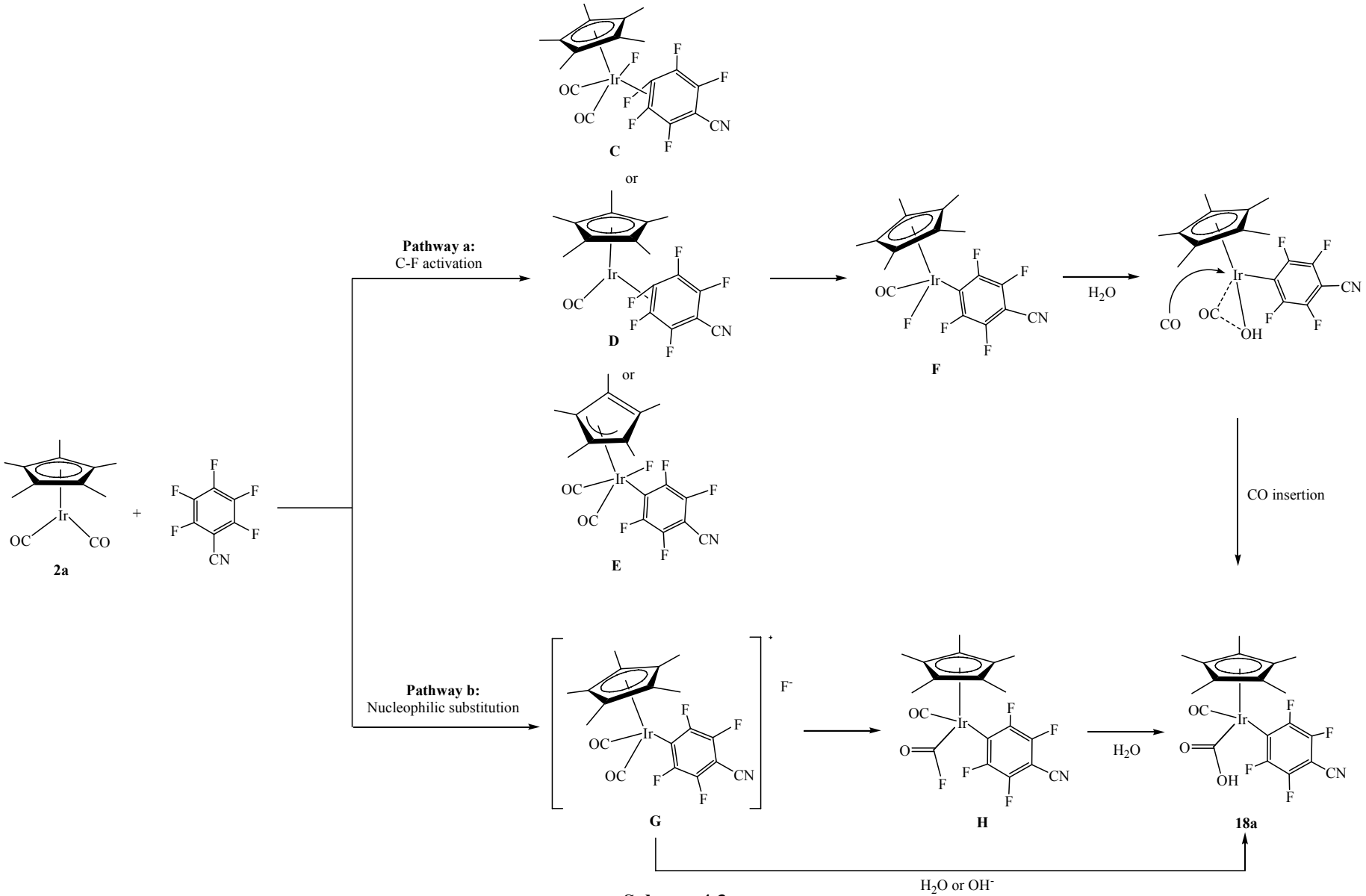
2a
C
or
D
or
E
Pathway a:
C-F activation
F
H2O
CO insertion
Pathway b:
Nucleophilic substitution
G
H
18a
H2O or OH-

Scheme 4.3

4.3 C-F activation by photochemical activation

It was described previously that complexes such as $LRh(PMe_3)(C_6F_5)(F)$ (where L = Cp or Cp*) could be obtained photochemically from the reaction of $LRh(PMe_3)(C_2H_4)$ with C_6F_6. We have also found that **2a** reacted photochemically with C_6F_6 to give $Cp^*Ir(CO)(\eta^2\text{-}C_6F_6)$, **15** and $[Cp^*Ir(CO)(C_6F_5)]_2$, **16** with the loss of one CO ligand per molecule of **2a**. However, CO dissociation is not likely to be so facile at room temperature in the absence of photoactivation. UV irradiation should promote CO dissociation and hence increase the rate of reaction for pathway **a**. However, UV irradiation of a solution of **2a** in C_6F_5CN did not give **18a** but a mixture of other products suggesting that pathway **a** is unlikely.

4.4 Regioselectivity and substituent effect

Cleavage of C-F bonds in substituted fluoropyridines and fluoroarenes by the platinum group metals is known.[14] For the nickel triad, activation of C_5F_5N, for example, occurs predominantly at the *2*-position for Ni, and at the *4*-position for Pt and Pd. The difference in regiochemistry has been accounted for with differing mechanisms.[15] For nickel complexes, the observed preference for C-F activation at the *2*-position suggests that the reaction takes place via a three-centred transition state in a concerted oxidative addition reaction (a). Reaction via a tight ion pair (b) or Meisenheimer intermediate (c) would result in activation at the *4*-position as observed for platinum[16] and palladium[15b] complexes, and in nucleophilic substitution by various transition metal anions.[17]

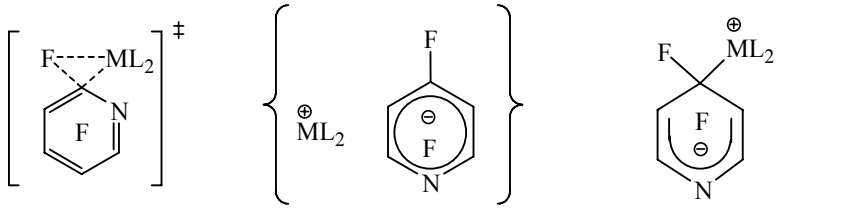

a) Concerted b) Electron transfer/ tight ion pair c) S_NAr/ Meisenheimer

Figure 4.1. Possible intermediates and transition states for C-F activation of C_5F_5N by transition metals.[15d]

Highly fluorinated aromatic compounds are susceptible to nucleophilic substitution. Presence of electron-withdrawing substituent(s) favors the reaction by stabilizing the negative charge in the intermediate such as in the case of a CN group (Scheme 4.4),[18] and fluoride is a good leaving group for nucleophilic aromatic substitution. In such systems, nucleophilic attack occurs predominantly at the position *para* to the functional group present.[19]

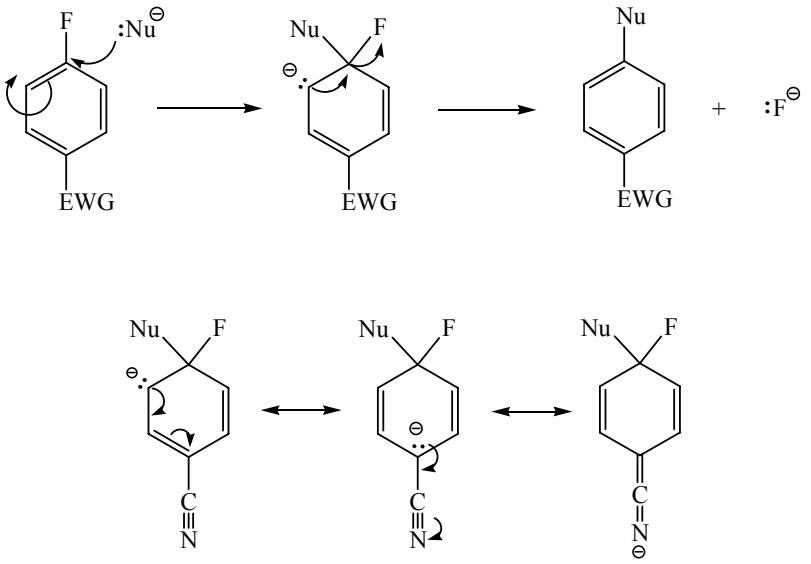

Scheme 4.4

For example, polyfluoroaromatic nitrogen heterocyclic systems are activated towards nucleophilic aromatic substitution relative to the corresponding benzenoid compounds. C_5F_5N reacts with various nucleophiles such as MeO^-, NH_3, $C_6F_5^-$, OH^- to give only *para*-substituted products. Attack at the *4*-position (para to N) is strongly preferred because the negative charge in the intermediate can be placed on the electronegative N and it avoids electron-pair repulsion arising from fluorine at the *5*-position (Scheme 4.5).

The reaction of **2a** with C_6F_5CN and C_5F_5N was observed to be highly regioselective, giving rise to only *para*-substituted products, Cp*Ir(CO)(COOH)(*p*-C_6F_4CN), **18a** and Cp*Ir(CO)(COOH)(*p*-C_5F_4N), **22a**, respectively. This is consistent with a nucleophilic aromatic substitution mechanism where the rate of reaction is enhanced by a good leaving group, a strong nucleophile and a stable intermediate.

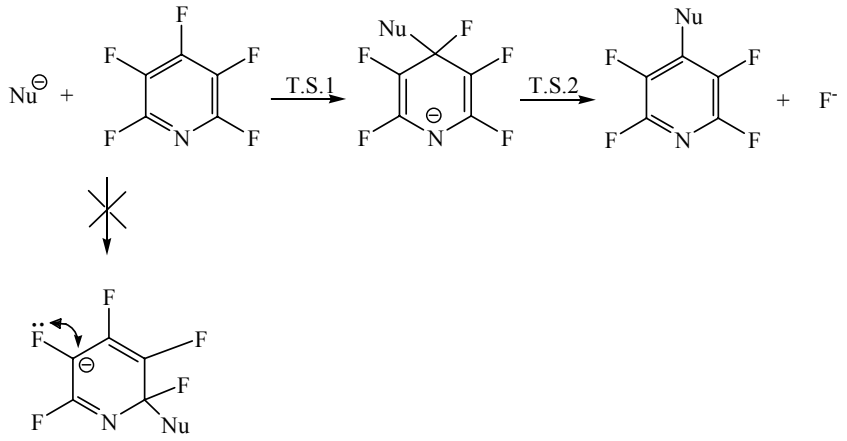

Scheme 4.5

The electron-withdrawing power of substituents can be quantified using the Hammett substituent constant σ (Table 4.1). Electron-withdrawing substituents make σ positive while electron-donating groups make σ negative.[20] It can be seen that reaction only occurred with fluoroarenes containing substituents that are highly electron-withdrawing (large positive σ_p) or can stabilize negative charges in the transition state by conjugation (large positive $\sigma^-_{p)}$.

Table 4.1. Correlation between σ values[21] and outcome of the reaction between **2a** and C_6F_5X. X indicates no reaction.

Substituent	σ_p	σ^-_p [a]	Outcome of reaction
OMe	-0.268	-0.2	X
NH_2	-0.66	-0.13	X
H	0	0	X
F	+0.06	+0.02	X
COOMe	+0.39	+0.68	X
CF_3	+0.54	+0.73	X
CN	+0.66	+1.00	√
NO_2	+0.78	+1.04	Mixture
CHO	+0.22	+1.13	Mixture

[a]Modified constant (σ^-_p) used where delocalization of electrons can take place across the entire π-system (through-conjugation).[22]

C-F activation of fluoroarene, on the other hand, is not likely to be so substituent dependant and can occur even with C_6F_6 and fluoroarene carrying electron-donating substituent such as OMe. For example, the reaction of $CpRh(PMe_3)(C_2H_4)$ with pentafluoroanisole (*p*-C_6F_5OMe) was non-regioselective and occurred under photoirradiation to give two isomeric η^2-arene complexes.[23]

4.5 Nucleophilicity of 2a

Nucleophilic aromatic substitutions by organic and organometallic nucleophiles are well known, although the organometallic nucleophiles are usually metal anions. The following order (in decreasing nucleophilicity) was made by empirical observations on the reactivity of the anions: $[Re(CO_5)]^-$ ~ $[CpFe(CO)_2]^-$ > $[CpRu(CO)_2]^-$ $[Mn(CO)_4(PPh_3)]^-$ > $[Mn(CO_5)]^-$ > $[CpMo(CO)_3]^-$ > $[Fe(CO_4)]^{2-}$ > $[Co(CO_4)]^-$.[17c] Strong nucleophiles react with hexafluorobenzene to afford stable complexes while weaker nucleophiles are unreactive. $[Mn(CO_5)]^-$ has been reported to react with C_6F_5CN and C_5F_5N, but $[Co(CO_4)]^-$ failed to react.[17f] Although neutral transition metal carbonyls have been known to act as nucleophiles in oxidative addition reactions to simple alkyl halides,[24] there have not been any literature reports on nucleophilic substitution on fluoroarenes by neutral transition metal carbonyls. In our case, we have a neutral, 18-electron organometallic complex **2a** acting as a nucleophile in nucleophilic substitution of fluoroarenes. We believe that the iridium centre is sufficiently electron-rich for the complex to act as a nucleophile because the Cp analogue $CpIr(CO)_2$ is known to act as a 2-electron donor in several iridium-osmium complexes.[25] Cp*, being more electron-donating than Cp, will make the iridium center more electron-rich and hence more nucleophilic.

Boron halides are known to be Lewis acids and bind to electron-pair donors such as $:NR_3$ to form a Lewis adduct. To show that the iridium center in **2a** is electron-rich enough to act as a 2-electron donor, **2a** was reacted with $BF_3{\cdot}OEt_2$. White solid precipitated out of a solution of **2a** in hexane immediately upon addition of an ethereal solution of $BF_3{\cdot}OEt_2$ and

the supernatant turned from yellow to colourless. The white solid was soluble in dcm initially but decomposed to a yellow insoluble solid upon standing. It also turned yellow upon removal of solvent under reduced pressure. Monitoring of the reaction by IR spectroscopy, in which $BF_3{\cdot}OEt_2$ was added dropwise to a dcm solution of **2a** until it turned colourless, shows that the two CO stretching vibrations were blue-shifted by *ca*. 100 cm^{-1} (**2a**: ν_{CO} 2009, 1937; **31**: ν_{CO} 2118 (s), 2078 (s) cm^{-1}), consistent with the donation of electron density from iridium to boron. The ^1H NMR spectrum also shows a downfield shift in the Cp* resonance from δ 2.18 to δ 2.26. The ^{11}B NMR spectra shows a resonance at δ -1.18 when it was calibrated with the resonance of $BF_3{\cdot}OEt_2$ set to δ 0.00, demonstrating that the Ir-BF_3 adduct formed is a slightly stronger coordination complex than $BF_3.OEt_2$. The MS (FAB^+) shows a low intensity cluster of peaks around 451 corresponding to $Cp^*Ir(CO)_2(BF_3)$. Repeating the reaction with less than half molar equivalents of $BF_3{\cdot}OEt_2$ resulted in CO stretching vibrations due to both unreacted **2a** and the product. These results suggest that an Ir-BF_3 adduct has been formed, thus demonstrating that the iridium center can act as an electron-pair donor.

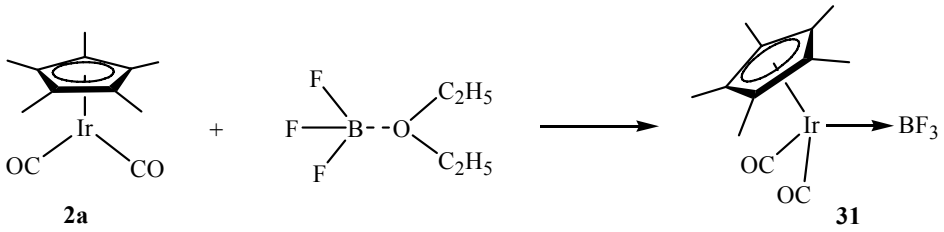

2a **31**

Scheme 4.6

Reaction of C_6F_5CN with the rhodium analogue of **2a**, $Cp^*Rh(CO)_2$ did not lead to the formation of the corresponding metallocarboxylic acids. The IR and ^1H NMR spectra show only the presence of unreacted starting material. Rhodium, being above iridium in the same group is expected to be less electron-rich and hence less nucleophilic.

4.6 Attempted detection and isolation of intermediate

It would seem that pathway **b** involving a cationic intermediate **G** (Scheme 4.3) was the most likely reaction pathway; this is also corroborated by the large number of literature reports on the formation of metallocarboxylic acid via nucleophilic attack of water or hydroxide ions on cationic metal carbonyl complexes.[3,5,7,9] Since the reaction of $CpIr(CO)(PPh_3)$ with alkyl halides (RX) was reported to produce a stable ionic species, $[CpIr(CO)(PPh_3)(R)]^+[X]^-$ via a bimolecular mechanism,[24a] we thought that the reaction of **2a** with fluoroarene may thus similarly produce an ionic intermediate, $[Cp^*Ir(CO)_2R_F]^+F^-$ which is susceptible to attack by water or hydroxide ion to produce the metallocarboxylic acid.

The alternative pathway to the formation of metallocarboxylic acid via a fluoroacyl intermediate has no literature precedence although fluoroacyl complexes have been synthesized by other routes. The reaction of XeF_2 with the iridium carbonyl complexes $[Ir(CO)_3L_2]^+$ (L = PMe_3, PMe_2Ph, PEt_2Ph, $PEtPh_2$) and $[Ir(CO)_2Cl(PMe_3)_2]$, have been reported to afford fluoroacyl complexes. $[Ir(CO)_3(PEt_3)_2]^+$, for example, gave $[Ir(CO)_2F(COF)(PEt_3)_2]^+$, which was isolated as the BF_4^- or PF_6^- salt.

It was hoped that by performing the reaction under anhydrous conditions, it would be possible to detect the intermediate of the reaction before the nucleophilic attack of the carbonyl by water (**G**) or the hydrolysis step (**H**) (Scheme 4.3). The reaction of **2a** with C_6F_5CN at room temperature, with dried molecular sieves to remove water, gave an off-white precipitate in a pale yellow supernatant. The IR spectrum of the crude mixture (taken in C_6F_5CN) gave weak intensity peaks corresponding to **18a** (from reaction with trace amounts of moisture). The residue obtained after removal of volatiles was not soluble in C_6D_6 or $CDCl_3$, suggesting that it was ionic. The residue, however, dissolved in methanol to give $Cp^*Ir(CO)(COOMe)(p\text{-}C_6F_4CN)$, **18b**. The result suggests that the intermediate could be the ionic species $[Cp^*Ir(CO)_2(C_6F_4CN]^+[F]^-$, **G** and that nucleophilic attack by methanol on one of the carbonyl group resulted in the formation of the ester **18b**.

In the reaction of **18a** with HBF_4, $[Cp^*Ir(CO)_2(p\text{-}C_6F_4CN)]^+[BF_4]^-$, **20** was isolated as a product from the dehydration of **18a** (Section 5.2). If the intermediate was indeed

$[Cp^*Ir(CO)_2(p\text{-}C_6F_4CN)]^+[F]^-$, it might be possible to convert the counter-anion from F^- to BF_4^- to isolate the intermediate as **20** by salt exchange with $AgBF_4$ (Scheme 4.7).

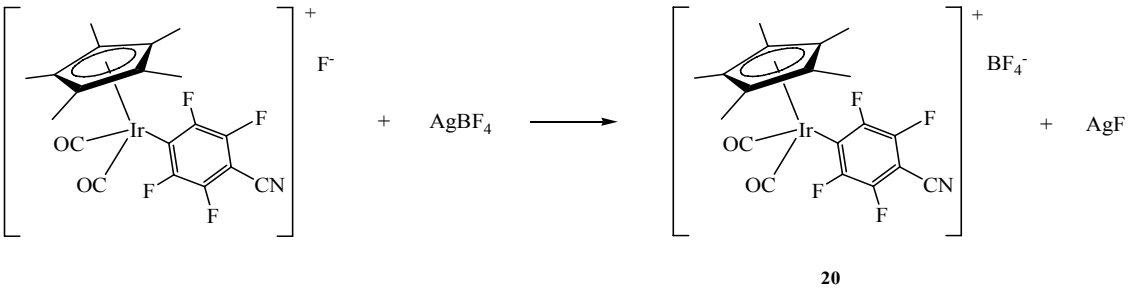

20

Scheme 4.7

Attempts were made to synthesize **20** from **2a** by (i) reacting **2a** with anhydrous C_6F_5CN followed by addition of $AgBF_4$ under an inert atmosphere and (ii) by a one-pot reaction of **2a** and $AgBF_4$ in anhydrous C_6F_5CN. An immediate precipitation of tan solids upon addition of $AgBF_4$ was observed in (i). In (ii) a tan precipitate was also obtained at the end of the reaction. The tan solid darkened upon exposure to moist air, consistent with the expected formation of AgF by exchange of F^- with BF_4^-. However, the presence of **20** was not evident in the ^1H and ^{19}F NMR spectra. Instead, a complicated mixture of products was observed in the spectra. Addition of water to the product mixtures did not give **18a**. Similarly, salt exchange was attempted with TMSOTf without success. The reaction of **2a** with C_6F_5CN under anhydrous conditions in the presence of HBF_4 also failed to give **20**.

Another approach to convert the intermediate to the BF_4^- salt was made by reacting the intermediate with $BF_3{\cdot}OEt_2$. Presence of **20** was not observed in the ^1H and ^{19}F NMR spectra. However, the ESI spectrum (negative ion mode) shows a strong intensity peak corresponding to BF_4^- suggesting that F^- is present in the reaction mixture.

The above attempts to isolate and characterize the intermediate were unsuccessful probably due to the instability of the intermediate. An increase in the electron-density on iridium by phosphine substitution may make it possible to arrest the reaction in the intermediate stage as the reduction in electrophilicity of the remaining CO ligand may be sufficient to disfavour nucleophilic attack by water or hydroxide ion on the carbonyl carbon (Scheme 4.8). Precedence to this has been observed in the iron complex $[CpFe(CO)_2(PPh_3)]^+$,

which reacted with KOH to form the stable [CpFe(CO)(CO_2H)(PPh_3)]. The more electron-rich [CpFe(CO)$_2$(dppe)]$^+$ failed to react with KOH..

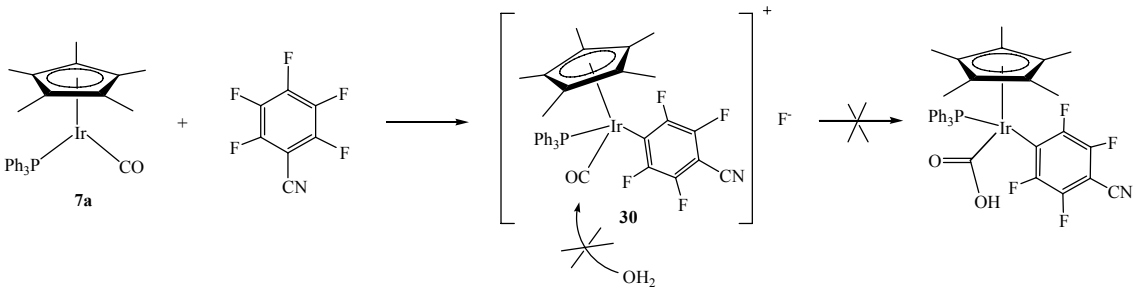

Scheme 4.8

Reaction of the phosphine substituted complex Cp*Ir(CO)(PPh_3), **7a** with C_6F_5CN resulted in the formation of a product that still contain the CO ligand (as indicated by terminal CO stretching vibrations the IR spectrum) and phosphine ligand (as shown by the aromatic proton resonances in the ^{1}H NMR spectrum). MS (FAB$^+$) shows the molecular ion peak corresponding to the formulation [Cp*Ir(CO)(PPh_3)(*p*-C_6F_4CN)]$^+$. If the reaction of **2a** with C_6F_5CN occurred via the same pathway, [Cp*Ir(CO)$_2$(*p*-C_6F_4CN)]$^+$ would be formed and the reaction is likely to be via intermediate **G**.

4.7 Kinetic studies

There are a few possible routes for the formation of **18a** from the proposed intermediate **G**. The rate-determining step (r.d.s.) may involve: (i) nucleophilic attack by water molecule on the carbonyl carbon with F^- acting as a base to partially abstract a proton from the attacking water molecule in the transition state and hence increasing the nucleophilicity of the water molecule. This is aided by hydrogen bonding between F^- and H_2O - general base catalysis, (ii) nucleophilic attack by OH^- on the carbonyl carbon - nucleophile catalysis or (iii) nucleophilic attack by F^- on the carbonyl carbon followed by hydrolysis of the fluoroacyl group- nucleophile catalysis (Scheme 4.9).

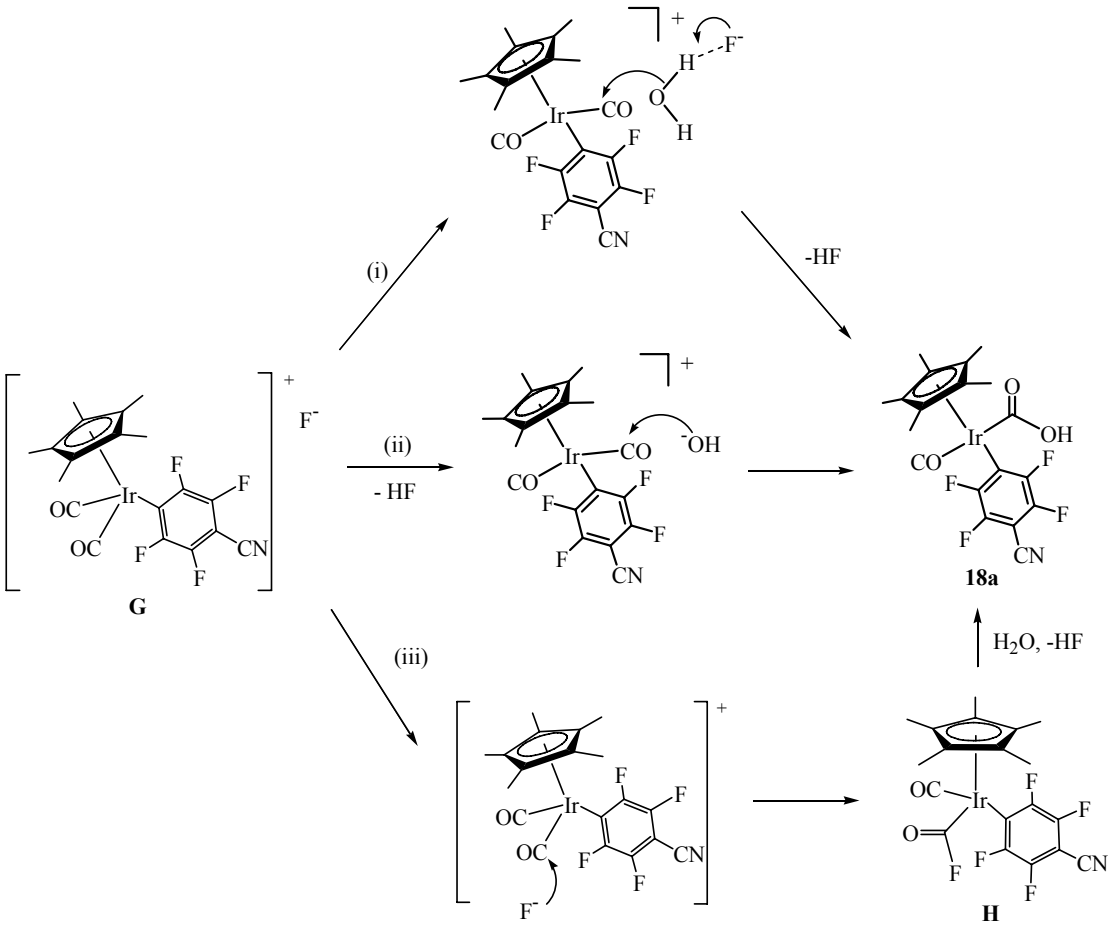

Scheme 4.9

If the r.d.s. is the general base-catalyzed attack by H_2O, the reaction in H_2O would be expected to be faster than D_2O due to kinetic isotope effect, which favours the breaking of O-H bond to O-D bond. If the r.d.s. involves nucleophilic attack by OH^-, k_{H2O}/k_{D2O} is generally

unity or inverse because OD^- is a better nucleophile that OH^-.[26] If the r.d.s. involves nucleophilic attack by F^-, no kinetic isotope effect would be expected.

It was found that the reaction in H_2O was slightly faster than the reaction in D_2O with k_{H2O}/k_{D2O} of 1.2 at room temperature. This value is relatively small compared to the generally observed value of 2 or above for general base catalysis.[26b, 27] However, there are several literature reports where the kinetic isotope effect is much smaller than 2 for reactions that proceed via general base catalysis. For example, a kinetic isotope effect of $k_H/k_D = 1.38$ was observed in the transesterification (ethanolysis) of 2'/3'-*O*-peptidyl adenosine where the molecule acts as a general base of its own external peptidyl transfer. The small kinetic isotope effect suggests a significant movement of a proton towards the 2'-oxyanion concurrent with the attack of the neutral ethanol molecule.[28] In our case, there might be strong hydrogen bonding and significant H-F bond formation in the transition state, leading to a small kinetic isotope effect.

A similar pathway is proposed for the formation of the iridium alkoxycarbonyls **18b-d**. The rate-determining step involves the base-catalyzed attack of the alcohol molecule on the carbonyl carbon. This is supported by experimental evidence that the rate of formation of the acid **18a** is faster than for the methyl ester, **18b** followed by the isopropyl ester, **18c**. The reaction of **2a** with C_6F_5CN in the presence of water to form **18a** took 8 h to complete, while the same reaction in methanol or isopropanol to form their corresponding esters **18b** and **18c** gave a 98 % and 82 % conversion, respectively, after 22 h of stirring at room temperature; complete conversion was obtained after approximately 2 d. If rate-determining step is the nucleophilic attack by F^-, the reaction time required for all the alcohols would be similar.

Water, being more acidic than methanol and isopropanol (Table 4.2) is more susceptible to proton abstraction by F^- and hence the reaction to form **18a** would be expected to be the fastest. Using the same argument, the reaction in isopropanol would be the slowest since it is the least acidic among the three. Hence the reaction of **2a** with C_6F_5CN in a 1:1 molar ratio of MeOH: ^{i}PrOH under anhydrous condition gave a 7:1 ratio of Ir-COOMe:Ir-COO^{i}Pr (from ^{19}F NMR integration).

Table 4.2. pK_a values of water and some alcohols.

R-OH	**pK_a**
H-OH (water)	15.8
Me-OH (methanol)	16.4
Et-OH (ethanol)	16.8
^{i}Pr-OH (isopropanol)	17.2

In order to test the proposal that fluoride ion promotes the formation of the metallocarboxylic acid or alkoxycarbonyl from the intermediate by forming hydrogen bonds with water or alcohol molecules, the effect of addition of fluoride on the rate of reaction was studied. Reaction of **2a** with C_6F_5CN in the presence of water and tetrabutylammonium fluoride (Bu_4NF), or tetramethylammonium fluoride (Me_4NF) resulted in the formation of the decarboxylated product Cp*Ir(CO)(H)(*p*-C_6F_4CN), **19a** (see Section 5.3). However, it was found that the reaction of **2a** with C_6F_5CN in methanol to give **18b** proceeded to completion in 8 h in the presence of 5 equivalents of $[Me_4N]F$, but failed to complete even after 22 h in the absence of $[Me_4N]F$. Hence, the formation of **G** from the reaction of **2a** with C_6F_5CN may be reversible, with the equilibrium lying to the left. Addition of F^- promotes the second step (nucleophilic attack on carbonyl carbon) by partial abstraction of proton from H_2O or ROH, thereby shifting the equilibrium of the first step to the right by consuming the intermediate **G** (Scheme 4.10).

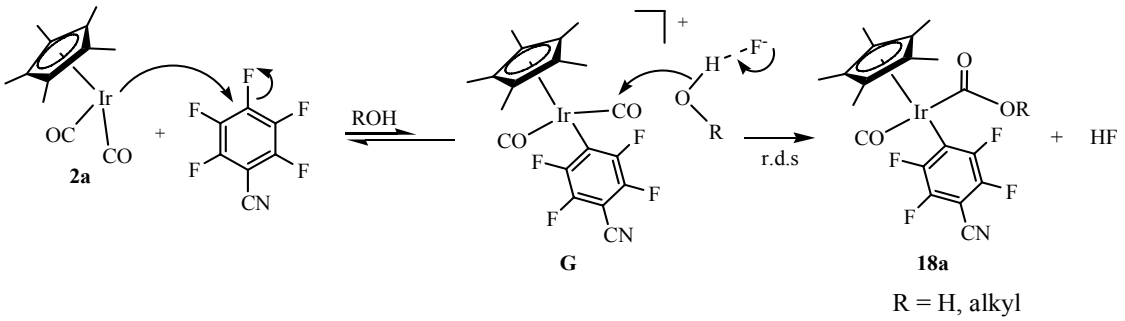

Scheme 4.10

4.8 Conclusion

The evidences presented in Sections 4.3 to 4.7 are consistent with a nucleophilic aromatic substitution mechanism. The reaction only occurs with fluoroaromatics containing highly electron-withdrawing substituents and give only *para*-substituted products. With the Rh analogue $Cp^*Rh(CO)_2$ where the metal center is less electron-rich, no reaction was observed. The formation of the metallocarboxylic acid can be suggested to involve two nucleophilic substitution steps. The first step involves a nucleophilic attack of the iridium center on the *para*-carbon of the fluoroarene; the second step involves the base-catalyzed attack of water or alcohol on one of the carbonyl carbon to form the carboxylic group.

The reaction is highly dependent on the electronic properties of the various species involved. If the metal center is not electron-rich enough, or the substituent on the fluoroarene is not electron-withdrawing enough, reaction will not occur. If the metal center is too electron-rich, as in the case of $Cp^*Ir(CO)(PPh_3)$, the carbonyl group in the intermediate is not electrophilic enough to undergo nucleophilic attack by water. If the fluoroarene contains highly electron-withdrawing groups, it will be very susceptible to nucleophile attack, i.e. 1,3-$C_6F_4(CN)_2$ can undergo attack by other nucleophiles such as methanol in addition to nucleophilic attack by **2a**. Similarly, a stronger nucleophile such as pyridine or amine would compete with **2a** for the initial attack at the fluoroarene.

4.9 Experimental

General experimental as described in Section 2.6. $Cp^*Ir(CO)_2$, **2a** and $Cp^*Ir(CO)(PPh_3)$, **7a** were synthesized and purified as described in Section 2.6. All other reagents were purchased commercially and used without further purification. For reactions under anhydrous condition, pentafluorobenzonitrile was dried using molecular sieve prior to use.

4.9.1 Reaction of 2a with $BF_3{\cdot}OEt_2$

i) To a solution of **2a** (10.0 mg, 26.1 μmol) in hexane in a Schlenk tube was added $BF_3{\cdot}OEt_2$ (3.3 μl, 26.0 μmol). Fine white solids precipitated from a yellow solution. An additional 50 μl of $BF_3{\cdot}OEt_2$ was added. The solution turned colourless immediately upon stirring with the precipitation of more white solid. The mixture was filtered via a cannula and the solid was washed with hexane (3 x 2.0 ml). The solid was soluble in dcm but upon standing, it slowly turned into an insoluble yellow solid.

ii) $BF_3{\cdot}OEt_2$ was added dropwise into a solution of **2a** (10.0 mg, 26.1 μmol) in dcm until the solution turned colourless. An IR spectrum of the reaction mixture was taken without removal of solvent. Attempts to crystallize out the product from dcm/cyclopentane or dcm/hexane solutions were unsuccessful. The solution slowly turned yellow upon standing.

NMR scale reaction:

iii) Complex **2a** (5.0 mg, 13.0 μmol) was dissolved in $CDCl_3$ (0.5 ml) in an NMR tube fitted with a rubber septum. A drop of $BF_3{\cdot}OEt_2$ was added immediately prior to NMR analysis. The ^1H NMR spectrum shows that **2a** was totally consumed.

iv) Complex **2a** (7.0 mg, 18.3 μmol) was dissolved in $CDCl_3$ (0.4 ml) in an NMR tube fitted with a rubber septum. $BF_3{\cdot}OEt_2$ (0.1 ml, 8.1 μmol withdrawn from a 10μl/ml $BF_3{\cdot}OEt_2$ in $CDCl_3$ solution) was added to the NMR tube immediately prior to NMR analysis. An IR spectrum taken after NMR analysis shows a mixture of **2a** and **31**.

31:

IR (dcm): ν_{CO} 2118 (s), 2078 (s) cm^{-1}. IR ($CDCl_3$): ν_{CO} 2106 (s), 2065 (s) cm^{-1}. ^1H NMR ($CDCl_3$): δ 2.26 (s, Cp*). ^{19}F NMR ($CDCl_3$): δ -77.12 (s. 4F, B*F*$_4$). ^1H NMR (dcm, no-d)*: δ 2.35 (s, Cp*). ^{11}B NMR ($CDCl_3$): δ -1.18. MS FAB$^+$ (*m*/*z*): 451 $[M]^+$.

* A reference NMR tube containing the same volume of $CDCl_3$ was locked and shimmed as usual and then replaced with the "no-d" sample (crude aliquot in CH_2Cl_2).[29] ^1H chemical shifts were referenced with the resonance of CH_2Cl_2 set to δ 5.30.

4.9.2 Reaction of Cp*Rh(CO)$_2$ with C_6F_5CN

Cp*Rh(CO)$_2$ (6.0 mg, 20.4 μmol) was dissolved in C_6F_5CN (0.5 ml) and stirred at room temperature for 16 h. The IR spectrum shows only peaks due to the starting materials.

4.9.3 Reaction of 2a with C_6F_5CN under anhydrous conditions

To a Carius tube containing **2a** (12.0 mg, 31.3 μmol), dried molecular sieves and C_6F_5CN (1.0 ml) was added. The mixture was stirred at room temperature for 1 d. The volatiles were removed under reduced pressure and the residue was extracted with C_6D_6 and $CDCl_3$ subsequently. The ^1H and ^{19}F NMR spectra of the extracts show no resonances due to protons or fluorines. Methanol (3.0 ml) was added and the reaction was left to stand at room temperature for 3 d. ^1H NMR, ^{19}F NMR and IR analyses showed that the product has been converted to **18b**.

4.9.4 Attempted salt exchange reactions

With $AgBF_4$

i) To a Carius tube containing **2a** (20.0 mg, 52.2 μmol) was added anhydrous C_6F_5CN (1.0 ml). The solution was degassed by three cycles of freeze-pump-thaw and stirred at room temperature for 2 d. To half the solution, anhydrous $AgBF_4$ (10.0 mg, 51.3 μmol) was added under an argon atmosphere and the mixture was stirred for 3 h. Immediate precipitation of a

tan solid was observed. Volatiles were removed under reduced pressure, and ^{1}H and ^{19}F NMR spectra of the dcm extract and residue were taken. The residue was soluble in methanol but did not convert to **18b**.

ii) To a Carius tube containing **2a** (10.0 mg, 26.1 μmol) and anhydrous $AgBF_4$ (8.0 mg, 41.1 μmol) was added anhydrous C_6F_5CN (0.5 ml). The solution was degassed by three cycles of freeze-pump-thaw and stirred at room temperature for 16 h. A tan precipitate in orange solution was obtained. The ^{1}H and ^{19}F NMR spectra show complicated mixtures.

With $BF_3{\cdot}OEt_2$

To a Carius tube containing **2a** (10.0 mg, 26.1 μmol) was added anhydrous C_6F_5CN (1.0 ml). The solution was degassed by three cycles of freeze-pump-thaw and stirred at room temperature for 18 h. $BF_3{\cdot}OEt_2$ (2 x 6 μl, 47.3 μmol) was added. No colour change was observed. The volatiles were removed under reduced pressure. The ^{1}H and ^{19}F NMR spectra (d_6-acetone) were complicated, and an ESI-MS^- spectrum (acetone) shows highest m/z at 87 [BF_4^-].

*In all the attempted salt exchange reactions described above, the expected cationic dicarbonyl species $[Cp^*Ir(CO)_2(p\text{-}C_6F_4CN)]^+[BF_4]^-$, **20**, was not detected by ^{1}H NMR, ^{19}F NMR or IR spectroscopy. Product mixture gave complicated ^{1}H NMR and ^{19}F NMR spectra suggesting a mixture of unidentified products.

With TMSOTf ($CF_3SO_3SiMe_3$)

To a Carius tube containing **2a** (11.1 mg, 29.0 μmol) and dried molecular sieve was added anhydrous C_6F_5CN (1.0 ml). TMSOTf (10 μl, 55.3 μmol) was added and the mixture was stirred at room temperature for 3 h. The resultant mixture gave complicated ^{1}H NMR and ^{19}F NMR spectra suggesting a mixture of unidentified products. The IR spectrum (KBr) shows no peak in the CO stretching region.

4.9.5 Reaction of Cp*Ir(CO)(PPh_3) with C_6F_5CN

To a Carius tube containing Cp*Ir(CO)(PPh_3), **7a** (5.0 mg, 8.09 μmol) was added C_6F_5CN (0.5 ml) and distilled H_2O (0.1 ml). The reaction mixture was degassed by three cycles of freeze-pump-thaw and stirred for 40 h. The volatiles were removed under reduced pressure to give a pale brown oil.

IR (dcm): ν_{CN} 2248 (w), 2210 (w), ν_{CO} 2062 (s), 2019 (w) cm^{-1}.

^1H NMR ($CDCl_3$): δ 7.8-7.3 (m, 15 H, aromatic), 1.87 (s, 15H, Cp*CH_3). ^{19}F NMR ($CDCl_3$): δ - 31.7 (m, 2F), - 58.0 (m, 2F), -64.4 (s, 1F). MS FAB^+ (*m*/z): 792 $[M]^+$. HR-MS FAB^+ (*m*/z): calcd for $C_{36}H_{30}F_4NOP^{[193]}Ir$: 792.1625, found: 792.1649.

4.9.6 Rate of reaction in D_2O vs H_2O

i) To a Carius tube containing **2a** (10.3 mg, 26.9 μmol) was added C_6F_5CN (0.5 ml) and D_2O (0.2 ml). The reaction mixture was degassed by three cycles of freeze-pump-thaw and stirred at room temperature for 2¾ h. The volatiles were removed under reduced pressure and the integration ratio of the Cp* resonance of **2a**:**18a**-deuterated in the ^1H NMR spectrum ≈ 1:1.5

ii) To a Carius tube containing **2a** (10.0 mg, 26.1 μmol) was added C_6F_5CN (0.5 ml) and deionized H_2O (0.2 ml). The reaction mixture was degassed by three cycles of freeze-pump-thaw and stirred at room temperature for 2¾ h. The volatiles were removed under reduced pressure and a ^1H NMR spectrum of the residue was taken in $CDCl_3$.

Integration ratio of the Cp* resonance of **2a**:**18a** in the ^1H NMR spectrum ≈ 1:1.8

4.9.7 Rate of formation of methyl vs isopropyl ester

Reaction of 2a with C_6F_5CN in methanol

To a Carius tube containing **2a** (10.0 mg, 26.1 μmol) was added C_6F_5CN (0.25 ml) and methanol (0.5 ml). The reaction mixture was degassed by three cycles of freeze-pump-thaw and stirred at room temperature for 8 h. A 0.3 ml aliquot was taken out of the reaction

mixture and the volatiles were removed under reduced pressure. A ^{1}H NMR spectrum of the residue was taken in $CDCl_3$. The remaining solution was allowed to react for another 14 h. The percentage conversion of **2a** to **18b** after 8 and 22 h were 63% and 98%, respectively (from integration ratio of the Cp* resonance).

Reaction of 2a with C_6F_5CN in isopropanol

The reaction was repeated in isopropanol. The percentage conversion of **2a** to **18c** after 8 and 22 h were 57 % and 82%, respectively.

Competitive reaction in methanol/ isopropanol

A mixture of methanol (0.500 ml), isopropanol (0.945 ml) and C_6F_5CN (0.500 ml) was pre-dried with molecular sieve and syringed into a Carius tube containing **2a** (10.0 mg, 26.1 μmol). The reaction mixture was degassed by three cycles of freeze-pump-thaw and stirred at room temperature for 22 h. The volatiles were removed under reduced pressure, and the ^{1}H and ^{19}F NMR spectra of the residue were taken in $CDCl_3$.

Integration ratio of the ^{19}F NMR resonances of **18c**: **18b** was ≈ 1:7

4.9.8 Reaction of 2a with C_6F_5CN in the presence of 5 equivalent of Me_4NF

To a Carius tube containing **2a** (10.0 mg, 26.1 μmol) and Me_4NF (25.0 mg, 269 μmol) was added anhydrous C_6F_5CN (0.25 ml) and methanol (0.5 ml). The mixture was degassed by three cycles of freeze-pump-thaw and stirred at room temperature for 8 h. The volatiles were removed under reduced pressure and the residue was redissolved completely in $CDCl_3$. The ^{1}H NMR spectrum shows complete conversion of **2a** to **18b**.

References

[1] Katz, N. E.; Szalda, D. J.; Chou, M. H.; Creutz, C.; Sutin, N. *J. Am. Chem. Soc.* **1989**, *111*, 6591-6601.

[2] Bennett, M. A. *J. Mol. Catal.* **1987**, *41*, 1-20.

[3] Mandal, S. K.; Ho, D. M.; Orchin, M. *J. Organomet. Chem.* **1992**, *439*, 53-64.

[4] Barrientos-Penna, C. F.; Gilchrist, A. B.; Klahn-Oliva, A. H.; Hanlan, J. L.; Sutton, D. *Organometallics* **1985**, *4*, 478-485.

[5] Catellani, M.; Halpern, J. *Inorg. Chem*. **1980**, *19*, 566-568.

[6] Ford, P. C.; Rokicki, A. In *Nucleophilic Activation of Carbon Monoxide: Applications to Homogeneous Catalysis by Metal Carbonyls of the Water Gas Shift and Related Reactions*; Stone, F. G. A.; West, R. Eds.; Advances in Organometallic Chemistry, vol 28; Academic Press, Inc.: New York, 1988, pp 139-217.

[7] Katz, N. E.; Szalda, D. J.; Chou, M. H.; Creutz, C.; Sutin, N. *J. Am. Chem. Soc.* **1989**, *111*, 6591-6601.

[8] Campora, J.; Palma, P.; Rio, D. D.; Alvarez, E. *Organometallics* **2004**, *23*, 1652-1655.

[9] Bennett, M. A. *J. Mol. Catal.* **1987**, *41*, 1-20.

[10] Elliot. O. I. P; Haslam, C. E.; Spey, S. E.; Haynes, A. *Inorg. Chem*. **2006**, *45*, 6269-6275.

[11] (a) Bromberg, S. E.; Lian, T.; Bergman, R. G.; Harris, C. B. *J. Am. Chem. Soc.* **1996**, *118*, 2069-2072. (b) Lees, A. J. *J. Organomet. Chem*. **1998**, *554*, 1-11.

[12] (a) Pinkes, J. R.; Masi, C. J.; Chiulli, R.; Steffey, B.D.; Cutler, A.R. *Inorg. Chem.* **1997**, *36*, 70-79. (b) Gibson, D. H.; Mehta, J. M.; Ye, M.; Richardson, J. F.; Mashuta, M. S. *Organometallics* **1994**, *13*, 1070-1072. (c) Gibson, D. H.; Ong, T. S. *J. Am. Chem. Soc.* **1987**, *109*, 7191-7193. (d) Gibson, D. H.; Owens, K.; Ong, T. S. *J. Am. Chem. Soc*. **1984**, *106*, 1125-1127. (e) Carlos, F.; Barrientos, P.; Gilchrist, A. B.; Sutton, D. *Organometallics* **1983**, *2*, 1265-1266. (f) Sweet, J.; Graham, W. A. G.; *Organometallics* **1982**, *1*, 982-986. (g) Grice, N.; Kao, S. C.; Pettit, R. *J. Am. Chem. Soc*. **1979**, *101*, 1627-1628.

[13] (a) Blake, A. J.; Cockman, R. W.; Ebsworth, E. A. V.; Holloway, J. H. *J. Chem. Soc., Chem. Commun.* **1988**, 529-530. (b) Ebsworth, E. A. V.; Robertson, N.; Yellowlees, L. J. *J. Chem. Soc., Dalton Trans.* **1993**, 1031-1037.

[14] Torrens, H. *Coord. Chem. Rev.* **2005**, *249*, 1957-1985.

[15] (a) Burling, S.; Elliott, P. I. P.; Jasim, N. A.; Lindup, R. J.; McKenna, J.; Perutz, R. N.; Archibald, S. J; Whitwood, A. C. *Dalton Trans.* **2005**, 3686 -3695. (b) Jasim, N. A.; Perutz, R. N.; Whitwood, A. C.; Braun, T.; Izundu, J.; Neumann, B.; Rothfeld, S.; Stammler, H.-G. *Organometallics* **2004**, *23*, 6140-6149. (c) Cronin, L.; Higgitt, C. L.; Karch, R.; Perutz, R. N. *Organometallics* **1997**, *16*, 4920-4928. (d) Braun, T.; Perutz, R. N. *Chem. Commun.* **2002**, 2749-2757. (e) Braun, T.; Perutz, R. N. In *Routes to Fluorinated Organic Derivatives by Nickel Mediated C-F Activation of Heteroaromatics*; Screttas, C. G.; Steele, B. R., Eds.; *Perspectives in Organometallic Chemistry*; Royal Society of Chemistry: U. K., 2003; pp 136-151.

[16] Hintermann, S.; Pregosin, P. S.; Rűegger, H.; Clark, H. C. *J. Organomet. Chem.* **1992**, *435*, 225-234.

[17] (a) Kiplinger, J. L.; Richmond, T. G.; Osterberg, C. E. *Chem. Rev.* **1994**, *94*, 373-431. (b) Bruce, M. I.; Stone, F. G. A. *Angew. Chem. Int. Ed.* **1968**, *7*, 747-753. (c) Booth, B. L.; Haszeldine, R. N.; Perkins, I. *J. Chem. Soc. (A)* **1971**, 927-929. (d) Booth, B. L.; Haszeldine, R. N. Perkins, I. *J. Chem. Soc., Dalton Trans.* **1975**, 1843-1846. (e) Booth, B. L.; Haszeldine, R. N.; Taylor, M. B. *J. Chem. Soc. (A)* **1970**, 1974-1978.

[18] Berdeniuc, J.; Jedlicka, B.; Crabtree, R. H. *Chem. Ber*. **1997**, *130*, 145-154.

[19] (a) Reinhold, M.; McGrady, J. E.; Perutz, R. N. *J. Am. Chem. Soc.* **2004**, *126*, 5268-5276. (b) Bosque, R.; Clot, E.; Fantacci, S. Maseras, F.; Eisenstein, O.; Perutz, R. N.; Renkema, K. B.; Caulton, K. G. *J. Am. Chem. Soc.* **1998**. *120,* 12634-12640.

[20] Johnson, C. D. In *The Hammett Equation*, Cambridge University Press: U. K., 1973; Chapter 1, pp1-26.

[21] (a) Zuman, P. In *Substituent Effects in Organic Polarography*; Plenum Press: New York, 1967; Chapter 3; pp 43-129. (b) Gordon, A. J.; Ford, R. A. In *The Chemist's Companion: A Handbook of Practical Data, Techniques, and References*; Wiley: New York, 1972, pp 145-155.

[22] Jackson, R. A. In *Mechanisms in Organic Reactions*; The Royal Society of Chemistry: U. K., 2004; Chapter 3; pp 45-71.

[23] Ballhorn, M.; Partridge, M. G.; Perutz, R. N.; Whittlesey, M. K. *Chem. Commun.* **1996**, 961-962.

[24] (a) Hart-Davis, A. J.; Graham, W. A. G. *Inorg. Chem.* **1970**, *9*, 2658-2662. (b) Oliver, A. J.; Graham, W. A. G. *Inorg. Chem.* **1970**, *9*, 243-247. (c) Hart-Davis, A. J.; Graham, W. A. G. *Inorg. Chem.* **1971**, *10*, 1653-1657.

[25] Jiang, F.; Biradha, K.; Leong, W. K.; Pomeroy, R. K.; Zaworotko, M. J. *Can. J. Chem.* **1999**, *77*, 1327 - 1335.

[26] (a) Slebocka-Tilk, H.; Neverov, A. A.; Brown, R. S. *J. Am. Chem. Soc.* **2003**, *125*, 1851-1858. (b) Bender, M. L.; Pollock, E. J.; Neveu, M. C. *J. Am. Chem. Soc.* **1962**, *84*, 595-599.

[27] Fife, T. H.; Singh, R.; Bembi, R. *J. Org. Chem*. **2002**, *67*, 3179-3183.

[28] Changalov, M. M.; Ivanova, G. D.; Rangelov, M. A.; Acharya, P.; Acharya, S.; Minakawa, N.; Foldesi, A.; Stoineva, I. B.; Yomtova, V. M.; Roussev, C. D.; Matsuda, A.; Chattopadhyaya, J.; Petkov, D. D. *Chembiochem*, **2005**, *6*, 1-6.

[29] Hoye, T. R.; Eklov, B. M.; Ryba, T. D.; Voloshin, M.; Yao, L. J. *Org. Lett.* **2004**, *6*, 953-956.

Chapter 5: Reactivity of Metallocarboxylic Acid

5.1 Properties of metallocarboxylic acids

The similarities and differences in the properties of metallocarboxylic acids (or hydroxycarbonyl complexes) in comparison to organic carboxylic acids are summarized in Table 5.1.

Table 5.1. Comparison of the properties of metallocarboxylic acids with typical organic carboxylic acids.[1,2]

	Organic Carboxylic acids, RCOOH	**Metallocarboxylic acids, L_nMCOOH**
Structure	Can exist as dimers in solid, liquid and gaseous states, held by H-bonds. Typical O-H···O separation: 2.63 to 2.65Å	Can exist as dimers in solid state and in solutions, held by H-bonds. Longer (and weaker) H-bonds. e.g. 2.695(8) Å for O-H···O separation in *trans*-$Pt(COOH)(C_6F_5)(PEt_3)_2$ 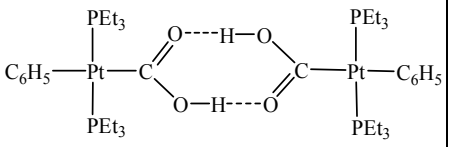
NMR	Resonance for COOH ^{1}H NMR: δ 10- 13 ^{13}C NMR: δ 165- 185	Resonance for COOH ^{1}H NMR: δ 7- 11 ^{13}C NMR: δ 170- 220

IR	ν_{OH} 2500-3300 cm^{-1} ν_{CO} 1650- 1740 m^{-1}	ν_{OH} 2700-3500 cm^{-1} ν_{CO} 1570-1650 cm^{-1} Shifted ca. 100 cm^{-1} to lower energy compared to typical organic carboxylic acids. Could indicate contribution from a dipolar resonance hybrid: 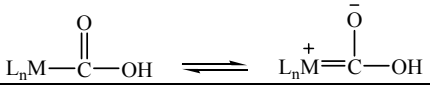
Acid-base properties	Mainly acidic (can be slightly basic). 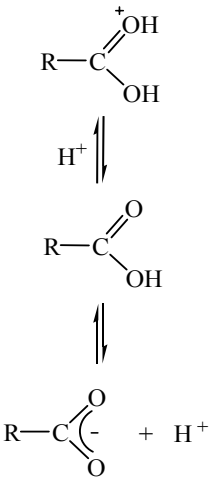	Amphoteric. Reacts with strong acid to give the corresponding metal carbonyl cation. 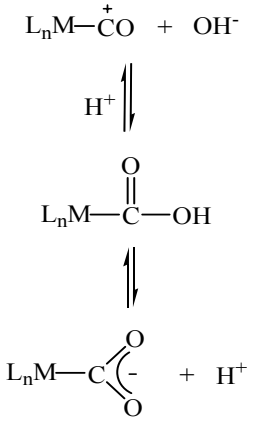
Decarboxylation	For 3-ketoacids only. Proposed pathway: 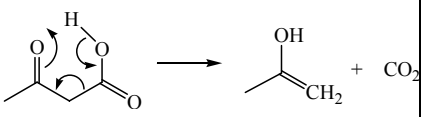	By β-H elimination. $L_nMCOOH \rightarrow L_nMH + CO_2$
Esterification	Undergoes acid-catalyzed esterification. $RCOOH + R'OH \overset{H^+}{\rightleftharpoons} RCOOR'$	Forms ester readily without acid catalyst.

X-ray structural studies of metallocarboxylic acids, such as those containing Pt, Ir and Re metal centers, have been reported.[1,2] Hydrogen-bonded dimers predominate in the solid state, while in solution, there is an equilibrium between the monomeric and dimeric forms.

Metallocarboxylic acids are often difficult to isolate and purify because many such complexes spontaneously lose carbon dioxide to give the metal hydride or its conjugated base. This decarboxylation process can be promoted by heat, the presence of base, or in solvents such as acetone and benzene. The decomposition pathway may be via β-hydride transfer to the metal or deprotonation to give an anionic M-CO_2 intermediate (Scheme 5.1).[1]

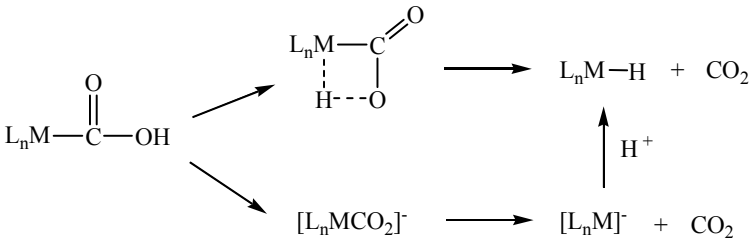

Scheme 5.1

Nevertheless, there are other metallocarboxylic acids that do not decarboxylate under mildly basic conditions, but instead form the corresponding carboxylate salts. For example, Cp*Re(CO)(COOH)(N_2Ar) forms the carboxylate salt when treated with aqueous hydroxide. In the presence of excess NaOH or KOH, decarboxylation occurs to give the corresponding hydride species, Cp*Re(CO)(H)(N_2Ar) (Scheme 5.2).[2,3]

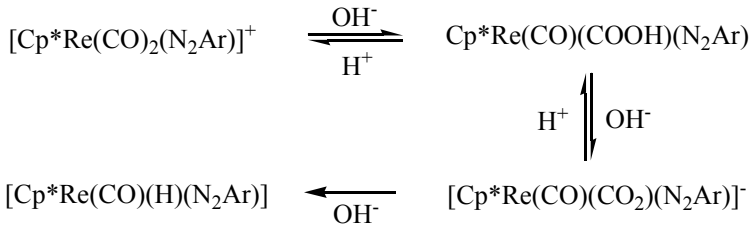

Scheme 5.2

While some metallocarboxylic acids are basic enough to ionize spontaneously to their corresponding metal carbonyl cations in solvents such as formamide, others are known to dehydrate in the presence of strong acids to form their corresponding metal carbonyl cation by

electrophilic attack on the carboxylate oxygen. This is the reverse of the reaction that is frequently used to form them (eq 1).[2]

$$L_nMCOOH \underset{OH^- \text{ or } H_2O}{\overset{H^+}{\rightleftharpoons}} L_nMCO^+ \qquad (1)$$

Although metallocarboxylic acids are known to be poor acids, for example, they do not protonate 1,8-bis(dimethylamino)naphthalene,[1a] they react readily with alcohols at room temperature without the need for any added catalyst to form esters. The proposed mechanism of the reaction is shown in Scheme 5.3.[4] It involves the initial dissociation of the metallocarboxylic acid to generate a metal carbonyl cation and a hydroxide anion. The conjugate base of the alcohol is then generated by reaction with the hydroxide ion, and the last step is reversible. The existence of the ionization step is supported by the observed ease of CO exchange between free ^{12}CO and Pt($^{13}CO_2H$)(C_6H_9)(dppp),[5] and the observation that the rate of esterification followed the order of acidity of the alcohol, viz., $CH_3OH > C_2H_5OH \approx C_6H_5CH_2OH > (CH_3)_2CHOH$. The acid was regenerated when Pt(CO_2CH_3)(C_6H_9)(dppp) was dissolved in 'wet' $(CD_3)_2SO$ for several hours, which, together with the ease of transesterification, supports the reversibility of the last step.[5]

$$MCOOH \rightleftharpoons MCO^+ + OH^-$$
$$OH^- + ROH \longrightarrow RO^- + H_2O$$
$$MCO^+ + RO^- \rightleftharpoons MCOOR$$

Scheme 5.3

The reactivity of the metallocarboxylic acids synthesized, Cp*Ir(CO)(COOH)(*p*-C_6F_4CN), **18a** and Cp*Ir(CO)(COOH)(*p*-C_5F_4N), **22a** will be discussed in the next few sections.

5.2 Reaction with tetrafluoroboric acid … dehydration

Addition of tetrafluoroboric acid, HBF_4 to a solution of **18a** in dcm resulted in the formation of a colourless oil that was sparingly soluble in dcm but completely soluble in acetone. The IR spectrum of the product shows two terminal CO stretches at 2124 and 2090 cm^{-1} which are blue-shifted with respect to those in **2a** (2009 and 1937 cm^{-1}). Such high CO stretching frequencies are typical of cationic transition metal carbonyl complexes. The ^1H NMR spectrum shows that the resonance due to the methyl protons of the Cp* ligand (δ 2.27) was deshielded with respect to **18a** suggesting that the Cp* ligand is attached to a more electron-poor iridium center. The high resolution FAB mass spectrum (+ve ion mode) shows the molecular ion peak at 558.0662 corresponding to the formulation $[C_{19}H_{15}O_2F_4N^{193}Ir]^+$. The peak corresponding to the BF_4^- anion can be seen in the negative ion mode. These are consistent with the formation of the ionic product $[Cp^*Ir(CO)_2(p\text{-}C_6F_4CN)]^+[BF_4]^-$, **20** from the dehydration of **18a**.

Complex **20** dissolved completely in methanol to give Cp*Ir(CO)(COOMe)(*p*-C_6F_4CN), **18b** which has been fully characterized, including by single crystal X-ray crystallography. The ORTEP plot of **18b** is shown in Figure 5.1. The structural discussion will be covered in Section 5.6.

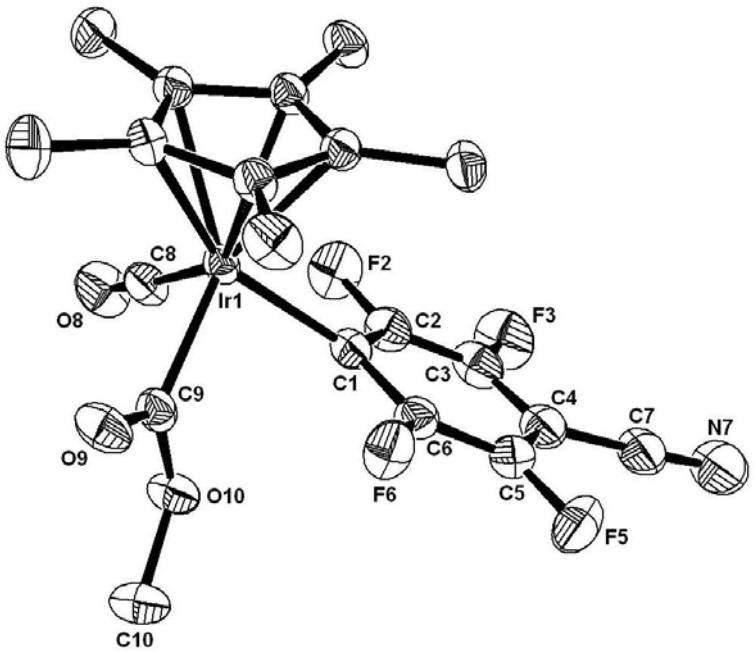

Figure 5.1. ORTEP diagram of **18b.** Thermal ellipsoids are drawn at 50% probability level. The hydrogen atoms have been omitted for clarity.

The formation of **18b** probably occurred via nucleophilic attack of methanol or methoxide ion on one of the CO ligand (Scheme 5.4). The carbonyl groups in **20** are highly electrophilic due to the positive charge on the iridium complex.

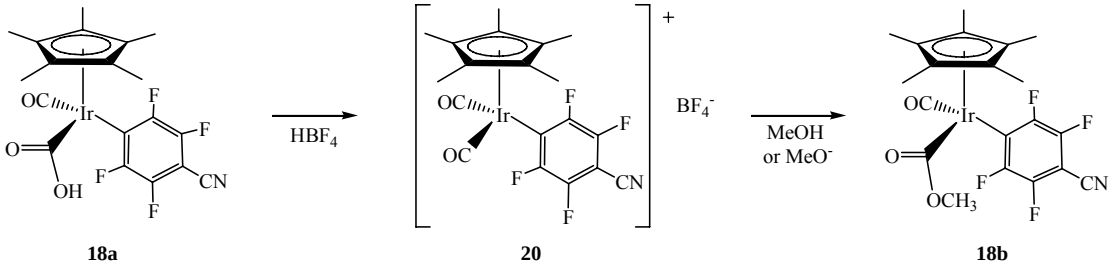

18a **20** **18b**

Scheme 5.4

5.3 Reaction with base and quaternary ammonium salts … decarboxylation

While complex **18a** was stable in solution in the absence of base, it decomposed into a mixture of unidentified species upon heating. Treatment of **18a** with aqueous NaOH resulted in the formation of a species, **19a** that has a hydride resonance at δ -14.53 and a Cp* methyl resonance at δ 1.49 in the ^{1}H NMR spectrum. Complex **18a** also underwent a similar reaction in the presence of quaternary ammonium salts such as tetrabutylammonium fluoride

(Bu_4NF), tetraethyl ammonium bromide (Et_4NBr), tetramethylammonium fluoride (Me_4NF) or bis(triphenylphosphoranylidene) ammonium chloride (PPNCl), to give **19a**. The ^{19}F NMR and IR spectra are also consistent with the formulation of **19a** as the decarboxylation product, Cp*Ir(CO)(H)(*p*-C_6F_4CN).

In order to confirm its structure, **19a** was converted to its corresponding chloride, Cp*Ir(CO)(Cl)(*p*-C_6F_4CN), **19b** by stirring in $CDCl_3$ (Scheme 5.5).

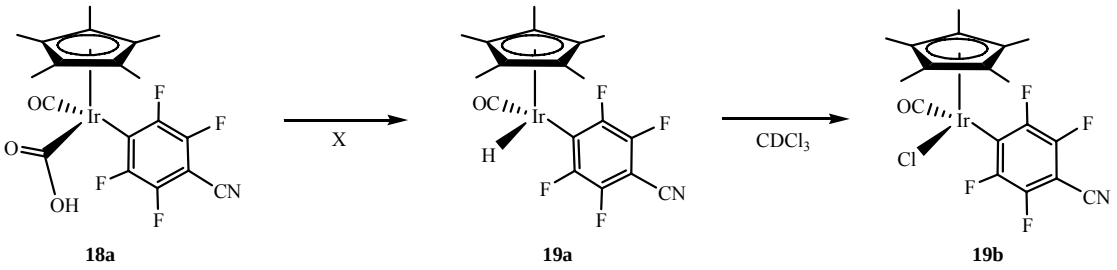

18a **19a** **19b**

X = NaOH, Bu_4NF, Et_4NBr, Me_4NF or PPNCl

Scheme 5.5

The structure of **19b** was confirmed by spectroscopic characterization and by a single crystal X-ray crystallographic analysis. The ORTEP diagram of **19b** is shown in Figure 5.2. The structural discussion will be covered in Section 5.6.

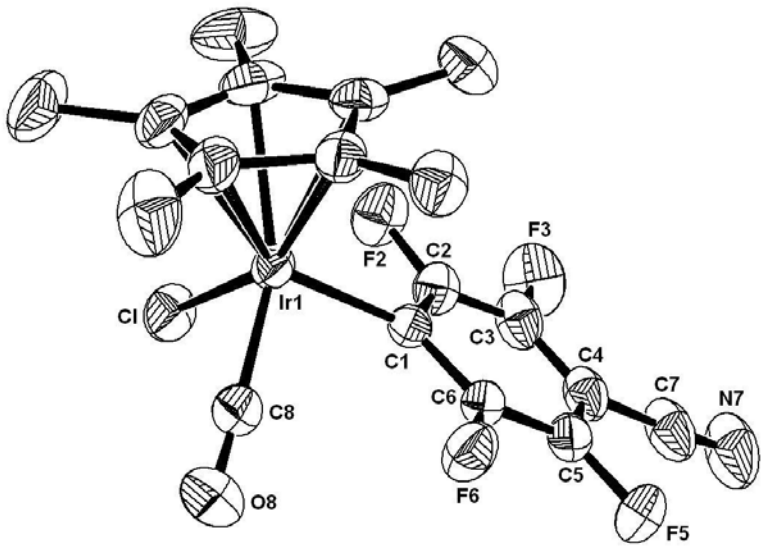

Figure 5.2. ORTEP diagram of **19b**. Thermal ellipsoids are drawn at 50% probability level. The hydrogen atoms have been omitted for clarity.

The reaction of **2a** with 1,3-$C_6F_4(CN)_2$ in C_6D_6 also gave a hydride species, Cp*Ir(CO)(H)[2,4-$C_6F_3(CN)_2$], **28** (see Section 3.3) even without the addition of base or heating. Presumably, the initially formed metallocarboxylic acid underwent spontaneous decarboxylation (Scheme 5.6). The decarboxylation may have proceeded via the deprotonation pathway outlined in Section 5.1. Presence of a more electron-withdrawing ligand [1,3-$C_6F_3(CN)_2$] would stabilize the anionic intermediate formed, favoring decarboxylation.

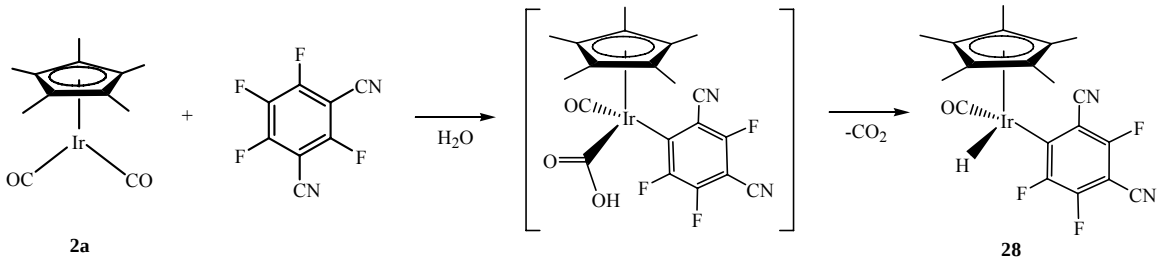

Scheme 5.6

5.4 Reaction with alcohols: esterification

The reaction of **2a** with C_6F_5CN in alcoholic solvents, namely methanol, isopropanol or cyclopentanol, produced the corresponding esters, Cp*Ir(CO)(COOR)(*p*-C_6F_4CN), **18** (R = Me, **b**; ^{i}Pr, **c**; c-C_5H_9, **d**). The esters **18b**, **c** and **d** can also be formed by stirring a solution of **18a** in the respective alcohols (Scheme 5.7). The reaction of **2a** with C_5F_5N in methanol similarly produced Cp*Ir(CO)(COOMe)(*p*-C_5F_4N), **22b**.

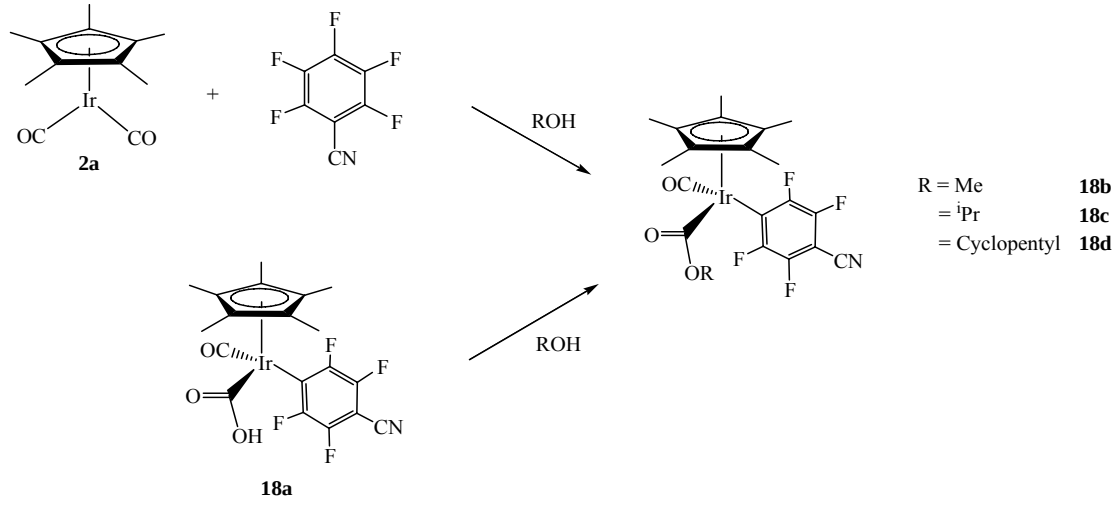

Scheme 5.7

All four complexes, **18b**, **c**, **d** and **22b** were isolated as white powders that are moderately air-stable in their solid state but air-sensitive in solution. The peaks corresponding to the protons of the methyl, isopropyl or cyclopentyl groups can be observed in the ^{1}H NMR spectra. For **18b-d,** the presence of the terminal carbonyl, ester and tetrafluorobenzonitrile groups is supported by their characteristic bands in the IR spectra. The terminal carbonyl vibration appears at ~2040 cm^{-1} while the carbonyl vibration of the ester group appears at 1661, 1652 and 1653 cm^{-1} for the methyl, isopropyl and cyclopentyl ester, respectively. The latter bands are at higher frequencies than that for the carboxylic acid group in **18a** (1630 cm^{-1}), consistent with the expected increase in carbonyl stretching frequency in going from a carboxylic acid to an ester.

When a solution of **18a** in a 1:1 molar ratio of MeOH:^{i}PrOH was stirred at room temperature for 4 h, only the methyl ester **18b** was formed. This observation is in line with the acidity of the alcohols; methanol, being more acidic, forms the methoxide ion more readily than isopropanol. The order of nucleophilicity or basicity of the alcohols, on the other hand, is reversed. Thus it is the methoxide ion rather than methanol which is the actual species that attacks the carbonyl cation.

When a solution of **18b** was stirred in a THF/ H_2O (1:1, v/v) solvent mixture at room temperature for 18 h, a 67 % conversion to **19a** was observed. A control reaction involving stirring a solution of **18b** in anhydrous THF shows that **18b** remained unreacted. Hence, **18b** must have been hydrolysed by water to give **18a**, which underwent decarboxylation to yield **19a**.

A solution of **18b** in isopropanol gave a 98% conversion to the isopropyl ester, **18c** after 2 d while the reverse reaction gave a 35% conversion to the methyl ester, **18b**. The slow rate of transesterification suggests that the ester does not ionize as readily as many other reported alkoxylcarbonyls (see Section 5.1), and unlike the metallocarboxylic acid, the alcohol probably attacks the carbonyl carbon of the ester in the neutral form (Scheme 5.8). Hence, the rate of esterification parallels the basicity or nucleophilicity of the alcohols, with isopropanol being more nucleophilic than methanol.

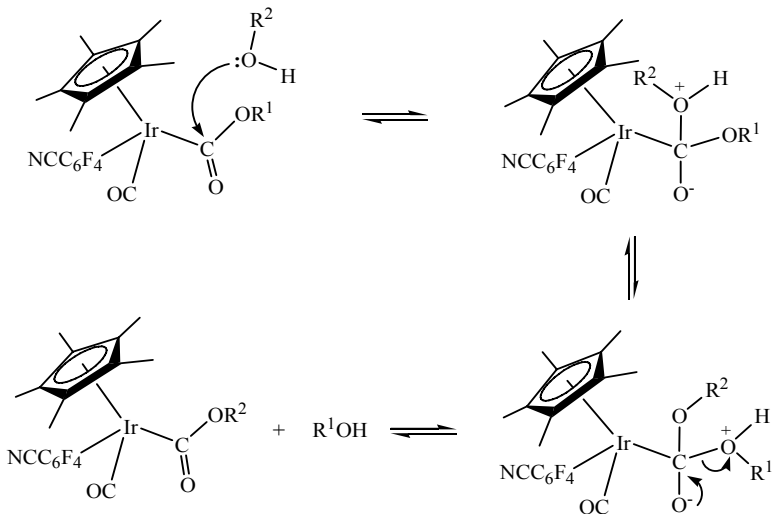

Scheme 5.8

This trend is the reverse observed for the analogous reaction of **2a** with C_6F_5CN in water or alcohols where the reaction in water occurs most readily. It also supports the general base catalysis mechanism proposed in Section 4.7, in which the fluoride ion in the proposed intermediate, $[Cp^*Ir(CO)_2(p\text{-}C_6F_4CN)]^+[F]^-$ aids in the partial deprotonation of the water or alcohol molecule to increase their nucleophilicity in attacking the carbonyl carbon (Scheme 5.9).

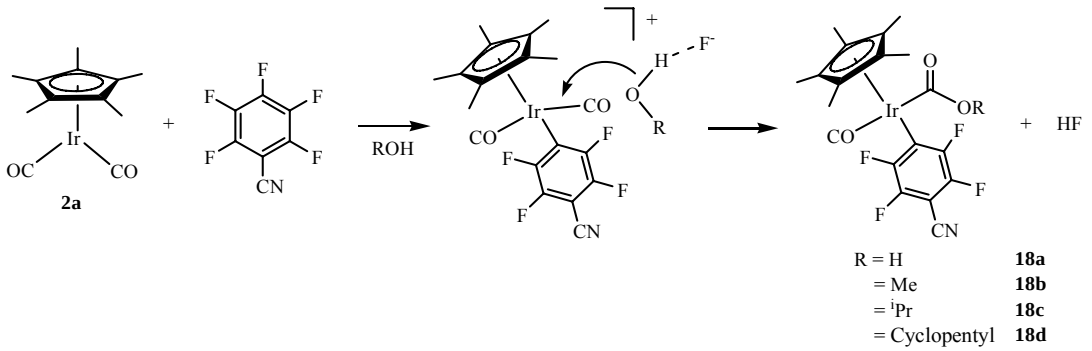

Scheme 5.9

While metallocarboxylic acids are usually unstable to heat, alkoxylcarbonyls are usually more thermally stable. We have been able to use this to advantage in order to get **2a** to react with perfluoroarenes carrying a less electron-withdrawing substituent (with respect to CN). Thus, while **2a** did not react with $C_6F_5CF_3$ at room temperature, partial conversion to the corresponding alkoxycarbonyl could be achieved at higher temperatures in an alcoholic solvent. Heating a solution of **2a** with $C_6F_5CF_3$ in methanol resulted in partial conversion of **2a**

to the methoxycarbonyl complex, Cp*Ir(CO)(COOMe)(*p*-$C_6F_4CF_3$), **24a** (5% conversion wrt **2a** from ^{1}H NMR integration). The reaction was repeated by heating a solution of **2a** with $C_6F_5CF_3$ in n-propanol at 110 °C. The reaction did not complete after 18 h and a mixture of unreacted **2a** and the n-propylcarbonyl complex, **24b** was obtained (37% conversion wrt **2a** from ^{1}H NMR integration) (Scheme 5.10). Further heating at a higher temperature did not increase the yield of **24b**. Instead, the solution turned from colourless to brown with some decomposition to a hydrido species, which is proposed to be Cp*Ir(CO)(H)(*p*-$C_6F_4CF_3$), **25** on the basis of its spectroscopic characteristics.

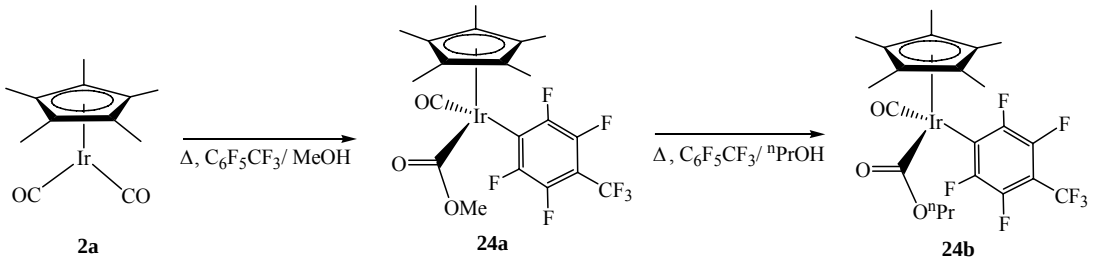

Scheme 5.10

Reaction of **2a** with a stoichiometric amount of 1,3-$C_6F_4(CN)_2$ in methanol gave two products which were identified to be 2,4,5-trifluoro-6-methoxy-isophthalonitrile and Cp*Ir(CO)(COOMe)[2,4-$C_6F_3(CN)_2$], **29** on the basis of spectroscopic data (Scheme 5.11). The ^{1}H NMR spectrum of **29** shows a singlet at δ 1.96 due to the methyl protons of the Cp* ligand and a singlet at δ 3.48 due to the methoxy protons on the ester group. This chemical shift is close to that of the methoxy protons on **18b** (δ 3.44) and smaller than that of the methoxy protons on 2,4,5-trifluoro-6-methoxy-isophthalonitrile (δ 4.38), suggesting that there is no methoxy substitution on the fluoroarene ring.

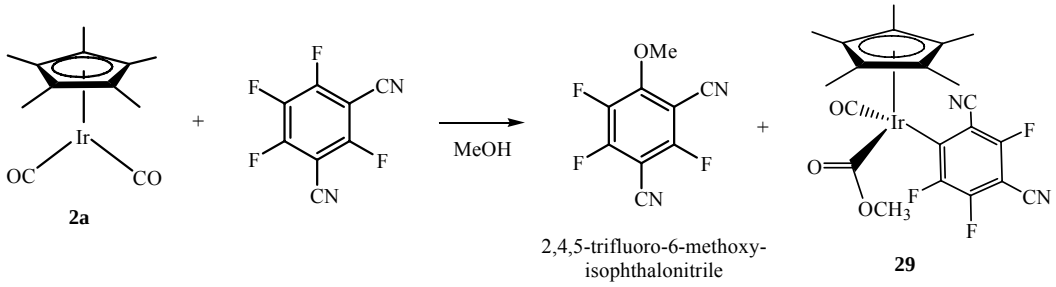

Scheme 5.11

The dicarbonitrile 1,3-$C_6F_4(CN)_2$, which carries two electron-withdrawing cyano groups, is highly susceptible to nucleophilic attack. While there was no evidence of nucleophilic attack by methanol on C_6F_5CN, C_5F_5N or $C_6F_5CF_3$ in the reactions of **2a** with these fluorinated compounds in alcoholic media, it was found that methanol was able to attack 1,3-$C_6F_4(CN)_2$ directly at room temperature to afford 2,4,5-trifluoro-6-methoxy-isophthalonitrile. This methoxyl substituted product was, however, inert to attack by **2a**. This reaction also suggests that the nucleophilicity of **2a** is higher than methanol; in a large excess of methanol (the reaction solvent), the ratio of 2,4,5-trifluoro-6-methoxy-isophthalonitrile to **29** produced was only 1:5.

The reaction of **2a** with alcohols demonstrates the ease of esterification when there is an OH functionality. In an extension to this, **2a** was reacted with the bifunctional ligand 3-chloropropanol-1-ol to afford a product **22c** in which the Cl functionality remained on the other end of the ligand (Scheme 5.12). This idea may be extended to the preparation of other iridium complexes with different dangling functional groups, which may in turn be converted to other functional groups, including attachment to other metal complexes to form hetero-dinuclear complexes.

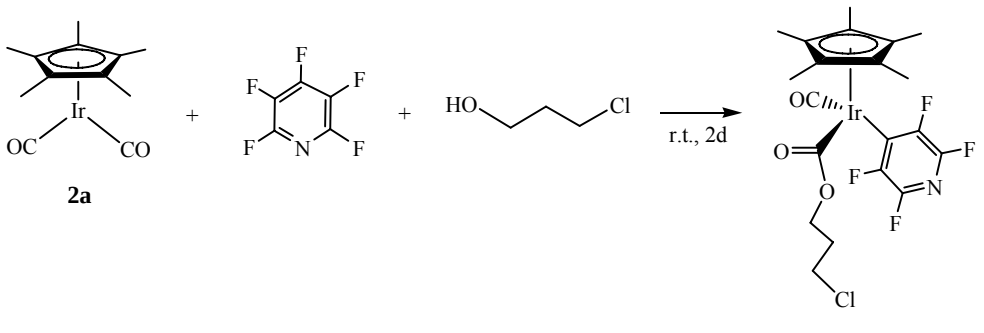

2a **22c**

Scheme 5.12

5.5 Reaction with the osmium cluster $Os_3(CO)_{10}(NCCH_3)_2$

$Os_3(CO)_{10}(NCCH_3)_2$ is a derivative of $Os_3(CO)_{12}$ which contains labile acetonitrile ligands that can be easily replaced by other nucleophiles such as PR_3, C_5H_5N, HX (X = Cl, Br, I), C_2H_4 or RCOOH.[6] Its reaction with organic acids is known to form clusters of the general formula $Os_3(\mu\text{-}H)(CO)_{10}(\mu\text{-}O_2CR)$.[7] We were interested to find out if **18a** would react with $Os_3(CO)_{10}(NCCH_3)_2$ to give an analogous product.

Compound **18a** reacts readily with $Os_3(CO)_{10}(NCCH_3)_2$ in dcm at room temperature to afford compound **21**. The pattern of the CO stretching bands in the IR spectrum is typical of triosmium clusters of the type $Os_3(CO)_{10}(\mu\text{-}H)(\mu\text{-}OOCR)$,[8] with an additional peak (2046 cm^{-1}) for the CO attached to the iridium metal centre. The molecular structure of **21** has been confirmed by a single crystal X-ray crystallography. The ORTEP diagram of **21** is shown in Figure 5.3; the structural discussion will be covered in Section 5.6.

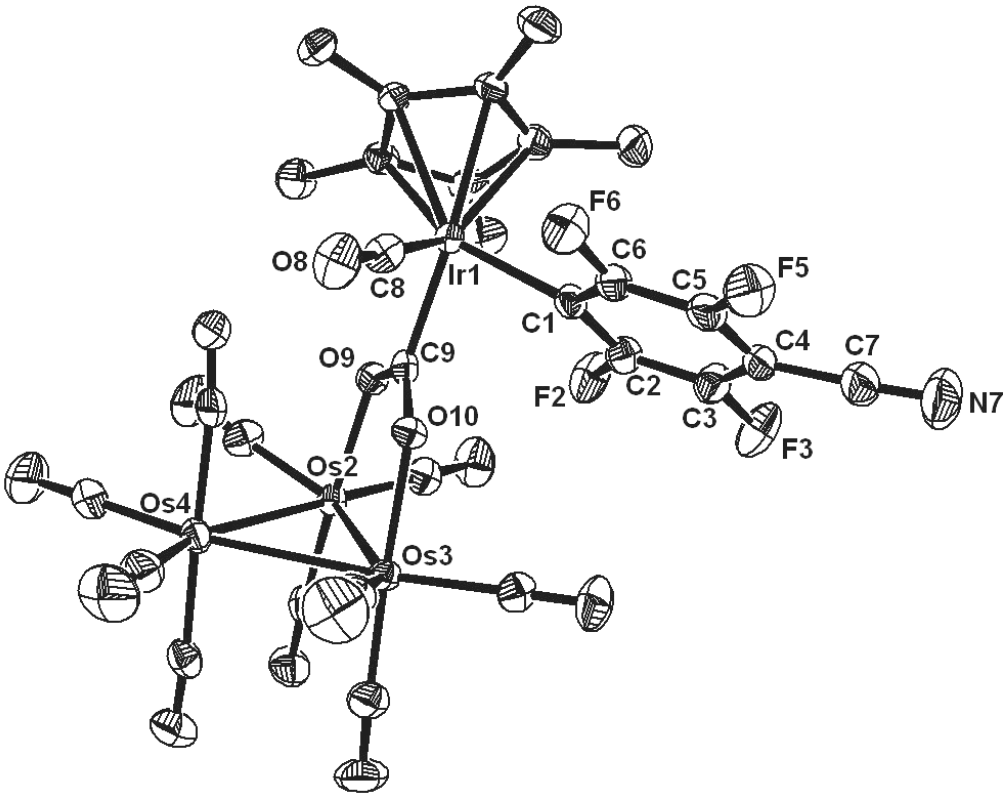

Figure 5.3. ORTEP diagram of **21**. Thermal ellipsoids are drawn at 30% probability level. The hydrogen atoms have been omitted for clarity.

The ^{1}H NMR spectrum of **21** shows a singlet at δ 1.85 assignable to the methyl groups on the Cp* ring and a doublet at δ –10.41, the chemical shift of which is characteristic of the resonance exhibited by a bridging hydride adjacent to a μ,κ^{2} *O*-carboxylato bridge.[9] The splitting could be due to coupling with a F nuclei. The ^{19}F NMR spectrum of **21** shows four sets of multiplets of equal intensities (Figure 5.4); a similar spectrum was obtained for the product $Os_3(CO)_{10}$(μ-H)(μ-OOC[IrCp*(CO)(*p*-C_5F_4N)], **23** obtained from an analogous reaction with the pentafluoropyridine analogue, **22a**.

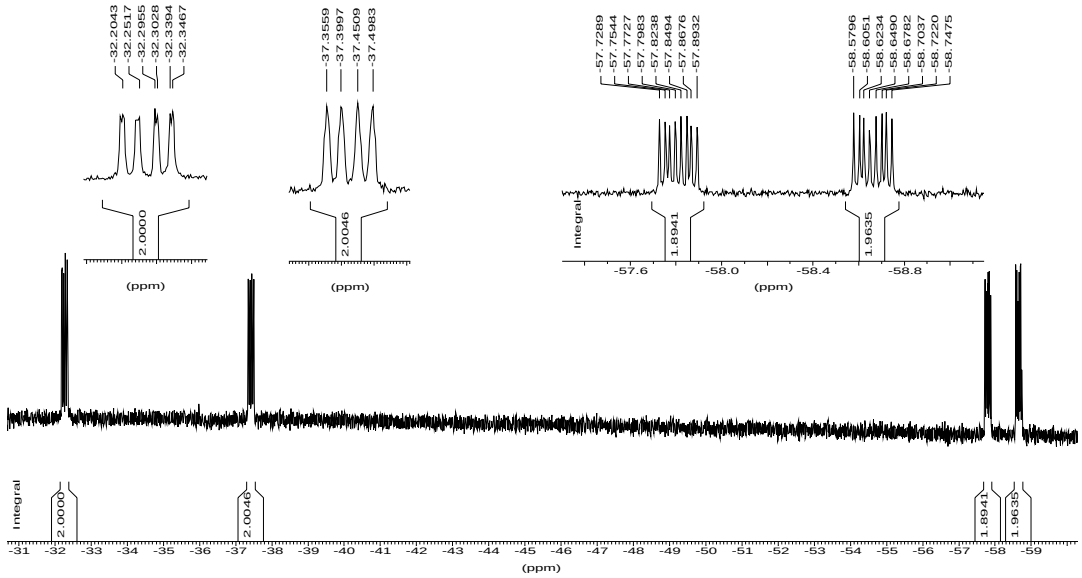

Figure 5.4. ^{19}F NMR spectrum of **21**.

The ^{19}F COSY spectrum of **23** (Figure 5.5) shows correlation between almost all pairs of fluorine resonances. This indicates that **23** has four chemically non-equivalent fluorine atoms, and suggests that there is restricted rotation about the Ir-C1 bond brought about the bulky triosmium cluster.

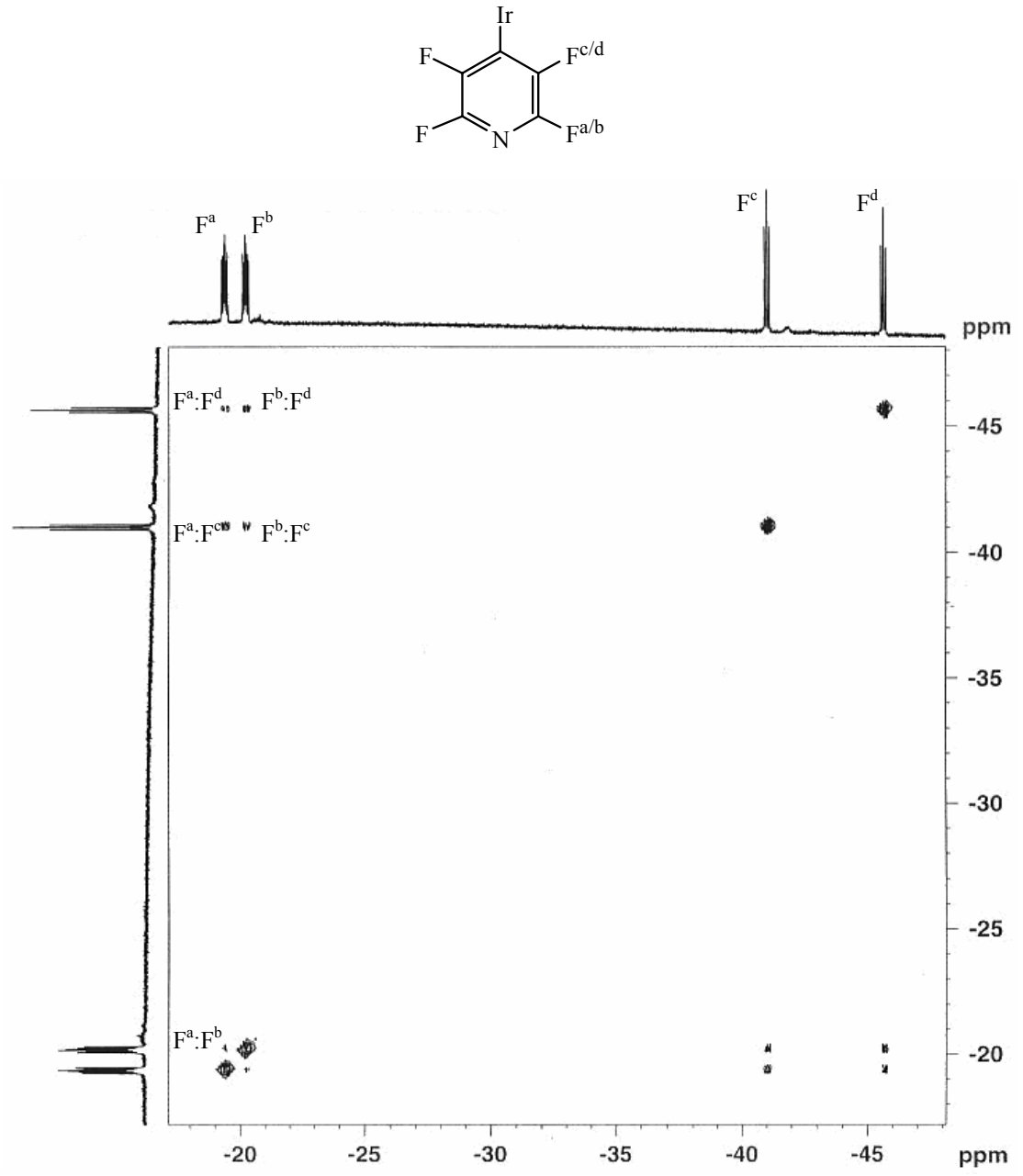

Figure 5.5. ^{19}F COSY spectrum of **23**.

5.6 Crystallographic discussion

X-ray diffraction quality crystals of **18a** were obtained by slow evaporation from a C_6F_5CN solution while that of **18b**, **19b** and **21** were grown from a solution of methanol (**18b**) or dichloromethane (**19b**, **21**) at 5 ºC. Selected bond parameters and a common atomic numbering scheme for **18a, 18b**, **19b** and **21** are tabulated in Table 5.2.

Table 5.2. Selected bond distances (Å) and angles (º) for **18a**, **18b**, **18b** and **21**.

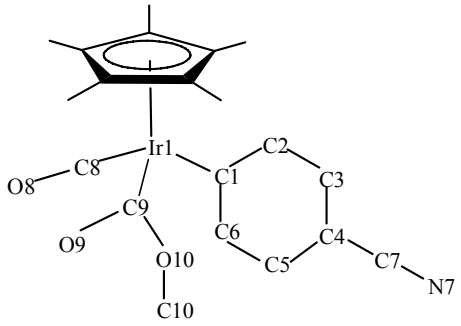

	18a	**18b**	**19b**	**21**
Ir1-C1	2.090(8)	2.068(3)	2.082(6)	2.075(5)
Ir1-C8	1.906(10)	1.873(3)	1.878(6)	1.861(6)
Ir1-C9	2.040(6)	2.047(3)	-	2.052(5)
C8-O8	1.143(12)	1.127(4)	1.118(8)	1.143(7)
O9-C9	1.227(9)	1.200(4)	-	1.261(6)
O10-C9	1.330(10)	1.369(4)	-	1.281(6)
O10-C10	-	1.441(4)	-	-
Ir1-Cl1	-	-	2.4072(16)	-
C(8)-Ir(1)-C(1)	89.8(4)	93.41(13)	92.5(2)	93.5(2)
Ir1-C1-C*$_{Ar}$	173.0(10)	169.9(2)	177.6(4)	170.6(4)
C*$_{CN}$-C4-C*$_{Ar}$	176.2(10)	172.9(4)	179.2(8)	173.4(7)
C(8)-Ir(1)-C(9)	86.9(3)	89.09(12)	-	86.1(2)
C(9)-Ir(1)-C(1)	88.9(3)	88.84(11)	-	86.7(2)
O(9)-C(9)-O(10)	118.8(6)	119.9(3)	-	123.5(5)
O(9)-C(9)-Ir(1)	122.9(5)	126.3(2)	-	118.9(4)
O(10)-C(9)-Ir(1)	118.3(5)	113.84(19)	-	117.6(4)
C(10)-O(10)-C(9)	-	117.2(2)	-	-
C(1)-Ir(1)-Cl(1)	-	-	89.48(16)	-
C(8)-Ir(1)-Cl(1)	-	-	88.8(2)	-
O(9)-Os(2)-Os(4)	-	-	-	92.08(10)
O(9)-Os(2)-Os(3)	-	-	-	80.89(10)
O(10)-Os(3)-Os(4)	-	-	-	90.41(10)
O(10)-Os(3)-Os(2)	-	-	-	81.26(9)

[a] C*$_{Ar}$ = centroid of the fluoroarene C_6 plane.
[b] C*$_{CN}$ = centroid of the CN bond.

All the complexes may be described as three-legged piano stools. The Ir1-C8 bonds of the complexes are slightly longer, and the C8-O8 bonds shorter, than the corresponding bonds in **2a** [1.841(5) Å and 1.847(6) Å, and 1.147(7) Å and 1.157(7) Å respectively]. This indicates that the Ir centres in the fluoroarene complexes are less electron-rich than the Ir center in **2a**, resulting in less π back-bonding from the Ir to the CO ligand.

For **18b**, the difference in the two C-O bond lengths of the carboxylate group are very distinctive; the O9-C9 bond length of 1.200(4) Å is shorter than a typical C=O double bond, and the O10-C9 bond length of 1.369(4) Å is typical of a C-O single bond. In the previously reported fac-$Re(CO)_3$(dpy)C(O)OMe complex, the difference in the C-O bond distances is similarly very pronounced [1.210(9) Å and 1.384(10) Å respectively].[10] In **21**, the C-O bond lengths [1.261(6) Å and 1.281(6) Å] lie between those for a C-O single and double bond, indicating partial double bond character.

The O(9)-C(9)-O(10) bond angle for **18a**, **18b** and **21** are close to the ideal trigonal angle of 120°. The angle is largest for **21** probably because the carboxylate group is bridging across two metal centers. It can be seen from the Ir1-C1-C^*_A and C^*_{CN}-C4-C^*_A bond angles in **18a**, **18b**, **19b** and **21** that the CN group is bent out of the fluoroarene plane, and that the Ir1-C1 bond is also at an angle to this plane.

5.7 Conclusion

The metallocarboxylic acids **18a** and **22a** are relatively stable in several solvents at room temperature under an inert atmosphere. They do not decarboxylate spontaneously. They share many properties typical of metallocarboxylic acids such as dehydration in the presence of an acid, decarboxylation in the presence of a base, and esterification in alcohols without any acid or base catalyst. However, no hydrogen-bonded dimers typical of metallocarboxylic acids and organic carboxylic acids were observed in the X-ray structure of **18a**.

5.8 Experimental

General experimental procedures are as described in Section 2.6. Cp*Ir$(CO)_2$, **2a** was synthesized and purified as described in Section 2.6. $Os_3(CO)_{10}(CH_3CN)_2$ was synthesized by a literature method.[11] All other reagents were purchased commercially and used without further purification.

For the X-ray structural determination of compound **21**, the metal hydride position was placed in a calculated position with the program XHYDEX,[12] and refined with a fixed isotropic thermal parameter and riding on one of the osmium atoms that it was are attached to. All non-hydrogen atoms were given anisotropic thermal parameters in the final model.

5.8.1 Reaction of Cp*Ir(CO)(COOH)(*p*-C_6F_4CN), 18a with HBF_4

To a Carius tube containing **18a** (10.0 mg, 17.4 μmol) in dcm (4 ml) was added HBF_4 (3 drops). The reaction mixture was stirred at room temperature for 16 h. The volatiles were removed under reduced pressure. The oily residue obtained was sparingly soluble in dcm and completely soluble in acetone, and was identified to be [Cp*Ir$(CO)_2$(*p*-C_6F_4CN)][BF_4], **20**. IR (dcm): ν_{CN} 2246 (w), ν_{CO} 2124 (s), 2090 (s) cm^{-1}. ^{1}H NMR: (d_6-acetone): δ 2.27 (s, 15H, Cp*CH_3). ^{19}F NMR (d_6-acetone): δ - 33.92 (m, 2F, F_{meta}), - 58.88 (m, 2F, F_{ortho}), -74.02 (s, 4F, BF_4). MS FAB$^+$ (*m*/*z*): 558 $[M]^+$, 530 $[M - (CO)]^+$, 502 $[M -2(CO)]^+$. HR-MS FAB$^+$ (*m*/*z*): calcd for $C_{19}H_{15}O_2F_4N^{[193]}Ir$ $[M]^+$: 558.0663, found: 558.0662.

Addition of methanol to the residue resulted in complete conversion to Cp*Ir(CO)(COOMe)(*p*-C_6F_4CN), **18b**.

5.8.2 Decarboxylation

i) Compound **18a** (22.8 mg, 39.7 μmol) and PPNCl (20.0 mg, 34.8 μmol) was dissolved in d_6-benzene (1 ml) in a Carius tube. The reaction mixture was degassed by three cycles of freeze-pump-thaw and stirred at room temperature for 16 h. The ^{1}H NMR shows the presence of a hydrido species identified as Cp*Ir(CO)(H)(*p*-C_6F_4CN), **19a**. [A control experiment in

which a degassed solution of **18a** (10.0 mg, 17.4 μmol) in d_6-benzene (1 ml) was stirred for 16 h at room temperature gave no hydride resonance in the ^{1}H NMR spectrum.] On stirring the mixture in $CDCl_3$ at room temperature for 16 h, the solution changed from colourless to a pale orange. Removal of volatiles under reduced pressure followed by extraction with toluene (3 ml) afforded a mixture of **19b** and PPNCl (22.2 mg) in a 4:1 ratio from the ^{1}H NMR integration. Yield of **19b** ≈ 79%. X-ray diffraction quality crystals of **19b** were grown from a concentrated dichloromethane solution at 5 ºC.

The reaction was repeated with **18a** (10.0 mg, 17.4 μmol) and Me_4NF (1.6 mg, 17.2 μmol) in d_6-benzene (1 ml) (stirred for 16 h), and with **18a** (6.5 mg, 11.3 μmol) suspended in aq NaOH (0.1 M, 1 ml, 0.1 mmol) (stirred for 15 min). Compound **19a** was produced in both reactions.

19a: IR (KBr): ν_{CN} 2235 (w), ν_{IrH} 2120 (w), ν_{CO} 2017 (s) cm^{-1}. IR (dcm): ν_{CN} 2240 (w), ν_{IrH} 2120 (vw), ν_{CO} 2014(s) cm^{-1}. ^{1}H NMR ($CDCl_3$): 2.08 (s, 15H, Cp*CH_3), -14.71 (s, 1H, *Ir-H*). ^{1}H NMR (C_6D_6): 1.49 (s, 15H, Cp*CH_3), -14.53 (s, 1H, *Ir-H*). ^{19}F NMR ($CDCl_3$): δ -32.36 (m, 2F, F_{meta}), -60.32 (m, 2F, F_{ortho}). ^{19}F NMR (C_6D_6): δ -32.99 (m, 2F, F_{meta}), -60.60 (m, 2F, F_{ortho}). MS FAB$^+$ (*m*/*z*): 530 $[M - H]^+$.

19b: IR (dcm): ν_{CN} 2240 (w), ν_{CO} 2053 (s) cm^{-1}. ^{1}H NMR ($CDCl_3$): 1.94 (s, 15H, Cp*CH_3). ^{19}F NMR ($CDCl_3$): δ -34.98 (m, 2F, F_{meta}), -58.89 (m, 2F, F_{ortho}). MS FAB$^+$ (*m*/*z*): 538 $[M - (CO) + H]^+$, 530 $[M - Cl]^+$. HR-MS FAB$^+$ (*m*/*z*): calcd for $C_{18}H_{15}F_4NO^{[193]}Ir$ $[M - Cl]^+$: 530.0714, found: 530.0697.

ii) To a Carius tube containing Cp*$Ir(CO)_2$, **2a** (10.1 mg, 26.3 μmol) and Me_4NF (242.9 mg, 2.60 mmol) was added C_6F_5CN (0.5 ml) and deionized H_2O (0.1 ml). The reaction mixture was degassed by three cycles of freeze-pump-thaw and stirred overnight at room temperature. The ^{1}H NMR spectrum showed that **2a** has been consumed, with the formation of **19a**.

Similar results were obtained with Me_4NF (1 and 10 equivalents wrt **2a**), Bu_4NF (100 equiv), and Et_4NBr (100 equiv).

5.8.3 Reaction of 2a with fluoroarenes and fluoropyridines in alcohols.

Reaction of 2a with C_6F_5CN in methanol

To a Carius tube containing **2a** (19.1 mg, 49.8 μmol) was added methanol (1.0 ml) and C_6F_5CN (0.5 ml). The resultant mixture was degassed by three cycles of freeze-pump-thaw and left to stand at room temperature for 2 d. The volatiles were removed under reduced pressure and the residual solid was re-crystallized from methanol to give white crystals of Cp*Ir(CO)($COOCH_3$)(*p*-C_6F_4CN), **18b**. Yield: 27.4 mg (93%). X-ray diffraction quality crystals of **18b** were grown from a concentrated methanol solution at 5 ºC.

IR (KBr): ν_{CN} 2236 (w), ν_{CO} 2038 (s), 1650 (m) cm^{-1}. IR (dcm): ν_{CN} 2239 (w), ν_{CO} 2041, 1659 (s) cm^{-1}. ^1H NMR ($CDCl_3$): δ 3.44 (s, 3 H, OCH_3), 1.95 (s, 15H, Cp*CH_3). ^1H NMR (CH_2Cl_2): δ 3.36 (s, 3 H, OCH_3), 1.91 (s, 15H, Cp*CH_3).^{19}F NMR ($CDCl_3$): δ -35.07 (m, 2F, F_{meta}), -59.35 (m, 2F, F_{ortho}). ^{19}F NMR (CH_2Cl_2): δ -36.32 (m, 2F, F_{meta}), -62.53 (m, 2F, F_{ortho}). Anal. Calcd for $C_{20}H_{19}F_4NO_3Ir$: C, 40.81; H, 3.08; N, 2.38. Found: C, 41.29; H, 3.22; N, 2.19. MS FAB^+ (*m*/*z*): 590 $[M + H]^+$, 558 $[M – (OCH_3)]^+$, 530 $[M – (OCH_3) - (CO)]^+$. HR-MS FAB^+ (*m*/*z*): calcd for $C_{20}H_{19}F_4NO_3Ir$ $[M + H]^+$: 590.0930, found: 590.0926.

Alternatively, complex **18a** (5.0 mg, 13.0 μmol) was dissolved in methanol and stirred at room temperature for 16 h. The ^1H NMR spectrum showed partial conversion to **18b** (82%). Further stirring of the solution at room temperature (3 d) did not increase the amount of **18b**.

The reaction of **2a** (10.5 mg, 27.4 μmol) and C_6F_5CN (0.5 ml) in CD_3OD (0.3 ml) afforded Cp*Ir(CO)($COOCD_3$)(*p*-C_6F_4CN). The ^1H NMR spectrum shows complete consumption of **2a** and the resonance at δ 3.36 due to $COOCH_3$ disappeared.

^1H NMR (CH_2Cl_2): 1.91 (s, 15H, Cp*CH_3). ^{19}F NMR (CH_2Cl_2): δ -37.13 (m, 2F, F_{meta}), -63.68 (m, 2F, F_{ortho}).

Reaction of 2a with C_6F_5CN in isopropanol

Complex **2a** (19.5 mg, 50.9 μmol) was dissolved in isopropanol (1.0 ml) in a Carius tube and C_6F_5CN (0.5 ml) was added. The resultant mixture was degassed by three cycles of freeze-pump-thaw and left to stand for 2 d. The volatiles were removed under reduced pressure and the residual solid was re-crystallized from isopropanol to give white crystals of Cp*Ir(CO)(COO^iPr)(*p*-C_6F_4CN), **18c**. Yield: 20.5 mg (65%).

IR (dcm): ν_{CN} 2238 (w), ν_{CO} 2040 (s), 1652 (m). ^{1}H NMR ($CDCl_3$): δ 5.02 {sep, $^3J_{HH}$ = 6.2, 1H, O*CH*(CH_3)$_2$} 1.95 (s, 15H, Cp*C*H*$_3$), 1.05, 0.95 (dd, 6H, OCH(C*H*$_3$)$_2$. ^{19}F NMR ($CDCl_3$): δ -34.58 (m, 2F, F_{meta}), -59.81 (m, 2F, F_{ortho}). Anal. Calcd for $C_{22}H_{22}F_4NO_3Ir$.1/2IPA: C, 43.65; H, 4.05; N, 2.17. Found: C, 43.81; H, 3.87; N, 2.30. MS FAB$^+$ (*m*/*z*): 618 $[M + H]^+$, 558 $[M – (OC_3H_7)]^+$, 530 $[M – (COOC_3H_7)]^+$, 502 $[M – (COOC_3H_7) – (CO)]^+$. HR-MS FAB$^+$ (*m*/*z*): calcd for $C_{22}H_{23}F_4NO_3Ir$ $[M + H]^+$: 618.1244, found: 618.1255.

Alternatively, **18c** can be prepared from **18b** in 98% conversion (from ^{1}H NMR) by stirring a solution of **18b** in isopropanol for 2 d. The reverse reaction to obtain **18b** from **18c** by stirring a solution of **18c** in methanol for 2 d resulted in only 35% conversion to **18b**.

Reaction of 2a with C_6F_5CN in cyclopropanol

To a Carius tube containing **2a** (8.3 mg, 21.6 μmol) was added C_6F_5CN (0.25 ml) and cyclopropanol (0.5 ml). The solution was degassed by three cycles of freeze-pump-thaw and stirred at room temperature for 2 d during which the solution turned from yellow to almost colourless. The volatiles were removed under reduced pressure. 1,3,5-triphenylbenzene (3.3 mg, 10.8 μmol) was added as a standard for quantification. A ^{1}H NMR spectrum of the mixture was taken immediately in $CDCl_3$. Yield of Cp*Ir(CO)($COOC_5H_9$)(*p*-C_6F_4CN), **18d**: 96% (^{1}H NMR integration).

IR (dcm): ν_{CN} 2239 (w), ν_{CO} 2040 (s), 1653 (w) cm^{-1}. IR (KBr): ν_{CN} 2239 (w), ν_{CO} 2031 (s), 1654 (m), 1628 (m) cm^{-1}. ^{1}H NMR ($CDCl_3$): 5.16 (m, 1H, OC*H*<), 1.63 (m, 4H, ring H), 1.41 (m, 4H, ring H), 1.96 (s, 15H, Cp*C*H*$_3$). ^{19}F NMR ($CDCl_3$): δ - 34.63 (m, 2F, F_{meta}), - 59.68

(m, 2F, F_{ortho}). MS FAB$^+$ (*m*/*z*): 644[M + H]$^+$, 574[M – (C_5H_9)]$^+$, 558[M – (OC_5H_9)]$^+$, 530[M – ($COOC_5H_9$)]$^+$. HR-MS FAB$^+$ (*m*/*z*): calcd for $C_{24}H_{25}F_4NO_3{}^{[193]}Ir$ [M + H]$^+$: 644.1395, found: 644.1409.

Reaction of 2a with C_5F_5N in methanol

Complex **2a** (19.6 mg, 51.1 μmol) was dissolved in methanol (1.0 ml) in a Carius tube and C_5F_5N (0.5 ml) was added. The resultant mixture was degassed by three cycles of freeze-pump-thaw and left to stand for 2 d. The volatiles were removed under reduced pressure and the residue was washed with hexane to recover unreacted **2a** (0.9 mg, 5%). The product was re-crystallized from methanol to give white crystalline solid, Cp*Ir(CO)($COOCH_3$)(*p*-C_5F_4N), **22b**. Yield: 25.7 mg (89%).

IR (dcm): ν_{CN} 2236 (w), ν_{CO} 2042 (s), 1661(m) cm^{-1}. ^{1}H NMR ($CDCl_3$): δ 3.45 (s, 3 H, O*CH*$_3$), 1.96 (s, 15H, Cp*C*H*$_3$). ^{19}F NMR ($CDCl_3$): δ -20.88 (m, 2F, F_{meta}), -43.64 (m, 2F, F_{ortho}). Anal. Calcd for $C_{18}H_{18}F_4NO_3Ir$: C, 38.29; H,3.21; 2.48. Found: C, 38.54; H, 3.33; N, 2.43. MS FAB$^+$ (*m*/*z*): 566 [M + H]$^+$, 534 [M – (OCH_3)]$^+$, 506 [M – (OCH_3)-(CO)]$^+$. HR-MS FAB$^+$ (*m*/*z*): calcd for $C_{18}H_{19}F_4NO_3Ir$ [M + H]$^+$: 566.0925, found: 566.0936.

Reaction of 2a with octafluorotoluene, $C_6F_5CF_3$ in methanol.

Complex **2a** (10.0 mg, 26.1 μmol) was dissolved in methanol (2.0 ml) in a Carius tube and $C_6F_5CF_3$ (0.5 ml) was added. The resultant mixture was degassed by three cycles of freeze-pump-thaw and heated at 70 °C for 4 h. The IR spectrum shows the presence of peaks due to unreacted **2a** and a new CO stretch. The solution was heated for another 5 h at 90 °C. A mixture of Cp*Ir(CO)($COOCH_3$)(*p*-$C_6F_4CF_3$), **24a** and unreacted **2a** was observed in the ^{1}H NMR spectrum (5% conversion to **24a** from ^{1}H NMR integration).

IR (dcm): ν_{CO} 2037(s) cm^{-1}. ^{1}H NMR ($CDCl_3$): δ 3.49 (s, 3 H, O*CH*$_3$), 1.96 (s, 15H, Cp**CH*$_3$). MS FAB$^+$ (*m*/*z*): 601 [M – (OMe)]$^+$, 573 [M – (COOMe)]$^+$, 545 [M – (COOMe)-(CO)]$^+$. MS FAB$^-$ (*m*/*z*): 631 [M - H]$^-$.

Reaction of 2a with $C_6F_5CF_3$ in 1-propanol.

The reaction was repeated by heating **2a** (10.0 mg, 26.1 μmol) and $C_6F_5CF_3$ (0.25 ml) in 1-propanol (2.0 ml) at 110 °C for 18 h in a Carius tube. The reaction was monitored by IR spectroscopy and shown to be incomplete. The solution was heated for a further 16 h at 130 °C. IR and ^{1}H NMR analysis still showed the presence of starting materials. (37% conversion to Cp*Ir(CO)(COO^{n}Pr)(*p*-$C_6F_4CF_3$), **24b** from ^{1}H NMR integration). Further heating at 130 °C for 65 h did not increase the yield of product. Instead, the solution turned from colourless to brown with some decomposition to a hydrido species, which was proposed to be Cp*Ir(CO)(H)(*p*-$C_6F_4CF_3$), **25**.

24b:

IR (hexane): ν_{CO} 2044 (s), 1669 (w) cm^{-1}. ^{1}H NMR ($CDCl_3$): δ 3.88 (m, 2H, OC*H*$_2$CH$_2$CH$_3$), 1.96 (s, 15H, Cp*C*H*$_3$), 1.41 (m, 2H, OCH$_2$C*H*$_2$CH$_3$), 0.67 (t, 3H, $^3J_{HH}$ = 7.2, OCH$_2$CH$_2$C*H*$_3$). ^{19}F NMR ($CDCl_3$): δ 20.02 (m, 3H, C*F*$_3$), -36.58 (m, 2F, F$_{meta}$), - 67.32 (m, 2F, F$_{ortho}$). MS FAB$^+$ (*m*/*z*): 661 [M + H] $^+$, 601 [M – (OC_3H_7)]$^+$, 573 [M – (OC_3H_7)-(CO)]$^+$, 545 [M – (O C_3H_7)-2(CO)]$^+$. HR-MS FAB$^+$ (*m*/*z*): calcd for $C_{22}H_{23}O_3F_7{}^{[193]}$Ir [M + H]$^+$: 661.1159, found: 661.1154.

25:

^{1}H NMR ($CDCl_3$): δ 1.96 (s, 15H, Cp*C*H*$_3$), -14.76 (s, 1H, Ir-*H*). ^{19}F NMR ($CDCl_3$): δ 19.94 (m, 3H, C*F*$_3$), -34.31 (m, 2F, F$_{meta}$), - 68.03 (m, 2F, F$_{ortho}$).

Reaction of 2a with 1,3-$C_6F_4(CN)_2$ in methanol

i) To a Carius tube containing **2a** (10.0 mg, 26.1 μmol) and 1,3-$C_6F_4(CN)_2$ (104.2 mg, 0.521 mmol) was added methanol (0.5 ml). The solution was degassed by three cycles of freeze-pump-thaw and left to stand for 4 h during which the solution was turned from yellow to colourless. The ^{19}F NMR spectra showed the presence of unreacted 1,3-$C_6F_4(CN)_2$ and 4-methoxybenzene-1,3-dicarbonitrile, C_6F_3[4-(OMe)-1,3-$(CN)_2$] in a 1:2 integration ratio.

ii) The reaction was repeated with stoichiometric amounts of 1,3-$C_6F_4(CN)_2$ in methanol: To a Carius tube containing **2a** (10.5 mg, 27.4 μmol) and 1,3-$C_6F_4(CN)_2$ (5.2 mg, 26.0 μmol) was added methanol (0.5 ml). The solution was degassed by three cycles of freeze-pump-thaw and left to stand for 4 h. The ^1H and ^{19}F NMR spectra showed the presence of $C_6F_3(OMe)(CN)_2$ and another product proposed to be Cp*Ir(CO)(COOMe)[2,4-$C_6F_3(CN)_2$], **29**, in a 1: 5 ratio.

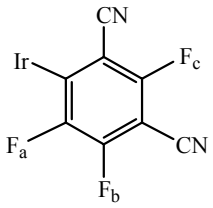

IR (dcm): ν_{CO} 2046 (s) cm^{-1}. ^1H NMR ($CDCl_3$): δ 3.48 (s, 3H, OC*H*$_3$), 1.96 (s, 15H, Cp**CH*$_3$). ^{19}F NMR ($CDCl_3$): δ - 26.79 (d, $^3J_{FF}$ = 14.4, 1F, F_c), -32.47 (m, 1F, F_b), -45.79 (d, $^3J_{FF}$ = 26.8, 1F, F_a). MS FAB$^+$ (*m*/z): 597[M + H]$^+$, 565 [M – (OMe)]$^+$, 537 [M – (COOMe)]$^+$, 509 [M – (COOMe) – (CO)]$^+$.

Reaction of 1,3-$C_6F_4(CN)_2$ with methanol

1,3-$C_6F_4(CN)_2$ (20.0 mg, 100 μmol) was dissolved in methanol and left to stand at room temperature for 5 h. The volatiles were removed under reduced pressure to give a white solid identified to be 2,4,5-trifluoro-6-methoxy-isophthalonitrile.

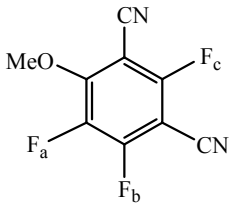

^1H NMR ($CDCl_3$): δ 4.38 (d, $^5J_{HF}$ = 5Hz, 3H, OC*H*$_3$). ^{19}F NMR ($CDCl_3$): δ - 25.39 (apparent d, 1F, F_c), -40.49 (apparent d, 1F, F_b), -80.88, (m, 1F, F_a). MS EI$^+$ (*m*/z): 212 [M]$^+$. {Literature: ^{19}F NMR (d_6-DMSO): δ - 24 (d, 1F,), -38 (d, 1F), -75, (dd, 1F).[13]

Reaction of 2a with $C_6F_3(CN)_2(OMe)$.

A solution of **2a** (10.0 mg, 26.1 μmol) and $C_6F_3(OMe)(CN)_2$ (5.6 mg, 26.4 μmol) in toluene (2 ml) was stirred for at room temperature for 1 d. The IR and ^{1}H NMR spectra show only peaks due to the starting materials.

Test for stability of 18b to hydrolysis

To a solution of **18b** (10.0 mg, 17.0 μmol) in THF (1 ml) was added deionized water (1 ml). The solution was degassed by three cycles of freeze-pump-thaw and stirred at room temperature for 18 h. The volatiles were removed under reduced pressure and the residue was completely dissolved in $CDCl_3$. A ^{1}H NMR spectrum was taken. A 67% conversion of **18b** to **19a** was observed from the integration ratio of the Cp* resonances in **18b** and **19a**.

Control: A solution of **18b** (10.0 mg, 17.0 μmol) in anhydrous THF (1 ml) was stirred at room temperature for 20.5 h. The ^{1}H and ^{19}F NMR spectra showed only the presence of **18b**.

Reaction of 2a with pentafluoropyridine and 3-Chloro-propan-1-ol

To a Carius tube containing **2a** (19.0 mg, 49.5 μmol) was added C_5F_5N (0.5 ml) and 3-chloro-propan-1-ol (0.25 ml). The solution was degassed by three cycles of freeze-pump-thaw and stirred at room temperature for 2 d during which the solution was turned from yellow to almost colourless. The volatiles were removed under reduced pressure to give a pale brown oil, **22c**. The oil was completely dissolved in $CDCl_3$ and ¼ of the solution was transferred to an NMR tube containing 1,3,5-triphenylbenzene (6.3 mg, 20.5 μmol). A ^{1}H NMR spectrum was taken immediately. Yield: 96% (^{1}H NMR integration).

IR (dcm): ν_{CO} 2046 (s), 1653 (w). ^{1}H NMR ($CDCl_3$): 4.01 (m, 2H, $OCH_2CH_2CH_2Cl$), 3.29 (m, 2H, $OCH_2CH_2CH_2Cl$), 1.97 (s, 15H, Cp*CH_3). 1.85(m, 2H, $OCH_2CH_2CH_2Cl$), ^{19}F NMR ($CDCl_3$): δ - 20.57 (m, 2F, F_{meta}), - 43.38 (m, 2F, F_{ortho}). MS FAB$^+$ (*m*/*z*): 628 $[M + H]^+$, 534 $[M – (OC_3H_7Cl) + H]^+$, 506 $[M – (OC_3H_7Cl)-(CO)]^+$, 478 $[M – (OC_3H_7Cl)-2(CO)]^+$. HR-MS FAB$^+$ (*m*/*z*): calcd for $C_{20}H_{22}O_3ClF_4N^{[193]}Ir$ $[M + H]^+$: 628.0845, found: 628.0848.

5.8.4 Reaction with $Os_3(CO)_{10}(CH_3CN)_2$

Reaction of 18a with $Os_3(CO)_{10}(CH_3CN)_2$

Complex **18a** (33.0 mg, 57.4 μmol) and $Os_3(CO)_{10}(CH_3CN)_2$ (54.0 mg, 57.9 μmol) was dissolved in dcm (10 ml) to give a yellow solution. The solution was stirred at room temperature for 16 h, after which the solvent was removed under reduced pressure. The residue obtained was redissolved in the minimum of dichloromethane and chromatographed on TLC plates. Elution with dichloromethane: hexane (2:3 v/v) afforded two yellow bands leaving an immovable brown band on the baseline. The major band, B1 (R_f = 0.34) was identified to be **21** (50.2 mg, 61%). The minor band, B2 (R_f = 0.14) was identified to be $Os_3(CO)_{10}(\mu\text{-H})(\mu\text{-OH})$ (1.1 mg, 2%). {ν_{CO}/ cm^{-1} (hexane): 2112(w), 2071(s), 2062(m), 2025(vs), 2002(m), 1990(w), 1985(w); literature ν_{CO}/ cm^{-1} (cyclohexane): 2110(w), 2072(s), 2060(m), 2027(vs), 2025(w), 2006(m), 1989(w)}[14]

X-ray diffraction quality crystals of **21** were grown from a concentrated dichloromethane solution at 5 ºC.

21: IR (dcm): ν_{CN} 2240 (w), ν_{CO} 2109 (w), 2071 (vs), 2059 ν(s), 2046 (sh), 2020 (vs), 2011 (vs), 1978 (w) cm^{-1}. ^{1}H NMR ($CDCl_3$): 1.85 (s, 15H, C*H*$_3$), -10.41 (d, 1H, *OsHOs*). ^{19}F NMR ($CDCl_3$): δ -32.25 (m, 1F, F_{meta}), -37.39 (m, 1F, F_{meta}), -57.84 (m, 1F, F_{ortho}), -58.69 (m, 1F, F_{ortho}). Anal. Calcd for $C_{29}H_{16}F_4NO_{13}IrOs3$: C, 24.44; H, 1.13; N, 0.98. Found: C, 24.62; H, 1.07; N, 0.96. MS FAB$^+$ (*m*/*z*): 1424 [M - H]$^+$.

Reaction of 22a with $Os_3(CO)_{10}(NCCH_3)_2$

Complex **22a** (19.0 mg, 34.5 μmol) was reacted with $Os_3(CO)_{10}(CH_3CN)_2$ (38.0 mg, 40.7 μmol) according to the procedure described above. TLC separation gave a major yellow band (R_f = 0.51) identified to be **23** (22.5 mg, 47 %).

IR (dcm): ν_{CO} 2109 (w), 2071 (vs), 2060 (s), 2046 (sh), 2019 (vs), 2011 (vs), 1975 (w) cm^{-1}. ^{1}H NMR ($CDCl_3$): 1.85 (s, 15H, C*H*$_3$), -10.41 (d, 1H, Os*H*Os). ^{19}F NMR ($CDCl_3$): δ -19.38

(m, 1F, F_{meta}), -20.20 (m, 1F, F_{meta}), -41.02 (m, 1F, F_{ortho}), -45.65 (m, 1F, F_{ortho}). HR-MS FAB^+ (*m*/*z*): calcd for $C_{27}H_{15}O_{13}F_4N^{[191]}Ir^{[188]}Os^{[192]}Os_2$ $[M - H]^+$: 1399.8868, found: 1399.8800.

Table 5.3. Crystal data for **18b**, **19b** and **21**.

Compound	**18b**	**19b**	**21**
Empirical formula	$C_{20}H_{18}F_4IrNO_3$	$C_{18.50}H_{16}Cl_2F_4IrNO$	$C_{29}H_{16}F_4IrNO_{13}Os_3$
Formula weight	588.55	607.42	1425.23
Temperature	223(2)	243(2)	223(2)
Crystal system	Triclinic	Triclinic	Monoclinic
Space group	$P\bar{1}$	$P\bar{1}$	$P2_1/n$
Unit cell dimensions			
a (Å)	8.2139(5)	7.2622(3)	9.3815(4)
b (Å)	9.1750(6)	11.3491(5)	15.4499(7)
c (Å)	14.0581(9)	14.6705(6)	23.8611(11)
α (°)	73.4480(10)	68.1550(10)	90
β (°)	84.5460(10)	83.0620(10)	90.2070(10)
γ (°)	75.8680(10)	74.4150	90
Volume (Å^3)	984.45(11)	1080.75(8)	3458.5(3)
Z	2	2	4
Density calc. (Mg m^{-3})	1.986	1.867	2.737
Absorption coefficient (mm^{-1})	6.839	6.465	14.907
F(000)	564	578	2568
Crystal size (mm^3)	0.42 x 0.32 x 0.24	0.32 x 0.22 x 0.08	0.34 x 0.22 x 0.14
Theta range for data collection (°)	2.38 to 26.37	2.02 to 30.49	2.16 to 30.47
Index ranges	$-10 \le h \le 10$	$-10 \le h \le 10$	$-12 \le h \le 12$
	$-10 \le k \le 11$	$-14 \le k \le 15$	$0 \le k \le 21$
	$0 \le l \le 17$	$0 \le l \le 20$	$0 \le l \le 32$
Reflections collected	15037	16485	53029
Independent reflections	4034 [R(int) = 0.0231]	6182 [R(int) = 0.0297]	10163 [R(int) = 0.0426]
Completeness to theta (%)	= 26.37°; 100.0	= 30.49°; 93.8	= 30.47°; 96.4
Max. and min. transmission	0.2906 and 0.1613	0.6258 and 0.2315	0.2294 and 0.0807
Data / restraints / parameters	4034 / 0 / 268	6182 / 100 / 303	10163 / 0 / 465
Goodness-of-fit on F^2	1.063	1.104	1.133
Final R indices [$I>2\sigma(I)$]	R1 = 0.0171, wR2 = 0.0422	R1 = 0.0427, wR2 = 0.1253	R1 = 0.0332, wR2 = 0.0711
R indices (all data)	R1 = 0.0177, wR2 = 0.0424	R1 = 0.0478, wR2 = 0.1288	R1 = 0.0382, wR2 = 0.0731
Largest diff. peak and hole (e.Å^{-3})	1.001 and -0.439	2.888 and -0.498	1.701 and -1.215

References

[1] (a) Bennett, M. A.; Robertson, G. B.; Rokicki, A.; Wickramasinghe, W. A. *J. Am. Chem. Soc.* **1988**, *110*, 7098-7105. (b) Elliot, P. I. P.; Haslam, C. E.; Spey, S. E.; Haynes, A. *Inorg. Chem.* **2006**, *45*, 6269-6275.

[2] Bennett, M. A. *J. Mol. Catal.* **1987**, *4*1, 1-20.

[3] (a) Barrientos-Penna, C. F.; Gilchrist, A. B.; Klahn-Oliva, A. H.; Hanlan, J. L.; Sutton, D. *Organometallics* **1985**, *4*, 478-485. (b) Catellani, M.; Halpern, J. *Inorg. Chem.* **1980**, *19*, 566-568.

[4] Mandal, S. K.; Ho, D. M.; Orchin, M. *J. Organomet. Chem*. **1992**, *439*, 53-64.

[5] Bennett, M. A.; Rokicki, A. *Organometallics* **1985**, *4*, 180-187.

[6] (a) Nicholls, B. J. N.; Vargas, M. D. *Inorg. Synth.*, **1990**, *28*, 234-235. (b) Richmond, M. G. *Coord. Chem. Rev.* **1997**, *160*, 237-294.

[7] Ainscough, E. W.; Brodie, A. M.; Coll, R. K.; Coombridge, B. A.; Waters, J. M. J. *Organomet. Chem.* **1998**, *556*, 197-205.

[8] Banford, J.; Mays, M. J.; Raithy, P. R. *J. Chem. Soc. Dalton Trans.* **1985**, 1355-1360.

[9] Frauenhoff, G. R. *Coord. Chem. Rev.* **1992**, *121*, 131-154.

[10] Gibson, D. H.; Sleadd, B. A.; Vij, A. *J. Chem. Crystallogr.* **1999**, *29*, 619-622.

[11] Nicholls, B. J. N.; Vargas, M. D. *Inorg. Synth.*, **1990**, *28*, 232-235.

[12] Orpen, G. XHYDEX: A Program for Locating Hydrides in Metal Complexes; School of Chemistry, University of Bristol: UK, **1997**.

[13] Nobuo, I.; Akio, T.; Takashi, I.; Masatoshi, M.; Kazuhiro, K. *Ger. Offen.* DE 3530941, **1986**.

[14] D. Roberto, E. Lucenti, C. Rovenda and R. Ugo, *Organometallics*, **1997**, *16*, 5974-5980.

Chapter 6: Catalytic Investigation on Cyclopentadienyl Iridium Complexes

6.1 Oppenauer-type oxidation of primary and secondary alcohols catalyzed by iridium complexes

The oxidation of alcohols to carbonyl compounds is a fundamental and important reaction in organic synthesis. Metal-catalyzed oxidation of alcohols using environmentally friendly oxidants is of interest as the reaction can be carried out with high selectivity under milder and less toxic conditions. The Oppenauer oxidation, which employs aluminum alkoxide as the catalyst, is a gentle method for oxidizing primary or secondary hydroxyl compounds to their corresponding carbonyl compounds through the use of an excess of a carbonyl hydrogen acceptor such as benzophenone or acetone.[1]

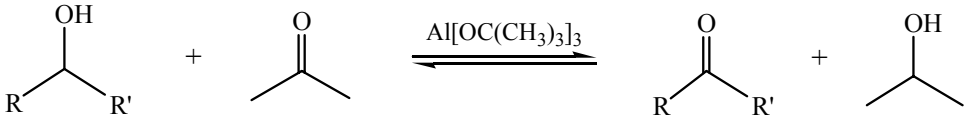

Scheme 6.1

The advantage of Oppenauer oxidation over other oxidative methods for alcohols is that carboxylic acid products from over-oxidation are avoided. Several transition-metal-catalyzed systems for the Oppenauer-type oxidation have also been reported, such as those using ruthenium and iridium complexes as catalyst (Chart 6.1), acetone as the hydrogen acceptor and potassium carbonate or triethylamine as the base.[1b,2]

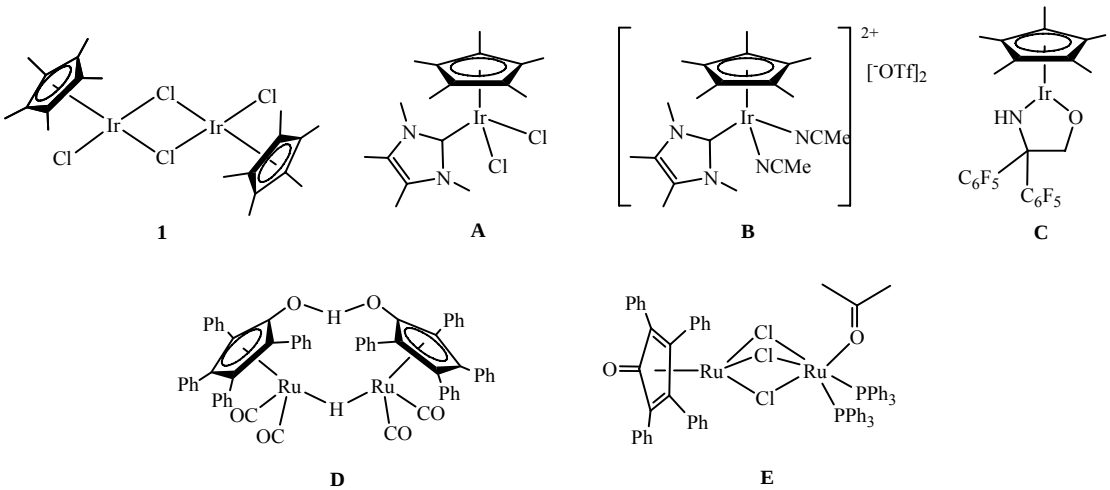

Chart 6.1

The mechanism of the iridium-catalyzed Oppenauer-type oxidation proposed by Fujita *et. al.* is shown in Scheme 6.2.[2a, b]

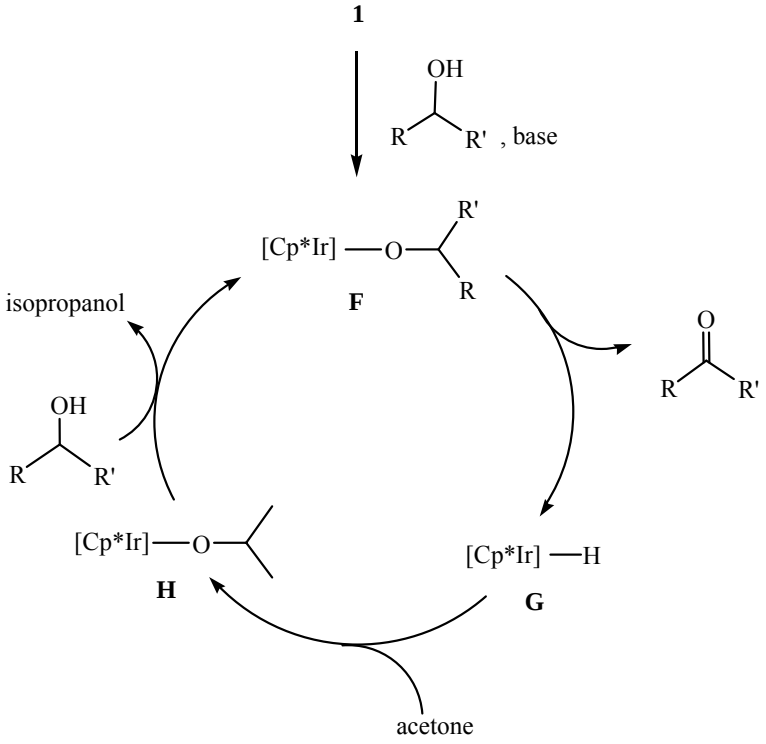

Scheme 6.2

A base such as K_2CO_3 would stimulate the formation of the metal alkoxide **F** by trapping the hydrogen chloride generated in the first step of the reaction. The corresponding carbonyl product and the iridium hydride complex **G** would be formed by *β*-hydrogen elimination. Insertion of acetone into the metal-hydride bond would generate the metal isopropoxide **H** and exchange of the alkoxy moiety would regenerate the metal alkoxide **F** with the production of isopropanol as a by-product.

The results for the oxidation of cyclopentanol by various iridium complexes are summarized in Table 6.1. It can be seen that complex **1** can catalyze oxidation with an amine as a base (entry 1). $Cp^*Ir(CO)(Cl)_2$, **9a** shows comparable activity to **1** with K_2CO_3 as base and probably goes through a similar catalytic cycle as **1**, forming the metal alkoxide intermediate by losing a chloride ligand to generate hydrogen chloride. However, with triethylamine as base, only 22% conversion was achieved after 4 d at room temperature (entries 3 and 4). In-situ conversion of **2a** to **9a** was attempted in a one-pot oxidation of

cyclopentanol (**2a**, CCl_4, cyclopentanol, K_2CO_3 and acetone was added together) but the yield of the ketone was poor.

Table 6.1. Iridium catalyzed oxidation of cyclopentanol.

Entry	Iridium complex	Base	Conv. of alcohol (%)[a]
1	**1**	Et_3N[b]	100%
2	**2a**	K_2CO_3	0%
3	**9a**	K_2CO_3	100%
4	**9a**	Et_3N[b]	Trace, 22% after 4 d
5[c]	**9b**	K_2CO_3	0%
6	**2a**/ CCl_4[d]	K_2CO_3	Trace
7	**2b**/ CCl_4[d]	K_2CO_3	Trace conversion after 5 d
8	$IrCl_3$	K_2CO_3	0%, 22% after Δ for 4 d[e]
9	Cp*Ir(PMe_3)Cl_2, **32a**	K_2CO_3	0%, trace after Δ for 4 d[e]
10	Cp*Ir(PPh_3)Cl_2, **32b**	K_2CO_3	0%

The reaction was performed at room temperature for 6 h with cyclopentanol (1.0 mmol), iridium complex (1 mol%) and base (0.01 mmol) in acetone (10 ml) unless otherwise stated.
[a] Determined by ^{1}H NMR.
[b] 1.0 mmol of base used.
[c] **9b** was synthesized from the reaction of **2b** with CCl_4 under irradiation from a xenon lamp and used for the catalytic run without isolation.
[d] 0.5 ml of CCl_4 used.
[e] 2d heating at 70 ºC followed by another 2 d heating at 75 ºC in Carius tube.

We were interested to find out if it was possible to utilize the amine functionality in the Cp*^ ligand as an internal base for the Oppenaeur-type oxidation of cyclopentanol. An attempt to synthesize $(Cp^{*\wedge}IrCl_2)_2$ from the reaction of Cp*^H with iridium trichloride in refluxing methanol following the literature method for the preparation of $(Cp^*IrCl_2)_2$, **1** was unsuccessful. However, since **9a** shows promising catalytic activity, we surmise that it would be worthwhile to test the amine-functionalized analogue Cp*^Ir(CO)Cl_2, **9b** for its catalytic potential. The reaction of CCl_4 with **2a** is known to produce **9a** readily, so we tested the activity of a **2b**/CCl_4 mixture; the activity was similar to that for **2a** (entries 6 and 7). To check that this procedure indeed produced **9b**, it was also first obtained by irradiating a solution of **2b** in CCl_4 using a xenon lamp before a solution of cyclopentanol in acetone was

added and stirred for 6 h. A ^{1}H NMR spectrum taken shows that cyclopentanone was not produced. Addition of K_2CO_3 followed by another 6 h of stirring did not result in conversion to the product either (entry 5). With $IrCl_3$, there was no oxidation of the alcohol at room temperature; after 4 d of heating, only a 22% conversion was achieved (entry 8). An attempt to generate **1** in situ from the reaction of $IrCl_3$ with Cp*H in refluxing acetone failed (literature preparation uses methanol).

The phosphine complexes were found to be inactive for the oxidation of alcohol (entries 9 and 10). From the proposed catalytic cycle (Scheme 6.1), it seems that only one vacant coordination site is required. Changing the catalyst from **9a** to Cp*Ir(PR_3)Cl_2 should still allow the loss of the chloride ligands to generate a vacant coordination site. However, no conversion of cyclopentanol was obtained with the phosphine complexes. It is possible that more than one vacant coordination site is required for the catalysis, and that phosphine ligands are difficult to be lost to generate that additional coordination site.

6.2 Transfer hydrogenation of ketones catalyzed by iridium complexes

Transfer hydrogenation is the addition of hydrogen to a substrate from a source other than gaseous hydrogen.[3] A useful class of hydrogen-transfer catalyst based on Ru, Rh and Ir diamines has been developed for the reduction of ketones to secondary alcohols.[4] The hydrogen transfer agent is typically isopropanol and converts to acetone upon donation of hydrogen (Scheme 6.3).

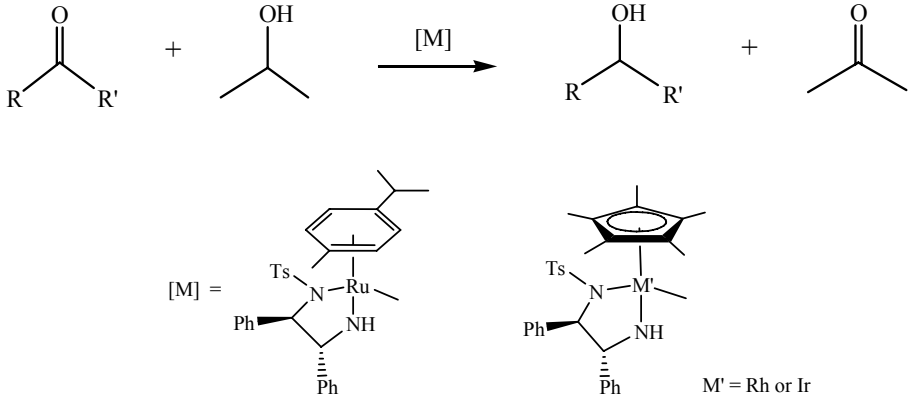

Scheme 6.3

This process is essentially the reverse of the Oppenauer-type oxidation described in Section 6.1, and complex **1** has been known to catalyze transfer hydrogenation of quinoline in isopropanol.[5] The catalytic results for the complexes studied here are summarized in Table 6.2. It shows the same trend as the Oppenauer-type oxidation described in Section 6.1, with compound **1** and **9a** showing good catalytic activity while the phosphine complex **32a** gave no conversion. The presence of acetone as a side product was detected in the ^{1}H NMR spectrum.

Table 6.2. Iridium catalyzed transfer hydrogenation of cyclopentanone.

Entry	Ir complex	Base	Conv. of ketone (%)[a]
1	**1**	K_2CO_3	100%
2	**9a**	Na_2CO_3	100%
3	**32a**	Na_2CO_3	0%

The reaction was performed at room temperature for 6 h with cyclopentanone (1.0 mmol), iridium complex (0.01 mmol) and base (0.1 mmol) in isopropanol (10 ml).
[a] Determined by ^{1}H NMR spectroscopy.

6.3 One-pot oxidation and methylenation

Multicatalytic processes involving the use of more than one metal complex to catalyze independent reactions in a one-pot synthesis enhances the efficiency of organic synthesis as it avoids the need to isolate and purify the intermediates produced in each step of the reaction. Lebel *et. al.* have developed a one-pot process for the conversion of alcohols to alkenes, thus avoiding the isolation and purification of the potentially air-sensitive aldehyde intermediate. The procedure combines the palladium-catalyzed aerobic oxidation of alcohols with the rhodium-catalyzed methylenation of carbonyl derivatives (Scheme 6.4).[6]

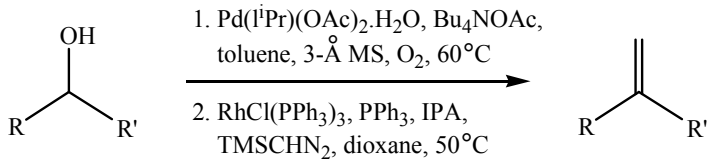

Scheme 6.4

The feasibility of replacing the palladium catalyst with complexes **1** or **9a** to effect an Oppenauer-type oxidation of primary and secondary alcohols into carbonyl complexes before

the methylenation step was investigated as the Oppenauer-type oxidation is simpler and safer, using acetone as the oxidant at room temperature instead of pure oxygen at 60 ºC. Hence the compatibility of **1** or **9a** with the Wilkinson's catalyst $RhCl(PPh_3)_3$ in a one-pot synthesis of alkenes was studied (Scheme 6.5).

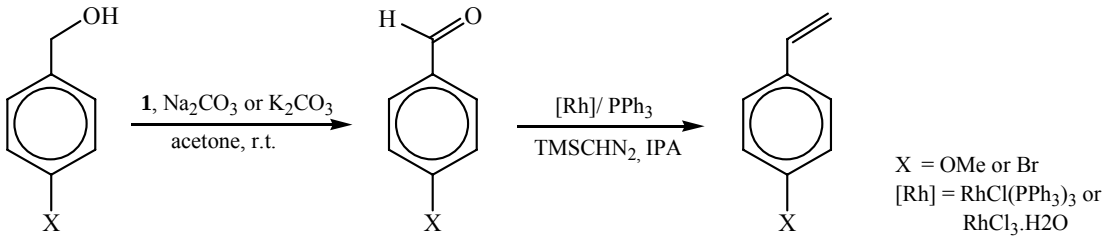

Scheme 6.5

Oxidation of 4-methoxylbenzyl alcohol and 4-bromobenzyl alcohol were performed using **1** as the catalyst (10 mol% [Ir]) to effect quantitative conversion to 4-methoxylbenzaldehyde and 85% conversion to 4-bromobenzaldehyde respectively. When the reaction was repeated with lower catalyst loading (1 mol% [Ir]), a 92% conversion of 4-methoxylbenzyl alcohol to the corresponding aldehyde was achieved in 14 h at room temperature. The reaction mixture was filtered into a flask containing the second catalyst $RhCl(PPh_3)_3$ generated in situ from the reaction of $RhCl_3.3H_2O$ with PPh_3 followed by addition of $TMSCHN_2$. The ^1H NMR spectrum of the crude reaction mixture showed complete consumption of the aldehyde but only trace amounts of the corresponding alkene was produced. The reaction was repeated with $RhCl(PPh_3)_3$ that was pre-synthesized but only trace conversion to the alkene was achieved. The same procedure was followed for 4-bromobenzyl alcohol using dioxane instead of THF as solvent in the second step. Flash column chromatography of the product mixture gave 4-bromostyrene in only 4% yield.

One-pot reactions in which **1** or **9a** was added together with $RhCl(PPh_3)_3$/ PPh_3 were unsuccessful due to reaction of **1** and **9a** with PPh_3 to form $Cp^*Ir(PPh_3)Cl_2$. Other metal complexes were tested for their ability to catalyze the oxidation of the alcohol but their catalytic activity was poor {$Ir(CO)(Cl)(PPh_3)_2$: trace conversion; $RuCl_2(PPh_3)_3$: 36% conversion of 4-methoxybenzyl alcohol to 4-methoxybenzaldehyde in 7 h}.

6.4 Conclusion

Complex **9a** catalyzes the Oppenauer-type oxidation of cyclopentanol to cyclopentanone and transfer hydrogenation of cyclopentanone to cyclopentanol quantitatively using K_2CO_3 or Na_2CO_3 as base. The amine-functionalized analogue, however does not show any catalytic activity. One-pot oxidation/ methylenation procedures using **1** and $RhCl(PPh_3)_3$ did not give good yield of the alkenes, probably due to incompatibility of the two catalytic conditions.

6.5 Experimental

General experimental procedures and instrumentation are as described in Section 2.6. $RhCl(PPh_3)_3$ and $RuCl_2(PPh_3)_3$ were synthesized using reported procedures.[7,8] All other chemicals were obtained commercially and used without further purification. Yields of products were calculated by ^{1}H NMR integration.

6.5.1 Oppenauer-type oxidation of primary and secondary alcohols by iridium complexes

In a typical run, the cyclopentanol (1.0 mmol) was syringed into a suspension of the iridium complex (0.01 mmol) and base (0.01 mmol) in acetone (10 ml) in a Schlenk tube. The mixture was stirred for 6 h at room temperature. Aliquots (0.5 ml) were drawn and concentrated by blowing with a stream of argon. The residue was completely dissolved in $CDCl_3$ (0.5 ml) for ^{1}H NMR quantification. Cyclopentanone was identified by comparing its ^{1}H NMR and IR spectra with that obtained from a commercial sample.

Spectroscopic data of Ir complex after reaction:

IR (dcm): 2019 (w) cm^{-1}. ^{1}H NMR ($CDCl_3$): δ 2.63 (s, 15H, Cp*C*H*$_3$).

For entry 5, a solution of **2b** (5.0 mg, 11.4 μmol) in CCl_4 (0.5 ml) was irradiated using a xenon lamp for 3 h. Compound **9b** precipitated out of the solution as yellow solids (ν_{CO} = 2058 cm^{-1} in dcm). A solution of cyclopentanol (50 μl, 0.55 mmol) in acetone (10 ml) was added and the solution was stirred at room temperature for 6 h. No conversion to

cyclopentanone was observed in the ^{1}H NMR spectrum. K_2CO_3 (20.0 mg, 0.145 mmol) was added and the reaction mixture was stirred for another 6 h. No conversion to cyclopentanone was observed.

For entries 6 and 7, CCl_4 (0.5 ml) was added together with the starting materials. The reaction mixture was briefly purge-filled with argon three times and stirred at room temperature.

For entries 8-10, the reaction mixture was degassed by three cycles of freeze-pump-thaw and heated at 70 ºC in a Carius tube.

Attempted synthesis of **1** using acetone as solvent:

A suspension of $IrCl_3$ (10.0 mg, 0.335 mmol) and Cp*H (80 μl, 0.51 mmol) in acetone (8 ml) was heated at 75 ºC in a Schlenk tube fitted with a water-cooled condenser for 2 d. A suspension of brown solids in a reddish brown solution was obtained. Complex **1** was not present in the crude mixture.

6.5.2 Transfer hydrogenation of cyclopentanone catalyzed by iridium complexes

In a typical run, cyclopentanone (88 μl, 0.99 mmol) was syringed into a suspension of the iridium complex (0.01 mmol) and base (0.01 mmol) in isopropanol (10 ml) in a Schlenk tube. Aliquots (0.5 ml) were drawn and concentrated by blowing with a stream of argon. The residue was completely dissolved in $CDCl_3$ (0.5 ml) for ^{1}H NMR quantification.

6.5.3 One-pot oxidation and methylenation

Oxidation of 4-methoxylbenzyl alcohol and 4-bromobenzyl alcohol

i) By complex 1

4-methoxylbenzyl alcohol (15 μl, 0.13 mmol) was syringed into a suspension of **1** (5.0 mg, 6.3 μmol) and K_2CO_3 (10.0 mg, 0.072 mmol) in acetone (10 ml) in a Schlenk tube. The mixture was stirred at room temperature for 6 h. The same procedure was followed using 4-bromobenzyl alcohol (12.6 mg, 67.4 μmol) as the substrate. Quantification of the product

formed is as described in 6.5.1. Conversion to 4-methoxybenzaldehyde: quantitative. Conversion to 4-bromobenzaldehyde: 85 %.

ii) By $RuCl_2(PPh_3)_3$

4-methoxylbenzyl alcohol (120 µl, 0.97 mmol) was syringed into a solution of $RuCl_2(PPh_3)_3$ (10.0 mg, 10.4 µmol) and K_2CO_3 (14.0 mg, 0.1 mmol) in acetone (7 ml) in a Schlenk tube. The mixture was refluxed for 3 h. The ^1H NMR spectrum showed incomplete conversion to 4-methoxylbenzaldehyde. H_2O (35 µl, 1.9 mmol) was added and the mixture was refluxed for another 4 h to give 36 % conversion to 4-methoxylbenzaldehye.

Synthesis of 4-methoxystyrene

i) Using in situ generated $RhCl(PPh_3)_3$

4-methoxylbenzyl alcohol (150 µl, 1.27 mmol) was syringed into a suspension of **1** (5.0 mg, 6.3 µmol) and Na_2CO_3 (14.0 mg, 0.132 mmol) in acetone (10 ml) in a Schlenk tube. The mixture was stirred at room temperature for 14 h to yield a 92 % conversion into 4-methoxylbenzaldehyde. The mixture was filtered into a flask containing $RhCl(PPh_3)_3$ generated in-situ from the reaction of $RhCl_3.3H_2O$ (6.6 mg, 25 µmol) with PPh_3 (157.0 mg, 0.60 mmol) in THF (5 ml) for 30 min at 50 ºC. Isopropanol (38 µl, 0.5 mmol) and $TMSCHN_2$ (2.46 ml of 2M solution in ether) was added and the solution was stirred at room temperature for 14 h. H_2O_2 (3 ml) was added and the organic layer was extracted with dichloromethane (3 x 10 ml). The combined organic extract was washed with brine (10 ml) and the volatiles were removed under reduced pressure. A ^1H NMR spectrum of the crude reaction mixture was taken in $CDCl_3$. The aldehyde was completely consumed but only trace amounts of the corresponding alkene was produced.

ii) Using isolated $RhCl(PPh_3)_3$

Using the same procedure as described in (i), 4-methoxylbenzaldehyde was produced in situ and filtered into a solution containing $RhCl(PPh_3)_3$ (11.0 mg, 11.9 µmol), PPh_3 (150.0

mg, 0.57 mmol) and isopropanol (37 µl, 0.5 mmol) in THF (5 ml). $TMSCHN_2$ (2.46 ml of 2M solution in ether) was added and the solution was stirred at room temperature for 3 h. The work up is as described in (i). Spot TLC shows complete consumption of the aldehyde but only trace amounts of the corresponding alkene was produced.

Synthesis of 4-bromostyrene

4-bromobenzyl alcohol (93.0 mg, 0.497 mmol) was syringed into a suspension of **1** (4.0 mg, 5.0 µmol) and Na_2CO_3 (10.0 mg, 94.3 µmol) in acetone (5 ml) in a Schlenk tube. The mixture was stirred at room temperature for 14 h. Acetone was removed under reduced pressure the residue was extracted with dioxane (3 ml). 2 ml of the extract was added to a Schlenk tube containing $RhCl(PPh_3)_3$ (8.0 mg, 8.6 µmol), PPh_3 (90.0 mg, 0.344 mmol) and isopropanol (25 µl, 0.32 mmol) in dioxane (3 ml) at 50 ºC. $TMSCHN_2$ (2.46 ml of 2M solution in ether) was added and the solution was stirred at 50 ºC for 1 h. The work up is as described for the synthesis of 4-methoxystyrene. The product was purified by column chromatography (1% ether/pentane, v/v). 4-bromostyrene was obtained as a colourless oil (4.0 mg, 4 %).

References

[1] (a) Oppenauer, R. V. Recl. Trav. Chim. Pays-Bas **1937**, *56*, 137-144. (b) Hanasaka, F.; Fujita, K.; Yamaguchi, R. *Organometallics* **2005**, *24*, 3422-3433.

[2] (a) Fujita, K.; Furukawa, S.; Yamaguchi, R. *J. Organomet. Chem*. **2002**, *649*, 289-292. (b) Hanasaka, F.; Fujita, K.; Yamaguchi, R. *Organometallics* **2004**, *23*, 1490-1492.

[3] Sakaguchi, S.; Yamaga, T.; Ishii, Y. *J .Org. Chem*. **2001**, *66*, 4710-4712.

[4] (a) Mashima, K.; Abe, T.; Tani, K. *Chem. Lett*. **1998**, 1199-1200. (b) Wu, X.; Li, X.; Hems, W.; King, K.; Xiao, *J. Org. Biomol. Chem*. **2004**, *2*, 1818-1821. (c) Murata, K.; Ikariya, T. *J. Org. Chem*. **1999**, *64*, 2186-2187. (d) Inoue, S.; Nomura, K.; Hashiguchi, S.; Noyori, R.; Izawa, Y. *Chem. Lett*. **1997**, 957-958.

[5] Fujita, K.; Kitatsuji, C.; Furukawa, S.; Yamaguchi, R. *Tetrahedron Lett.* **2004**, *45*, 3215-3217.

[6] Lebel, H.; Paquet, V. *J. Am. Chem. Soc*. **2004**, *126*, 11152-11153. (b) Jensen, D. R.; Schultz, M. J.; Mueller, J. A.; Sigman, M. S. *Angew. Chem. Int. E*d. **2003**, *42*, 3810-3813. (c) Lebel, H.; Paquet, V. *J. Am. Chem. Soc*. **2004**, *126*, 320-328.

[7] Osborn, J. A.; Wilkinson, G. *Inorg. Synth*. **1990**, *28*, 77-79.

[8] Hallman, P.S.; Stephenson, T. A.; Wilkinson, G. *Inorg. Synth*. **1970**, *12*, 237-238.

Conclusion

Photolysis of aminoethyl-functionalized cyclopentadienyl iridium dicarbonyl complexes $Cp^XIr(CO)_2$ (Cp^x = Cp^ or Cp*^) in cycloalkanes resulted in the formation of hydridoalkyl species $Cp^XIr(CO)(R)(H)$ and dihydride species $Cp^XIr(CO)(H)_2$. There is no observed intramolecular coordination of the amine group to form chelate complexes. Under a carbon monoxide atmosphere, the cyclopentadienyl iridium system can be photochemically activated to promote the carbonylation of cyclohexane to produce cyclohexanecarboxaldehyde (Scheme I). Spectroscopic evidence suggests that the acyl species $[Cp^*Ir(CO)(COC_6H_{11})(H)]$ may be an intermediate in the formation of the aldehyde.

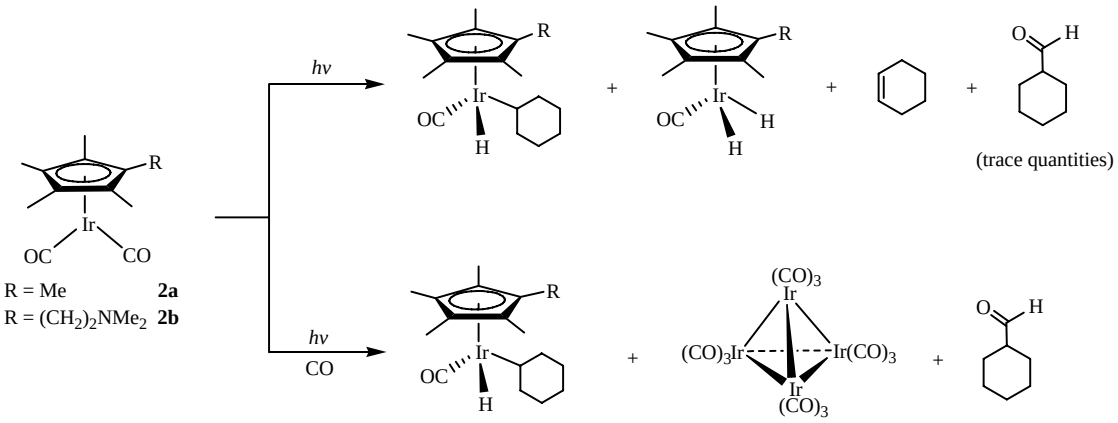

Scheme I

$Cp^*Ir(CO)_2$, **2a** was found to react with fluorinated solvents. Complex **2a** reacted photochemically with C_6F_6 to give the η^2-arene complex $Cp^*Ir(CO)(C_6F_6)$, **15** and the C-F activated dimeric complex $[Cp^*Ir(CO)(C_6F_5)]_2$, **16**. A highly regioselective reaction of **2a** with C_6F_5CN proceeded in the presence of water to produce the metallocarboxylic acid $Cp^*Ir(CO)(COOH)(p\text{-}C_6F_4CN)$, **18a**, where the substituent in the arene ring is in the *para* position. Similar reactions occurred with perfluoroarenes carrying one or more highly electron-withdrawing groups and with pentafluoropyridine. On the basis of various experimental studies, the formation of **18a** was suggested to occur via two nucleophilic substitution steps: (i) attack by **2a** on the *para*-carbon of the fluoroarene and (ii) attack by

water or hydroxide ion, probably via a general base-catalyzed route, on one of the carbonyls to form the carboxylic group (Scheme II).

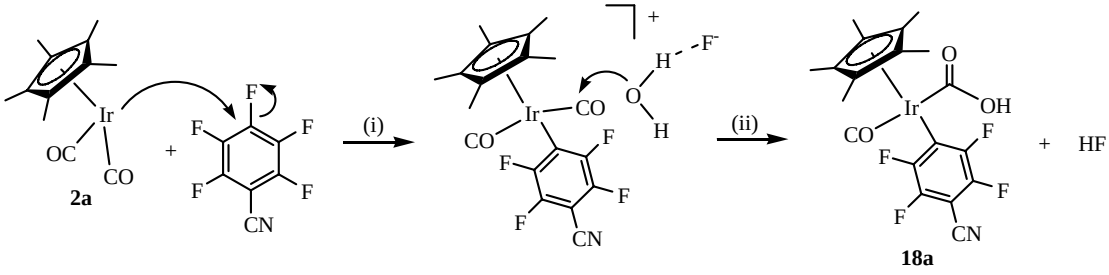

Scheme II

The properties and reactivity of **18a** were compared to other known metallocarboxylic acids, and it was found that **18a** shows many properties typical of these, such as dehydration in the presence of a strong acid, decarboxylation in the presence of a base and esterification in alcohols without an acid or base catalyst.